NASA Contractor Report 189735

P-328

A SUPERCONDUCTING LARGE-ANGLE MAGNETIC SUSPENSION

James R. Downer,
George V. Anastas, Jr.,
Dariusz A. Bushko,
Frederick J. Flynn,
James H. Goldie,
Vijay Gondhalekar,
Timothy J. Hawkey,
Richard L. Hockney, and
Richard P. Torti

SatCon Technology Corporation
12 Emily Street
Cambridge, MA 02139

Contract No. NAS1-18853
December 1992

National Aeronautics and
Space Administration

Langley Research Center
Hampton, Virginia 23665-5225

NASA Contractor Report 189735

A SUPERCONDUCTING LARGE-ANGLE MAGNETIC SUSPENSION

James R. Downer,
George V. Anastas, Jr.,
Dariusz A. Bushko,
Frederick J. Flynn,
James H. Goldie,
Vijay Gondhalekar,
Timothy J. Hawkey,
Richard L. Hockney, and
Richard P. Torti

SatCon Technology Corporation
12 Emily Street
Cambridge, MA 02139

Contract No. NAS1-18853
December 1992

National Aeronautics and
Space Administration

Langley Research Center
Hampton, Virginia 23665-5225

THIS PAGE

INTENTIONALLY

LEFT BLANK

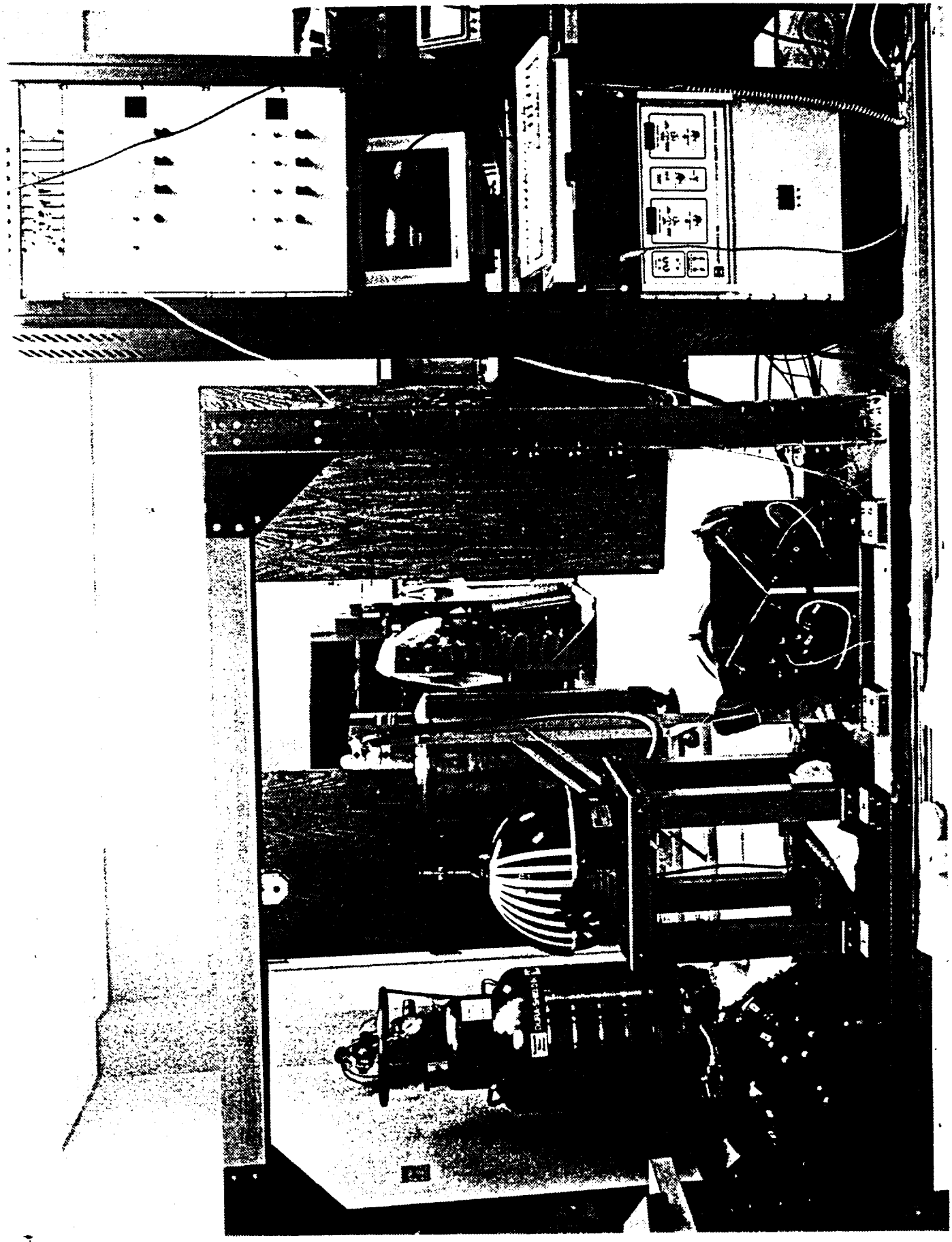

SUMMARY

SatCon Technology Corporation has completed a Small Business Innovation Research (SBIR) Phase II program to develop a Superconducting Large-Angle Magnetic Suspension (LAMS) for the NASA Langley Research Center. The Superconducting LAMS was a hardware demonstration of the control technology required to develop an advanced momentum exchange effector.

Phase I Results

The Phase I research defined a conceptual design for an advanced control moment gyro (CMG) type of momentum-exchange actuator sized for large spacecraft slew maneuvers. The key component of the CMG is a magnetic suspension system which combines the functions of conventional rotor bearings and mechanical gimbals. This type of suspension has been previously referred to as a LAMS system. In order to meet the needs of a demanding slew maneuver, LAMS design technology was expanded by incorporating a superconducting magnet. The inclusion of a superconducting magnet in the LAMS design and the goal of large amounts of angular freedom were challenges to the existing state of controller technology as applied to magnetic suspension systems.

Phase II Objectives

The Phase II research was directed toward the demonstration of the key technology required for the advanced concept CMG, the controller. The Phase II hardware consists of a superconducting solenoid ("source coil") suspended within an array of non-superconducting coils ("control coils"), a five-degree-of-freedom position sensing system, switching power amplifiers, and a digital control system.

Phase II Results

The Phase II results demonstrated the feasibility of suspending the source coil. Gimballing (pointing the axis of the source coil) was demonstrated over a limited range. With further development of the rotation sensing system, enhanced angular freedom should be possible.

Future Work

SatCon has proposed to retain the hardware in order to pursue an internal research and development (IR&D) program. SatCon is interested in making further developments on the rotation sensing system that was used in the LAMS testbed. SatCon will investigate the use of alternate software and hardware in order to achieve an enhanced angular range.

ACKNOWLEDGEMENT

This research in this final report was prepared under Contract NAS1-18853. The contract was sponsored by the National Aeronautics and Space Administration (NASA) and monitored by the NASA Langley Research Center (LaRC).

The authors would like to acknowledge the guidance and support provided by Nelson Groom, the Contracting Officer's Technical Representative.

THIS PAGE

INTENTIONALLY

LEFT BLANK

TABLE OF CONTENTS

1. INTRODUCTION

SatCon Technology Corporation has completed a Small Business Innovation Research (SBIR) Phase II program to develop a Superconducting Large-Angle Magnetic Suspension (LAMS) for the NASA Langley Research Center. The Superconducting LAMS was a hardware demonstration of the control technology required to develop an advanced momentum exchange effector.

1.1 Phase I Results

The Phase I research, completed in 1988, defined a conceptual design for an advanced control moment gyro (CMG) type of momentum-exchange actuator sized to provide the torque and angular momentum required to reorient a large spacecraft or other space-based payload through a large angle (a slew maneuver). Figure 1.1 shows the conceptual design of the advanced concept CMG. The Phase I design is described in more detail in Chapter 2.

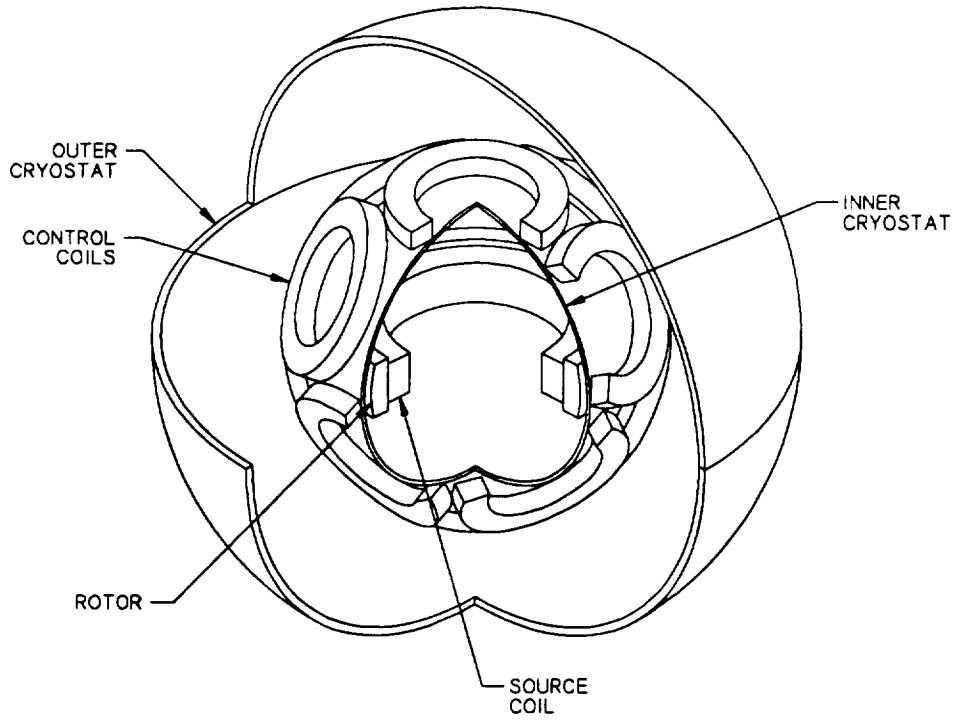

Figure 1.1. Advanced Concept CMG

The key component of the advanced concept CMG is a magnetic suspension system which combines the functions of conventional rotor bearings and mechanical gimbals. This type of suspension has been previously referred to as a large angle magnetic suspension (LAMS) system. In order to meet the needs of a demanding slew maneuver, LAMS design technology was expanded by incorporating a superconducting magnet. The inclusion of a superconducting magnet in the LAMS design and the goal of large amounts of angular freedom were challenges to the existing state of controller technology as applied to magnetic suspension systems.

1.2 Phase II Objectives

The Phase II research was directed toward the demonstration of the key technology required for the advanced concept CMG, the controller. The Phase II hardware consists of a superconducting solenoid ("source coil") suspended within an array of non-superconducting coils ("control coils"), a five-degree-of-freedom position sensing system, switching power amplifiers, and a digital control system. Figure 1.2 is a photograph of the hardware.

1.3 Phase II Results

The Phase II results demonstrated the feasibility of suspending the source coil. Gimballing (pointing the axis of the source coil) was demonstrated over a limited range. With further development of the rotation sensing system, enhanced angular freedom should be possible.

1.4 Organization of the Report

The remainder of this report documents the design, fabrication, and evaluation of the superconducting LAMS. Chapter 2 discusses the advanced concept CMG and introduces the overall design of the Phase II demonstration.

Chapters 3-6 describe the design and testing of the various hardware components. Chapter 3 presents the design and performance of the magnetic components. Chapter 4 describes the mechanical

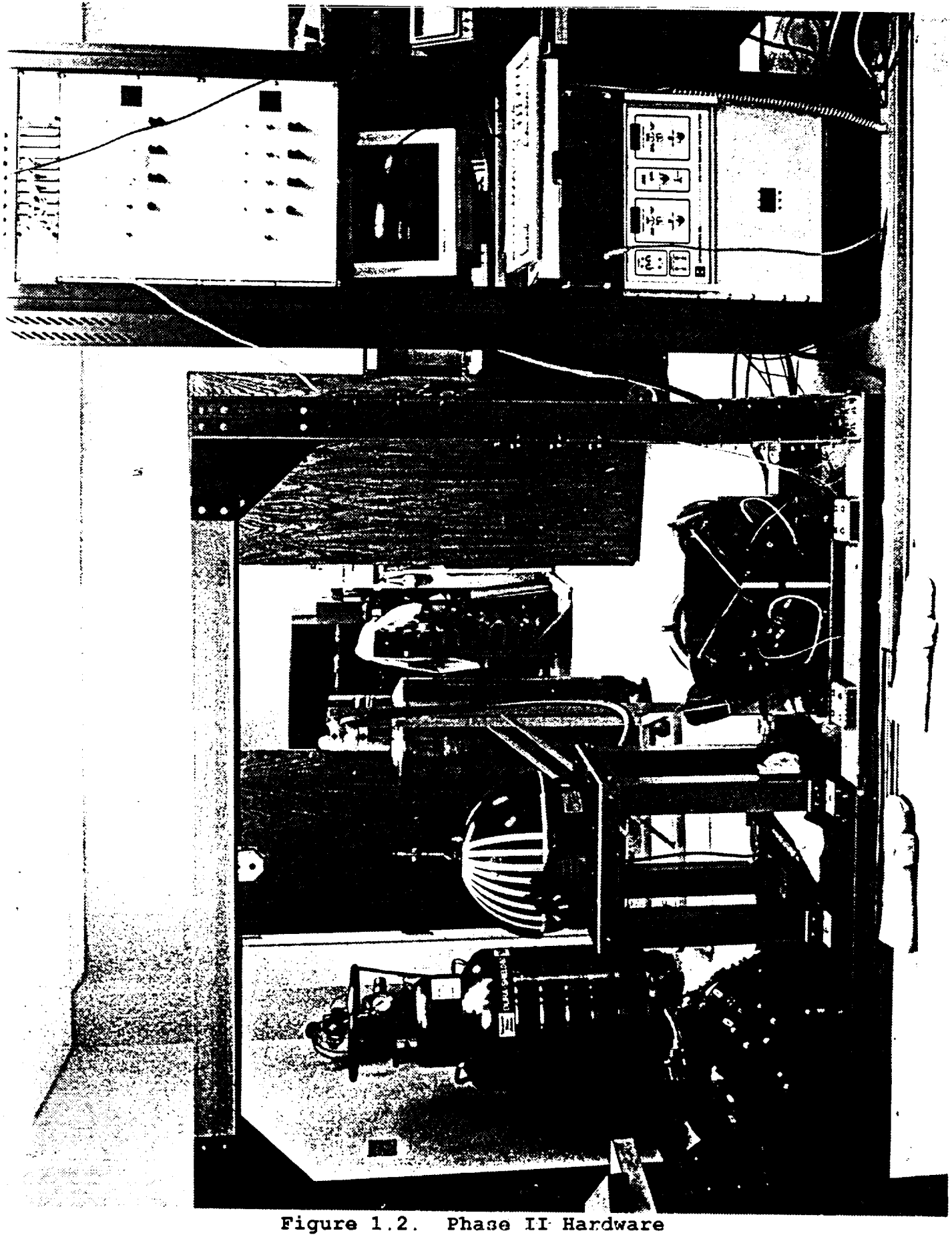

Figure 1.2. Phase II Hardware

support systems. Chapter 5 presents the design of the sensor systems which provide measurements of the position and orientation of the suspended body to the controller. The system electronics console consists of a digital signal processor, power amplifiers, and signal conditioning for the sensors. All of these electronic components are discussed in Chapter 6.

Chapter 7 describes the development of the controller for the superconducting LAMS demonstration. System modelling, compensation design, and digital implementation are all described.

Chapter 8 documents the performance of the integrated system. The test results include the initial suspension of the superconducting magnet and the evaluation of its gimballing capability. The final chapter contains conclusions and recommendations for further work.

In order that NASA personnel be able to operate the hardware, a number of appendices follow the main body of the report. Full sets of mechanical drawings and electronic schematics are included in Appendices A and B. Appendix C contains a manual for operation of the system, while Appendix D is a reprint of the manual provided by the manufacturer of the superconducting magnet. Appendix E contains a copy of the Computer Programming, Documentation and Material Report

1.5 Recommendations for Future Work

As currently configured, the rotation sensing system has a limited angular range. The performance of the superconducting LAMS is limited by the angular range of the rotation sensing system. The limitation is due to both the current software configuration and eddy-current shielding by the stainless-steel structure which supports the control coils.

SatCon believes that there are potential benefits to NASA and other Government agencies from further development of the rotation sensor. The advanced CMG will require a large angle capability in the angular sensing system. Further development of the sensor system will lead to the development of this capability.

The rotation sensing system will also be usable in other Government research programs. SatCon has proposed a modification of the sensing system to the Naval Weapons Center for sensing the rotational parameters required by a free gyro seeker of a multi-spectrum guidance system. The Navy's motivation in soliciting innovative sensors for the gyros of IR seekers is improved precision in angle, rate, and phase measurements in a smaller volume than current designs.

SatCon has proposed to retain the hardware in order to pursue an internal research and development (IR&D) program. SatCon is interested in making further developments on the rotation sensing system that was used in the LAMS testbed. SatCon will investigate the use of alternate software and hardware in order to achieve an enhanced angular range.

THIS PAGE

INTENTIONALLY

LEFT BLANK

2. SYSTEM OVERVIEW

This chapter discusses the design of the advanced concept CMG which was defined in the Phase I research. This baseline system is then used to develop the basic design for the Phase II hardware.

2.1 Phase I Design

The advanced concept CMG defined in the Phase I SBIR program has a specific torque (torque per unit of mass) that is a multiple order of magnitude improvement over conventional technology. Large spacecraft are defined as those having moments of inertia on the order of 100 kNms^2 (100,000 kg•m^2). The control-torque (27 kNm) and angular-momentum storage (45 kNms) required for rigid-body slewing of such large spacecraft are substantially greater than the capabilities of available momentum-exchange actuators. Table 2.1 presents the parameters (spacecraft moment of inertia, slew angle, and slew time) which define the slew. The table also presents the requirements (control torque, angular momentum, and mechanical power) for the advanced concept CMG. Torques of this magnitude are typically applied via a reaction-control (thruster) system. These systems, however, have deficiencies which make them unacceptable for many SDIO missions.

Table 2.1. Slew Actuator Requirements

Trajectory Parameters	
Slew Angle	1 rad.
Slew Time	4.4 sec.
Inertial Properties	
Forward-body Mass	6,000 kg
Forward-body Inertia	100 kNms^2
Actuator Requirements	
Max. Control Torque	27 kNm
Max. Angular Momentum	45 kNms

2.1.1 Deficiencies in Thruster Systems

Thruster systems expel a pressurized fluid in order to apply torque to a spacecraft. The fluid is stored, in tanks, on-board the spacecraft. These stores of fluid must be periodically replaced, thereby limiting the achievable mission length. Another disadvantage is that the fluid expelled by the reaction-control system (effluent) may also be detrimental to on-board optics. The advanced concept CMG described in this report would be used in large-spacecraft slewing applications where the disadvantages of reaction-control systems cannot be tolerated.

2.1.2 Conventional Angular Momentum Exchange Actuators

Another approach for controlling the attitude of a spacecraft or other payload is to apply equal and opposite torques to the payload and a flywheel. The net angular momentum of the flywheel and the payload will remain constant. This type of device is referred to as an angular momentum exchange actuator since any angular momentum which is gained (lost) by the payload is lost (gained) by the flywheel. The use of momentum exchange actuators has several advantages over thrusters (reduced maintenance and improved compatibility with optics). The use of momentum exchange actuators began in the early days of the space program and the design of these devices has steadily progressed to a state of relative maturity. Angular momentum may be exchanged between a flywheel and a payload in one of two ways. Either the spin rate (of a fixed orientation flywheel) or the orientation (of a fixed spin rate flywheel) may be varied. Devices of the latter type are referred to as CMGs and are discussed below.

2.1.2.1 Control Moment Gyro Principles. A control moment gyro (CMG) exchanges angular momentum by varying the angular orientation of a constant-speed flywheel through the use of either a single-degree-of-freedom or a two-degree-of-freedom gimbal system. Figure 2.1 describes this process in terms of applying a torque to a spacecraft over a fixed period of time. The torque is applied

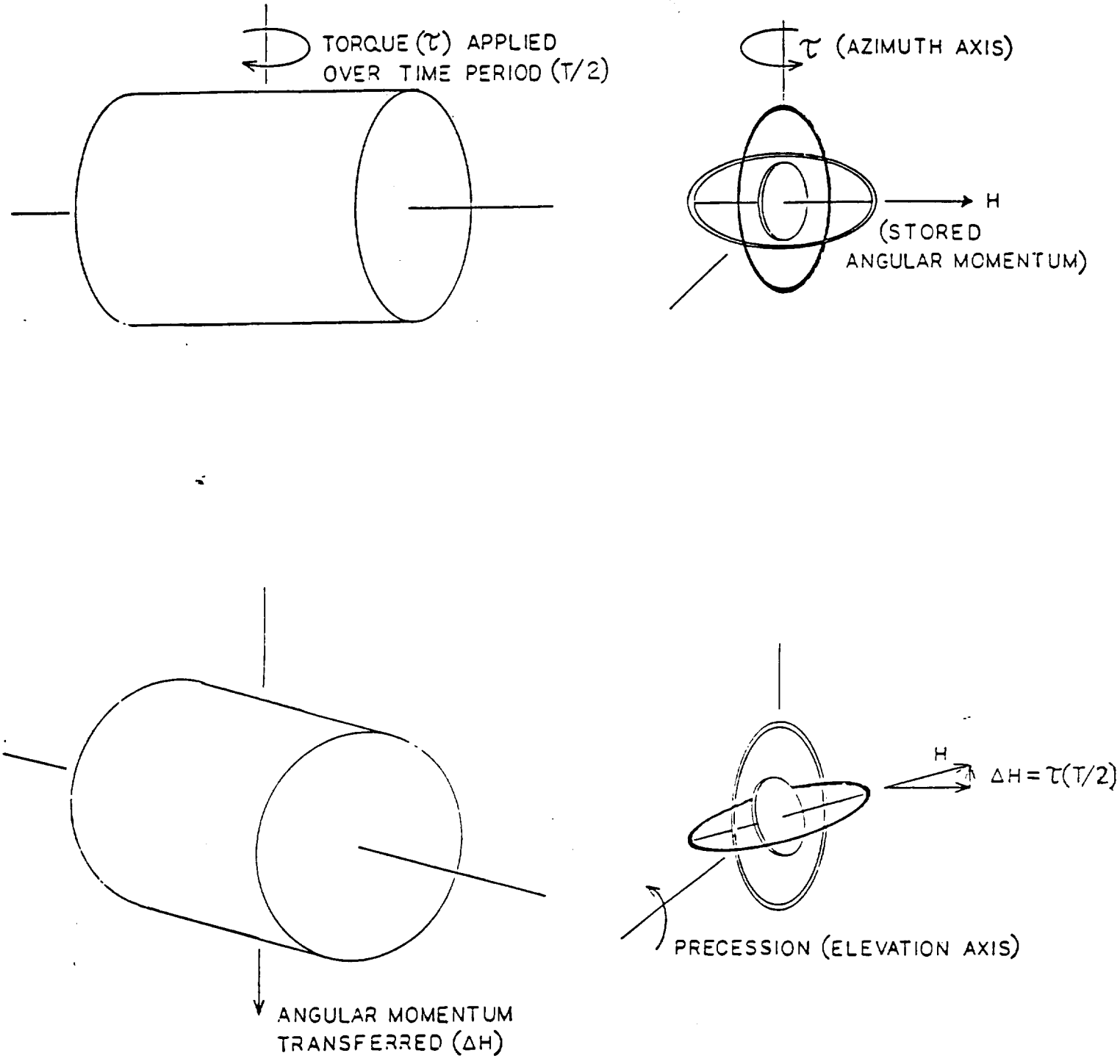

Figure 2.1. Operation of a CMG

through a torquer mounted to the azimuth-axis gimbal. The flywheel precesses about the elevation axis to conserve the net angular momentum of the flywheel and the payload. The Phase I study focused on the CMG type actuator design.

2.1.2.2 Conventional Technology CMGs. Table 2.2 shows an attempt at employing several commercially available CMGs an the slew actuator application. The table shows the number of CMGs which would have to be used to provide for slewing in two axes. Double gimballed CMGs are typically limited by the capacity of the gimbal torquers, while the single-gimballed CMGs are limited by angular momentum storage capacity. The mass and power consumption of the CMGs in the slew actuator application were obtained from manufacturers' data sheets.

Table 2.2. Conventional Technology CMGs

Model No.	Type	Torque (Nm)	Momentum (Nms)	Number Required	Mass (kg)	Power (W)
M4500	DGCMG	270	6,100	200	59,000	25,000
M2400	SGCMG	6,500	3,250	42	2,400	4,150

The number of units, mass, and power consumption are sufficiently large that available CMGs were eliminated from consideration.

2.1.3 Advanced-concept CMG

In addition to parts count, the use of conventional-technology CMGs is limited by the mass and power consumption of these devices. This section discusses an alternative design approach for a double-gimballed CMG which provides high control torque as well as reduced mass (increased specific torque) and reduced power consumption.

In order to meet the requirements of slewing large spacecraft, a number of advanced component technologies have been employed in the design of the advanced concept CMG. Each of the technologies

is relatively mature, but none of these has been previously used in the design of conventional CMGs.

Figure 2.2 is a partially cut-away view which shows the rotating components (superconducting coil and flywheel) and cryogenic housing of a two-degree-of-freedom CMG which employs a superconducting magnetic suspension system. The paragraphs which follow describe the configuration and design of the advanced CMG.

2.1.3.1 Large-angle Magnetic Suspension. One particularly large component of the mass of a double-gimballed CMG is that of the gimbal system. The use of a mechanical gimbal structure such as the one shown in Figure 2.1 is the conventional approach for CMG design. An early study [2.1] concluded that the mass of the gimbal system of a CMG was typically as large as that of the rotor. Later studies showed that an alternative approach which consolidates the functions of conventional bearing and gimbal systems could significantly reduce this mass penalty if limited gimballing (less than about 20 degrees) could be used [2.2,2.3]. A large-angle magnetic suspension (LAMS) is a five-axes, actively-controlled magnetic bearing which is designed to accommodate a certain amount of angular motion about the lateral axes of the flywheel. The later research [2.2] indicated that the mass of a LAMS can be made to be less than that of a gimbal system by as mush as a factor of five (depending on the amount of angular freedom).

The use of a LAMS in an angular momentum exchange actuator has the primary advantage that physical contact between the rotor and stator is eliminated. This leads to greatly extended life, increased reliability, and reduced vibrations. Several designs based on conventional magnet technology have been developed in previous research efforts [2.2,2.3]. These were sized for much lower control torque levels than those found in this application.

2.1.3.2 Superconducting LAMS. Based on the results of preliminary analyses, it became obvious these approaches would be excessively massive and inefficient. Thus, it was decided to turn the design

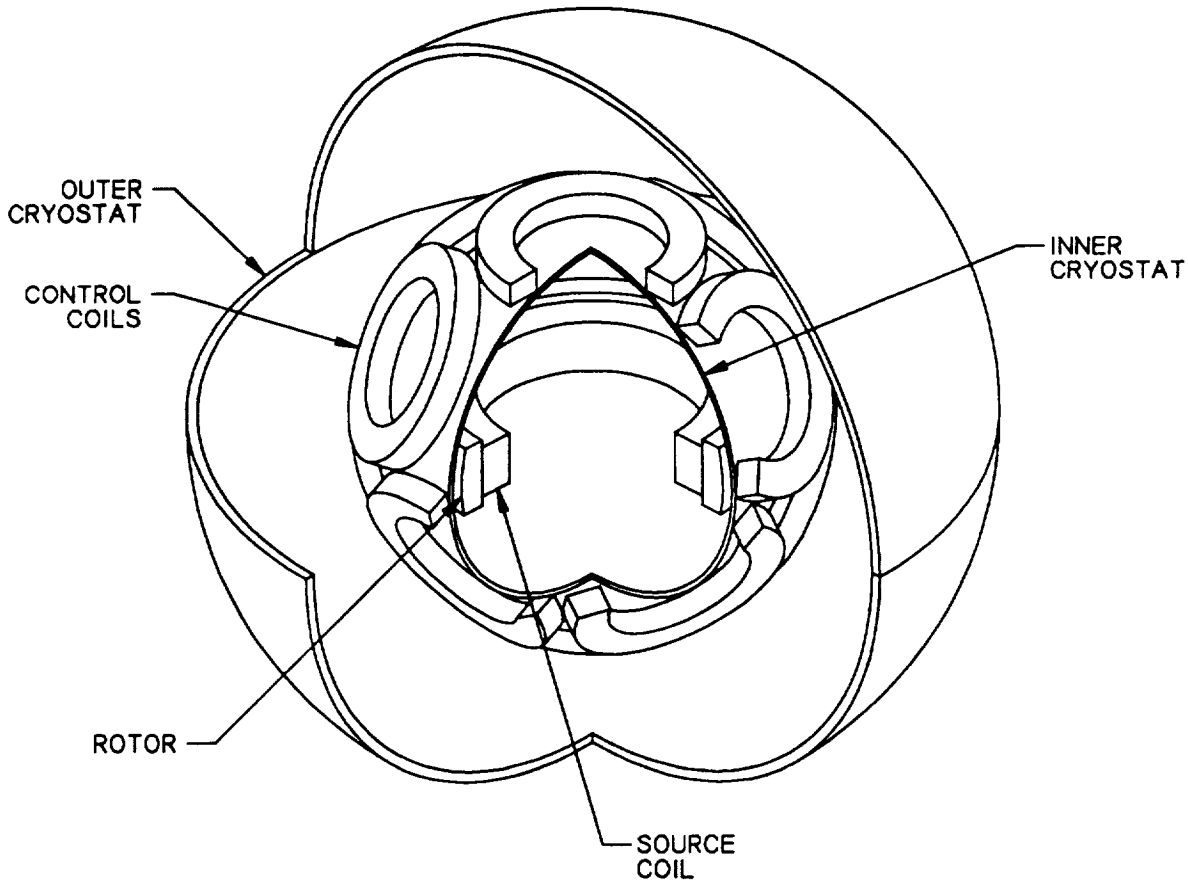

Figure 2.2. Advanced Concept CMG

toward a LAMS system based on superconducting technology. This promised significant reductions in power and weight for the following reasons:

1) The current density in a superconductor can be extremely high (on the order of 100 MA/m^2);

2) No field-shaping iron is required;

3) Higher flux density increases the force-producing capability of conventional coils.

A superconducting LAMS is an advanced design which may be used in a CMG to deliver large torques to a spacecraft without the need for an excessively massive magnetic core or the consumption of a large amount of power. The superconducting LAMS, as its name suggests, employs a superconducting coil and thus eliminate all conventional magnetic structures in order to produce an energy-efficient, light-weight design. The following paragraphs describe the construction and operation of a superconducting LAMS.

The superconducting coil (the "source" coil) is a solenoid which operates in persistent-current mode (without an electrical input). The current in the solenoid persists because of the lack of resistance in the superconducting material. The spherical case which surrounds the rotating components also serves as the cryostat for the superconducting solenoid. The superconducting LAMS employs a total of twelve (12) normal (non-superconducting) "control" coils which interact with the fields produced by the source coil solenoid in order to apply forces and torques. A simplified discussion can be used to describe the mechanisms which are used to apply forces and torques to the flywheel of the advanced concept CMG.

Figure 2.3(a) shows two coils which are attached to the outer surface of the case of the CMG. The interaction of the magnetic field (B) of the solenoid and the current density (J) in each differential section (dV) of the coil produces a force density (df).

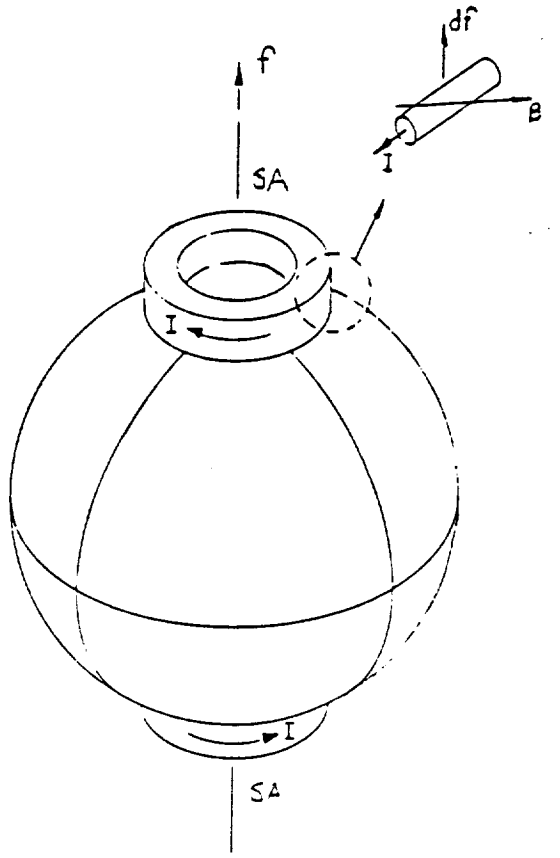

a) Thrust-force

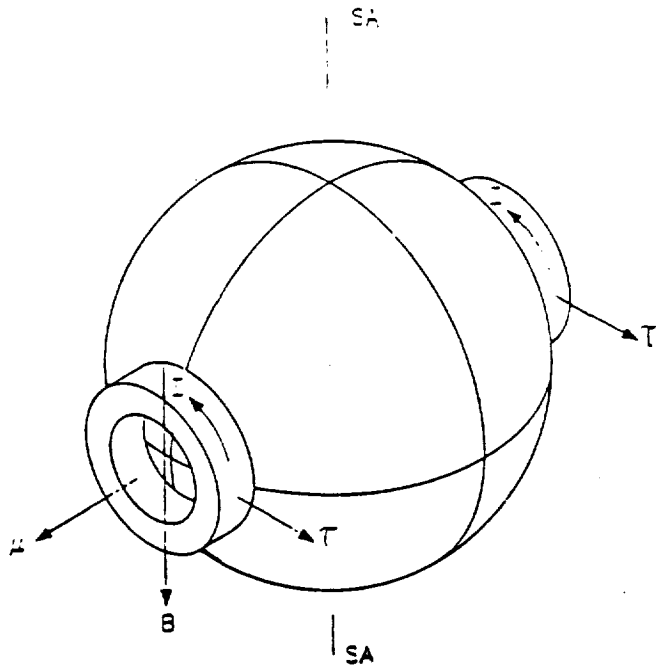

b) Torque

Figure 2.3. Superconducting LAMS Loading

The net force (f) produced by the two coils is found by integrating the force density over the volume of the coils.

Assuming that the spin axis of the flywheel (the axis of the solenoid) coincides with the z-axis, the net result of this interaction is a force which acts along the z-axis (a thrust force) as is shown in the figure.

The coils shown in Figure 2.3(b) which are perpendicular with the spin axis of the flywheel are used to apply torques to the flywheel. The figure also illustrates the torquing mechanism. Assuming that the spin axis is along the z-axis, the magnetic field (B), produced by the superconducting solenoid is nearly parallel to the z-axis and constant. The torque (τ) results from the interaction of the dipole moment (μ) produced by the current in the normal coil and the magnetic field.

2.1.3.3 Composite Flywheel. The angular-momentum storage device (flywheel) of available CMGs is typically made from a high-strength metal such as maraging steel. Advanced composite materials such as high-strength graphite fibers in an epoxy matrix [2.4], however, have much greater angular-momentum density (angular momentum per unit mass). This material is currently being used for advanced energy storage flywheels for space power applications. A high-strength graphite/epoxy composite flywheel is attached to the exterior of the superconducting source coil to provide angular momentum storage capacity. The outer diameter of the flywheel is machined to a spherical shape. This allows the flywheel to be completely gimballed without contact with the case.

2.1.3.4 Scissored-pair CMG Configuration. If a single CMG is to be used as a slew actuator, the amount of angular freedom of the gimbal system (the maximum gimbal angle) must be at least equal to the maximum slew angle. An alternative to the use of a single CMG is a pair of counter-rotating CMGs. This is a scissored pair configuration. Figure 2.4 shows this configuration schematically. The primary advantage of employing a scissored pair of CMGs is that

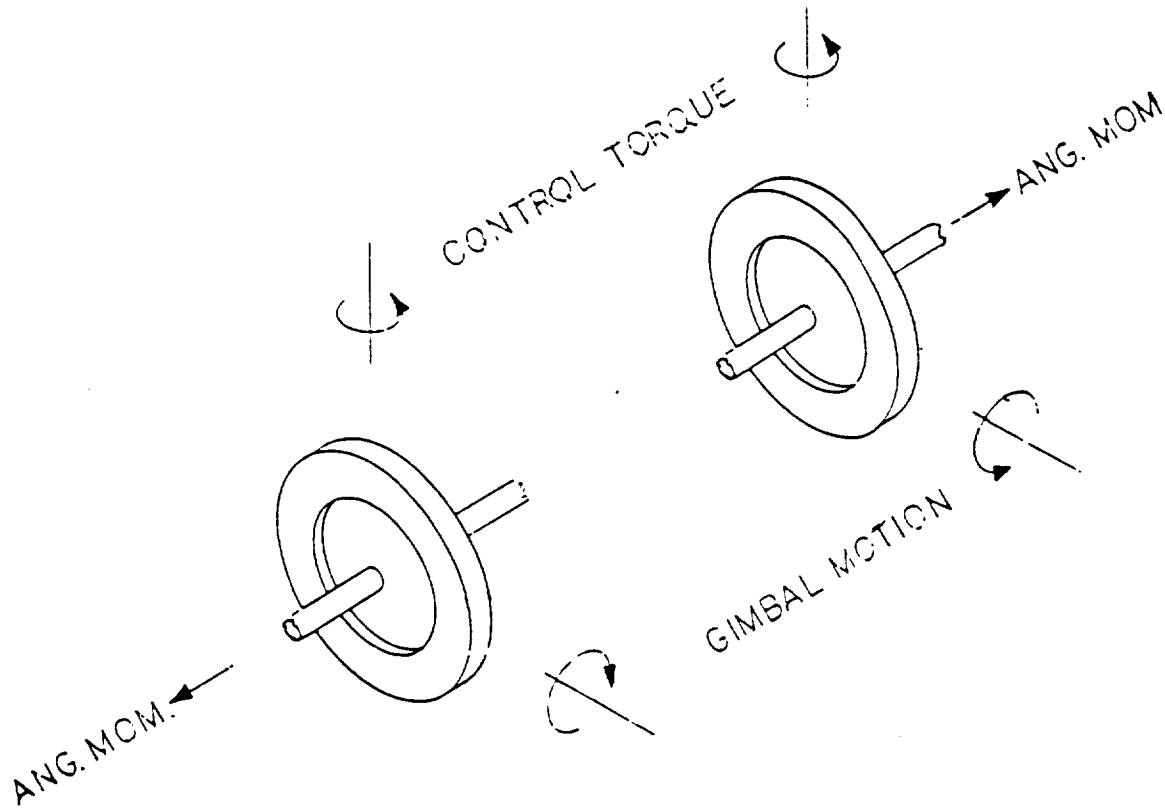

Figure 2.4. Scissored-pair Configuration

the requirement for a large-angle (equal to the maximum slew angle) is eliminated. This configuration is the baseline.

2.1.3.5 Advanced Concept CMG Performance. The goal for the Phase I SBIR research was to analytically verify the feasibility of the advanced concept CMG. The key to feasibility is the super-conducting LAMS. The approach to a feasibility analysis was to identify a preferred design and to quantify its advantages to SDI in the slew actuator application.

The design definition and benefits assessment required the development of a set of analytical tools and their use in a series of trade-off analyses of the various actuator configurations and component technologies. The final design was selected based on minimum mass and power consumption during the delivery of maximum control torque. An emerging technology, high purity aluminum

conductors cooled to the boiling point temperature of liquid hydrogen, was found to be the best choice for the control coils. These "hyperconductors" allowed substantial improvements in mass and power consumption over what is obtainable through the use of copper conductors.

Table 2.3 contains the performance parameters (mass tabulation and power consumption) for the key components of the superconducting LAMS. The reduced control torque requirement results from the use of two CMGs in a scissored-pair configuration. These represent a vast improvement over what could be achieved with more conventional technology.

Table 2.3. Superconducting LAMS Performance

Control Torque	13,500 Nm
Mass Tabulation	
Control Coils	65 kg
Dewar	57 kg
Stator Total	122 kg
Source Coil	57 kg
LAMS total	179 kg
Power	57 W

2.2 Phase II Hardware

In addition to the analysis of a baseline system, a laboratory scale technology demonstration experiment was identified and sized during Phase I. The purpose of the experiment was to use commercially available components in conjunction with a multi-input, multi-output control system and demonstrate the control laws for stabilizing and controlling the superconducting LAMS.

SatCon proposed that superconducting magnetic suspension technology be demonstrated in the laboratory by designing, developing, and testing a reduced-scale superconducting LAMS. The laboratory system was based around a commercially-available superconducting solenoid and an array of twelve room-temperature normal control

coils. For simplicity of construction, it was decided to suspend the cryostat for the superconducting magnet, rather than attempt to suspend the magnet within the cryostat.

The purpose of the Phase II experiment was to demonstrate the required control system technology. The controller is, of course, the key component of most magnetic suspension systems. This approach demonstrated one of the key scientific needs of the advanced concept CMG, but minimized the amount of engineering detail associated with technologies such as cryoresistivity, dewar fabrication, and composite flywheels. Extension of the results of the experiment to a rotating application is expected to be a challenging engineering task which is more appropriately performed as a Phase III development program.

2.3 References

2.1 Gross, S.: Study of Flywheel Energy Storage for Space Stations, NASA CR-171780, February 1984.

2.2 Downer, J.: Design of Large-angle Magnetic Suspensions, ScD Thesis, Massachusetts Institute of Technology, May 1986.

2.3 Oglevie, R. and Eisenhaure, D.: Advanced Integrated Attitude Control System (IPACS) Study, NASA CR-3912, November 1985.

2.4 Olszewski, M. and O'Kain, D.: "Advances in Flywheel Technology for Space Power Applications," Proceedings of the 21st Intersociety Energy Conversion Engineering Conference, San Diego, CA, August 1986.

3. MAGNETIC COMPONENTS

This chapter discusses the design, fabrication, and testing of the magnetic components for the superconducting LAMS. These components consist of the superconducting source coil and the room-temperature normal control coils.

3.1 Superconducting Source Coil and Dewar

Following extensive discussions with the probable fabricators, a detailed design of the superconducting coil and cryostat was proposed. This preliminary work evolved into the design illustrated in Figure 3.1. The superconducting coil and cryostat were constructed by Cryomagnetics, Inc. of Oak Ridge, TN and its subcontractor, Precision Cryogenic Systems of Indianapolis, IN. Cryomagnetics Inc. delivered coil, cryostat, attachments for the spherical envelope, power supply, helium transfer line, and diagnostics including both a level sensor and cryothermometer.

3.1.1 Superconducting Magnet and Cryostat Design

In brief, the superconducting solenoid is surrounded by a helium bath enclosed in a dual chamber vacuum dewar. The magnet is charged by means of removable current leads penetrating the dewar from the bottom through a thermally baffled stack. In a similar manner, liquid helium is filled through an inverted port. This port is normally sealed at its top. It utilizes a thin layer of helium gas for minimizing heat loss down the neck. The addition of an aluminum shield surrounding the superconductor aids in thermally tying the coil to liquid helium temperature thereby allowing operation at liquid levels well below the coil height and at full coil pitch.

3.1.1.1 Cryogenic System. The cryogenic system is illustrated in Figures 3.1, 3.2, and 3.3. The coil is centered on the envelope of the spherical cover and supported by brackets attached to the base of the inner shell. The cryostat dewar consists of three shells of

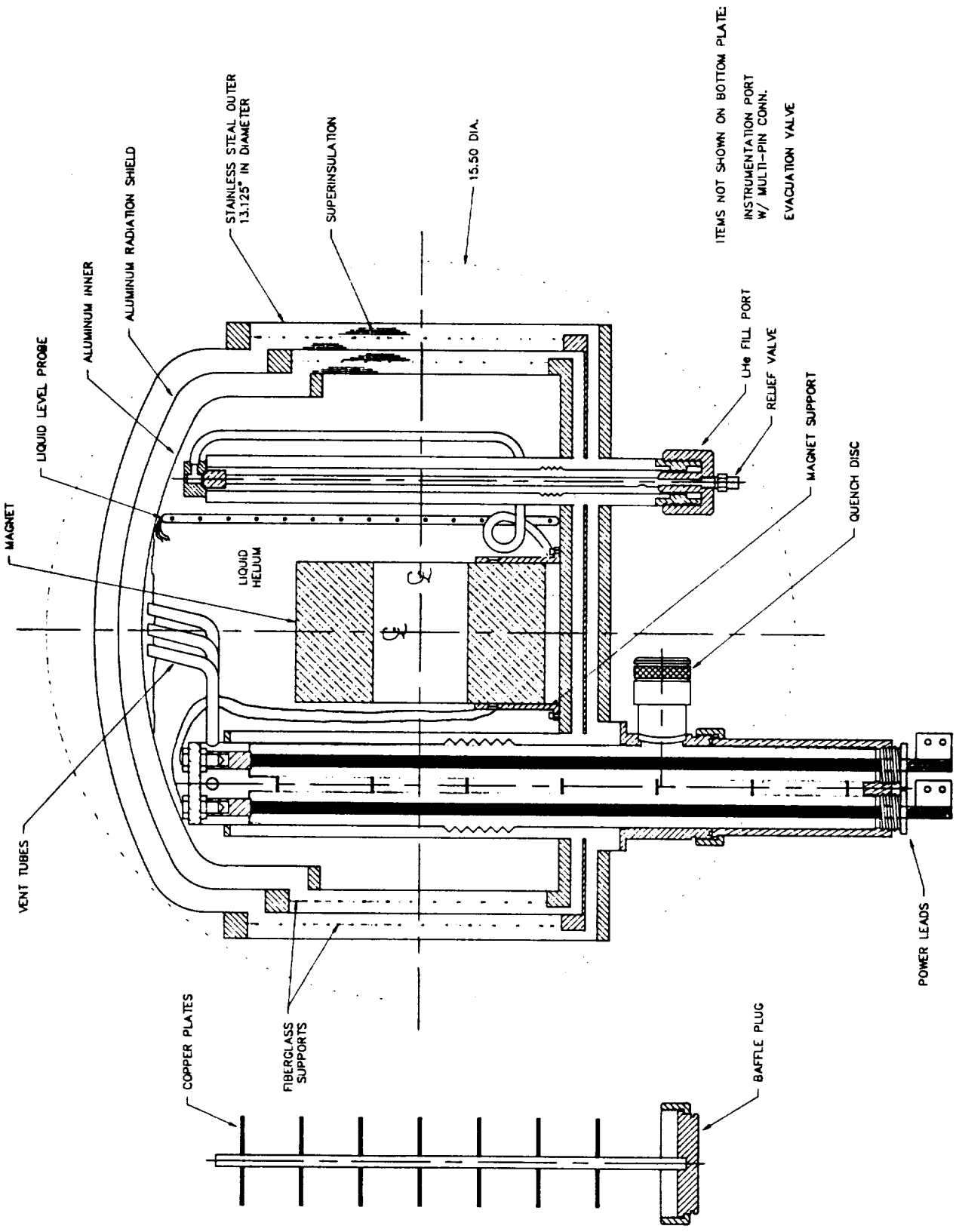

Figure 3.1. Magnet and Cryostat Design, Elevation View

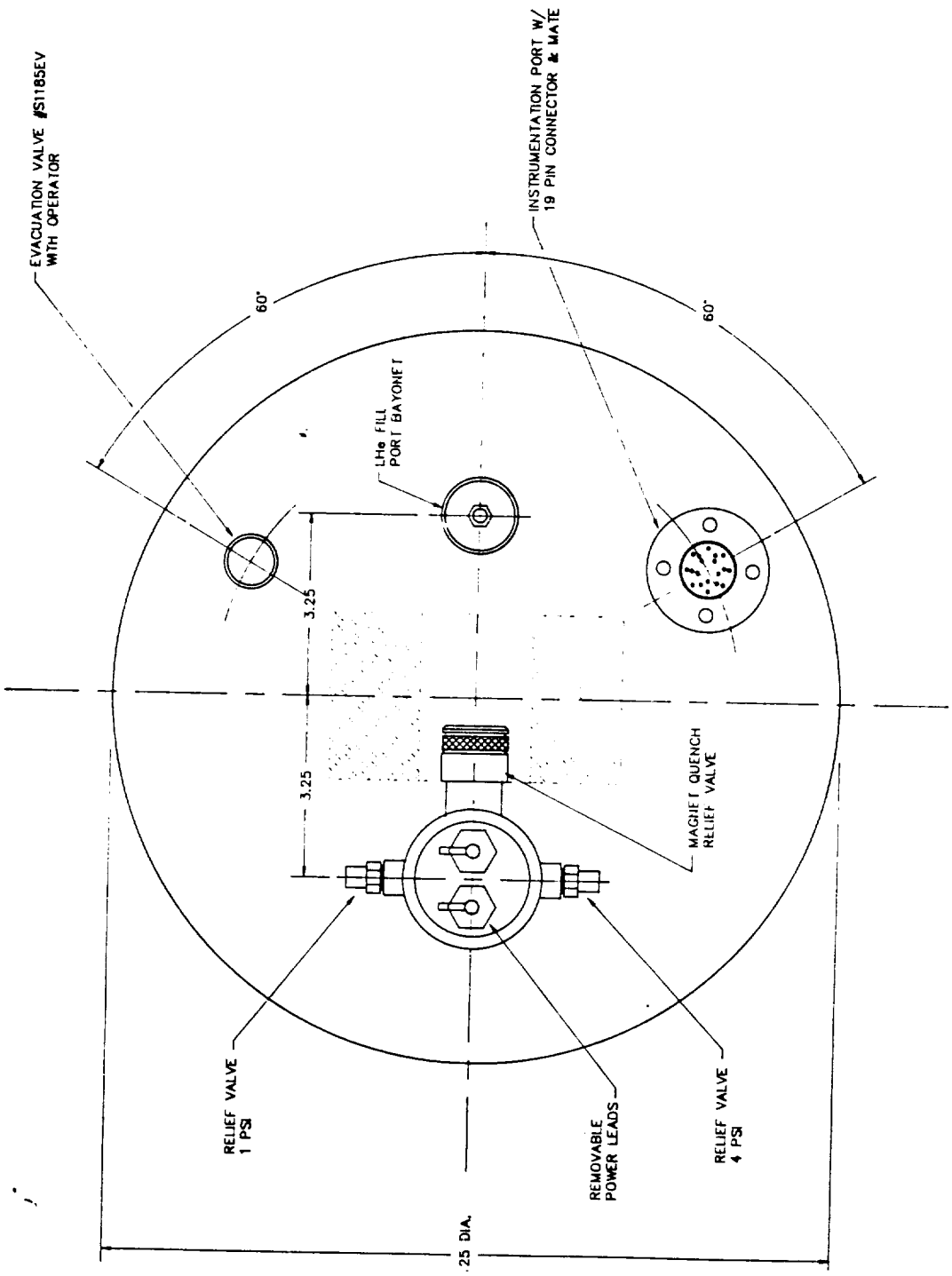

Figure 3.2. Magnet and Cryostat Design, Bottom View

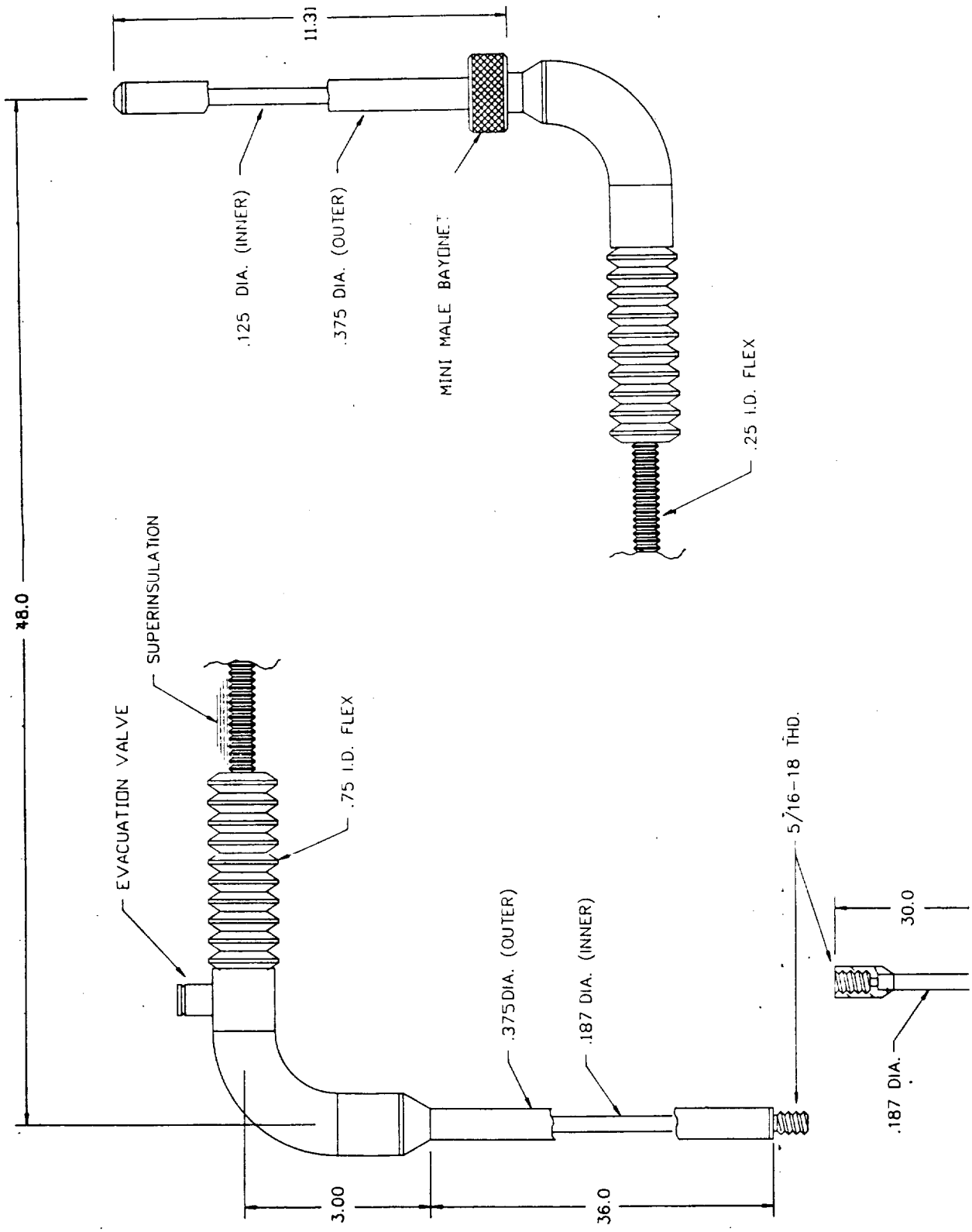

Figure 3.3. Liquid Helium Fill Line

domed metal welded to cylindrical side supports which are welded to their respective bases. The three penetrations into the helium bath provide access for power leads, helium filling, and diagnostics and persistent switch.

Several features of the design are directed toward allowing ±60° pitch of the magnetic axis without excessive loss of helium due to either pouring or increased heat loss to the vessel or feedthrus. In order to increase thermal tying of the coil to the 4° K thermal sink, the high thermal conductivity of aluminum is employed both in the fabrication of the inside shell of the dewar and by the addition of an additional shell bolted to the base which surrounds the coil. This arrangement helps to "pin" the temperature of the coil at 4° K even when the coil is not bathed in liquid. In this way, we will be able to operate the coil in the persistent mode with only enough liquid to wet the base of the inner dewar. To minimize thermal conduction through the coil input leads from the power lead stack, the leads will be guided away from the dewar wall and thermally connected to the base of the inner dewar before connection to the coil.

The three walled dewar assembly consists of two inner sections of 0.06" aluminum cylinders welded to the respective domes and bases and another section of stainless steel. The vacuum of both sections is common with the vacuum in both the power lead and helium fill ports. Each compartment is rigidly connected to the other by fiberglass cylinders attached to the grooved rings which join each dome to its respective cylinder. The space between the chambers is also filled with superinsulation to minimize radiation loss. The middle partition is thermally connected to the outer wall of the power lead port and should float near 100° K.

3.1.1.2 Magnet Power Connection. The power lead port is surrounded by single section vacuum dewar to minimize heat load into the helium bath from lead chamber which itself is cooled by venting helium gas. The inside wall is of stainless to minimize thermal conduction to the outside cap and is fitted with bellows to

accommodate linear thermal expansion. The bayonet shaped conductors at the top of the assembly connect to the superconducting coil input leads. Details of the leads are shown in Figure 3.4.

The power lead adapter involves an extension comprised of two 100 A copper leads surrounded by stainless steel shrouds to enhance vapor cooling. These are enclosed by insulating G-10 tubes. The current leads end in sleeves which engage the bayonets at the top of the port. The baffle adapter assembly uses offset copper plates to minimize convective heating up the port yet allow high throughput release during a quench.

3.1.1.3 Pressure Reliefs. In order to minimize liquid sloshing into the port, venting is from the top center of the helium vessel via tubes to the lead ports. The quench disc provides high throughput release in case of a magnet quench. The low pressure relief valve (~1 psi) prevents slow buildup of boiloff gas.

3.1.1.4 Helium Fill. The helium fill port is designed for fill flow up the port. This is accomplished by use of the PTL-202 LHe fill line shown in Figure 3.3, which is vacuum insulated, flexible and accommodates an upright liquid helium storage vessel. The bore of the port is insulated from the helium bath by a vacuum chamber the inside wall of which is of stainless to limit thermal conduction down the port. The bellows accommodates linear thermal expansion. The plugging assembly consists of an O-ring sealed cap to which is attached a stainless extension ending in a Kel-F cap. During fabrication, the procedure of soldering the Kel-F mount into the extension results in the creation a rough vacuum in this region. With the plug assembly in place, the Kel-F cap seals against the helium gas pressure. The volume between the cylinders filled with trapped helium gas is minimal and should reduce the extent of thermal oscillations.

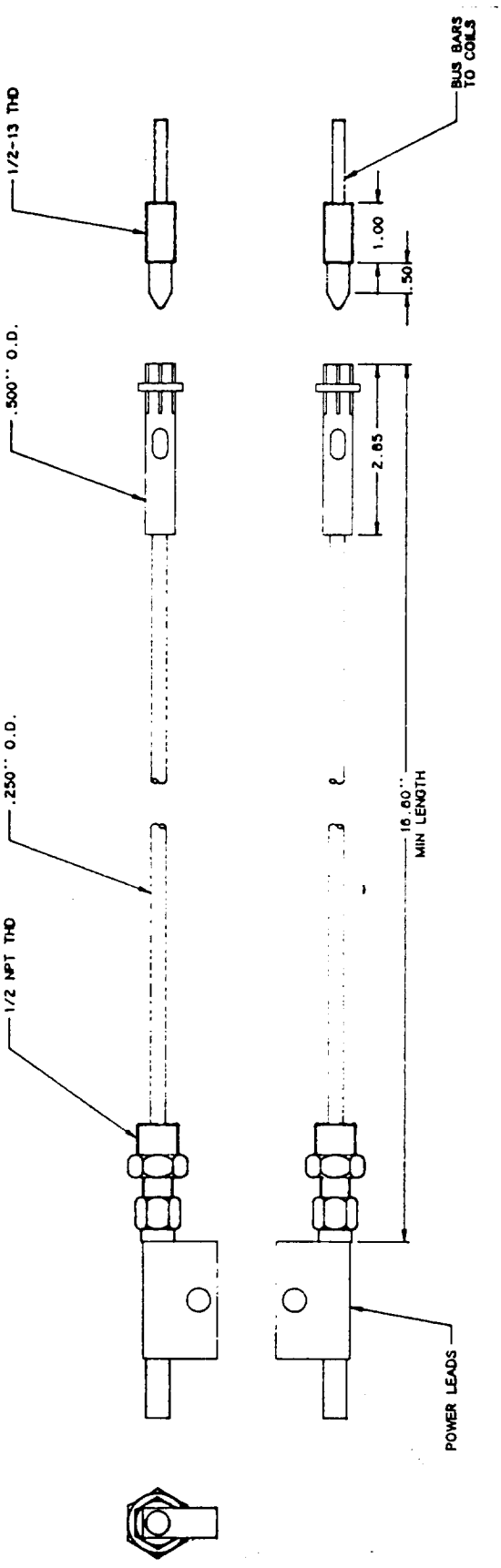

Figure 3.4. Details of Current Leads

3.1.1.5 Operating Procedure. A typical preparation for a suspension experiment proceeds in the following way:

1) The sphere is removed from its magnetic support assembly in order to access the bottom ports.

2) With the caps of both ports removed, the system is purged throughout with room temperature helium gas to eliminate the possibility of air and water vapor freezing at helium temperature.

3) Both the power lead and the helium fill assembly are connected.

4) Filling with liquid helium proceeds directly by pressure-forcing the liquid from its storage vessel in the usual way. It is estimated that the cool-down loss using this technique will be less than 2 liters. Alternatively, depending on its cost effectiveness, helium gas pre-cooled to liquid nitrogen temperature in a heat exchanger could be used to reduce liquid helium losses.

5) Once the liquid reaches the desired level as measure by the level sensor, charging of the coil with the power supply begins. The persistent switch is first energized to allow current changes. Ramp-up then proceeds at a rate consistent with inhibiting quenching and minimizing helium boiloff rates.

6) After charging to the desired field, the persistent switch is allowed to cool and the power supply is shut down, and the leads can be removed.

7) The baffle assembly is now fitted into the lead stack and the helium fill line is removed and replaced with the fill plug assembly.

3.1.1.6 Summary of Design. Table 3.1 is a summary of the features of the superconducting magnet and cryostat system.

Table 3.1. Features of Magnet and Cryostat System

Minimum spherical diameter size	15.500 inch
Estimated Combined Mass of Coil and Unfilled Dewar	48 lbs.
Capacity of Helium Container	7 liters
Coil Dimensions	
Inner Diameter	2.000 inches
Outer Diameter	5.400 inches
Length	3.000 inches
Total Coil Turns (two coaxial layers)	16,300
Design Magnetic Field at Center of Bore	8.2 Tesla
Maximum Current Density at Design Field	16 kA/cm^2
Stored Magnetic Energy	120 Joules
Quench Protection	Back-to-back Diodes, one for each of 3 coil sections
Diagnostics Sensor	Helium Level Cryothermometer
Power Supply:	
Capacity	100 A at 5 V
Ripple and Noise	< 100 mA p/p
Charge Rate	0-1 A/s

3.1.2 Superconductor Test Results

This section presents the results of tests conducted on the superconducting magnet system to verify the performance of the system. Tests were conducted to determine the superconducting characteristics of the magnet during persistent mode operation at

low currents and for run-up to full current. The magnetic fields produced by the superconducting magnet were measured and compared with theoretical predictions. The cryogenic capability and performance of the superconducting magnet system were also examined.

3.1.2.1 Mechanical and Electrical Inspection. Before power tests at low temperatures were attempted, a complete mechanical and electrical inspection, including testing of individual major components of the superconducting system, was undertaken.

Initial mechanical inspection of all the components of the superconducting magnet system was carried out to make sure the components were not defective or damaged during transit. For example, the dimensions of the cryostat, the fit of the spherical cover, and the diameter of the cryostat were measured for adherence to specifications. The positioning of sensor tabs, support tabs and lift tabs were checked for accuracy. The positioning, fit and assembly of power leads as well as helium fill ports were also examined.

The resistance across the leads of the source coil and the persistent switch was measured with a Fluke 75 multimeter to check for continuity. The operation of the power supply instrumentation was checked with a dummy load consisting of short-circuit leads. With the "dummy-load set-up" the power supply's current limit switches, charge rate, and voltage limit indicators could be checked for proper operation. The appropriate functioning of the temperature sensors and helium level sensors were also verified.

3.1.2.2 Cryogenic Capability Cooldown Tests. The dewar, operating in persistent mode and disconnected from the fill system, must be capable of maintaining the temperature of the source-coil at 4.2°K (liquid helium temperature) for times consistent with experimental runs (more than one hour).

The boil-off rate is the main limitation on the time the magnet can be in persistent mode. Additionally, excessive boil-off

of cryogens could freeze nearby vacuum container O-rings. Cooldown tests were conducted and boil-off rates monitored to verify the cryogenic capability of the dewar.

To bring the dewar to liquid helium temperatures, 4.2°K, it is first cooled down from room temperature (298°K) to 77°K using liquid nitrogen. Cooling the dewar first with relatively inexpensive liquid nitrogen ($0.27 per liter) minimizes the amount of helium used, which is relatively expensive ($6.50 per liter).

The dewar was filled with liquid nitrogen and the cooldown rate monitored. In practice, the fill rate was determined mainly by the set point of the storage vessel's relief valves and the size of the constriction in the fill line. Figure 3.6 of Section 3.1.2.4, shows a plot of temperature against time for the "liquid-nitrogen cooldown" of the superconducting magnet. The amount of time for the dewar to remain at liquid nitrogen temperatures was also noted. The dewar was then filled with liquid helium for gross loss rate determination at no power. The proper operation of the helium level detector and temperature probes were checked.

Before helium was introduced into the dewar, nitrogen had to be removed. It is important to remove completely all liquid nitrogen from the dewar because existing nitrogen would be frozen by the introduction of helium, with the risk of damage to the magnet. The subsequent steps were followed to effectively remove nitrogen and fill the dewar with liquid helium:

(i) Liquid nitrogen was blown out of the dewar with helium gas using lead cooling tubes until liquid ceased to spatter from the helium fill port. The overpressure on the tank was maintained between 2-4 psi.

(ii) The liquid helium transfer line was purged until it was cool enough to blow out liquid helium.

(iii) The dewar was then filled with liquid helium with the fill line up to 19.9 cm (level monitored by sensor).

During the filling of the dewar with liquid helium, the flow of helium was started at a slow, steady rate to make use of the cooling from helium vapor as it rose and escaped through the helium vent tubes. When the temperature dropped to around 10°K, the liquid helium transfer rate was increased until a 4°K temperature in the dewar was indicated by the temperature sensor. Figure 3.7 of Section 3.1.2.4, shows a plot of temperature against time for the "liquid helium cooldown."

3.1.2.3 Superconducting Magnet Characteristics. The maximum current achieved for the superconducting magnet before quench is 49 Amps. Tests were conducted for low currents (less than 10% of full field) and then from 50% full field current up to 100% field current (47.1 A). The magnetic fields were measured at the surface of the dewar, about 17 cm from the center of the magnet.

Figure 3.5 shows a diagram of the setup of the various components of the superconducting magnet system used for effective superconducting operation. As shown in Figure 4, the Integrated Cryogenics Incorporated current power supply model IPS-100 is connected to the current leads of the superconducting magnet. The dewar is securely placed on a sturdily built four-legged stand (not shown in Figure 3.5). The current and voltage limit switches and charge rate control assists in safe charging of the magnet.

The temperature and liquid helium level in the dewar are monitored by the Cryomagnetics model-70 temperature sensor and the Cryomagnetics model-12 helium level sensor respectively, which are connected to the dewar. The magnetic field of the superconducting magnet is measured with a (0.08 cm^2) Hall probe built and calibrated at SatCon.

If the procedure for operating the superconducting magnet is not carried out meticulously, quenching of the magnet could occur (at 47.1 A, 17 kJ is stored in the field). In addition to the risk of magnet damage, quenching could result in lethal voltages across the current leads of the superconducting magnet.

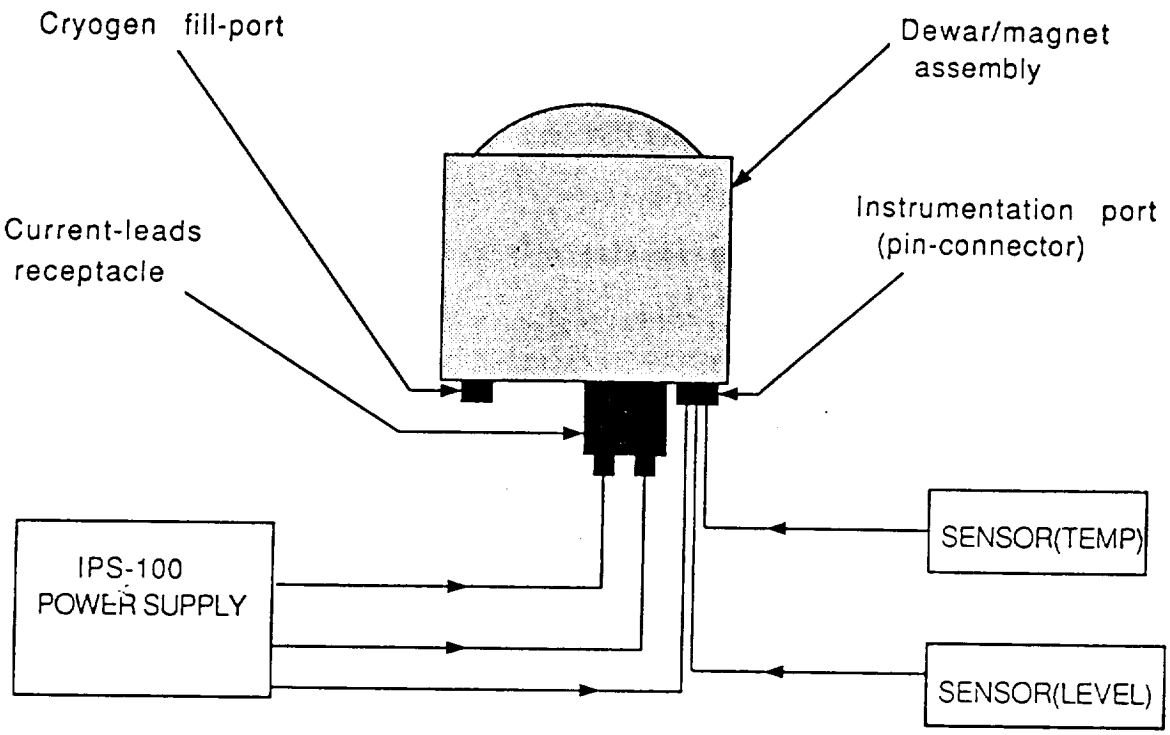

Figure 3.5. Superconducting Magnet System Component Setup

The superconducting assembly was set up as shown in Figure 3.5 after the dewar had been cooled to 4°K and filled with liquid helium. The magnet was charged as follows:

(i) The power leads and connections to the dewar were checked for fit and the instrument meters were read.

(ii) The amount of helium in the dewar was checked to make sure it was maintained at 19.9 cm.

(iii) The current limit, charge rate and voltage limit were set to the desired test values.

(iv) The persistent switch heater was then turned on, and the magnet charged by ramping the current to the set level.

(v) When the magnet voltage was zero (Ldi/dt ->0), the persistent switch was turned off. The switch cools down to superconducting within a few seconds and current can then circulate entirely in the dewar. The current supply could then be ramped down while the magnet remained in persistent mode. At this point, the current leads could be removed.

Discharging the magnet involved reconnecting the current leads, turning the persistent switch on, and ramping the current level down to zero.

For each current level test, the field produced by the magnet was measured using a Hall probe. The dewar temperature and the liquid helium loss rate were monitored. Results of these tests are presented in Section 3.1.2.4.

3.1.2.4 Test Results. Presented in this section are results of the testing done on the superconducting magnet system including the initial mechanical checks, electrical checks, and results of the superconducting characterization of the magnet system.

The components of the magnet system had been assembled appropriately and were in good working order. The outside diameter of the of the dewar was within 1.0% of the specified diameter of 13.125 inches. The height of the dewar is about 6% less than the specified height. The assembly, positioning and fit of the helium fill port and the power leads were adequate at room temperature. With the dewar filled with helium, however, accumulation of water ice on the power lead access nut made lead removal difficult, requiring the use of a heat gun for removal.

Operation of the power supply into a dummy load verified proper voltage and current limiting, ramping rates, and active quench detection and shutdown. The resistance between the leads across the superconducting magnet was about 9.2Ω at 298°K and became immeasurably low at 4°K with the persistent switch cold.

Shown in Figure 3.6 is a plot of the cooldown rate of the dewar when filled with liquid nitrogen. The dewar is originally at room temperature (298°K). It takes about one hour to reach liquid nitrogen temperatures of 77°K, as shown in Figure 3.6. After the dewar reached liquid nitrogen temperatures, it took approximately 30 minutes to completely fill with nitrogen. Once the dewar was filled with nitrogen, the time lapse before liquid nitrogen boiled off completely was approximately 66 hours. The liquid nitrogen boil-off rate was about 0.17 liters per hour corresponding to a heat input of 7 watts.

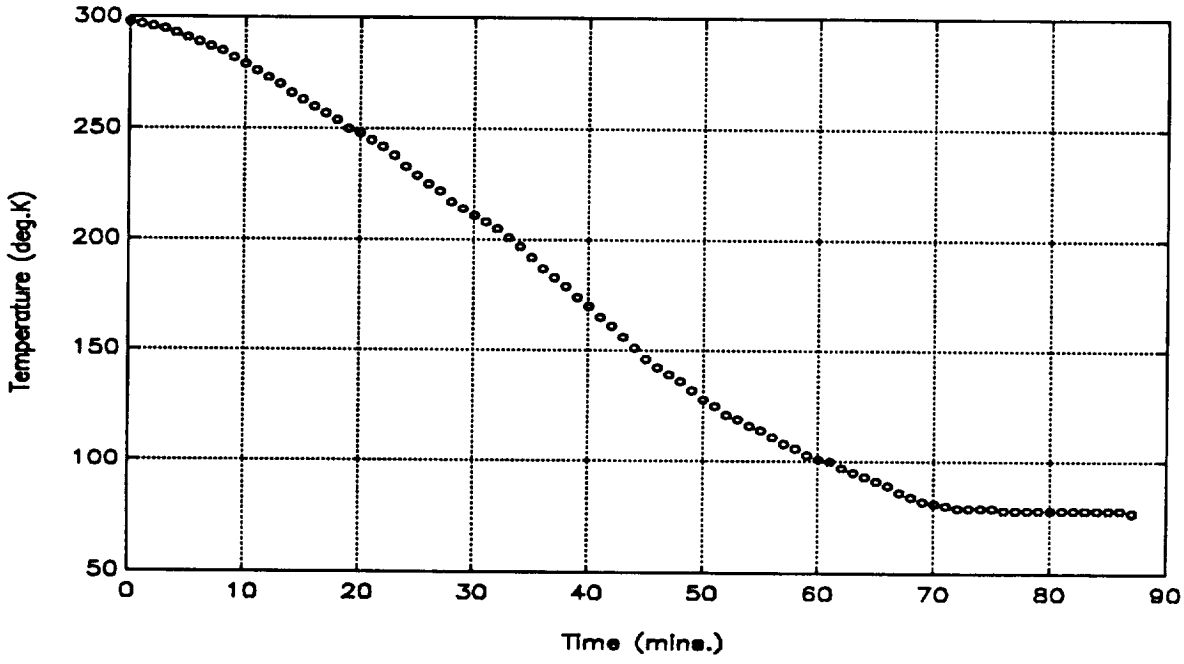

Figure 3.6. Liquid nitrogen cooldown of dewar from room temperature (298K).

Figure 3.7 shows the cooldown plot of the dewar when filled with liquid helium. The dewar was initially at 77°K before helium was introduced (after complete removal of liquid nitrogen had been done). The cooldown rate of the dewar during filling with helium is relatively high compared to liquid nitrogen, as shown in Figure

3.7. It takes about 12 minutes to reach 4°K from liquid nitrogen temperatures, and six more minutes to fill it to 19.9 cm.

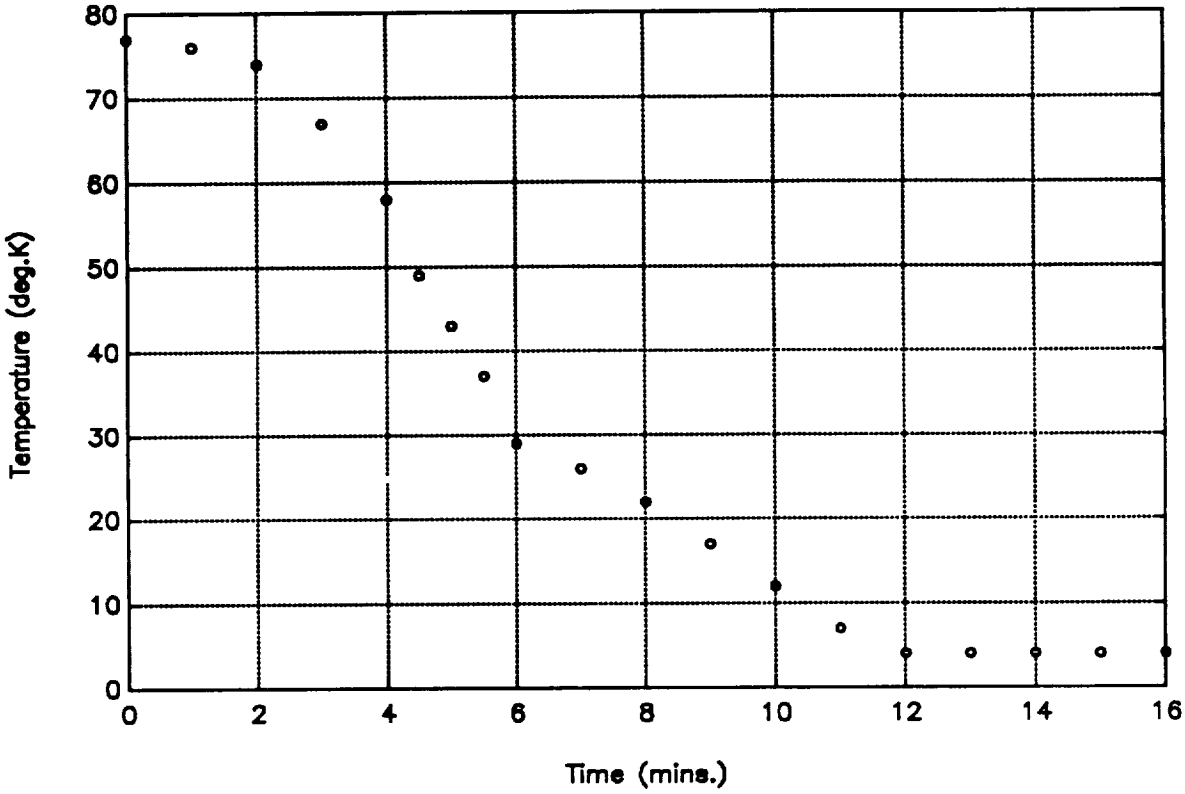

Figure 3.7. Cooldown of dewar from 77K to 4.2K using helium.

Shown in Figure 3.8 is the liquid helium filling curve. The dewar starts filling with liquid helium after about 12 minutes when it has cooled down to about 4.2°K. The fill rate of liquid helium is about 2.5 cm per minute. Figure 3.9 is a typical liquid helium loss curve, monitored during one of the tests when the magnet was in persistent mode.

In this particular case it took approximately 90 minutes for the helium level to reach 7.4 cm from a helium level of 19.9 cm. The best overall loss rate was about 0.1 cm per minute. If the dewar capacity is 11 liters and the readings are linear, this corresponds to a loss rate of 3.2 liters/hour or 2.4 watts.

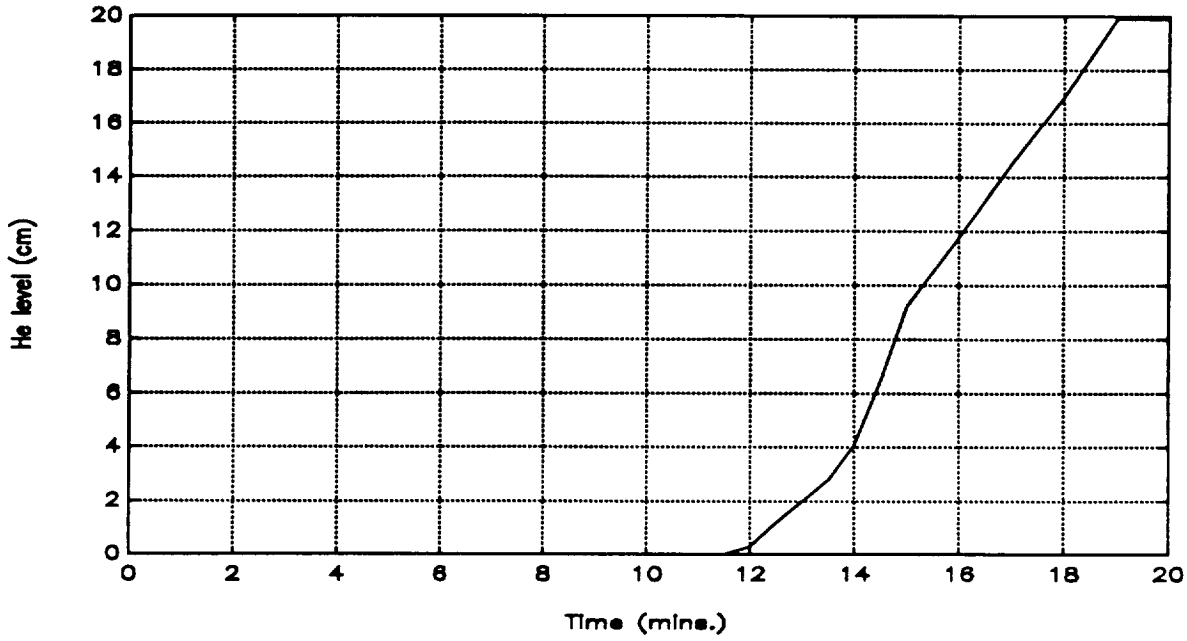

Figure 3.8. Liquid helium "fill-rate" of dewar.
Dewar starts filling with helium after it has been cooled to 4.2K.

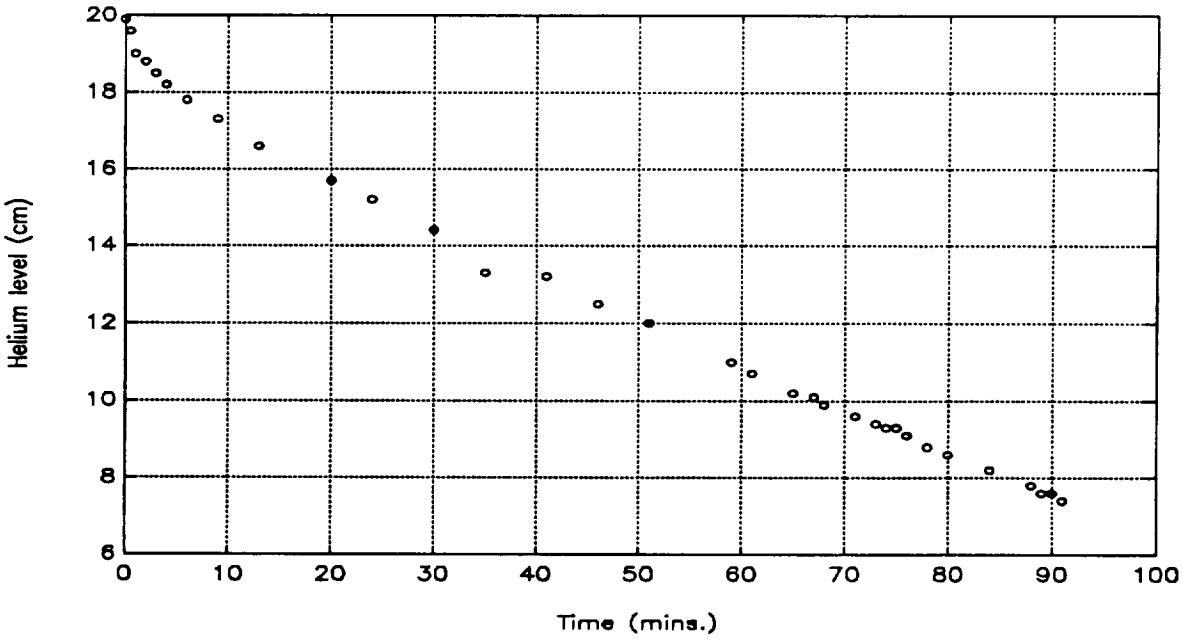

Figure 3.9. Liquid helium loss rate from dewar during persistent mode operation.

The magnetic fields produced by the magnet for low currents and full field current were measured and compared to predicted values from theoretical analysis. The position of the magnetic dipole was also determined.

For a typical low current of 5.0 A (about 10% of full field), the magnetic field on the dipole axis measured at the surface of the dewar (approximately 17 cm from the center of the magnet) was 249 gauss. For a full field current of 47.1 A, the field produced was 2600 gauss. The magnetic dipole was found to be rotated about 7 degrees from its nominal orientation along the sensor tabulations. Figure 3.10 shows a plot of the measured magnetic fields produced by the magnet from about 50% full field current to 100% full field current. The deviation of linearity between the field produced and the amount of current input to the magnet can be seen from Figure 3.10 to be slight.

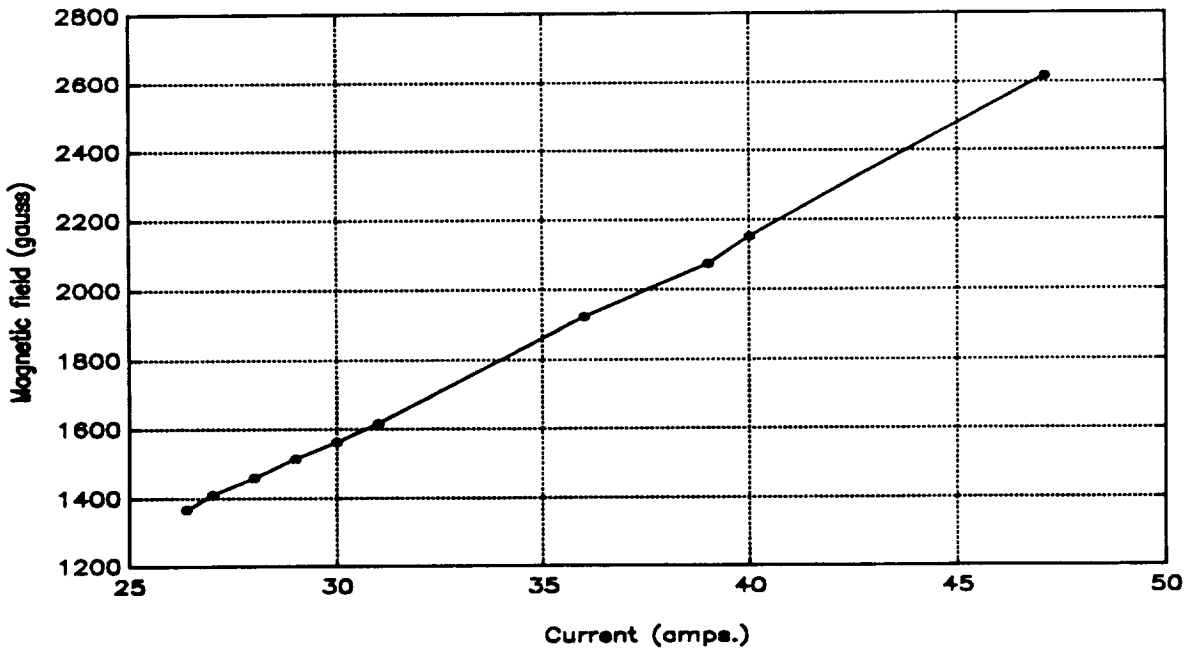

Figure 3.10. Plot of magnetic field produced by superconducting magnet against current input.

Shown in Figure 3.11 is the axial field profile from the center of the magnet from theoretical analysis for full field current. At the center, the predicted field is about 7.8 Tesla which is within 2.5% of the rated field (8.0 Tesla) at the center measured by Cryomagnetics, Incorporated. From Figure 3.11 the expected magnetic field at the surface of the dewar (17 cm from the center of the magnet) is 2500 gauss. This is within 4.5% of the field measured from real time operation of the superconducting magnet with full current (47.1 amps.)

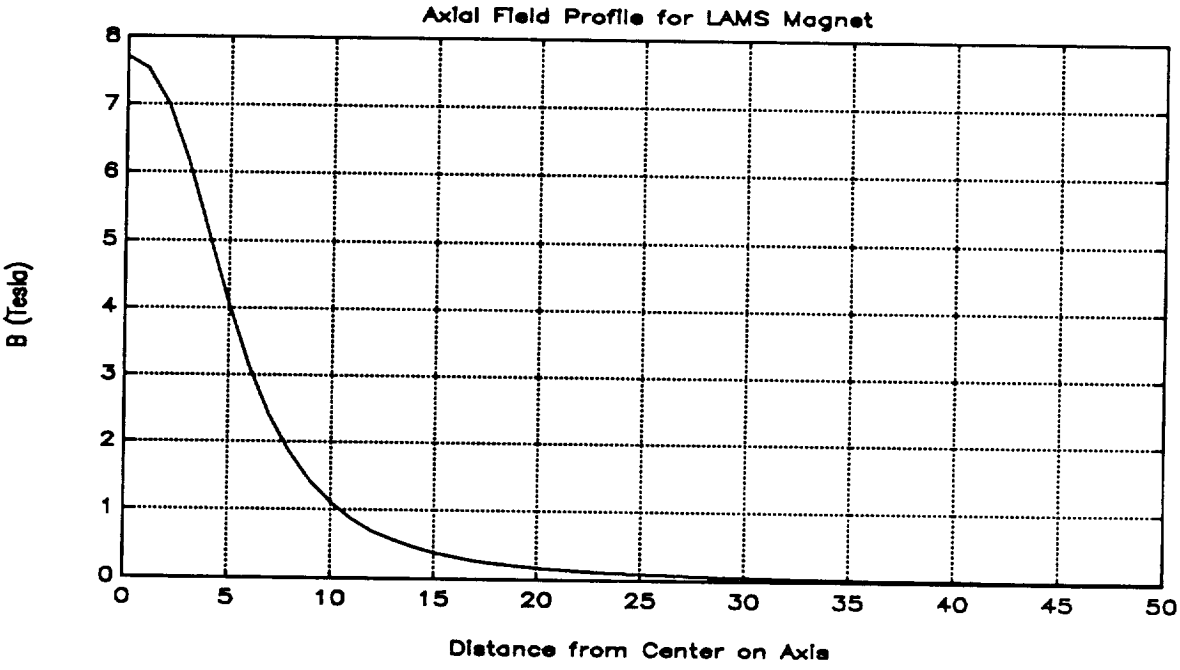

Figure 10. Theoretical simulation of axial field profile for the superconducting magnet. Distance on the x-axis is in centimeters.

3.1.3 Superconducting Magnet Summary

The superconducting magnet system is one of the major hardware subsystems for the LAMS project. The testing program was undertaken to verify compliance with specifications, to familiarize ourselves with the system operation, and to develop effective and safe techniques for handling the cryogenic liquids and the

charging/discharging of the magnet. The superconducting magnet and dewar were found to conform to or exceed design specifications. The sensor positioning tabs, support tabs and lift tabs were positioned on the dewar within 2.5%. The magnetic dipole position was rotated approximately 7 degrees from its nominal position along the sensor coil tab and within measurement error in other directions. This deviation is not detrimental to the overall operation of the LAMS.

The magnet supply and its associated instrumentation were found to operate adequately. The temperature and liquid helium level sensors and monitors gave consistent readings in their operating range.

It took about one hour to cool the dewar to liquid nitrogen temperatures (77°K) and about 30 minutes more to fill the dewar with nitrogen. The dewar can hold liquid nitrogen without replenishing up to about 65 hours. This suggests the technique of maintaining liquid nitrogen in the dewar for long periods between closely-spaced liquid helium runs.

The fill rate of liquid helium, once the dewar had cooled to 4.2°K (after 12 minutes), was about 2.5 cm per minute. The lowest boil-off rate was approximately 0.1 cm per minute (3.2 liters per hour), although the manufacturer suggests that optimum requires three or more refills, after which the loss rates will decrease substantially. In practice, the superconducting magnet should be able to operate in persistent mode for about one hour and forty minutes before refill with liquid helium is necessary. The liquid helium loss rate is much higher than is usual for a dewar of this size, probably due to the lack of a liquid nitrogen insulation jacket. The expected run time, while lower than hoped for, is adequate and within specifications, however.

A quench was experienced when the helium liquid level dropped to about 4.0 cm. From this experience, we do not expect to operate with helium level less than 5-6 cm.

The cryogen transfer line used, while otherwise suitable for transferring liquid helium to the dewar, was rather short for

connection to a dewar assembly 60 cm off the floor. The flexible length of the fill-line has been sent to Precision Cryogenics for modification at no charge.

The magnetic fields produced by the dipole increases proportionally with current. For a full field current of 47.1 A, the field produced at the center of the magnet was 80 kilogauss (8.0 Tesla). This was measured by Cryomagnetics Incorporated before assembly of the dewar/magnet component structure. The theoretical value of the field at the center of the magnet from simulation was within 2.5% of the measured value.

The magnetic field at the surface of the magnet 17 cm from the center of the magnet for full current field was 2600 gauss. This was within 4.5% of the theoretical value of 2500 gauss.

3.2 Control Coils

We determined the lightest control coil set that would allow the levitation of a 60 lb. spherical dewar of 8.5 inch radius, consistent with the equilibrium temperature inside the coils not exceeding 100°C for any orientation of the superconductor. The coils were then fabricated and evaluated.

3.2.1 Control Coil Design

This was done for both the 12 coil configuration, with the control coils arranged on the faces of a dodecahedron, and the 6 coil configuration with coils only on the 6 faces of the bottom half of a dodecahedron. For reasonable estimates of the thermal conductivity of the coils, levitation of the dewar is not possible with the 6 coil configuration for any size coils, without producing internal coil temperatures far in excess of 100°C, the temperature above which electrical insulation may start to break down. The six coil configuration would work only if the thermal conductivity of the coils were significantly increased, by using copper ribbon or carefully packed square cross-section wire, or by imbedding the wire in a medium of high thermal conductivity.) For the 12 coil configuration, levitation is possible; the optimal coil dimensions

are 4.5 inch inner diameter and 10.5 inch outer diameter for all control coils, with 2 inch length for the top and bottom coils and 1 inch length for the side coils.

3.2.1.1 Control Coil Requirements. The control coil current, power, and equilibrium temperature needed to support the dewar, for a given configuration, were found using a Matlab program written for this purpose, called CMG_MOD. The heart of this program is a routine which finds the mutual inductance between two circular filamentary coils at arbitrary distance and orientation, using Grover's expressions involving elliptic integrals. This routine was checked by comparing its result for a randomly chosen set of parameters with the mutual inductance calculated by the EFFI magnetics code developed at Lawrence Livermore National Laboratory, which does not use Grover's expressions but does the elliptic integrals numerically; the results were found to be in agreement to at least 4 significant figures. The mutual inductance between coils of finite cross-section is then found by summing over arrays of filamentary loops within the cross-section of each coil. The number of such loops needed to give a good approximation may be found by seeing how much the result changes when additional loops are added; we used enough loops to keep errors within a few percent. The mutual inductance between each control coil and the superconductor is then found for a series of slightly different orientations and positions of the superconductor, close to the desired equilibrium orientation and position. Taking the derivatives of the mutual inductances with respect to position and orientation of the superconductor gives us a matrix of the force and torque exerted on the superconductor by a given current in each control coil. By taking a Moore-Penrose pseudo-inverse of this matrix, we find the current in each of the control coils necessary to exert a given force and torque on the superconductor, viz. zero torque and an upward force equal to the 60 lb. weight of the dewar. Knowing the current in each coil, we can find the equilibrium surface temperature and internal temperature of each coil, using a

model for thermal conductivity and radiative and convective heat loss, for that orientation of the superconductor and that set of control coil dimensions. Looking at different superconductor orientations, the maximum internal temperature can be found for those control coil dimensions, and we can find the lightest set of control coils for which the internal temperature does not exceed 100°C. The pseudo-inverse of the matrix must be taken, rather than the inverse, because there are more coils than there are degrees of freedom of the superconductor, so there are many sets of control coil currents which will exert the desired force. The solution found by taking the pseudo-inverse is the one which minimizes the sum of the squares of the currents. For a set of pancake-like control coils with different lengths but the same inner and outer diameter, minimizing the sum of the squares of the currents also minimizes the difference between the average internal temperature and surface temperature of all the coils, and to fairly good approximation minimizes the maximum internal temperature of the hottest coil.)

3.2.1.2 Outer Diameter Optimization. The mutual inductance between a control coil and the superconductor is maximized (and the current and power needed to exert a given force or torque is minimized) when the outer diameter of the control coil is as large as it can be, and the distance from the center of the face of the control coil to the center of the superconductor is made as small as possible, subject to the constraint that the control coils cannot intersect each other. From the geometry of a dodecahedron, assuming all the control coils have the same outer diameter, the maximum outer diameter of a control coil is equal to 1.23 times the distance from the center of the dodecahedron to the center of the face of the coil. That distance is in turn fixed by the 8.5 inch radius of the dewar, and the requirement that there be a distance of 0.1 inches between the dewar and the coil to allow for motion of the dewar, and 1/16 inch for the thickness of the spindle on which the coil is wound. If the inner diameter of the coil were zero,

then the distance from the center of the dodecahedron to the center of the face of the coil would be 8.6625 inches. If the inner radius of the coil is finite, then the dewar can extend into the hole of the control coil a little, and the distance from the center of the dodecahedron to the center of the face of the coil can be slightly smaller. Given these constraints, and considering only coils with rectangular cross-section, there are only two parameters which may be varied for each control coil, the length and the inner diameter.

3.2.1.3 Inner Diameter Optimization. In order to determine the optimum inner diameter, we found the power required to levitate the dewar using six control coils, using several different values of the inner diameter and length (but with all coils having the same dimensions), keeping the orientation of the superconductor fixed at an angle of 30 degrees from vertical. At this orientation almost all of the power is in the bottom coil, and we expect the dependence of power on inner diameter to be the same for other orientations. The inner diameters used were 2.0, 4.5, 6.0, 7.0, and 8.0 inches, and the lengths were varied from 0.8 to 6 inches. The coils were assumed to be made of copper with a fill factor of 0.71, and the power was evaluated using the resistivity of copper at room temperature, 300°K. If the distance from the faces of the coils to the center of the dodecahedron was kept fixed at 8.56 inches, rather than allowing the dewar to further extend into the holes of the coils when the inner diameter was larger, we found that the power was minimized for a given coil weight when the inner diameter was 4.5 inches. It was almost as low, only a few percent higher, when the inner diameter was 2 inches, and was about 10% higher when the inner diameter was 6 inches. This was true over a range of coil weights from 16 to 32 pounds, so we presume it would be true also if the coils were not all the same weight, and if there were 12 coils rather than 6 coils. When the distance from the faces of the coils to the center of the dodecahedron was allowed to decrease at larger inner diameters, so that the surface

of the dewar remained at the same distance from the inner edge of the face of each coil, we found that the power was minimized when the inner diameter was 7 inches, for 20 lb coils (2 inches long), and at somewhat greater inner diameter for lighter coils and smaller inner diameter for heavier coils. In all cases, however, the power was rather insensitive to inner diameter; for the 20 lb. coils, decreasing the inner diameter to 4.5 inches or increasing it to 8 inches only resulted in an increase in power of 7%. An inner diameter of either 4.5 inches or 8 inches, for a fixed volume and outer diameter (about 10.5 inches in all these cases), results in a greater surface area, and should result in a lower internal temperature even though the power generated is slightly greater. Further changes in inner diameter will not result in much more increase in surface area. We conclude that, for coils in the general weight range of 15 to 30 lbs, the internal temperature is fairly close to a local minimum for a given coil weight when the inner diameter is 4.5 inches or 8 inches, with the absolute minimum probably being at 4.5 inches. We assumed an inner diameter of 4.5 inches and an outer diameter of 10.5 inches in all further studies.

3.2.1.4 Thermal Modelling. To determine the internal temperature expected for a given power dissipated in a control coil, we used an approximate formula relating the difference between surface temperature T_s and maximum internal temperature T_{max} to the thermal conductivity κ, the power P, and the coil dimensions:

$$T_{max} - T_s = 0.5\ P\kappa^{-1}[L^{-2} + (r_o - r_i)^{-2}]^{-1/2}$$

where L is the length, r_i is the inner radius and r_o is the outer radius. Since the thermal conductivity of copper is orders of magnitude greater than that of typical insulating materials and air, the thermal conductivity of the coil will be equal to the effective conductivity of the insulation and air between the copper, multiplied by a numerical factor depending on the fraction of the volume taken up by the copper and on the cross-sectional

shape of the copper wires. For circular cross-section copper wires with a fill factor of 0.71, as we have been assuming, this numerical factor is about 5. Whether the effective thermal conductivity of the insulation and the air is closer to the thermal conductivity of air or of insulation depends on such considerations as the surface area over which two wires make contact when they are pressed together, which is difficult to determine from first principles. However, the uncertainty is not too great because the thermal conductivity of typical insulation materials, which is generally within a factor of 2 of 0.005 W/in°K, is only about 6 times the thermal conductivity of air. Furthermore, if the temperature gradient in the coil is about 100°K/in and adjacent wires are more than 1/200 inch apart, as they surely will be, then the radiation transport between adjacent wires will be greater than the conductivity through air, which will effectively be like a vacuum as far as its thermal properties are concerned. An appropriately conservative estimate of the effective thermal conductivity of the insulation and the air would therefore be about 0.002 W/in°K, and the overall thermal conductivity of the coil, including the copper, would be about 0.01 W/in°K. The thermal conductivity might be as much as a factor of 2 greater than this, depending on the insulation material and on the spacing and amount of contact between adjacent wires, but it could hardly be much less than this. Even if the insulation and air were replaced by vacuum the thermal conductivity would be at least this great if the average distance between adjacent wires were greater than 0.01 inches.

The surface temperature of the coils depends on the radiative and convective heat flux. Because most of the power dissipation is typically concentrated in only one or two coils, the surface temperature of the hottest coils can be reduced if the surfaces of all of the coils are well coupled thermally to each other, as well as to the support structure or any other surface area that can be used to lose heat. We therefore assume in the analysis that all of the coils have the same surface temperature, and that the power

generated by all of the coils is evenly distributed over the total surface area of all the coils. In fact, some surfaces of the coils cannot lose heat as effectively as other surfaces, for example the surfaces facing the dewar and the surfaces facing the holes will have some of their radiation reflected back to them, and the undersides of coils will not lose heat by convection as well as the vertical and upper surfaces. As a preliminary model, we assume that these effects are compensated by the presence of additional surface area in the support structure which is thermally coupled to the coils, and that the total heat flux is equal to the convective heat flux from a vertical surface in still air, plus the blackbody radiative heat flux, over the surface area of all the coils. At a temperature T, the blackbody heat flux per degree is $4\sigma T^3$, where σ is the Stefan-Boltzmann constant. This is 5.5 $W/m^2°K$ at 300°K. The convective heat flux per degree from a vertical surface in still air is 6.1 $W/m^2°K$ at 300°K. At 350°K, the highest surface temperature that is plausible if the interior temperature is to be less than 100°C, the radiative heat flux rises to 8.8 $W/m^2°K$ and the convective heat flux to 6.6 $W/m^2°K$. Because there are so many other uncertainties in the heat flux, and in order to avoid the complications of self-consistently finding the heat flux and surface temperature, we simply use the value at 300°K, a total of 11.6 $W/m^2°K$. Other factors which can affect the heat flux are the possibility that the surfaces are not perfect blackbodies in the infrared, which will reduce the heat flux, and the possibility that a fan could be used to cool the coils, which will increase the heat flux.

3.2.1.5 Power Dissipation. To the extent that the internal temperature of the coils is greater than 300°K, the resistivity of copper, and hence the power dissipated, will be increased. A completely self-consistent calculation of the internal temperature and resistivity is difficult, because the surface temperature of a coil depends not just on the power dissipated in that coil, but, according to our assumption of good thermal coupling between coils,

on the power dissipated in all the coils, and can only be done iteratively. However, as noted previously, our model for the surface temperature has many uncertainties in it already, and self-consistently including the temperature dependence of the resistivity will not improve the accuracy of our surface temperature calculation very much. Therefore, we fix the surface temperature at the value we calculate using the room temperature resistivity of copper, and then self-consistently find the temperature difference between the interior and surface of each coil, including the temperature dependence of the resistivity. Using the relative increase in resistivity of copper, .0039/°K at 300°K, and assuming this linear rate of increase at all temperatures, and evaluating the resistivity at the average temperature inside the coil, which is assumed to be halfway between the surface temperature and the maximum interior temperature, we find that the self-consistent power dissipated in a coil is

$$P = P_0[1 + .0039(T_s-300)]/[1-.0039(T_{max} - T_s)]$$

where P_0, T_s, and T_{max} are the power, surface temperature and maximum interior temperature that were calculated using the room temperature resistivity of copper.

3.2.1.6 Final Control Coil Design. The maximum interior temperature was calculated for each coil, for various orientations of the superconductor, and various lengths of the control coils, for both the 6 coil and 12 coil configurations. It soon became clear that there was no set of coil dimensions that would allow the dewar to be levitated using only 6 coils, and keep the maximum interior temperature below 100°C, at least not for the thermal conductivity assumed. As an example, we calculated the maximum temperature for the six coil configuration making the optimistic assumption that the weight of the dewar could be reduced to 50 lbs., and used a 3 inch length for the bottom coil and 2 inch length for the side coils; these coils weigh respectively 33 lbs.

and 50 lbs. We also assumed that additional surface for cooling could be put in the place of the missing upper coils, so that the total surface area was equal to twice the surface area of the six coils. For the axis of the superconductor pointing vertically, which is the orientation that produces the greatest interior temperature, the maximum interior temperature in the bottom coil was found to be 232°C. Cooling the coils with a fan or by increasing the surface area would not change this result very much, since the surface temperature calculated was only 49°C. For the same reason, this high interior temperature does not depend very much on the uncertainties in modelling the heat flux from the surface. For this orientation almost all of the power is in the bottom coil (489W out of a total of 648W), so increasing the length of the side coils would not help much. Increasing the length of the bottom coil would also not decrease the power dissipated in it, since the additional current would be more than 3 inches further away from the superconductor than the face of the coil, and would contribute very little to the force on the superconductor. Only if the thermal conductivity of the coil were increased by a factor of 3.6, to 0.036 W/in°K, would the interior temperature fall to 100°C. This would be possible only if the space between the copper of the coils were solidly filled with an electrical insulator of rather good thermal conductivity, or if the fill factor of the coils were substantially increased by using copper ribbon, or carefully packed square cross-section wire. If the dewar weighed 60 lbs., then an even higher thermal conductivity would be needed to keep the interior temperature below 100°C. The greatest interior temperature of the side coils occurs when the superconductor axis is horizontal, pointing directly above the center of one of the side coils. The maximum temperature is then 185°C for the 50 lb. dewar, and even greater for the 60 lb. dewar. Even for this temperature, the side coils must weigh 33 lbs. each, which is a challenge mechanically. For these reasons we have concentrated on the twelve coil design.

With twelve coils we calculated the interior temperatures for several different orientations of the superconductor, for two sets of coil lengths: 1) 0.7 inch side coils with 1.5 inch top and bottom coils; and 2) 1 inch side coils with 2 inch top and bottom coils. The ratio of about 2 to 1 for the top and bottom coil length compared to the side coil length, was chosen because this results in the maximum interior temperature in the side coils being about equal to the maximum interior temperature in the top and bottom coils. The following table shows the maximum interior temperatures and power dissipated for the bottom (or top) coil and the hottest side coil, as well as the total power dissipated and the surface temperature, for various orientations of the superconductor. The azimuth of the superconductor axis is measured from the center of the nearest side coil, and the elevation is the angle above horizontal. To save computer time the results in the table were calculated using only one filamentary loop to represent each control coil; the correct results, using a sufficient number of loops, are about 10% higher in temperature and power. For the first case, 0.7 inch long side coils each weighing 11 lbs., and 1.5 inch long top and bottom coils each weighing 24 lbs., we find the results given in Table 3.2

Table 3.2. First Case Design

Azimuth	Elevation	Total power	T_s	Bottom coil Power	Bottom coil T_{max}	Max. side coil Power	Max. side coil T_{max}
0° or 36°	0°	1069W	79°C	0W	79°C	221W	122°C
18°	0°	1069W	79°C	0W	79°C	198W	118°C
0°	30°	878W	71°C	67W	92°C	269W	123°C
18°	30°	871W	71°C	66W	91°C	235W	117°C
36°	30°	863W	71°C	65W	91°C	157W	101°C
18°	45°	725W	64°C	122W	103°C	172W	98°C
18°	60°	622W	59°C	165W	112°C	95W	77°C
--	90°	560W	56°C	184W	114°C	19W	60°C

For the second case, 1 inch long side coils each weighing 7.3 kg, and 2 inch long top and bottom coils each weighing 14.6 kg, we find the results given in Table 3.3.

Table 3.3. Final Design

Azimuth	Elevation	Total power	T_s	Bottom coil Power	Bottom coil T_{max}	Max. side coil Power	Max. side coil T_{max}
0°	0°	793W	64°C	0W	64°C	102W	106°C
0°	30°	685W	59°C	53W	78°C	213W	113°C
18°	30°	678W	59°C	52W	78°C	186W	106°C
18°	60°	517W	52°C	139W	101°C	79W	[illegible]
--	90°	474W	50°C	155W	105°C	16W	[illegible]

Although it is possible that, with a little better cooling and higher thermal conductivity, the maximum temperature reached in the first case would be under 100°C, we have adopted the second case as a more conservative design, especially considering that the weights of the coils are quite reasonable. Note, however, that the increase in coil weight only reduces the maximum temperature by 10°C; the reason for this weak dependence of temperature on coil weight is that extra coil volume can only be added to the far face of the coil, away from the dewar, or inside the hole, where it does not do much good. Increasing the coil length to 3 inches hardly reduces the maximum temperature any further, so there is no point in being more conservative by using even longer coils. Even with the coil dimensions used in the second case, the maximum temperature from our model is 125°C, if we take into account the error introduced in the results given in the table by using only a single filamentary loop to represent each control coil. However, it is likely that the cooling and thermal conductivity will be a somewhat greater than we conservatively assumed in the model, and that the temperature will not exceed 100°C.

Because the predictions of interior temperature are somewhat uncertain, and the temperature cannot be reduced much by using

larger coils, it is important that the interior temperature be monitored during operation, perhaps by monitoring the coil resistance, and that the coils be designed to withstand temperatures somewhat in excess of 100°C, rather than relying on the predictions of the model to ensure that the coils do not burn out. In the worst case, if the maximum equilibrium interior temperature turns out to be well above 100°C, and too high for the coils to tolerate, then the only consequence will be that the coils cannot be operated indefinitely, but must be turned off before the equilibrium temperature is reached. The time required to reach equilibrium for these coils, which can be calculated using the specific heat of copper and ignoring the heat capacity of the insulation, is about 45 minutes, so the worst that could happen would be that the coils would have to be turned off after about half an hour and allowed to cool down. It is important to note that our results depend on the coils being thermally coupled to each other, and to the support structure. This should not be hard to do, but if it is not done then the surface of the hottest coil, and its interior, will be much hotter than we have calculated.

The effect of the power generated by the coils on helium loss from the dewar may be calculated by assuming, in the worst case, that the surface temperature of the dewar is equal to the surface temperature of the coils, which is 64°C in the worst case listed in the table, for the larger set of coils. Since this in only a factor of 1.13, in absolute temperature, above the temperature (room temperature) that the surface of the dewar would be if there were no power dissipated in the coils, the power absorbed by the dewar (and the helium loss rate) would be increased by only $(1.13)^4 = 1.64$ if the dewar absorbs a fixed fraction of the radiation that falls on its surface.

3.2.2 Control Coil Fabrication

This section describes the construction of the control coils. As described above, there are two distinct control coil types used in LAMS. These will be referred to as top/bottom coils and side

coils. The top/bottom coils are nominally located on the top and bottom faces of the dodecahedron while the side coils are located on all of the other faces. The dimensions of the coils are given in Table 3.4.

Table 3.4. Control Coil Dimensions

Dimension	Top/Bottom Coils	Side Coils
Inner Diameter	4.500 inches	4.500 inches
Outer Diameter	10.500 inches	10.500 inches
Axial Length	2.000 inches	1.000 inches

3.2.2.1 Bobbin Design. The control coils are wound on CE-type phenolic bobbins. The bobbins are made up of three separate pieces, two end plates and a winding mandrel. The detail drawings of the bobbins are given in Figures 3.12 and 3.13. Each bobbin drawing is a tabulated drawing to differentiate between top/bottom and side coils.

The two drawings differ in that the one shown in Figure 3.12 (SatCon Drawing No. 1016413) contains a slot across the diameter of the mandrel. This slot accommodates the mounting bracket for the capacitive position transducers used in the sensor system. The coils on the faces of the lower dodecahedron half have the sensor-mount slots.

3.2.2.2 Coil Turns. The number of turns in the two coils was determined in conjunction with the selection of the power amplifiers. Turns selection was a compromise between reducing the steady current required to support the weight of the source coil and dewar (large number of turns) and reducing the peak voltage required during transients (small number of turns). Table 3.5 contains the final turns selections.

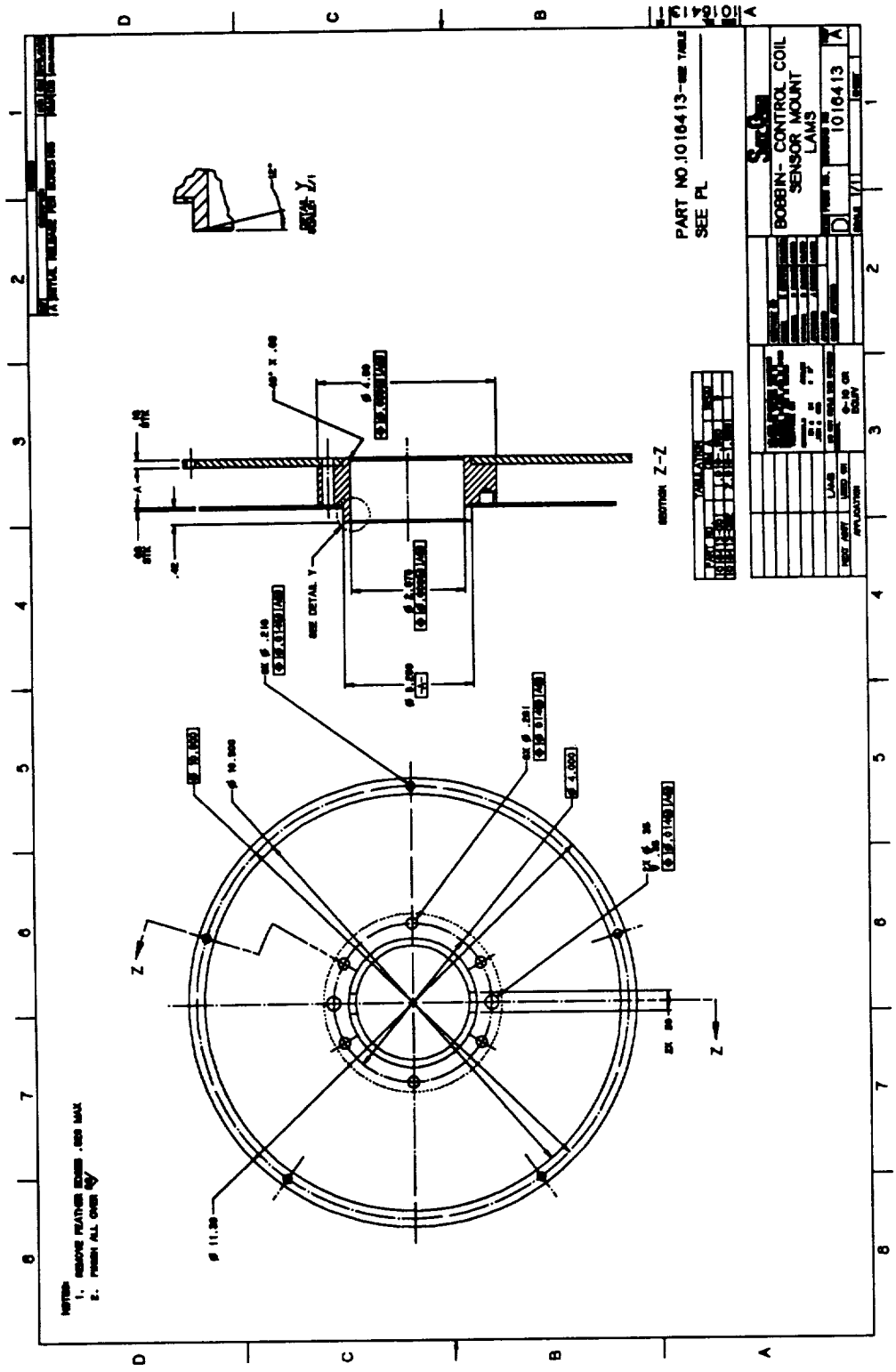

Figure 3.12. Control Coil Bobbin (Sensor Mount)

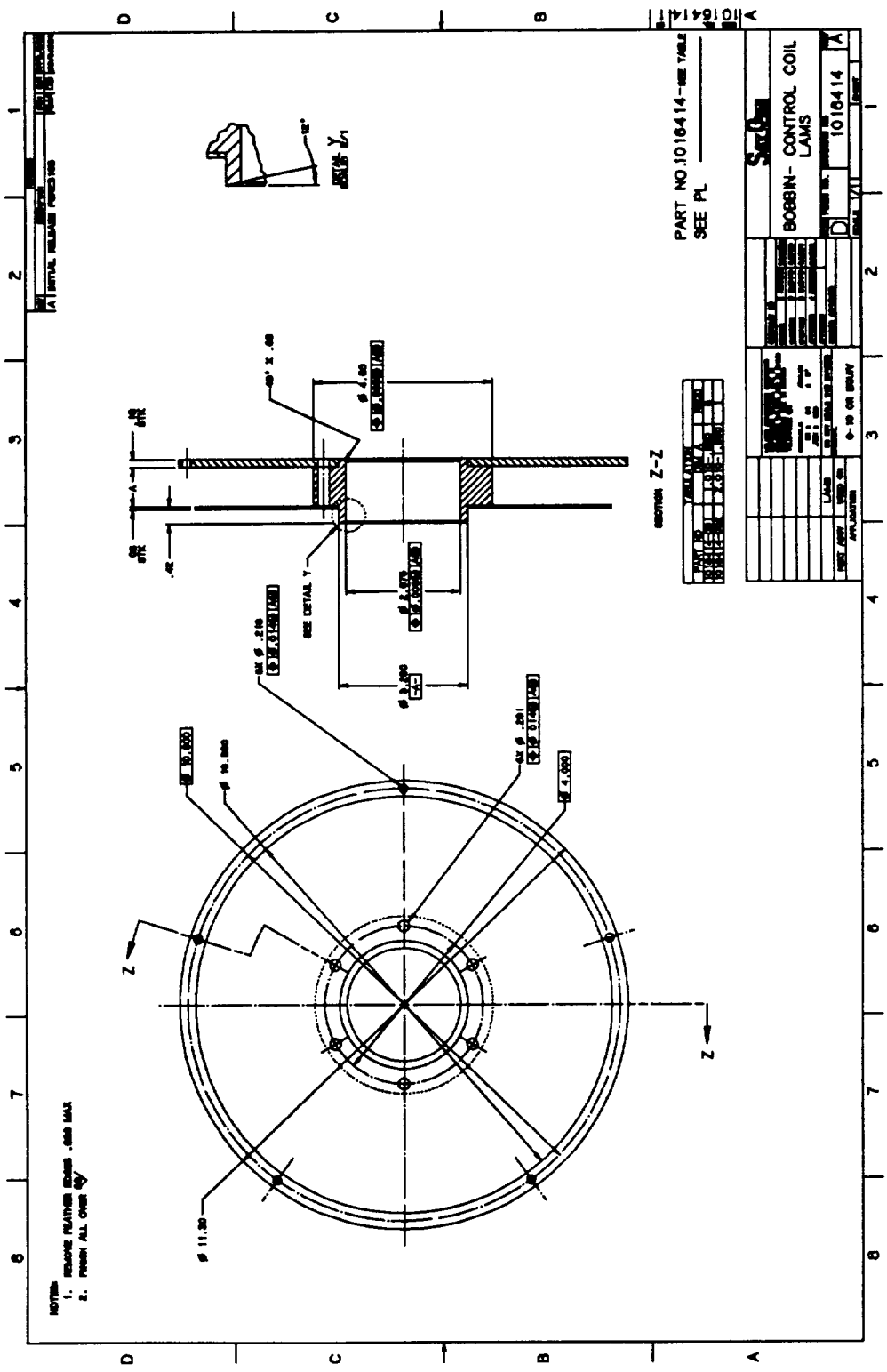

Figure 3.13. Control Coil Bobbin (Non-sensor Mount)

Table 3.5. Control Coil Turns and Wire Size

	Top/Side Coils	Bottom Coils
Number of Turns	730	700
Wire Size (AWG)	12	15

3.2.2.3 Coil Construction. The actual process of preparing the bobbins and winding the coils onto them is documented in the assembly drawings shown in Figures 3.14 and 3.15. As with Figures 3.12 and 3.13, these drawings differ only in the slot which accommodates the sensor mounting brackets.

Before winding, the thicker coil end plate is drilled and counter bored to accommodate fasteners for a barrier strip and to provide wire exit points. The attachment of the barrier strip is detailed in a sketch near the release block at the upper right-hand side of the drawing. The end plates were bonded to the mandrel with epoxy prior to delivery to the winder.

The tabulation block specifies wire size, insulation class, and preferred layout of the turns to the winder. The insulation is rated for a temperature of 220 °C. Heavy (double coating) ML (HML) film insulation is extremely tough and resistant to abrading. The direction of winding from the Start lead (inner diameter) to the Finish lead (outer diameter) is specified in Notes 6 and 7. Note 4 specifies the application and curing processes for the baking varnish which is used to encapsulate the windings.

3.2.2.4 Coil Fabrication. The bobbins were fabricated by a local machine shop (Loyal Machining of Chelsea, MA and returned to SatCon for modification and assembly. The modified bobbins were then delivered to the winder, ACR Electronics of Lynn, MA.

An initial shipment of five coils (both of the top/bottom coils and three side coils was received on August 17, 1990. They were returned to ACR on because of faulty encapsulation. The cure cycle of the baking varnish calls for the coil to be heated for 2.5 hours after it has achieved the desired temperature. The winder

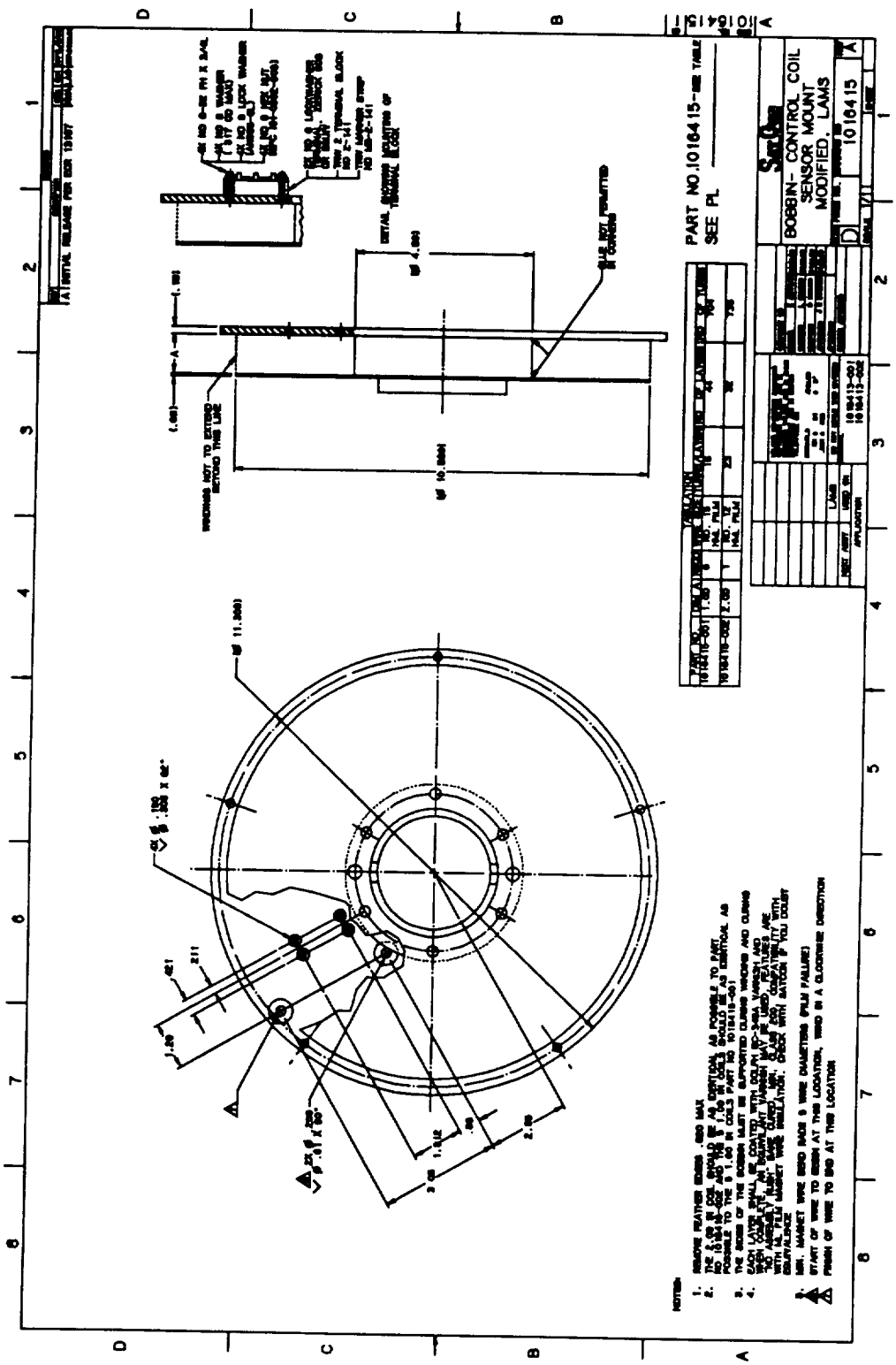

Figure 3.14. Control Coil (Sensor Mount)

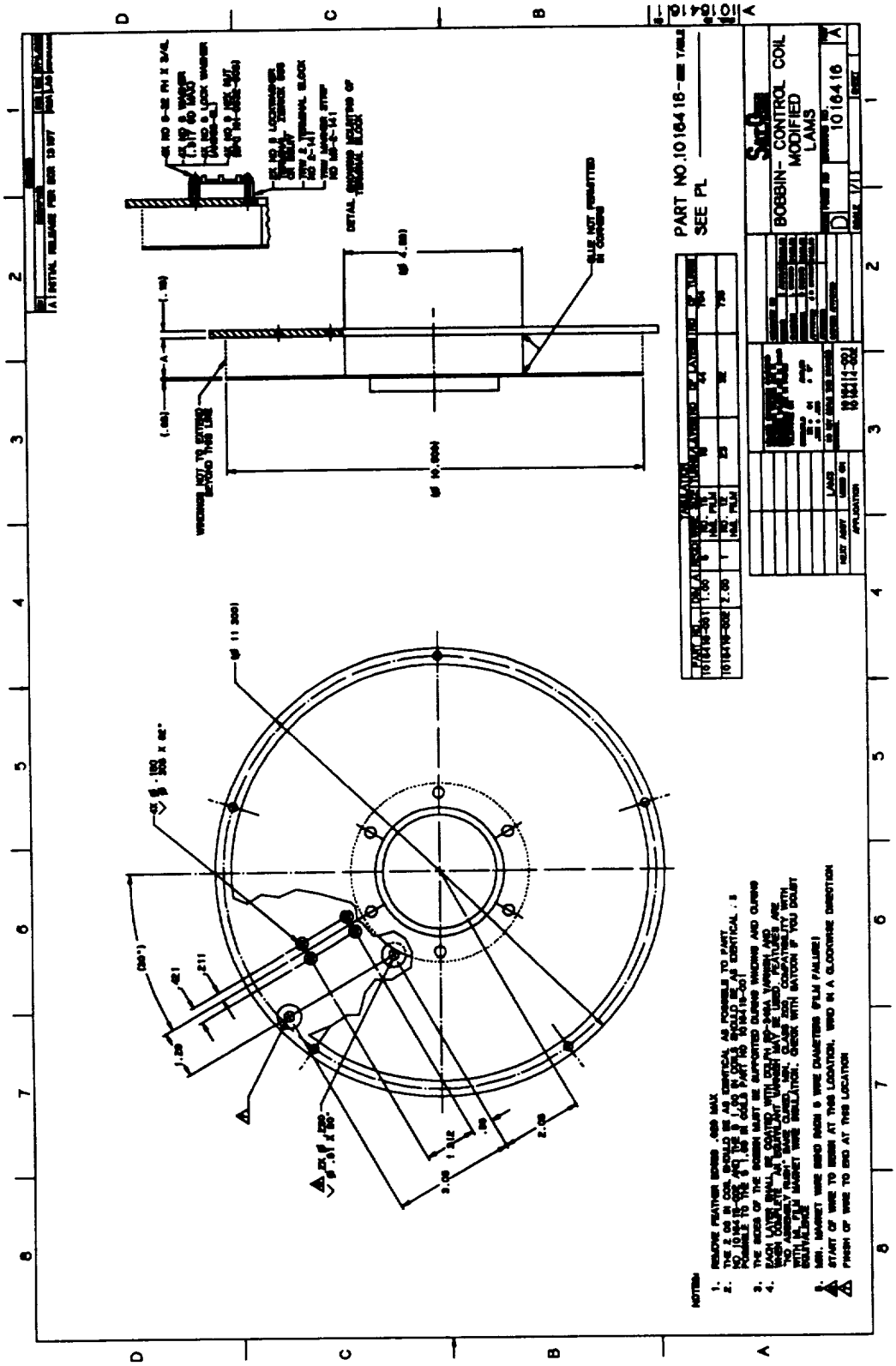

Figure 3.15. Control Coils (Non-sensor Mount)

apparently underestimated the time required for the coil to reach final temperature and the winding did not adequately cure. ACR corrected the faulty curing and returned the two coils.

3.2.3 Control Coil Testing

Presented in this section are results of tests conducted on the control to determine if the coils had been manufactured within design specifications; from theoretical analysis conducted at Satcon. The transient response and steady state thermal characteristics of the coils were also of particular interest. From the thermal characterization of the coils the limits to which the coil could be effectively used could be deduced. It was also important to ensure electrical/dynamic performance consistency among the different types of coils.

3.2.3.1 Initial Mechanical Checks. Prior to any electrical characterization, each of the control coils was uniquely identified and basic structural integrity was verified. Adherence to dimensional tolerances was also verified.

Sequence numbers were assigned to each coil for easy identification as described in Table 3.6. These are consistent with numbering schemes presented in the control design chapter.

Table 3.6. Control-coil Sequence Numbering

Sequence No.	Part Number	Description
1	1016415-002	2.0" thick, with slot
2-6	1016415-001	1.0" thick, with slot
7	1016416-002	2.0" thick, no slot
8-12	1016416-001	1.0" thick, no slot

The main difference between control coils with sequence numbers one (Coil-1) and seven (Coil-7) is that Coil-7 has a slot and Coil-1 has no slot. The electrical, dynamic and thermal characteristics of both these two-inch coils are expected to be the

same. Similarly, coils with sequence numbers 2 to 6, only differ primarily from coils with sequence numbers 8 to 12, by the presence of slots. Their dynamic characteristics, however, are expected to be identical. The presence of slots for some of the control-coils is to aid mechanical fastening.

The control-coils were inspected to ensure that they had been adequately assembled within specifications. The following checks where done :

1) The bobbins were inspected for possible failure of the epoxy glue joints.

2) The winding thickness of the coils (Dimension "-A-") were checked. This measurement was done at the outer periphery of the winding area to assure that the bobbin sides were well supported during the winding process.

3) It was verified that the coils were wound in the same direction (clockwise). If the winding direction was clockwise, then the barrier strips of the Start leads were marked positive and the Finish leads negative. If the direction was reversed, the Finish lead was marked positive and the start lead negative.

Shown in Table 3.7 of Section 3.2.3.4, are the results of the mechanical checks done on the control-coils.

3.2.3.2 Preliminary Electrical Characterization. The second step in the testing process was to determine the lumped electric circuit parameters which characterize the coils. Following initial checks that all of the coils had continuity between the Start and Finish leads, the nominal resistance, inductance, and frequency-dependant impedance were measured.

Continuity between the start and finish leads for all twelve coils were checked. Measurements were made of the nominal resis-

tances of each coil to ascertain consistency and to note any discrepancy. For each coil, the resistance was measured using a Fluke 8050A Digital Multimeter. The temperature at which the measurement was made was also recorded. Table 3.8 of Section 3.2.3.4 shows the results of the continuity and nominal resistance measurements.

The inductance of each of the coils were measured using a GenRad 1657 RLC Digital Bridge. For each coil, measurements were made at the low- (100 Hz) and high-frequency (1,000 Hz) settings of the bridge. Results of the inductance measurements of the coils are shown in Table 3.9 of Section 3.2.3.4.

Simulations of the impedance characteristics of the two types of coils (1" thick coil and 2" thick coil) are presented in Figures 3.21 and 3.22 of Section 3.2.3.4. Results of the impedance characteristics from simulation, was based on experimental resistance and inductance values of the coils. The break frequencies of the control-coils were deduced from their impedance characteristic. Real-time coil impedance behavior of the control coils were also determined experimentally. Figure 3.16 shows the experimental setup used for determining the magnitude and phase of the impedance of the coils.

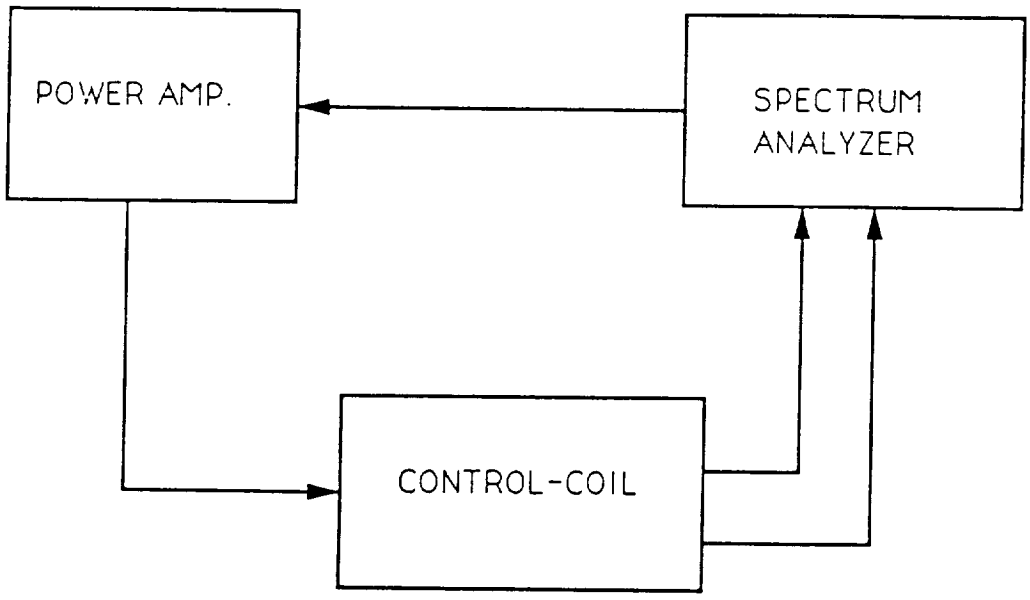

Figure 3.16. Experimental setup. (Impedance Characteristics)

The output of a Tektronics Spectrum analyzer is connected to a Power amplifier. The output of the amplifier is used as a voltage source for the control test coil. The spectrum analyzer monitors the voltage and current of the test-coil for various frequencies (from connections from the test-coil) and determines the impedance. Results of the magnitude and phase of the impedance of the coils using this setup is presented in Section 3.2.3.4.

3.2.3.3 Thermal Characterization. The transient response and steady state performance of the coils for a step input voltage was determined. Generally for a constant input voltage, the current decreases with time as the coil heats up and the resistance increases. The current level eventually stabilizes at a final temperature, after approximately four thermal time constants. Shown in Figure 3.17 is a flow diagram of the setup used for this experimental analysis.

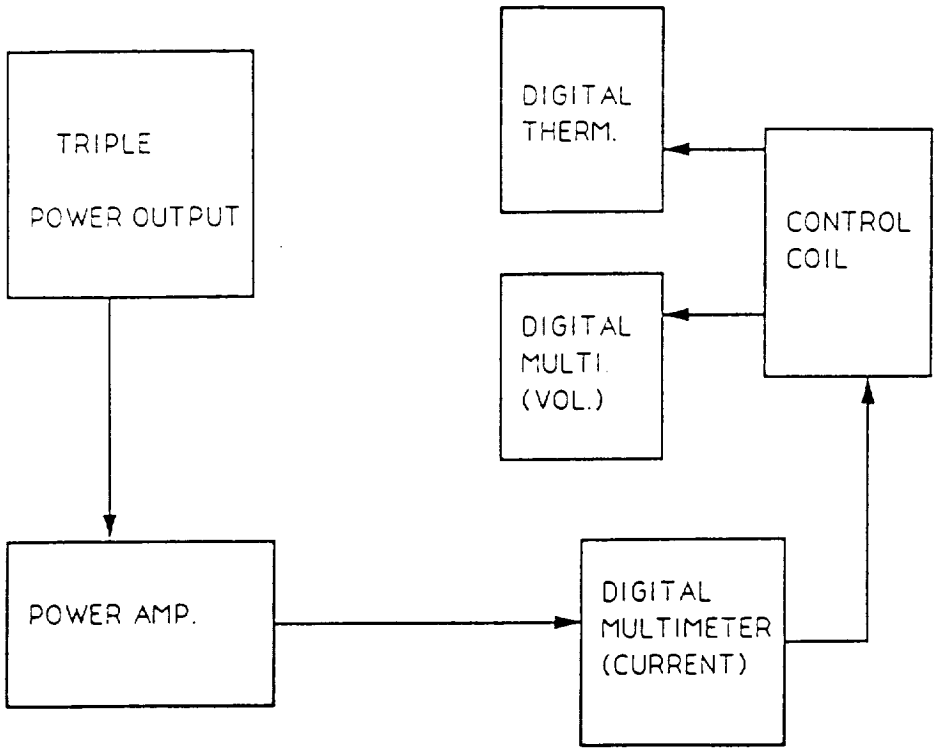

Figure 3.17. Experimental Setup for Thermal Characterization.

An HP 62368 Triple Output Power Supply is connected to a Copley Model 230 DC Servo amplifier as shown in Figure 3.17. The output of the power amplifiers is used as a voltage source for the test-coil. The current through the coils is monitored using a Fluke 75 Digital Multimeter, and the voltage by a Fluke 8050A Digital Multimeter. The surface temperature of the test-coil is measured by a Fluke 2166A Digital Thermometer. For each type of coil the following test procedure was carried out for initial coil currents of 5, 7 and 9 amperes:

1) A constant dc. voltage sufficient to produce the required initial current was applied to the coil.

2) Using the digital meters (Figure 3.17) the current and surface temperature values were recorded at one minute time intervals, until steady state was reached.

3) For each test the resistance as a function of time was calculated (voltage divided by current). The overall temperature of the coil was determined from the following expression:

$$T_h = \frac{R_h}{R_1} \cdot (T_1 + T_o) + T_o$$

where:

T_h = Average Coil Temperature
T_1 = Room Temperature
T_o = "Effective Zero Resistance" Temperature (- 234 °C)
R_h = Coil resistance at particular temperature
R_1 = Initial Coil resistance

Results of the plots of mean temperature against time for the two types of coils are shown in Section 3.2.3.4.

3.2.3.4 Results. This section contains the results of the mechanical, electrical, and thermal testing of the control coils.

Shown in Table 3.7 are the results of the mechanical checks conducted on the LAMS control-coils.

Table 3.7. Results of control-coil mechanical checks

SEQUENCE NO:	MECH.CHECK	DIMEN. ("A") "	WIND.DIRECTION
1	GOOD	2.0585	CLOCKWISE
2	GOOD	1.0125	CLOCKWISE
3	GOOD	1.018	CLOCKWISE
4	GOOD	1.038	CLOCKWISE
5	GOOD	1.0445	CLOCKWISE
6	GOOD	1.049	CLOCKWISE
7	GOOD	2.0345	CLOCKWISE
8	GOOD	1.011	CLOCKWISE
9	GOOD	1.056	CLOCKWISE
10	GOOD	1.058	CLOCKWISE
11	GOOD	1.053	CLOCKWISE
12	GOOD	1.046	CLOCKWISE

The control-coils had been well assembled. There was no observed failure of the epoxy glue joints for all the twelve coils, as shown in Table 3.7 under "MECH CHECK". The winding thickness for Coil-1 and Coil-7 were within 2.5% of the specified winding thickness of two inches. Coils 2-6, and coils 8-12 were within 2.4% of the specified winding thickness of one inch. All the coils were wound in a clockwise direction.

Table 3.8 shows the results of the continuity and nominal resistance checks. There was continuity between the start and finish leads of all the control-coils. The resistance for the two types of coils were consistent as shown in the table (within 2%). The "one-inch" coils had resistances ranging from 4.30 Ohms to 4.38 Ohms, while the "two-inch" coils had resistances of 2.36 Ohms and 2.38 Ohms.

Table 3.8. Continuity/nominal resistance results

COIL SEQ.NO:	CONTINUITY	RESIST.(Ohms)	TEMP.(DEG.C)
1	GOOD	2.36	23.0
2	GOOD	4.30	23.0
3	GOOD	4.31	23.0
4	GOOD	4.34	23.0
5	GOOD	4.37	23.0
6	GOOD	4.31	23.0
7	GOOD	2.38	23.0
8	GOOD	4.35	23.0
9	GOOD	4.35	23.0
10	GOOD	4.34	23.0
11	GOOD	4.28	23.0
12	GOOD	4.38	23.0

The results of the small-signal inductance tests is presented in Table 3.9.

Table 3.9. Small-signal Inductance Test Results

COIL SEQ. NUMBER	FREQUENCY (Hz)	INDUCTANCE (H)	FREQUENCY (KHz)	INDUCTANCE (H)
1	100	0.08574	1	0.08494
2	100	0.09152	1	0.09057
3	100	0.09247	1	0.09140
4	100	0.08963	1	0.8896
5	100	0.09112	1	0.09028
6	100	0.09046	1	0.08992
7	100	0.08628	1	0.08522
8	100	0.09272	1	0.09131
9	100	0.09140	1	0.09092
10	100	0.09045	1	0.08994
11	100	0.09021	1	0.08992
12	100	0.09107	1	0.09061

At low frequencies (100 Hz) the inductance of the one-inch thick coils varied from 90 mH - 93 mH and at 1,000 Hz the coil

inductances ranged from 90 mH - 91 mH. There is relative consistency among the inductances of the inch thick coils. The values of the inductances also remain fairly consistent for low and high frequencies. The two-inch coils also show consistency at both low and high frequencies, as shown in Table 3.9.

Using the experimentally determined values of the resistance and inductance of the control-coils, simulation of the impedance of the control-coils with change in frequency was carried out. Figure 3.18 shows the plot of impedance against frequency for Coil-1.

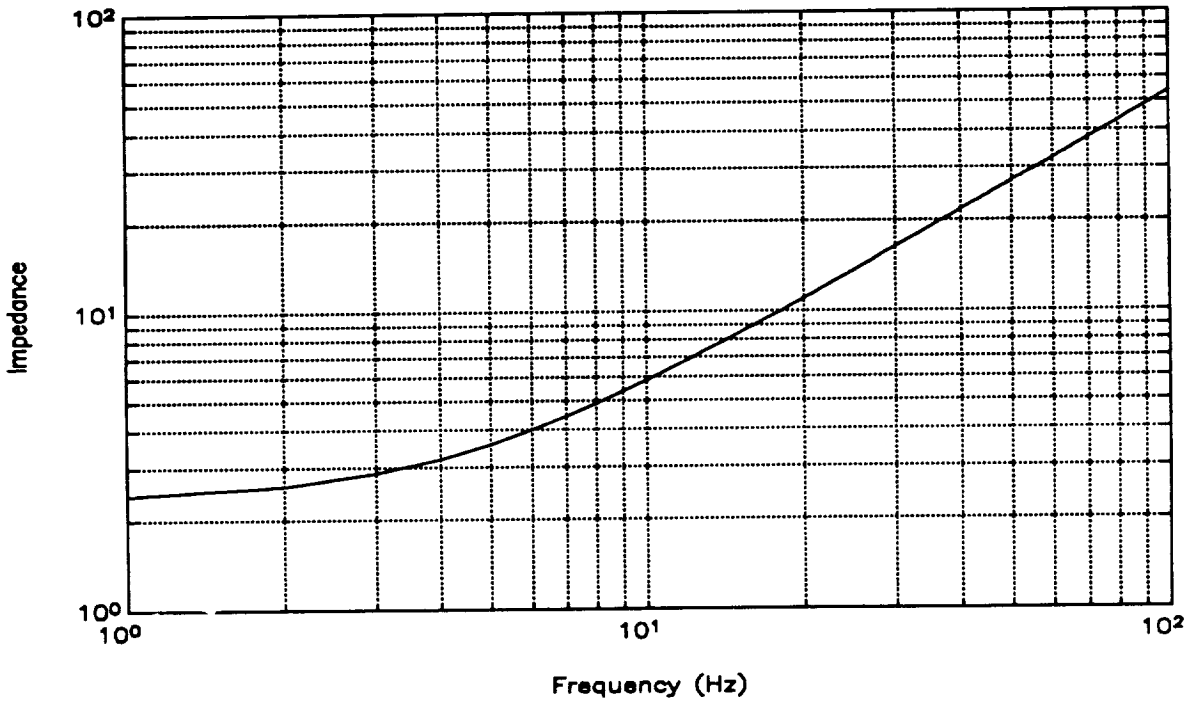

Figure 3.18. Impedance vs Frequency for Coil-1.

The impedance of the coil increases with increase in frequency as shown in Figure 3.18. At very low frequencies (frequencies less than 2.5Hz) the impedance of the coil is dominated by the resistive component of the coil. The break-frequency of the coil is 4.4 Hz. For frequencies above this value, the impedance of the coil is dominated by its inductance.

Shown in Figure 3.19 is the impedance against frequency plot of Coil-8. Coil-8 also shows the characteristic increase in

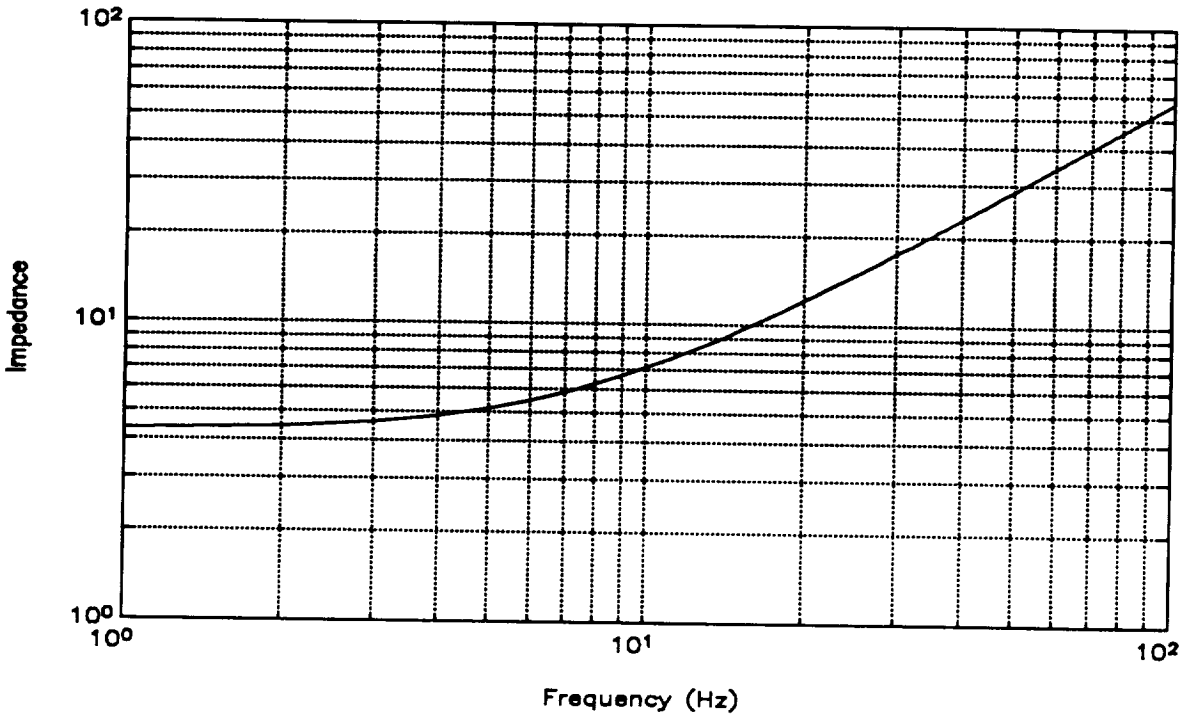

Figure 3.19. Impedance vs. Frequency for Coil-8

impedance with increase in frequency as in Figure 3.18. The break frequency of this coil is about 7.5 Hz. The impedance of the coil is dominated by inductance at frequencies above the break frequency.

Figure 3.20 shows the result of the plot of the magnitude of the impedance against frequency for Coil-1 using the experimental setup described in Section 3.3. The break frequency of the coil from this real-time experimental analysis was 4.9 Hz which compares well with values from simulation within 9.0% (using experimentally determined values of the inductance and resistance).

Shown in Figure 3.21 is the real-time impedance against frequency plot of Coil-8. The break frequency is about 7.3 Hz (the break frequency is within 2.0% of the break frequency deduced from simulation). Shown in Figure 3.22 and 3.23 are is the phase plots of the impedance of Coil-1 and Coil-8 respectively.

Figure 3.24 shows a plot of the average temperature of Coil-7 (2" coil) against time.

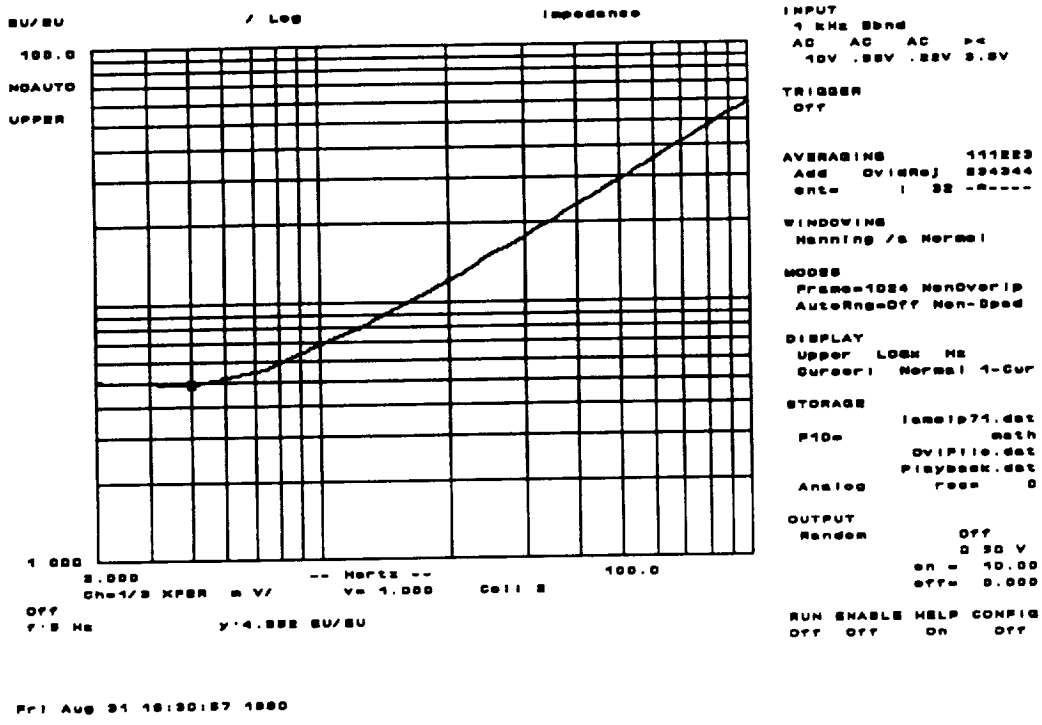

Figure 3.20. Spectrum Analyzer Plot of the Impedance of Coil-7.

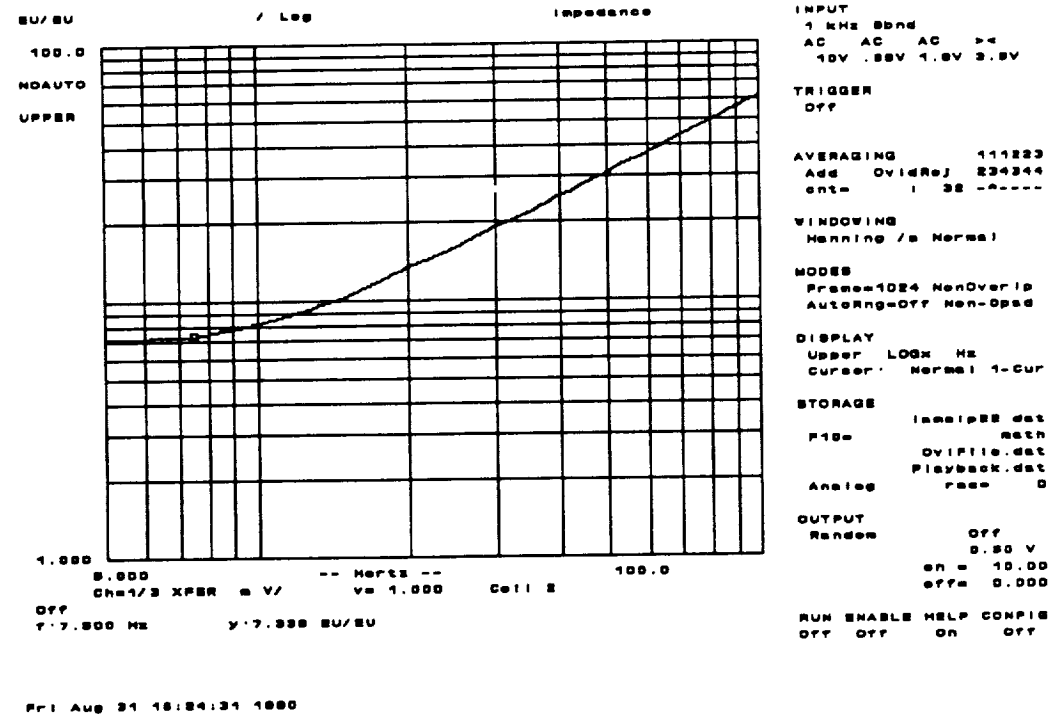

Figure 3.21. Real-time Impedance Behavior (Magnitude) of Coil-8.

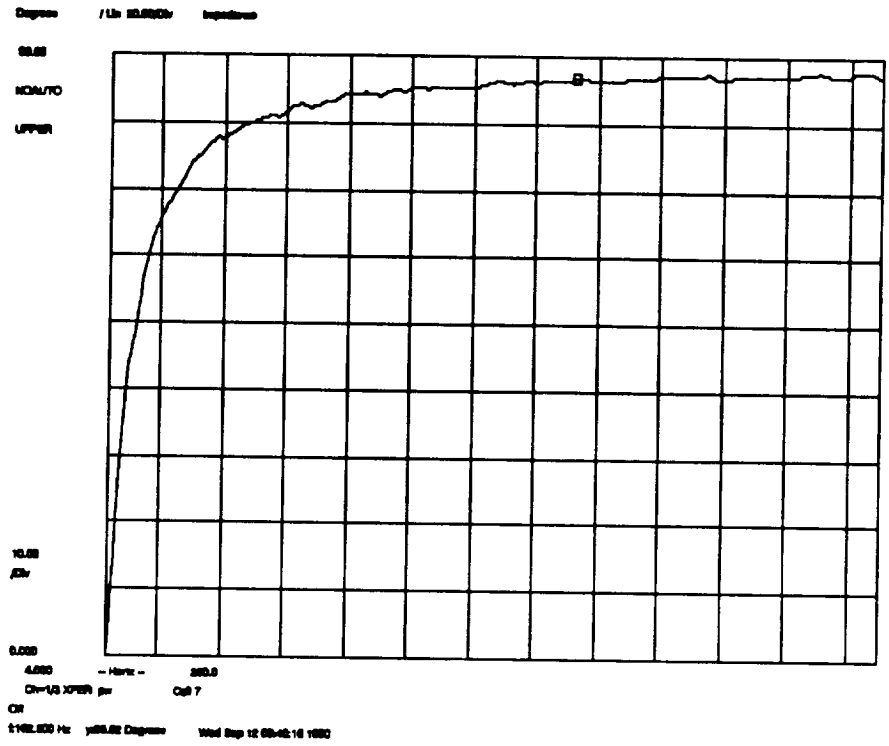

Figure 3.22. Phase plot of the impedance of Coil-1

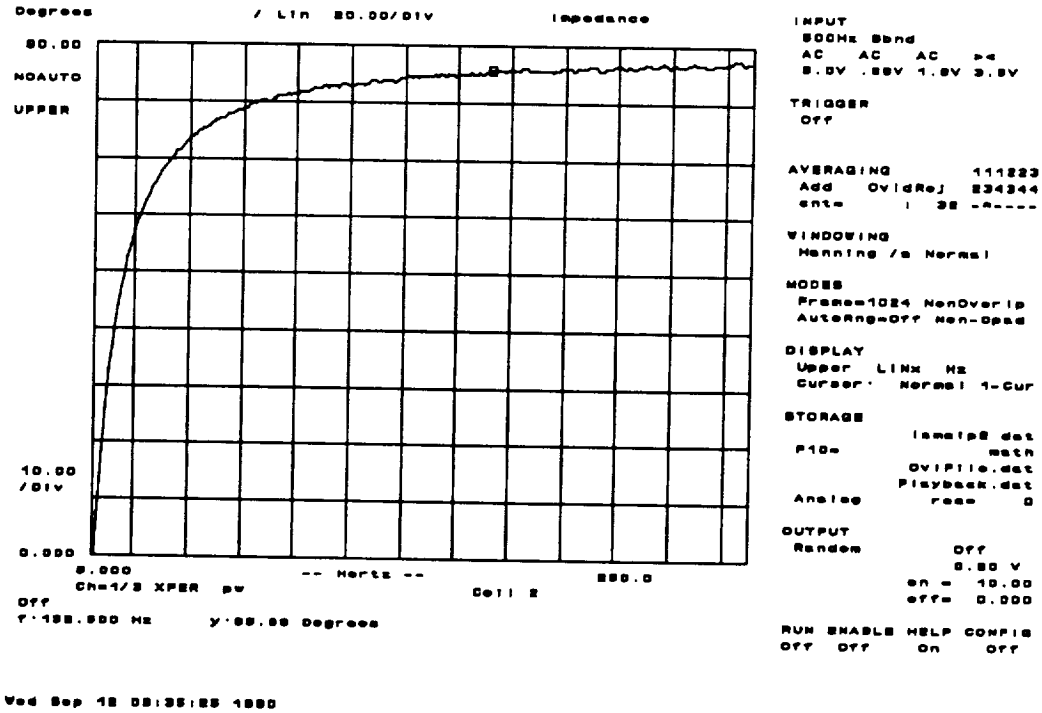

Figure 3.23. Phase Plot of Impedance (Coil-8)

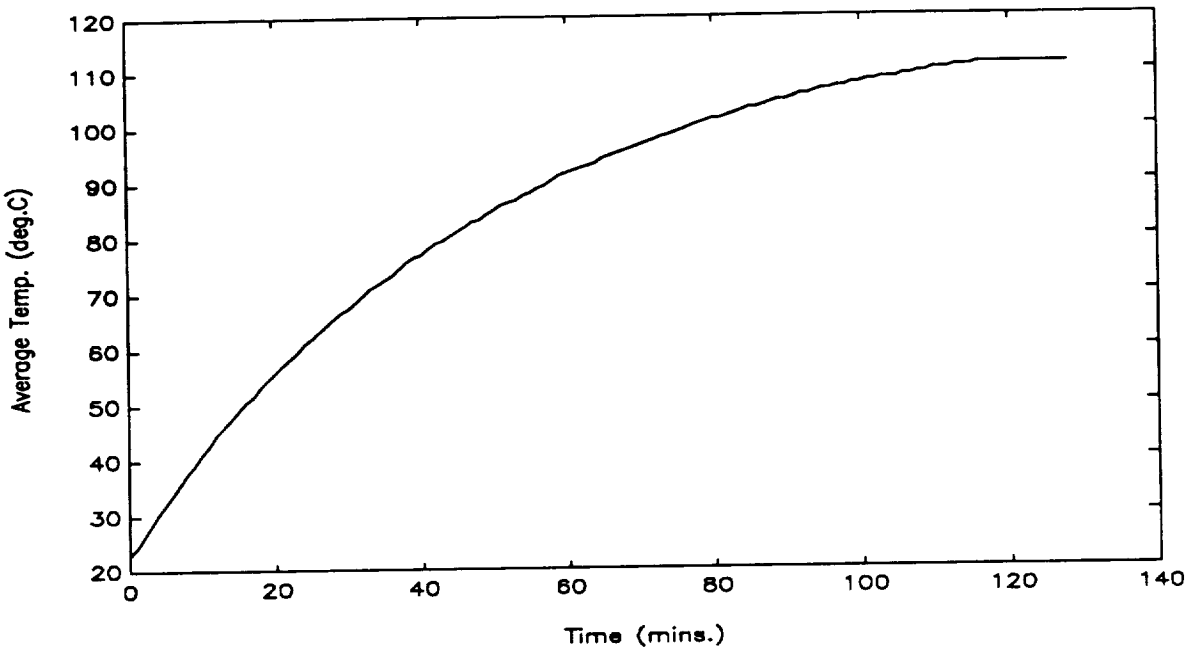

Figure 3.24. Average Coil Temperature (Coil-7) for 20 V Input

The average temperature of the coil increases with time as the resistance increases and the current decreases. The steady state temperature for this constant voltage input of 20.1 V and initial current of 9.13 amperes is about 110 °C. It takes about 120 minutes before the average temperature stabilizes. The time constant for Coil-7 (2" coils), is therefore about 30 minutes. Figure 3.25 is a plot of mean temperature against time (Coil-7) for a voltage input of 11.2 V (an initial current of 5.07 amperes).

For different input voltages/initial currents the thermal time constants are expected to be similar but the final steady state temperatures different. Figure 3.25 shows that steady state temperature is achieved after about 120 minutes. The time constant is then about 30 minutes; the same as in Figure 3.24. The final temperatures are however different as expected.

Figures 3.26 and 3.27 present the results of the thermal characterization of Coil-8 (1" thick coils). The constant voltage inputs are 29.9 V and 21.8 V with initial coil currents of 7.01 and

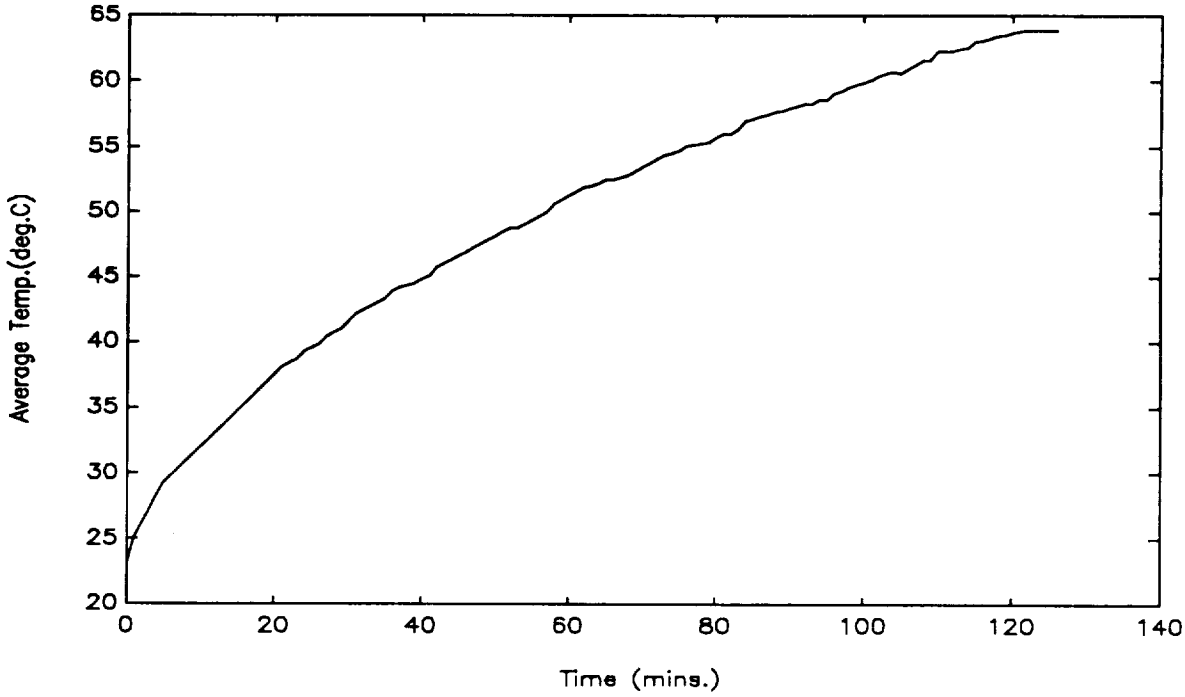

Figure 3.25. Average Temperature of Coil-7 for 11.1 V Input

5.18 amperes respectively. The thermal time constant for the inch thick coils is about 20 minutes as shown by both Figures 5.9 and 3.27. It takes about eighty minutes for steady-state temperature of the coil to be reached.

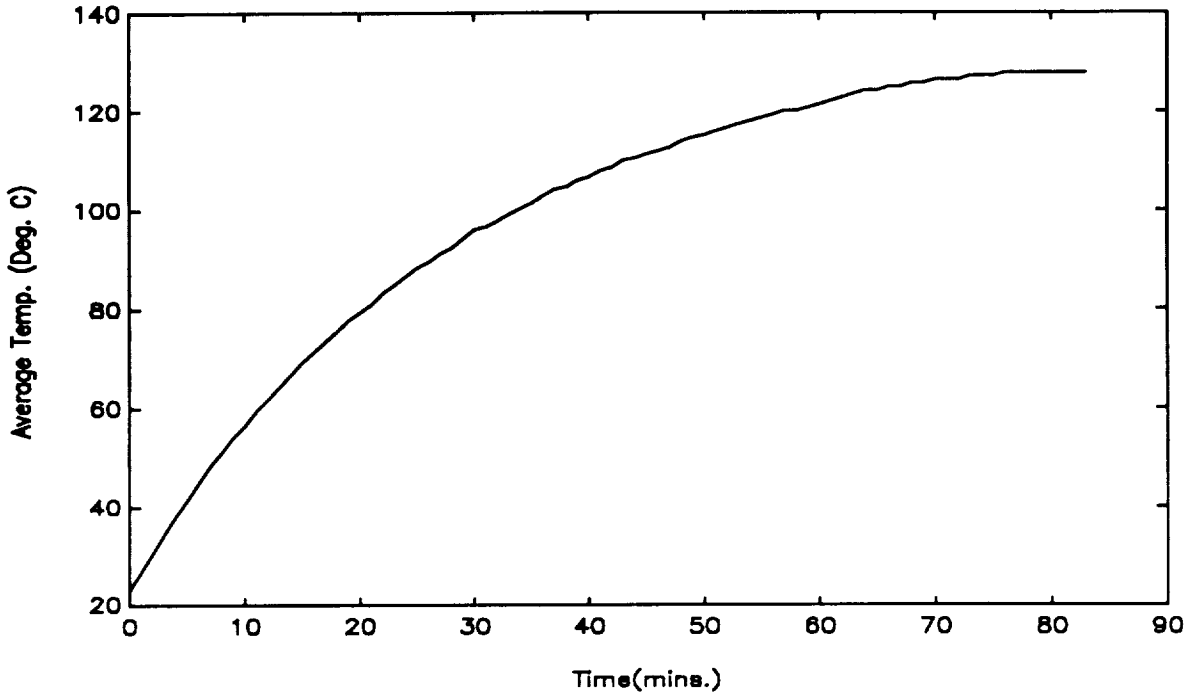

Figure 3.26. Average Temperature of Coil-8 for a 29.9 V input

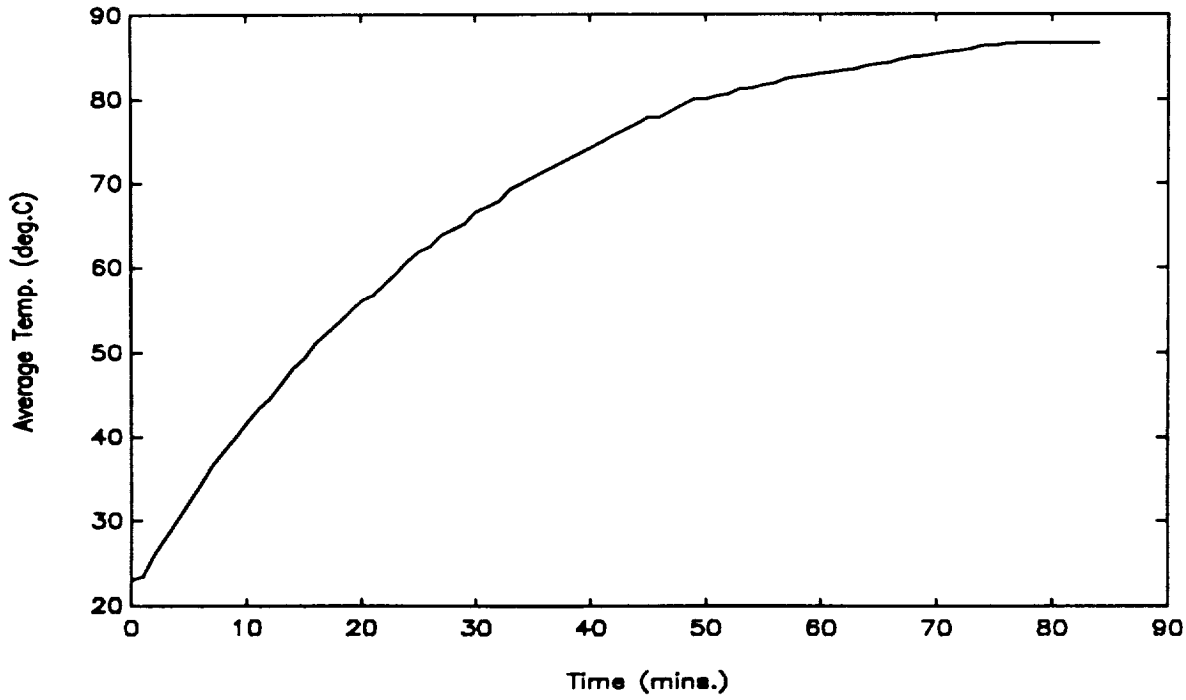

Figure 3.27. Average Temperature of Coil-8 for a 21.8 V Input

4. MECHANICAL SUPPORT SYSTEMS

This chapter describes the construction of the mechanical hardware for the superconducting LAMS prototype. The hardware provides support for all activities and operations which are necessary to perform system shakedown, testing, and routine maintenance. The mechanical hardware consists of five major components as shown in Figure 4.1:

1) crane-lift system,
2) base,
3) service stand,
4) weldment support structure, and
5) cryostat assembly.

The construction of these components is discussed in the sections which follow.

4.1 Crane-lift system

Use of the test bed requires repetitive cryostat refilling and magnet recharging operations. These service procedures can be performed only after gaining a full access to the service points of the cryostat (located at the bottom of the cryostat's outer shell). To access the cryostat the system has to be partially dismounted. This involves lifting and moving some relatively heavy and delicate components (the upper half of the control coil support structure and the cryostat assembly). The crane-lift system provides service assistance and assures quick and successful cryostat recharging. The recharging procedure is illustrated in Figure 4.2. Necessary procedural steps are as following:

1. Remove Lower Spherical Shell
2. Connect Diagnostics
3. Fill with Liquid Helium
4. Connect Power Leads with Persistent-mode Switch

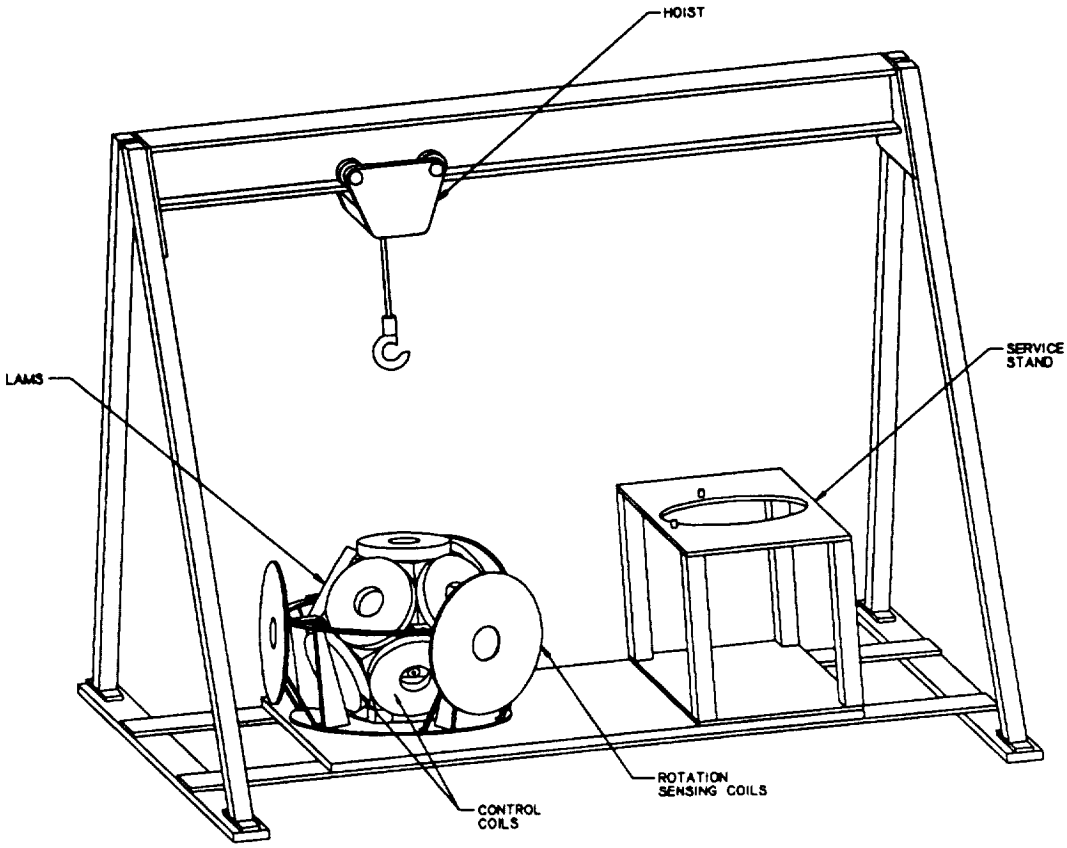

Figure 4.1. Overall Testbed Design

5. Energize and Charge
6. Disconnect Leads and Insert Thermal Baffle
7. Replace Lower Spherical Shell

The crane main bar and its supporting structure were tested for loads of 260 lbs. The lift mechanism components: medium duty ball bearing trolley and the mechanical wire rope hoist were also tested at 260 lbs. The main carrying bar and crane legs are fabricated separately and assembled together using appropriate mounting brackets and bolts.

Appendix A contains the pertinent detail drawings for the crane. Some of the machined parts of the crane were manufactured by Loyal Machining Co. of Chelsea, MA. The remainder of the parts were fabricated by SatCon personnel. The crane was assembled at SatCon.

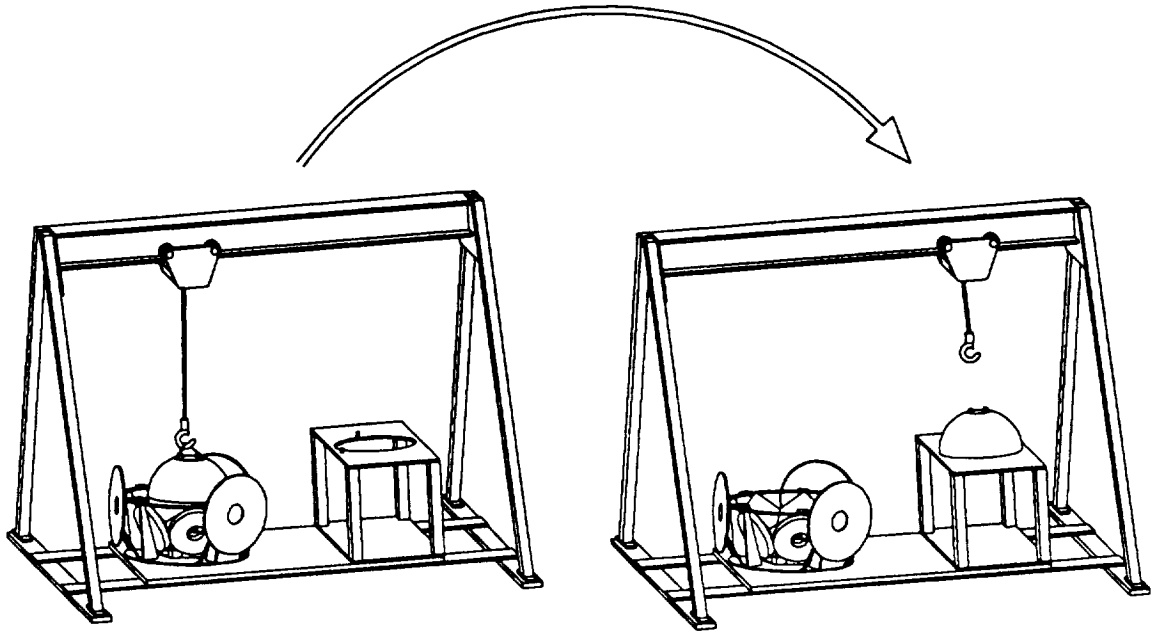

Figure 4.2. Recharging Procedure

4.2 Base

Four H-beams create a solid base which supports the crane, service stand, and the weldment support frame. Since each of the system components is firmly attached to the base, the base not only supports them but also localizes them in respect to each other. The base is a bolted beam assembly.

Appendix A also contains the detail drawings for the base. The base was fabricated and assembled by SatCon personnel.

4.3 Service Stand

The purpose of the service stand is to provide a temporary support for the cryostat during the recharging procedure. The service stand is constructed as a bolted frame structure and can carry up to 200 lbs load without observable deformation. After initial positioning the service stand is bolted down to the base.

Appendix A also contains the detail drawings for the service stand. All of the parts of the service stand were fabricated at SatCon by SatCon personnel.

4.4 Weldment Support Structure

The weldment support structure provides a structural linkage between the control coils and the base. Additionally, the structure provides a supporting frame for the angular position sensing coils and the cryostat assembly absolute location measuring probes (capacitive sensors). Twelve control coils are located in the centers of twelve pentagon shape plates. The combination of all twelve plates creates a dodecahedral structure. To provide easy access to the cryostat, the support structure is split horizontally along the edges of five pentagons creating two shell like substructures. Each substructure is a weldment consisting of six stainless steel plates. The use of stainless steel not only adds an extra structural strength to already an inherently rigid tetrahedral design but also eliminates undesired magnetic interactions. The requirement of high stiffness of the weldment comes from the necessity to limit its structural deflections under anticipated load to the level at least two order of magnitude lower then the required accuracy of the cryostat positioning when it is magnetically suspended. The control coils cover most of the pentagon plate area. Six high strength bolts and five sections of threaded rod are used to attach each coil to the weldment. Circular holes in the center of each pentagon plate provide visibility of the structure inside and in the case of the six bottom weldment plates, also accommodates a capacitive probe.

The system of six equally spaced probes provide information about the translational displacement of the cryostat assembly. The redundancy resulting from application of six instead of three capacitive probes makes the system less prone to error and greatly reduces fabrication tolerances of the weldments and the external shell of the cryostat assembly. Each sensor is positioned in the center of the pentagon plate hole through the mounting bracket.

The sensor mounting bracket consists of a cross bar which is attached to the inner edges of the plate hole. The cylindrical case of the sensor is threaded. The mounting bracket has a mating threaded hole. The radial location of each sensor face is fully adjustable by turning the sensor in and out. The counter nut secures the sensor in a desired position.

Bumpers which are integral parts of the control coil bobbins assure that no accidental contact of the cryostat assembly with the coil support structure will take place. To avoid a damage to the spherical shell of the cryostat assembly, the external surface of the bumpers are covered with a thin layer of a felt padding. Those padded bumpers located at the bottom six pentagons provide support for the cryostat assembly before the control coils are powered.

The cryostat assembly angular position sensing coils are positioned concentrically to the control coils but inside of the weldment. They are bolted down to the pentagon plates.

Five equally spaced mounting ears locate the halves of the weldments with respect to each other and provide firm connection points. To assure dimensional integrity of the support structure, both halves of the dodecahedron weldment were bolted together before the entire structure was welded.

The Appendix contains the detail drawings for the weldment. The weldment was fabricated by Merchant's Sheet Metal Co. of Worcester, MA. The control coil bobbins were manufactured by Loyal Machine and wound by ACR Electronics of Medford, MA. The sensing coils were wound by Roland Lund of Dorchester, MA. The phenolic parts used to mount the sensing coils were fabricated by the Stonebridge Co. of Holliston, MA. The parts were assembly and the protective surface was added to the control coil bumpers at SatCon by SatCon personnel.

4.5 Suspended Body

The cryostat assembly is a structural unit which is magnetically suspended inside the weldment support structure. A superconducting magnet is placed inside the cryostat tank. The

cryostat is of cylindrical shape with a thick bottom flat plate providing major structural support for the magnet, magnet powering port, liquid helium fill port, and the pressure relief valve. The top closing cap is in form of a rounded shell. There are three cryostat angular position sensing coils attached to the cryostat.

Three passively-tuned sensing coils are attached to the cylindrical walls of the dewar. The coils are mounted to circular phenolic plates.

Once both sensing coils were positioned and firmly bolted down to the cryostat, the entire assembly was placed inside the plastic spherical shell. The shell is made out of modified ABS plastic. The sphere plays a role of a target object for five capacitive sensors which are located in the lower half of the control coil support structure. The material of the sphere is partially conductive (volume resistivity of 5000 ohm-cm). This feature is necessary to assure successful operation of the capacitive sensors. The spherical container is horizontally split in half. Three equally-spaced brackets are attached to the upper sphere's edge to provide precise positioning of the two hemispheres with respect to each other. The wall of the spherical container was designed for a 0.250 inch thickness and has outer diameter of 16.4 inches. Special attention is given to sphere's external out of roundness which was kept within .010 of an inch. The upper hemisphere is not completely closed. There is a hole at the very top of it. The hole allows helium vapor to escape and provides access to the cryostat assembly lift brackets. A lift bracket was welded to the cryostat's top dome. The attachment of the upper hemisphere to the cryostat structure is provided by three mounting ears which are located circumferentially on the sphere's split edge. The sphere wall thickness is slightly enlarged at these locations to increase its local stiffness and to accommodate necessary attachment bolts. Three mounting brackets are welded in the corresponding locations on the side wall of the cryostat. Since only the upper hemisphere is bolted to the cryostat, the lower hemisphere need only by removed to get full access to the cryostat's service ports.

The detail drawings of the parts of the suspended body are given in Appendix A. The cryostat was manufactured by Precision Cryogenics of Indianapolis, IN under subcontract from Cryomagnetics Inc. of Oak Ridge, TN. Roland Lund also wound the passive sensing coils. Collins Manufacturing Co. of Fremont, NH fabricated the spherical shell as well as several parts for attaching the passive sensing coils and shell to the cryostat. All of the parts were assembled at SatCon by SatCon personnel.

THIS PAGE

INTENTIONALLY

LEFT BLANK

5. SENSOR SYSTEMS

The superconducting LAMS requires systems to monitor the position of the suspended body in five degrees-of-freedom. This chapter describes the methods used to sense translational motion along three orthogonal axes and a set of two Euler angles which describe the angular motion of the central axis of the solenoid.

5.1 Transducer Operating Principles

The three degrees of translation are sensed by capacitive devices operating at about 16 kHz. These devices are inherently simple and impose minimal constraints on the spherical surface and ambient magnetic fields requiring only an electrode impedance of $<<10^8\ \Omega$ and a target smoothness less than the required resolution.

The two rotational angles are determined from the mutual inductance between a set of stationary transmitting coils placed inside the control coil set operating at a frequency of ≈ 71 kHz and three passive coils moving with the cryostat/magnet. Both the transmitters and moving coils employ series capacitors which cancel inductance terms thereby enhancing sensitivity.

Ten transmitters determine both the angle of rotation in the horizontal plane, Φ, and Θ, the pitch angle around the horizontal plane, by measuring the coupling to the passive coils on the sphere.

5.1.1 Translational Sensors

There are available commercial devices for both capacitive and eddy current sensing which easily meet translational resolution and range requirements of one part in one thousand in 0.1". Both types are relatively inexpensive and easily implemented. Each also has its disadvantages. Eddy current sensors are affected by the electrical characteristics of the target material but only slightly sensitive to the continuously varying gas mixture between the sensor coil and target. Capacitive sensors with the required range (≈ 0.38 inch active diameter) have an impedance of $> 10^8\ \Omega$ and so

require only minimal conductivity on the spherical surface but could be affected by variations in the dielectric constant resulting from vapors exiting the helium dewar. For both methods, the surface flatness is a critical parameter. The electronics associated with these sensors has been shown to be reliable, accurate, and uncomplicated - a low frequency oscillator driving a constant current source with the voltage continuously sampled and applied to a digital signal processor (DSP). Further, we have had successful experiences with these techniques. The sensor units are Capacitec HPT-150 with an active diameter of 0.150 inches and are driven with a 15 kHz controller.

5.1.2 Rotation Sensing

A number of rotation sensing options were examined. All but two of these were eliminated by considering the key constraints in the system:

1) The ability to operate the sphere mechanically disconnected from its surroundings. The design for the superconducting coil system allows for operation without the low power ohmic umbilical used for diagnostics),

2) Insensitivity to ambient transient magnetic fields such as those induced by the control coils,

3) Insensitivity to the cryogenic environment surrounding the sphere,

4) Electronically robust hardware. (Supplies consistent analog signals to the DSP.

5) Minimum complexity in the hardware.

These considerations eliminated:

a) magneto-striction (requires power to sphere),

b) direct magnetometer analysis (since control fields track at the same rate as the rotating field requiring continuous evaluation of these fields in the DSP),

c) visible (but not necessarily infrared) optical methods which may be obscured by dewar vent gases or frost,

d) optical methods which require lock-on or pattern counting.

The remaining methods are listed below:

A) optical pattern locating (i.e. focusing an electronically recognizable pattern on the sphere onto a set of CCD arrays. Four linear arrays are necessary to unambiguously fix the position within the pitch range of ±60°. The position will be located by digital processing and

B) use of the variation of electromagnetic coupling between coils fixed externally and rotating with the sphere.

The CCD method as usually implemented is considered robust against false tracking but excessively complicated and relatively expensive. Estimated hardware cost alone is approximately $20,000. Such a system has little versatility compared to a system of mutual inductors which allows a choice of workable mechanical and electronic configurations.

5.1.2.1 Design Overview. As implemented here, mutual inductance sensing involves exciting outside static coils with a fixed current then coupling this energy into passive coils on the rotating body at a frequency well above the minimum response rates required for the control system. The power coupled into the cryostat of the superconductor must not cause excessive helium loss while induction in the control coil set must not interfere with proper operation.

Both the transmitting primary and passive secondary coil self-inductances are made resonant with series-placed capacitors. The change in mutual inductance (calculated from the coil voltage driven with a constant current) is then used to track rotation. The effective circuit is shown in Figure 5.1.

5.1.2.2 Simple Variometer. For coils inclined along the same axis but at large separation relative to diameter, the mutual inductance varies as the cosine of the angle of inclination. For the case of filamentary coils with one twice the radius of the other and separated by the radius of the smaller, the behavior closely approximates this. Such arrangements are commonly used as the basis of a "variometer"[1]. The deviation from a cosine variation for this case is shown in Figure 5.2.

Due to interference of key components, it is not practical to meet either of these geometrical limits. However, geometries which result in approximate cosine behavior can easily be corrected via the DSP. Figures 5.3 and 5.4 show these deviations for the practical geometries considered here.

5.1.2.3 Coil Complement. As the mechanical design of the control coil support structure progressed, it became apparent the none of the modified simple variometer configurations considered earlier were suitable. The 0.125" thick weldment almost completely enclosed the levitated sphere which would severely attenuate coupling between a sensor transmitting coil outside the structure and a passive coil moving with the dewar. Only at excitation frequencies below ~ 1 kHz, where the data rate would be low enough to limit control bandwidth, would the shielding effect be acceptable.

For this reason, the transmitting coils were placed inside the weldment. However, the necessarily close coupling between the active and passive coils, while increasing sensitivity to angle, limited range.

---

[1] Grover, F.W., Inductance Calculations, Dover 1962, p195

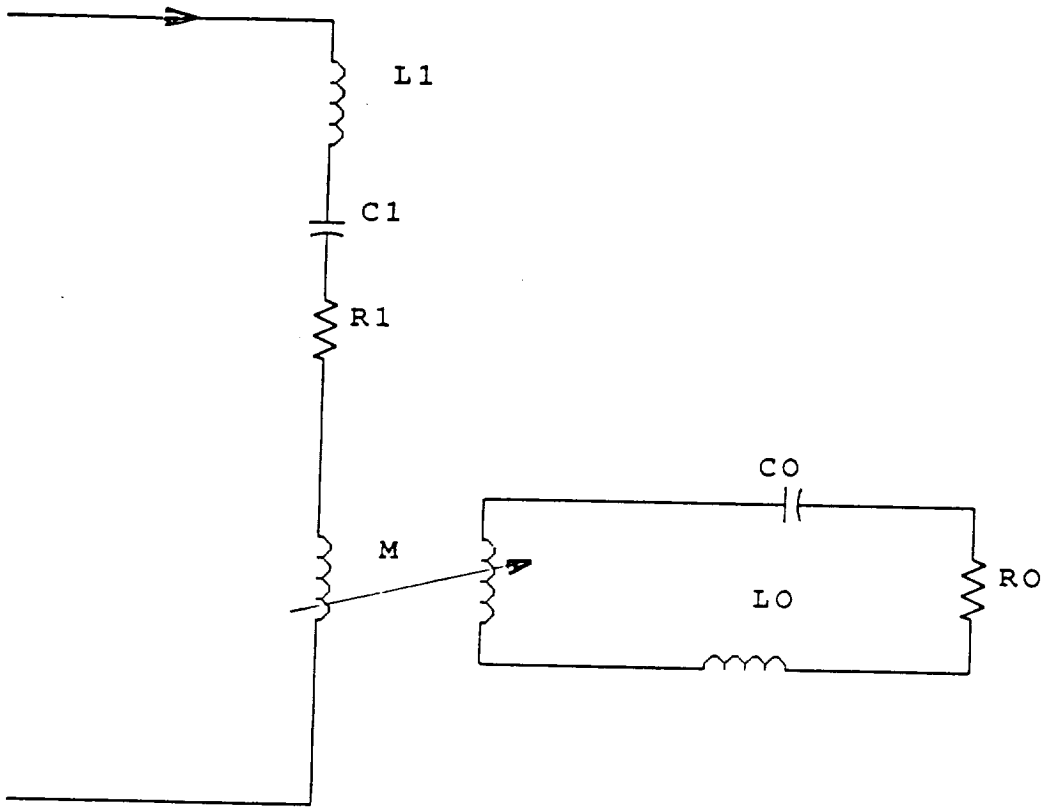

M is mutual inductance between coils; rotating coil components denoted by '0;' excited coil by '1.'

Figure 5.1. Single Coil Sensing Circuit

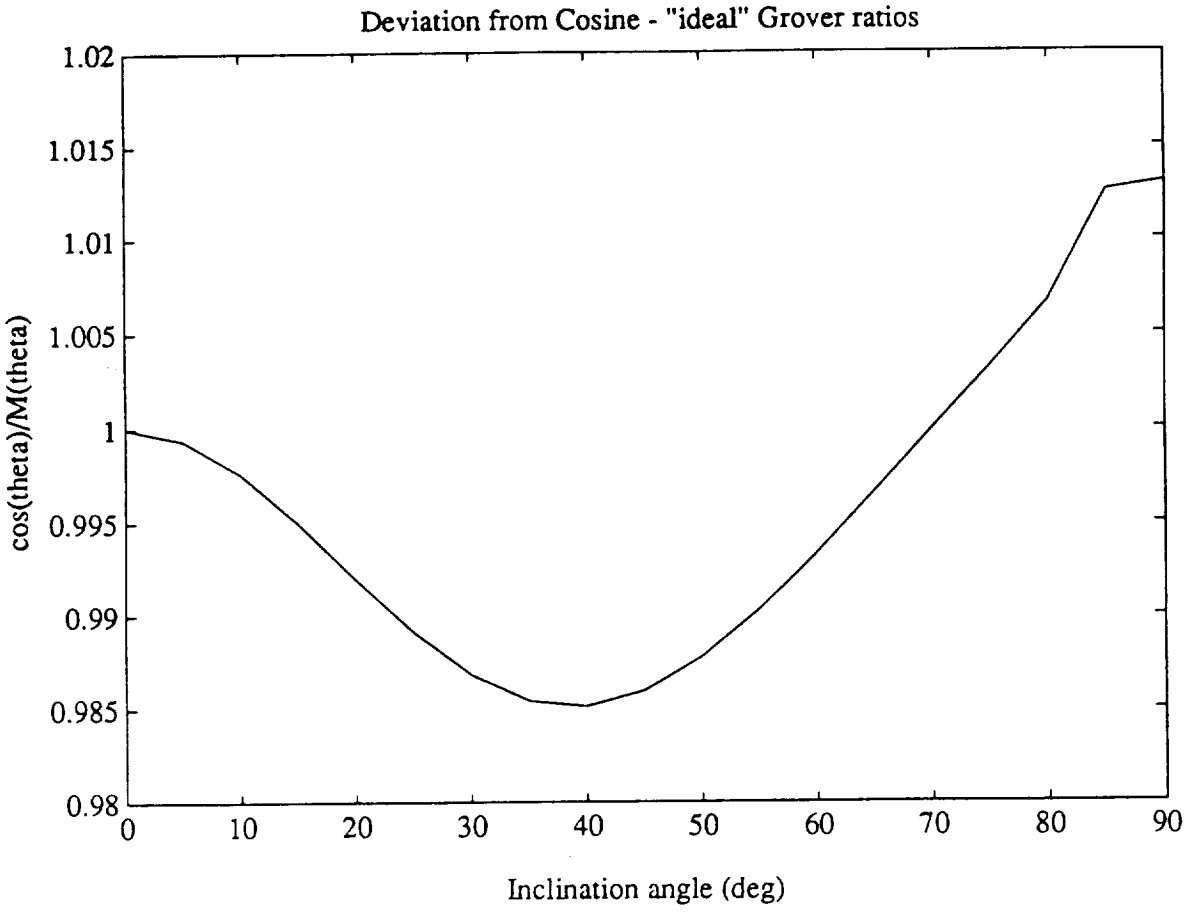

Figure 5.2. Deviation from Simple Trigonometric Function for Ideal Geometry

This led to expansion of the coil complement to ten transmitting coils and three passive coil moving with the sphere. With a useful range of about 40° in angular separation as measured in the three coil test fixture, the three pasive coils non-symetrically mounted on the dewar in conjunction with tramsmitters centered at each side mounted control coil position, allowed unique two degree of freedom angular position determination over ±60° in pitch and 360° in yaw.

For compatability with the oscillators in the control power amplifiers, the sensor coil system was operated at 71.5 kHz instead of 50 kHz. This slightly increased coupling while decreasing skin depth all of which had a negligible effect upon operation.

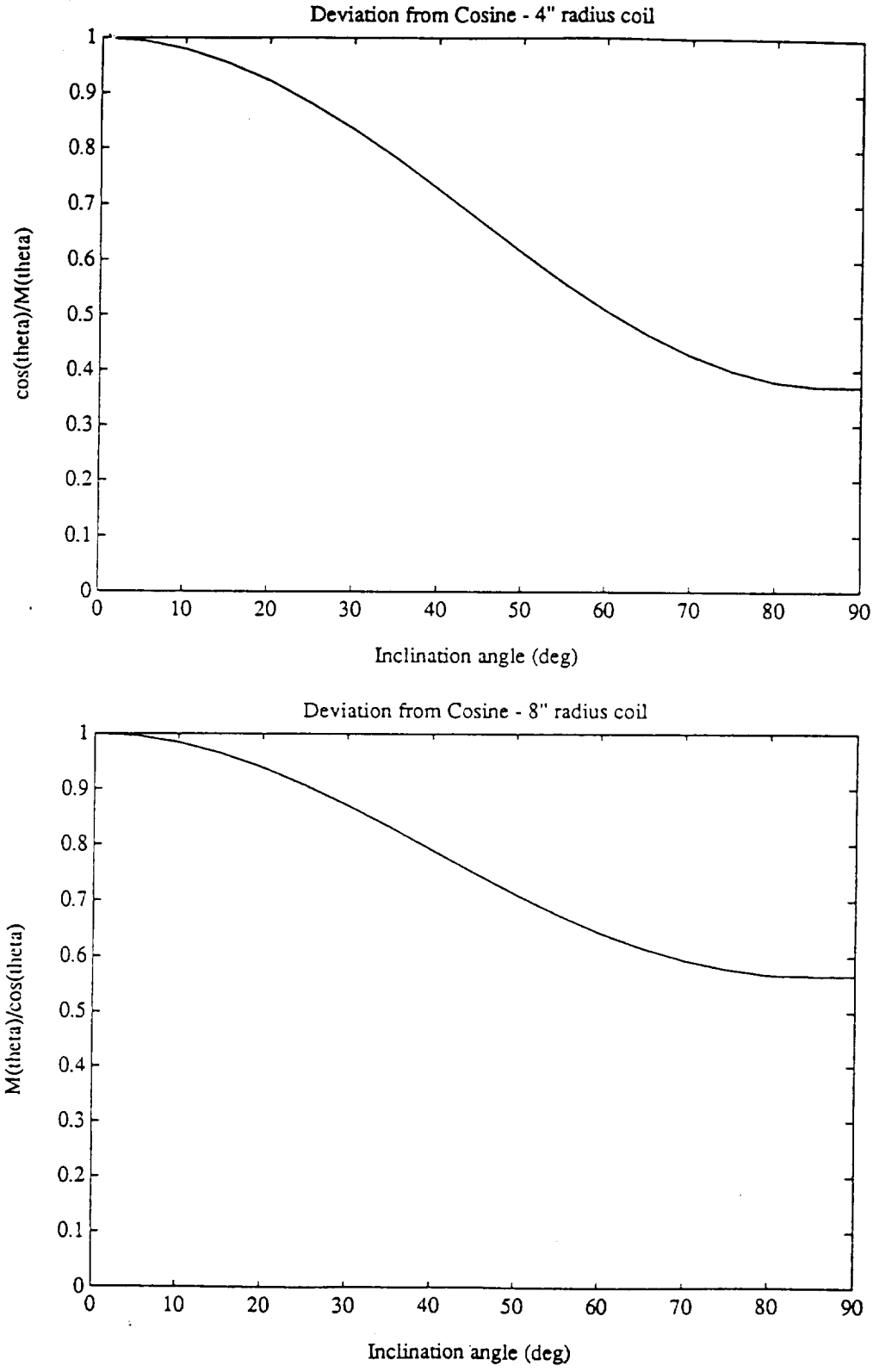

Figure 5.3. Deviation from Simple Trigonometric Function for Practical Coils Separated by 13 inches

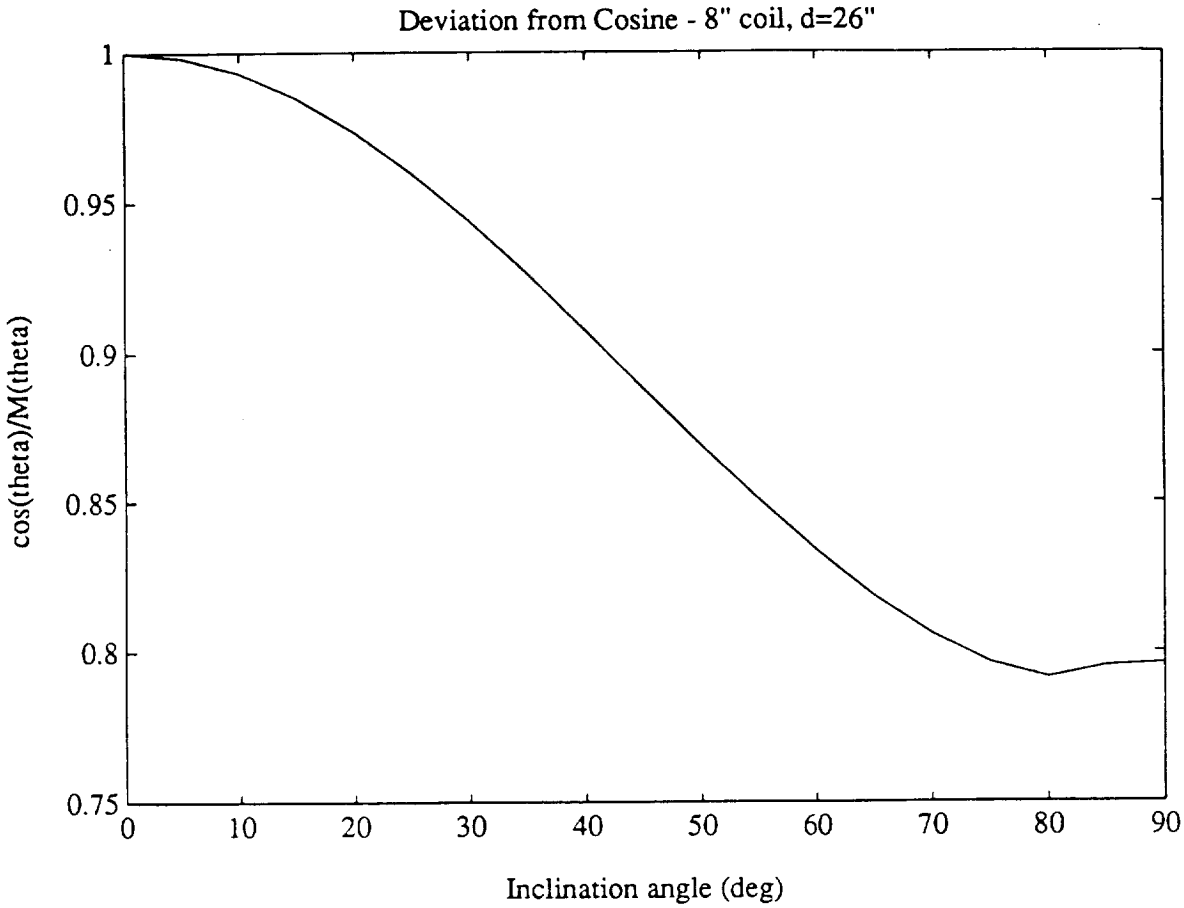

Figure 5.4. Deviation from Single Trigonometric Functions in Practical Coils Separated by 26 inches

5.1.2.4 Circuit. The coil set described above is excited with two distinct frequencies - one for the high resolution magnitude determination the other for the sense determination - allowing simultaneous acquisition of both types of information. Alternatively, a single exciting frequency could be used and each coil "scanned" in turn.

We will examine the consequences of this. Since the potential V1 across the excited coil is :

$$V_1 = I_1 \left[R_1 + i\omega L_1 - i\,(\omega\, C_1)^{-1} + \frac{\omega^2 M_1\,(M_1 + M_2 + M_3)}{i\omega\, L_0 - i\,(\omega\, C_0)^{-1} + R_0} \right] \qquad \text{Eq. (2)}$$

where the L's refer to coil self-inductances, C's the added capacitors, R's, the coil resistances, and M's the mutuals between the passive coil and the corresponding exciting coils (Figure 5.1).

In the case of continuous operation, three terms in M are present. The coils can then be connected (phased) so that the total dependance on the mutual inductance is approximately $\approx \cos^2\Theta$. With scanned operation, only one term in M is present reducing the magnitude of this term by a factor of 2. However scanning in this way allows eliminating the inner coils of the double set. The increase in electronics complexity associated with the switching and additional constraints on settling make this approach unappealing.

5.1.2.5 Coupling to Parasitic Elements. Such elements degrade the sensing measurement by supporting eddy currents which shield the passive coils or lower primary impedance thereby decreasing sensitivity for the save drive current.

These phenomena show in Equation 1 as reduced mutual inductance (M) of or a phase shift in the voltage across the transmitting coils. In general, the design approach was to first size the desired capacitance range to be much larger than typical stray capacitances, yet small enough to be practical in physical size. The required coil geometry and inductance range then determines the

number of turns. The copper area employed was as large a practical to minimize the effect of eddy currents in the external structure.

5.1.2.6 Cryostat and Conductors Surrounding the Passive Coils. In particular, elements such as the metal cryostat do not shield the passive coils, but can shunt induced current thereby decreasing sensitivity to the passive coil coupling. However, the inductive reactance of the cryostat (which can be estimated by one turn at approximately the diameter of the transmitting coil as 0.4 Ω) is not canceled by a capacitor as is the case for the passive coils. On the other hand, the resistance of an equivalent tuned passive coil is less than .001 Ω and can circulate a much greater induced current.

5.1.2.7 Superconductor. The superconductor, with its large number of turns has no effect upon the measurement sensitivity but may absorb enough energy to reduce its operating time from increased liquid helium boiloff. Assuming the oscillating magnetic field generated from one transmitter operating at ≈ 4 ampere-turns is completely absorbed into the superconductor, the energy absorbed per cycle can be calculated[2]. The increase in boiloff rate is much less than 0.1 liters/min, our measured quiescent boiloff rate). With an estimated capacity of 12 liters, this increase is compatible with our expected run times.

5.1.2.8 Sphere. The sphere must be conducting enough to support return current from the capacitive sensors. As a shunt for induced current, it behaves much the same as the cryostat. However, it can shield the passive sensing coil as well. The penetration at 71 kHz for stainless steel is approximately 0.05". To be non-shielding to the rotation sensor excitation frequency, the shell would have to be less than about 0.02" thick which is marginal mechanically.

---

[2] Wilson, Superconducting Magnets, Clarendon Press, Oxford 1983, chapt. 8.

Instead, a molded sphere of conducting plastic (ρ=~5000 Ω-cm) was fabricated. This had the virtue of a very long penetration depth, a low enough resistance for capacitive sensing, and good mechanical properties.

5.1.2.9 Control Coils. The control coils present both a possible shunt for induced current and source for interference into the control feedback loop. The inductance of a baseline configuration of ≈ 50 turns is about 800 μH.

5.1.2.10 Resonance Modeling. An key element in the rotation sensing system is the use of resonant circuits both in the exciting and passive coils to cancel the large inductive reactances. This increases the shunt current in the passive coil which increases the corresponding voltage contribution in the excited coil.

An examination of the behavior of the coil voltage around resonance will indicate the optimum operating range of Q's and whether the maximum sensitivity is adequate.

The calculation is an evaluation of Equation 1 (the circuit in Figure 5.1) with $M_1 + M_2 + M_3 = 2\ M_1$. This is only approximately true since it implies the variation in M with angle must be cosΘ.

The value of M was calculated with the angle of inclination set to 0° (maximum M). The inductances were for a one turn primary (1 μH) and a ten turn secondary (100 μH).

Values of C were chosen to obtain resonance at 50.3 kHz. The calculated maximum M for this geometry is about 0.4 μH for ten turns of the passive coil.

The plots in Figures 5.5 to 5.7 display impedance for the excited coil vs frequency. Ten separate responses for M_0 to $10M_0$ are overlayed in each plot. In Figure 5.5, the effect of decreasing the primary resistance on the sharpness of the dip at resonance is shown. The effect of varying M becomes more pronounced as R_1 decreases. A value of R_1 = .002 Ω is easily obtainable with the design coil. Figure 5.6 illustrates the change in peak width with a change in R_0 the secondary resistance. The

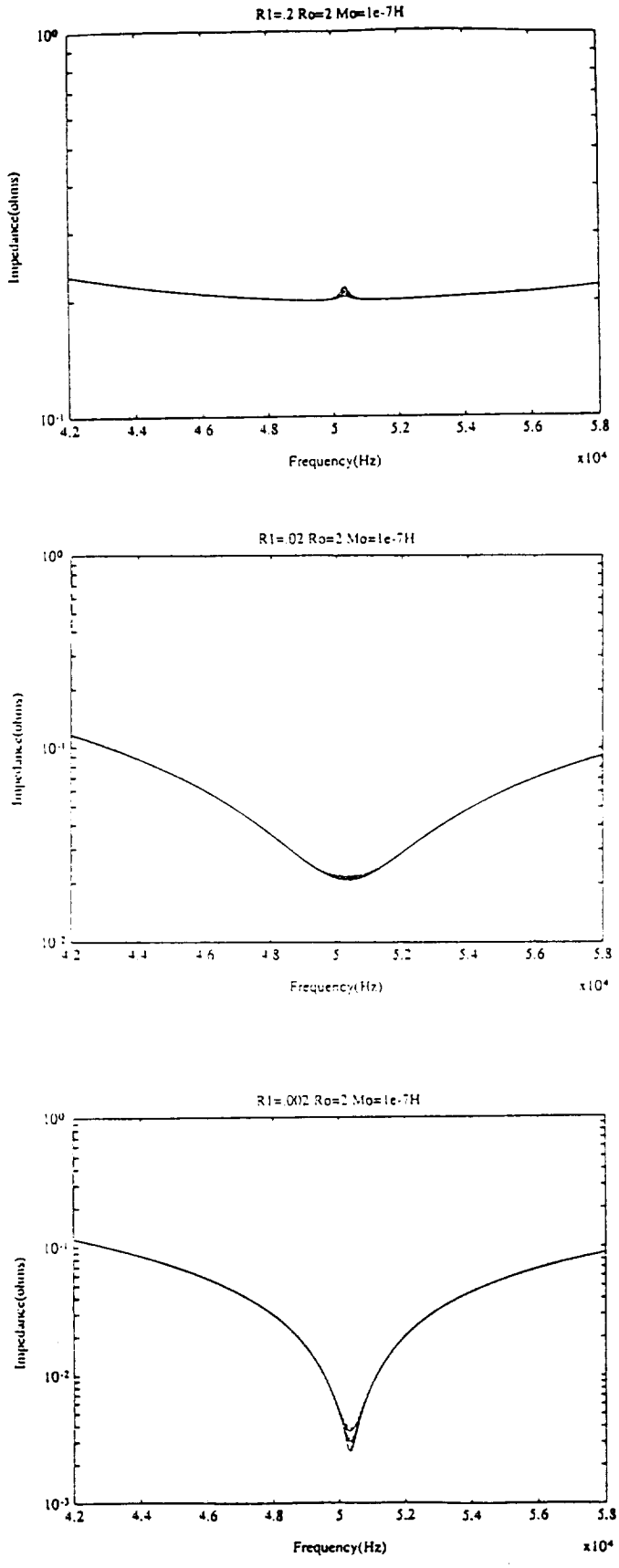

Figure 5.5. Variation in Response with Primary Resistance (Resonance at 30.3 kHz)

C-2

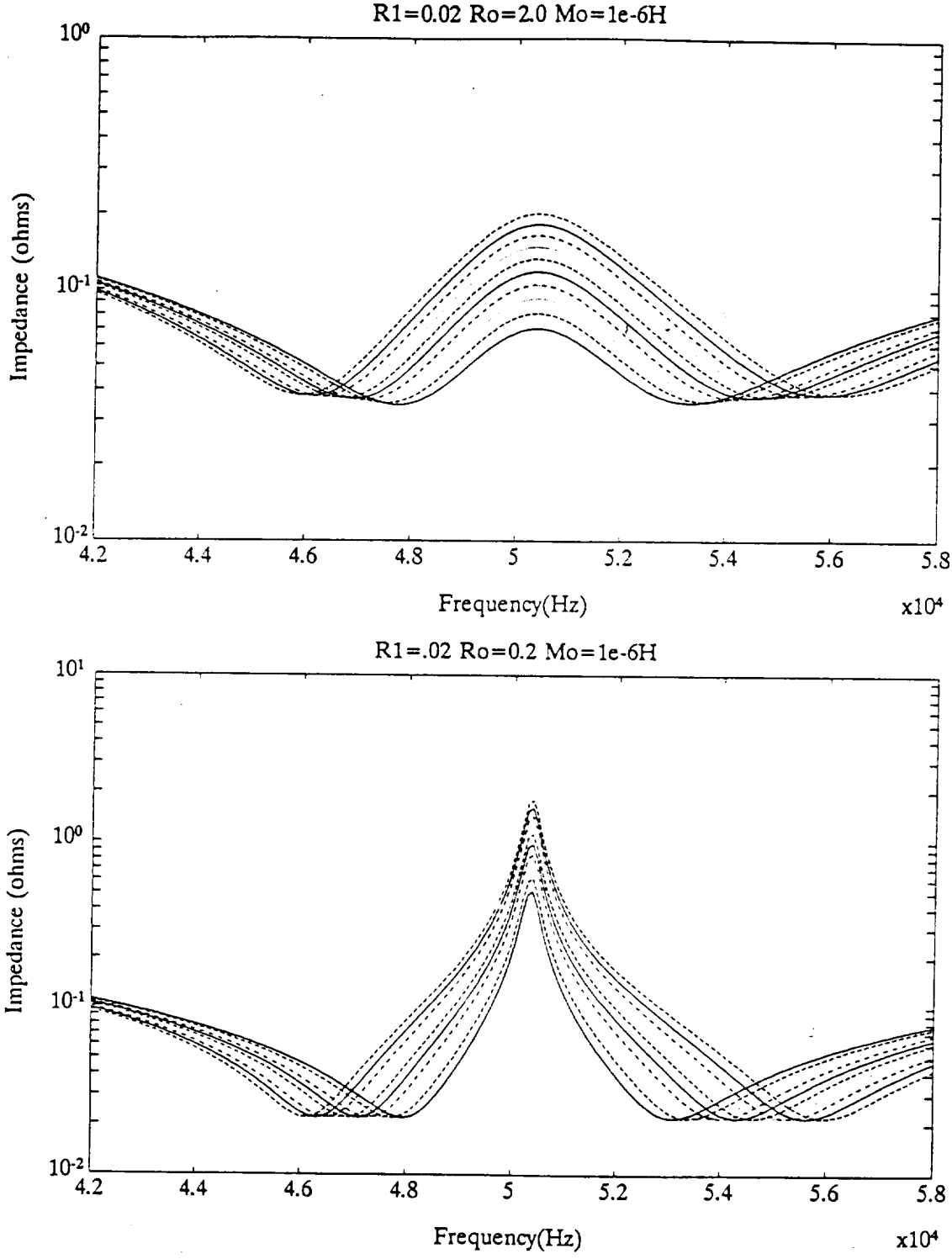

Figure 5.6. Variation in Response with Mutual Inductance from M_0 to $10M_0$

broadening at higher R_0 is accompanied by a decrease in the fractional impedance or sensitivity indicating a trade-off between tuning sensitivity and ultimately, resolution.

The importance of tuning is indicated in Figure 5.7 which shows the effect of a 1% shift in the capacitance of the passive coil. The fractional impedance change with M is decreased only slightly in the low Q (broad) curves of Figure 5.6 but results in a significant compression in the impedance range for the high Q plots.

It is expected that the main contribution to tuning shift will be the capacitance variation with temperature. Capacitors of the order of 0.1 μF (passive coil) with temperature coefficients << 1% over 10° C are available. Further, the passive coil turns can probably be increased by a factor of 2 to 3. The minimum resistance obtainable with a practical-sized coil and the increase in response time are limiting factors. Such an increase has the beneficial effect of both increasing the inductance (and thereby decreasing the capacitance into more temperature stable range) and increasing the sensitivity to M. We are also considering thermally tying this capacitor to the cold venting gas from the cryostat.

5.1.2.11 Response Times. The excited coil L/R at R_0 = .02 Ω is ≈ 50 μsec which is consistent with the required response for the control system.

The required system response time of < 50 μs limits the L_0 of the passive coil to about 400 μH or 20 turns.

5.1.2.12 Coil Set. The final design included ten transmitting coils mounted concentrically with the side mounted control coils but inside the weldment. There were wound with thirteen turns of #12 copper rolled to approximately 0.030" x 0.12" over a 7.75" diameter form. After bonding with epoxy in a form, the coils were self-supporting and could be fixed by fiber tabs to the weldment.

In a similar fashion, the three passive coils were wound of 25 turns over a 5.125" diameter form. These were mounted via

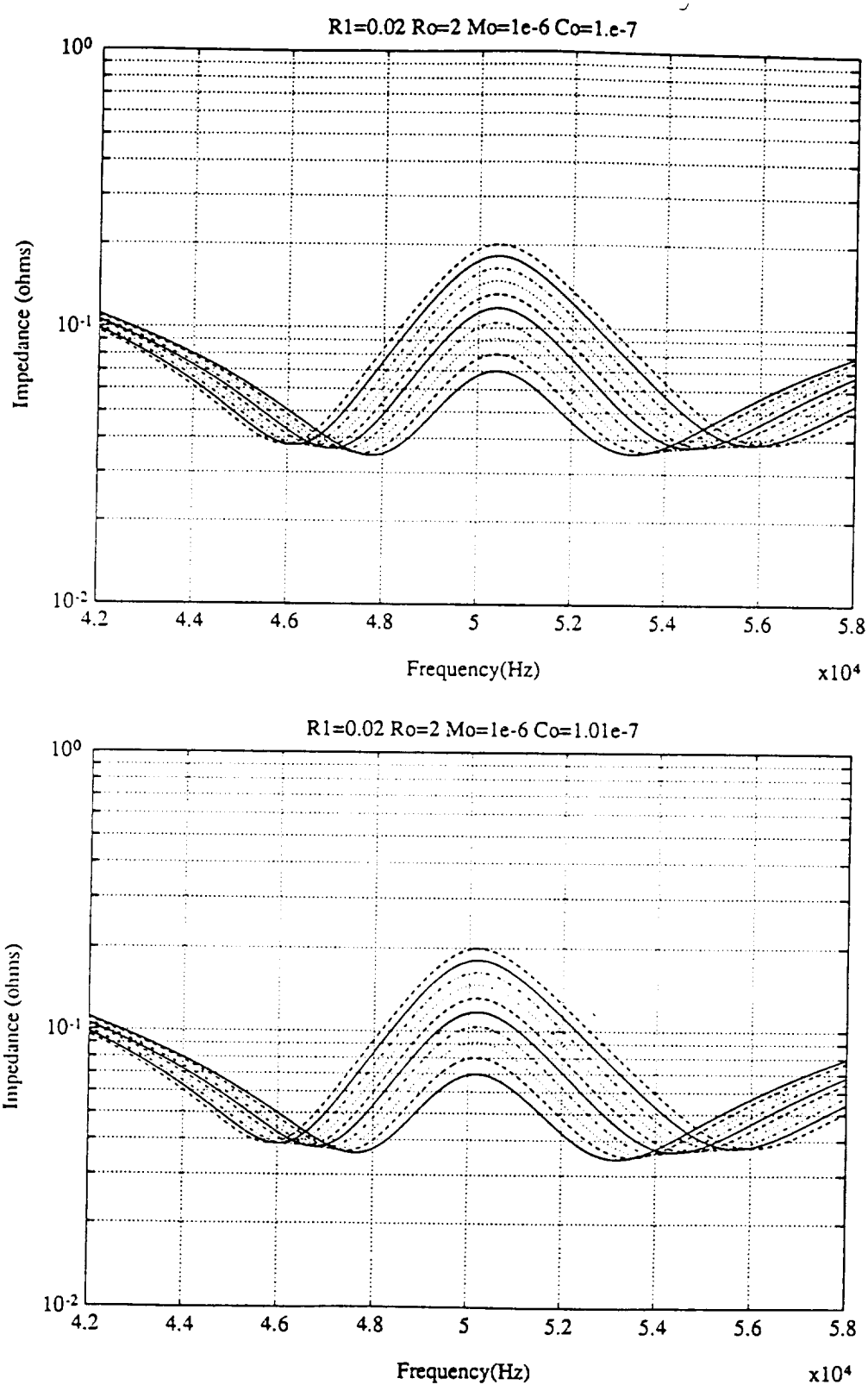

Figure 5.7. Variation in Response with 1% Capacitance Shift

tabulations on the magnet dewar concentric with and 135° on each side of the magnet axis.

5.1.2.13 Coil Excitation. Each transmitting coil-capacitor set was series resonant and driven with a constant current of about 0.02 A at 71.5 kHz. The ten sets were connected in series. The voltage across each coil was routed to the processor units described below where they were subsequently amplified, filtered, and demodulated for digitization by the DSP.

5.2 Transducer Performance

This section documents the process of verifying that the rotational and translational transducers operate as designed. The rotation and translation transducers are discussed separately.

5.2.1 Rotation Transducers

These transducers operate via the variation of the mutual inductance of two tuned coils. There are ten actively-excited "transmitting coils" mounted coaxially with the side control coils and three "passive coils" mounted on the cylindrical surface of the dewar. The ten transmitting coils are driven in series by a fixed-frequency oscillator with a constant current. The terminal voltage of each coil is used as the input to the sensor electronics described in some detail in Chapter 6.

This section discusses the steps which were taken to verify the operation of the transducers in conjunction with their electronics. Initially, the passive and transmitting coils were tuned with capacitors to the frequency of the oscillator. With the coils tuned, the outputs of the individual channels of the sensor electronics were calibrated with measured orientations of the passive coils.

5.2.1.2 Tuning of the Rotation Sensors. In this application, the "tuning" of the rotation sensors means simultaneous optimization of all adjustable components of the system. Referring to the block

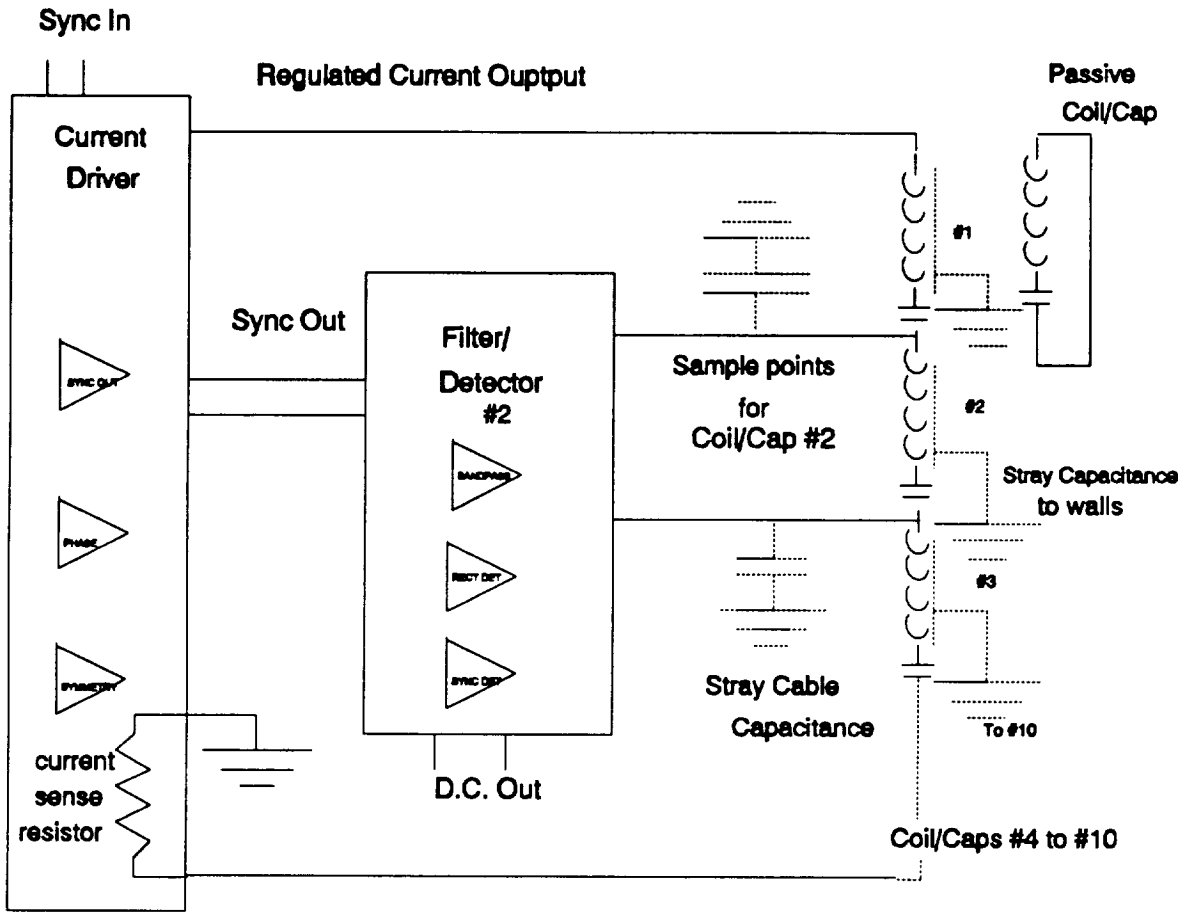

Figure 5.8. Block Diagram of Rotation Sensor System.

diagram of Figure 5.8, it can be seen that the number of adjustable components involved include:

1) The series capacitance of each of the ten transmitting coils

2) The capacitance of up to three passive coils

3) Regulated current from the driver

4) The phase and symmetry adjusts on ten driver boards

5) The output gain and bandwidth tune for each sensor channel

In addition, there are configuration options for the transmitting and passive coils, a choice of the sense of current flow around the coils, and the electronic detection mode - rectifier or synchronous phase.

If the response of each member of the ten coil set were identical to that of the two coils set used in the prototype tests, the obvious choice of configuration would be:

1) All ten coils in series with all currents in the same sense around coils

2) Use of synchronous phase detection channel for extended angular range

3) Use of one passive coil ("tail" coil) to simplify DSP processing for initial suspension tests but with the option for extension of all three passive coils. The additional information gained by use of all three would include roll angle.

The tuning process in this case was:

1) With the 71.5 kHz square wave supplied to the driver board by the DSP, adjust level for an undistorted current output of workable level

2) Adjust "symmetry" of output "sync" signal. This ensures that both positive and negative going components of the sensed waveform are integrated over the same time interval.

3) Adjust the "phase" control on the driver board so that square wave "sync" signal transitions occur at zero current crossing of the current waveform. This will assure peak D.C. output signal when RMS voltage is both maximum and in phase with current signal

4) Adjust bandpass filter on each channel processor board for maximum D.C. output at 71.5 kHz.

5) Find the series capacitance necessary to resonate each of the ten coil/capacitance sets. Capacitance can be varied with decade boxes. These are more lossy than the low dissipation polypropylene capacitors used in the final assemblies, but allow convenient determination of the optimum values. The optimum resonance is seen as the minimum RMS wave shape across each capacitance/coil set and should be low enough to show significant noise. Additionally the phase difference between this voltage and current should be close to zero.

6) Find the capacitance across each of the passive coils (closely placed to its corresponding transmitting coil) which gives the maximum in-phase voltage across the corr-esponding coil/capacitor pair. Since the current is fixed by the driver/regulator, the voltage is proport-ional to the impedance which should be real and a maximum

7) If any of the detector circuits saturate during these procedures, the drive current must be reduced to bring them out of saturation

8) The gains of the individual phase detectors are then adjusted to give identical peak values at maximum coupling between a passive coil and the sensed transmitter coil.

This procedure gave a usable range (single-valued with a resolution of greater than 0.1 volt/degree) of angular separation over 40°.

Examples of this response are shown in Figures 5.9 and 5.10 for each of the two detection modes. The data were obtained from two coils in series in the prototype test frame (Figure 5.11). Figure 5.9 shows the range with simple rectification detectors while Figure 5.10 shows the enhanced single-valued range obtainable with synchronous phase detection.

As can be seen in the data of Figure 5.12, obtained with the system tuned as described below, the range is about half that of the prototype. The lack of response near an angular displacement of 27°, which corresponds to a pitch of zero, precludes operation around the horizontal.

The strategy used to obtain more information is twofold. If the coil currents in adjacent coils are in opposite directions, the

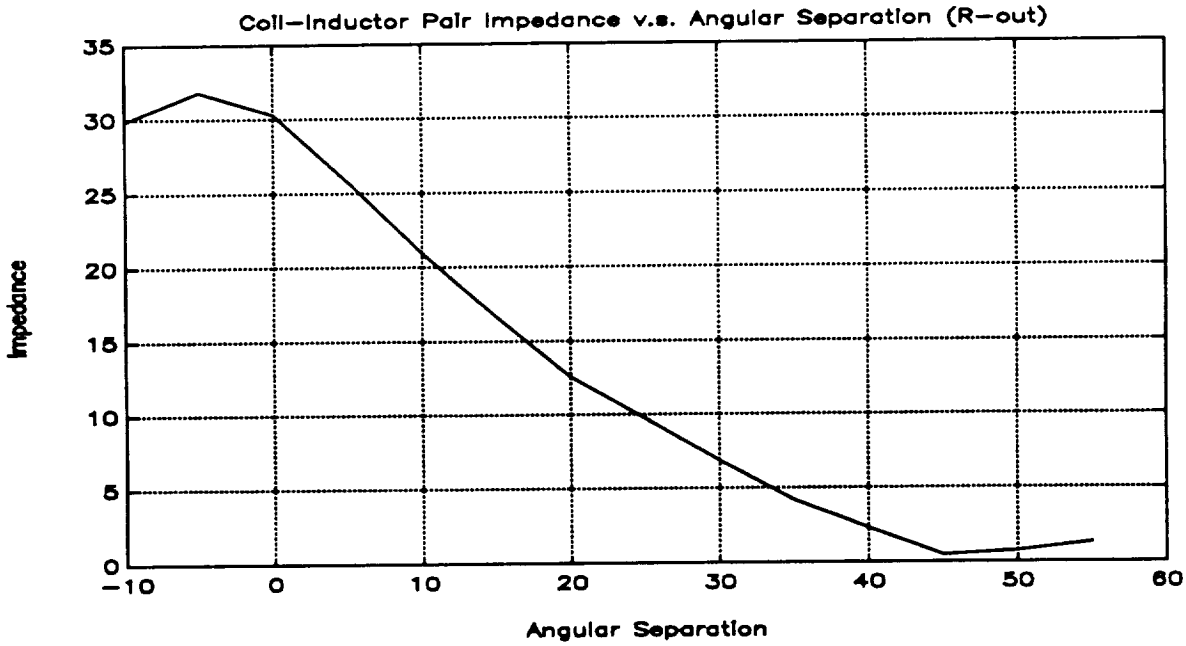

Figure 5.9. Response vs. Angular Separation for Rectifier Detection.

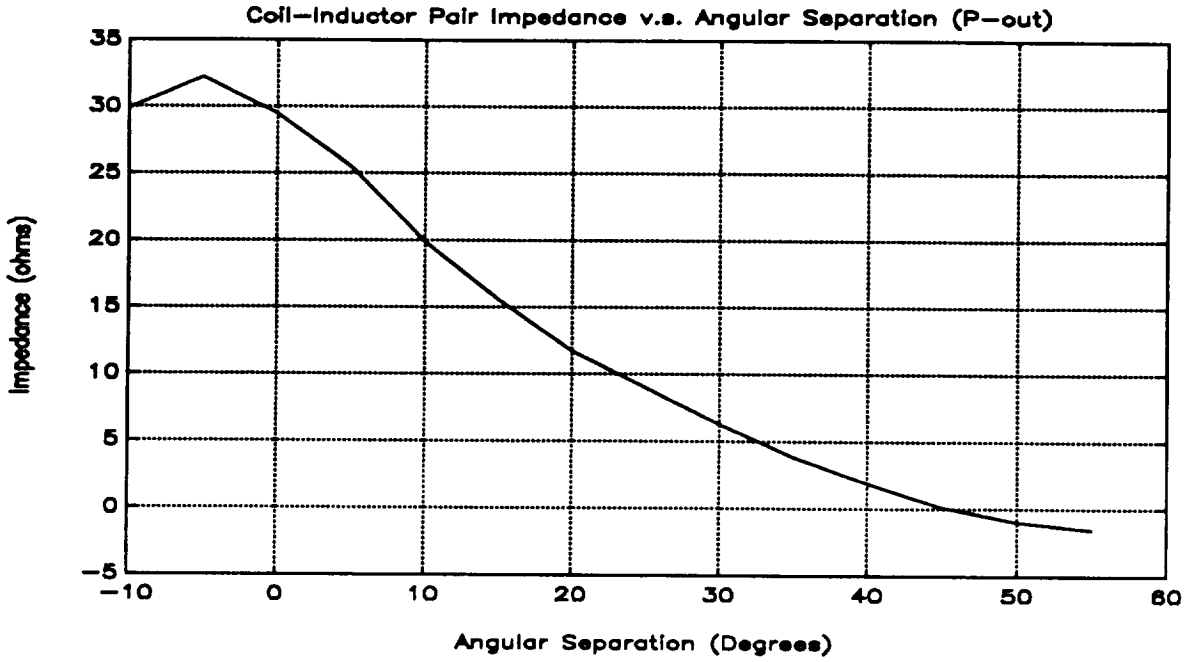

Figure 5.10. Response vs. Angular Separation for Synchronous Phase Detector.

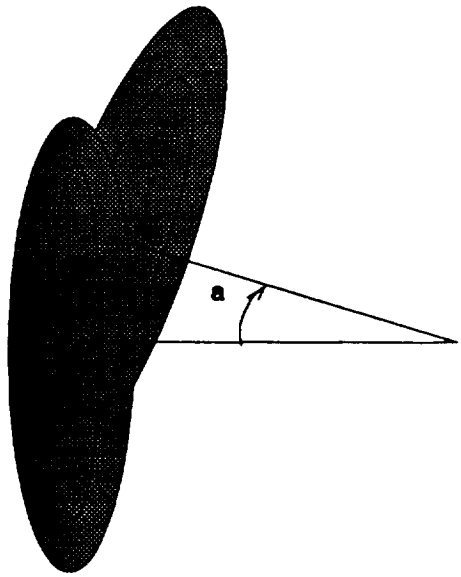

Figure 5.11. Geometry of coils used in obtaining the data of Figure 2 and 3. 'a' is the angular separation of the plots.

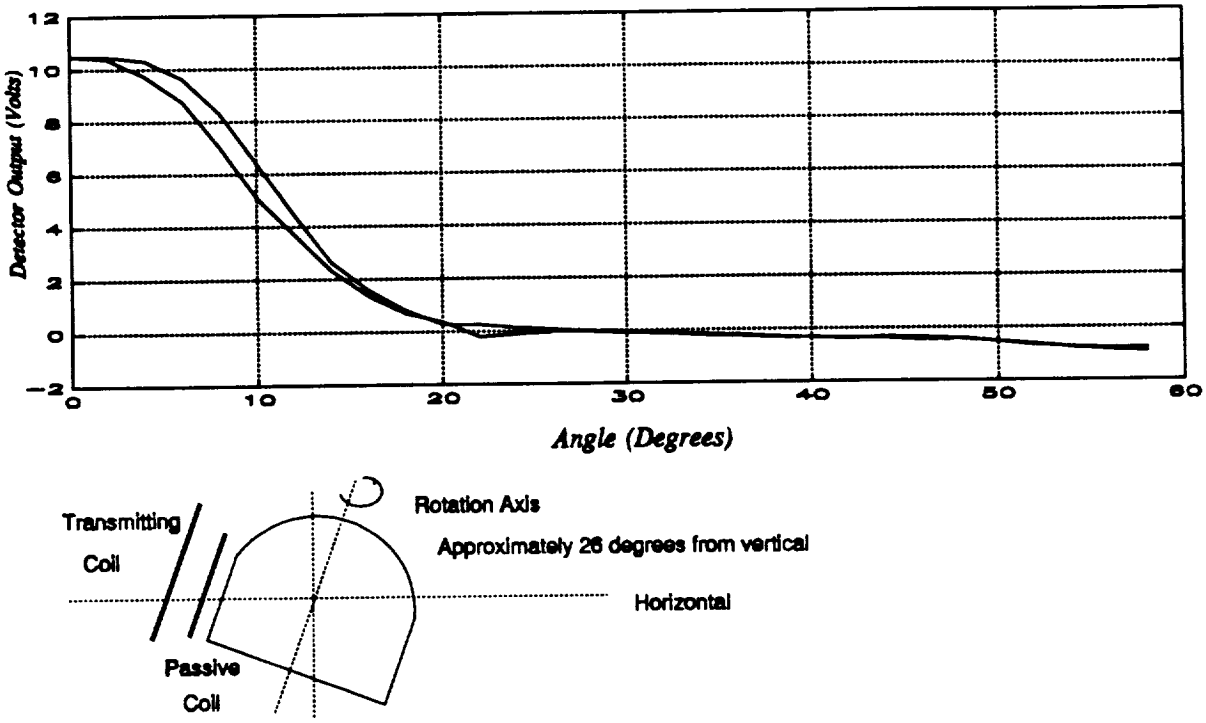

Figure 5.12. Response with East-West Rotation about Dewar.

flux in the region between adjacent is enhanced, not diminished, changing the monotonic fall of coupling between a passive coil and the transmitters. (There is the second option of using more than one passive coil which will give usable response from additional transmitting and a more unambiguous position determination.)

An example of this behavior is shown in Figure 5.13 which displays the response with the dewar upright (pitch of "zero"). The multi-valuedness make interpretation more difficult, however.

In order to tune for this configuration, certain steps in the procedure described above were altered in the following way:

1) The upper and lower coils are operated with currents in the opposite sense. This is simply achieved by reversing one set of leads.
2) The phase of the "sync" signal was adjusted along with the series capacitance of each transmitter to give the greatest range of detected signal level. This was done

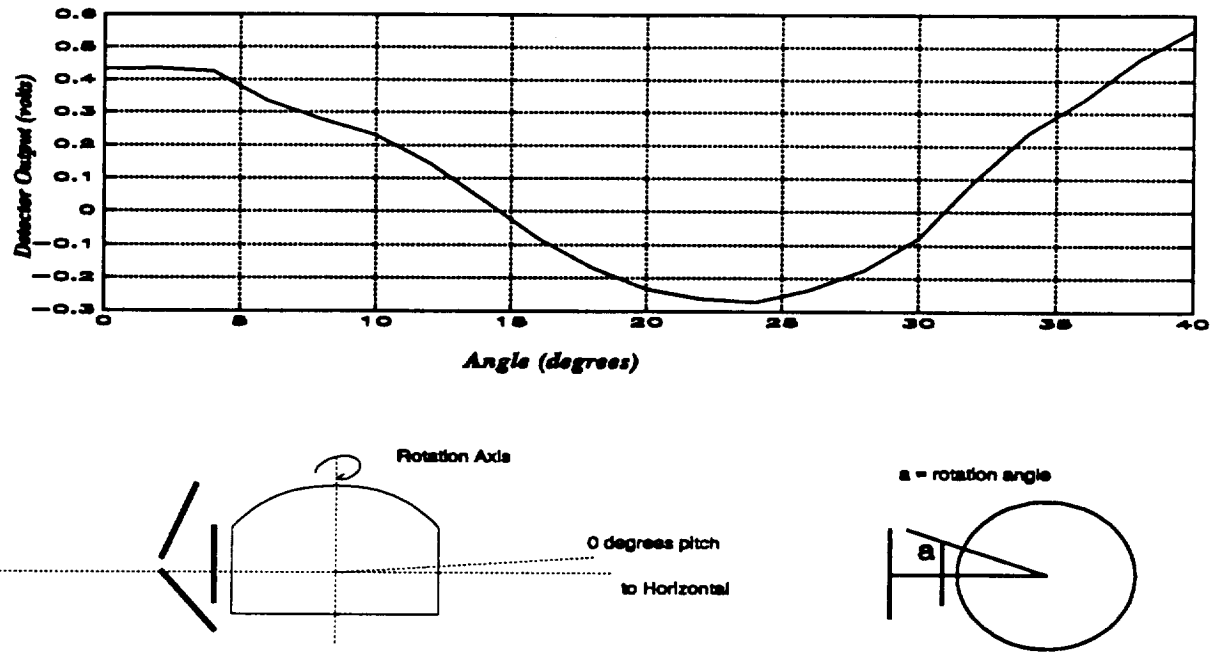

Figure 5.13. Response for Rotation above Dewar Apex with Zero Pitch.

by making a change and scanning the response with rotation of the dewar.

3) The bandpass adjust on each detector board was adjusted to give the first zero crossover in output at a convenient angle. Near 30° was chosen. This was set for all ten channels.

5.2.1.3 Calibration of the Rotation Sensors. It was necessary to determine the functional dependance of the impedance with angular separation with all coils operating and in place. Since the dewar had to be enclosed completely by the coil support weldment to achieve this, a procedure was developed which enabled both the rotational positioning of the dewar and the precise measurement of the angular coordinates.

First, a PVC ring support was fixed to the floor of the control coil frame. It was centered, machined to the correct height, and surfaced for supporting the dewar sphere at its suspended position with a minimum of friction.

Next, coil surfaces were marked with angles every two degrees for up to 60° in each direction of interest. These were made in an East-West great circle around the vertical axis of the dewar, a North-South great circle through the apex of the dewar, and an East-West circle or "latitude" 26° from the "equator" or mid-section gap between the two halves of the sphere.

An acrylic viewer able to be fit into the center bore holes of the control coils and marked with crosshairs was fabricated for sighting and reading the angular position.

A plastic nut with a centered hole was used to attach a passive coil to the dewar (Figure 5.14). The hole allowed a wire to be threaded through it and a hole in the acrylic viewer. Angular separation was calculated by measuring the length of the wire.

5.2.1.4 Calibration Results. The Calibration results are summarized in Figures 5.12 to 5.15 which exhibit the following features:

1) The maximum peak occurred for the passive coil centered approximately 6-7° South of the geometric centers of the control coils. The source of discrepancy is not known, but it is of little consequence since it can be canceled in software. This can be seen from Figure 5.15 in which the 0° refers to the alignment of the geometric centers between the passive coil and control coils.

2) The response curve falls twice as fast with angle as the prototype coil set. (Compare Figures 5.9 or 5.10 to 5.12 or 5.15)

3) Reversal of upper and lower coils currents gives a multivalued response for paths along the "equator". The interpretation of these responses in terms of an angle rotation algorithm will be addressed during the completion of the system integration.

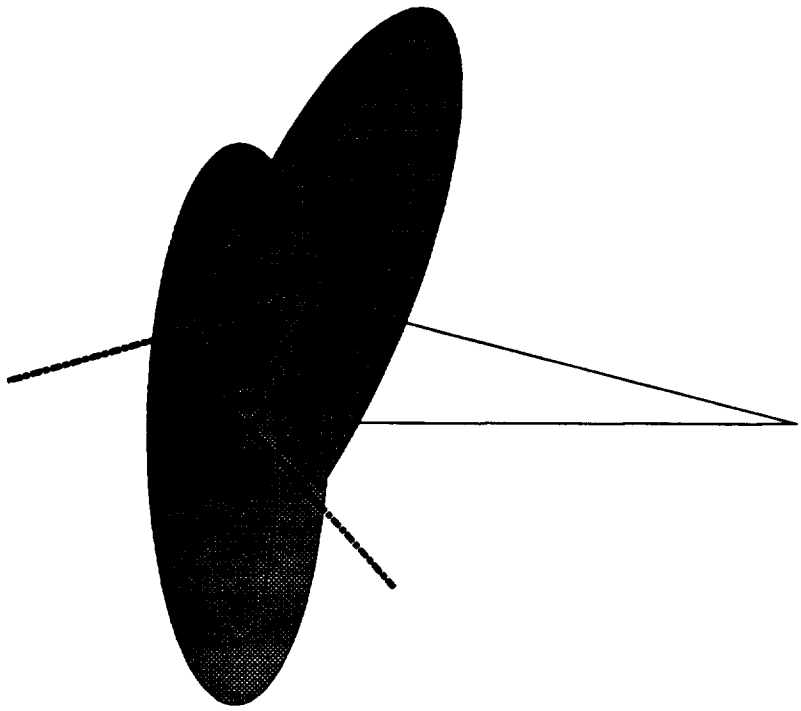

Figure 5.14. Measurement of Angular Separations with Wire Method.

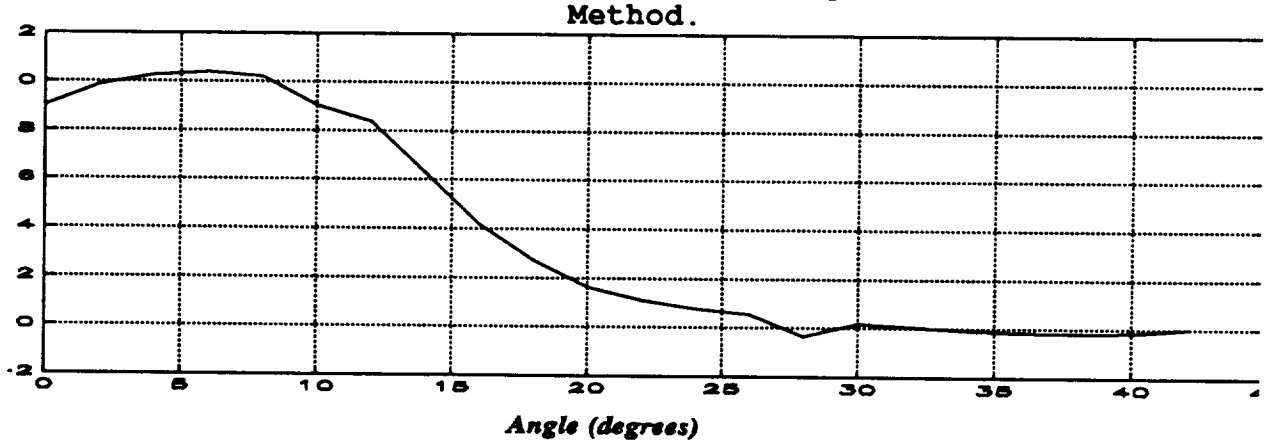

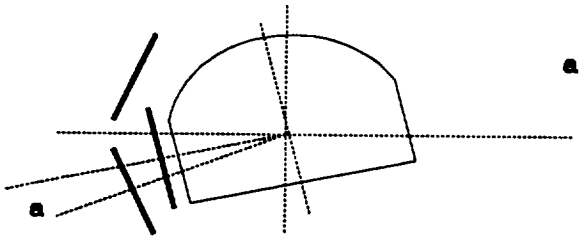

a = angular separation between geometrical centers of passive ant transmitting coils.

Figure 5.15. Response with North-South Pitch Change of Dewar. Angle is referenced to geometrical center of coils.

5.2.2 Translation Transducers

The translation transducers and their associated electronics are commercially-available from the Capacitec Corp. of Ayer, MA. They measure displacement by monitoring the capacitance of the air space between the transducer and the sensed surface (target). Each of the transducers is mounted along the axis of one of the lower control coils. The sensed surface is provided by a plastic sphere which surrounds the dewar.

5.2.2.1 Calibration Procedure. The calibration of the six capacitive sensors mounted at the center of the hexagonal faces of the lower half of the LAMS assembly have to be adjusted to have equal gains. The gain equalization is carried out to ensure that the displacement signals generated by each sensor can be read-in and processed directly by the control software without having to rescale each signal. The gain value is also adjusted to ensure that the sensor output voltage over the desired displacement range is compatible with the input range of the A/D convertor of the control computer I/O card.

An aluminum block with a step of 0.06" was constructed as a reference. The gain equalization procedure was carried out by reading the sensor output when reacting (i) against the flat face of the aluminum block (ii) against the 0.06" step. The capacitive sensor being linear over a range of 0.1", the output voltage difference for a known displacement of 0.06" gave the sensor gain. The calibration potentiometer on the charge amplifiers was used to equalize gains of all the sensors.

5.2.2.2 Calibration Results. All the sensors were calibrated to a nominal value of 90V/inch with a maximum deviation of 1% between individual sensor gains.

6. SYSTEM ELECTRONICS

In the simplest sense, the requirement for the LAMS system electronics is that they interface between the position sensors and the control coils in order to implement the algorithm required for proper control of the superconducting source coil in five degrees-of-freedom. This chapter discusses the design of these electronic components. Figure 6.1 shows the block diagram of the baseline control electronics with a DSP at its core.

6.1 Digital Signal Processor

The active control of the LAMS suspension will be via a Digital Signal Processor (DSP). The Texas Instruments (TI) TMS320C30 floating point DSP was chosen due to its capabilities as well as SatCon's experience with TI's DSPs and TI's support. This DSP has a rated capacity of 33 MFLOP/sec. The Spirit30 DSP board and development system by Sonitech International was selected for use in the superconducting LAMS system.

This section documents the process which lead to the selection of a DSP board for use as the LAMS system controller. The architecture of the control system is first reviewed in order to provide general requirements for the DSP. Commercially-available DSP boards are then identified. Finally, the results of the evaluation of a sample are reported.

6.1.1 DSP Requirements

The LAMS suspension algorithm is designed for stability and control in the local coordinate frame of the superconducting element. The local coordinate frame remains fixed with respect to the superconductor but, of course, rotates and translates with respect to the laboratory fixed coordinate frame. The control gains of the control coils as defined in the local coordinate frame vary with the orientation angles Θ_z and $\Theta_{x'}$. The gain variations are sinusoidal in nature.

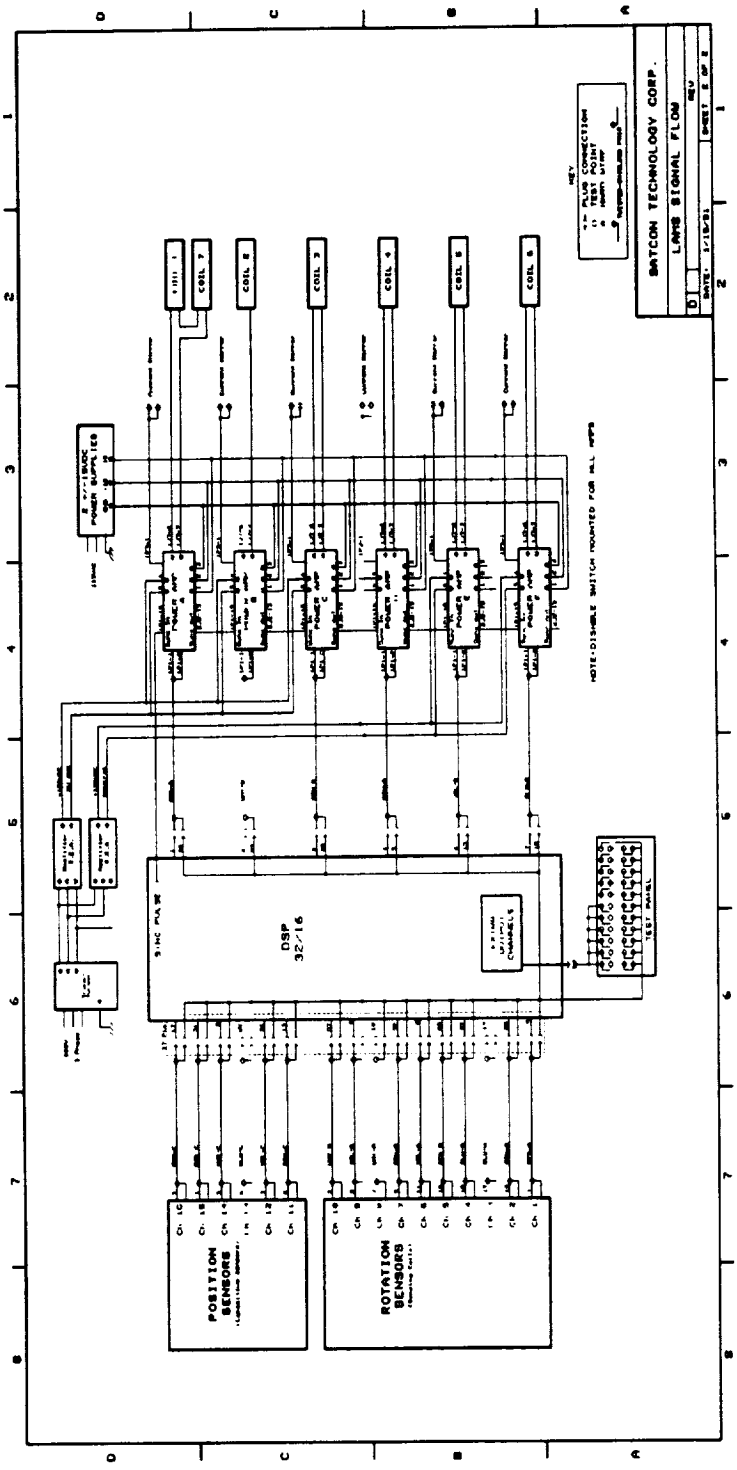

Figure 6.1. System Wiring Diagram

The control algorithm has three major functional blocks as described below.

(1) Data input and control signal output: This function is handled by the I/O boards in coordination with the DSP processor board.

(2) Transformation to and from the laboratory fixed to the superconductor local coordinate frame: This applies to transforming the displacement and rotation data as well as the control signals. The elements of the transformation matrices are sinusoidal functions of the orientation angles Θz and $\Theta x'$. Hence the transforms are essentially calculation of sine and cosine angles and matrix multiplications.

(3) Execution of the Kalman filter and the control algorithm in the superconductor local coordinate frame: This is mainly a series of matrix multiplications.

The computationally intensive actions are the evaluations of the sine and cosines of the Euler angles (Θ_z, $\Theta_{x'}$), taking products of these and performing matrix multiplications. The matrix multiplications are greatly assisted by the "multiply and add" instruction processing. The DSP architecture is optimized for such operations. However calculation of sine, cosines, the evaluation of the matrix elements and the data management and manipulation overheads will not be greatly assisted by the DSP architecture.

6.1.2 Available Options

In the selection of a Digital Signal Processor (DSP) board, the basic requirements were a strong development system and multiple Input/Output (I/O) capability. The Spirit30 DSP board made by Sonitech International was evaluated for use with the LAMS. A similar DSP board by Spectrum Research will not be available

until the middle of June 1990. Because of time constraints, the decision was not postponed to accommodate the late delivery of the Spectrum DSP board.

6.1.3 Evaluation of Sonitech Spirit30

The development system was found to be user friendly and to have many good and flexible features. Display of data memory in several formats (Hex, Integer, Floating Point etc) and the capability to plot acquired data were some of the features. The debugger provided a window display of the DSP's internal register set along with disassembled code. The capability to modify registers and program memory is also provided. The debugger is interrupt driven which eliminates the use of INT0 from the user and makes it more difficult to debug any interrupt driven code. The debugger was also fairly slow taking a few seconds to update the screen when using Single Step mode. Overall the development system had no major faults and those areas that were not ideal could be dealt with.

6.1.3.1 I/O Compatibility. Sonitech International's I/O compatible cards use serial data transfer between the I/O card and the DSP card. The configuration of the DSP card only allows for two serial channels thus limiting I/O capabilities. Sonitech did provide a parallel I/O connector for use with other vendors I/O cards particularly Spectrum Signal Processors. Sonitech claimed compatibility with the Spectrum I/O bus. Upon inspection of the two vendors busses the Sonitech bus had some minor differences and one major fault. Pin 11 of the Sonitech bus was connected to +5 Vdc and should have been GROUND. The other minor differences would not effect compatibility. The Sonitech Spirit30 board was connected to a Spectrum four channel I/O card after removing pin 11 from the Spirit30 connector. A simple echo program where an input signal is sampled and then echoed back was written. This program did not initially work due to the I/O strobe pulse width. A software delay was added to increase the I/O strobe pulse width

from 60 to 120 nanoseconds and the echo program ran successfully. This software delay was easily implemented due to the programmable wait state feature of the TI TMS320C30.

6.1.3.2 Multiple I/O Card Compatibility. Next three of the Spectrum four channel I/O cards were connected to the Sonitech Spirit30 card. The echo program was modified for the three cards but did not run. With the three I/O cards connected the Spirit30 card failed its own self test and the debugger could not be initialized. It was found the Sonitech Spirit30 board had brought out some clock signals unbuffered from the DSP to the I/O connector. It is believed that by hanging a long (18 inches) cable on the clock signals caused ringing which corrupted the data being clocked into the memory on the Spirit30 card. The clock pins on the I/O bus were not being used by the four channel I/O cards. The pins on the connector were removed and the echo program ran successfully. Sonitech was very supportive in helping to debug the problems that were found.

6.1.3.3 Other Features. The controller will be required to carry out a substantial amount of matrix multiplications. The C compiler supplied by Texas Instruments and some user routines supplied by Sonitech will be used. The availability of the SPOX operating system on the Sonitech board will provide assembly routines for doing these operations. However the overheads costs imposed by the SPOX operating system in relation to the LAMS application are not clear.

6.2 Power Amplifiers

This section presents the analysis of the requirements for the LAMS power amplifiers and provides the rationale for the selection of the Copley Controls Corporation Model Number 230H. The requirements analysis proceeded in sequence of four steps. These are itemized below and are summarized in the paragraphs which follow.

1) Determine the inertial properties of the suspended body (superconducting magnet, dewar, dewar enclosure, and associated hardware)

2) Determine the natural time constants (expressed as unstable system eigenvalues) of the unstable modes of the system. This included looking at both 12- and 6- coil operation as well as considering operation with the magnet in several attitudes.

3) Determine the corner frequencies of the control coils and compare these with the unstable frequencies.

4) Determine the excitation required to provide steady (levitation) and control current to the control coils.

6.2.1 Inertial Properties

Significant effort has been undertaken to calculate the mass distribution and inertia of the cryostat assembly. To assure an accurate result, each structurally continuous component of the assembly has been broken into a series of primitive structures (sphere, cylinder, ring, etc.). Inertia matrixes of each primitive structure could be easily calculated using commonly known formulae. For some unusually shaped parts of the cryostat (cryostat cap, big coil support structure, etc), specific expressions have been derived. Finally all partial matrixes have been combined yielding the results which are presented in Table 6.1.

6.2.2 Unstable Eigenvalue Calculation

The mutual inductance model was used to calculate the range of excitation and unstable time constants for the 12- and 6- coil LAMS over a range of Euler angles given by Θ_z= 0-360°, $\Theta_{x'}$= +-60°.

6.2.2.1 Steady Currents. The weight of the suspended mass (for a dewar and helium mass of 23.69 kg) is 232.4 Newtons. The control

Table 6.1. Cryostat Inertial Properties

Rotational inertia: (principal axis)	$I_{x'} = .362$ kg m^2 $I_{y'} = .337$ kg m^2 $I_{z'} = .407$ kg m^2
Total mass:	M = 23.75 kg (with He)
Mass center position:	$x' = 0.0$ m $y' = -0.0042$ m $z' = -0.0061$ m

coil excitation (expressed in ampere turns) required to support this weight at $\Theta_z = 36°$ and different values of $\Theta_{x'}$ were calculated. The orientation ($\Theta_z = 36°$) is the worst case current regardless of the value of $\Theta_{x'}$. For the 6-coil case, however, the difference is only 10% over those at $\Theta_z = 0°$ and these values were used. Tables 6.2 and 6.3 contain the steady currents required to support the weight of the suspended mass with 12 and 6 coils respectively.

Table 6.2. Steady Currents (12-Coil LAMS)

Angle $\Theta_{x'}$, degrees	30	60	90
I_{17o}	4,765	2,980	46
I_{28o}	-1,163	- 136	-1,098
I_{39o}	- 302	1,415	2,887
I_{410o}	- 302	1,415	2,887
I_{511o}	-1,163	-1,136	-1,098
I_{612o}	-2,743	-4,112	-3,621

6.2.2.2 Eigenvalues. The system eigenvalues were calculated under the assumption of a static load of 270 Newtons. This weight corresponds to an earlier, more conservative estimate of the mass of the suspended body.

Table 6.3. Steady Currents (6-Coil LAMS)

Angle Θ_x, degrees	30	60	90
I_{1o}	4,295	--	0
I_{2o}	-4,812	--	0
I_{3o}	- 392	--	3,483
I_{4o}	-3,200	--	2,123
I_{5o}	-2,895	--	-2,123
I_{6o}	- 80	--	-3,483

Tables 6.4 and 6.5 contain the system eigenvalues (expressed in radians per second^2) under this steady load condition.

Table 6.4. System Eigenvalues (12-coil LAMS)

Angle Θ_x, in degrees	30	60	90
Eigenvalues			
	-34.1	-91.7	94.6
	34.1	91.7	-94.6
	68.8	-13.9	0.0
	-68.8	13.9	- 0.0
	0.0	0.0	0.0
	0.0	- 0.0	0.0

Table 6.5. System Eigenvalues (6-coil LAMS)

Angle Θ_x, in degrees	30	60	90
Eigenvalues			
	239.4	-	0.7
	-230.6	-	0.2
	- 85.6	-	- 54.6
	40.1	-	168.3
	3.5	-	101.6
	0.0	-	0.0

6.2.3 Control Coil Characteristics

The time constants of the control coils were found, using Stefan's formula for self-inductance of a circular coil with rectangular cross-section [Eq. 90 in E. B. Rosa and F. W. Grover, "Formulas and Tables for the Calculation of Mutual and Self-Inductance", Bulletin of the Bureau of Standards, vol. 8, no. 1],

$$L/N^2 = \mu_0 a\{[1 + (3b^2+c^2)/9a^2]\ln[8a/(b^2+c^2)^{1/2}] - y_1 - b^2y_2/16a^2\}$$

where:

a = the mean of the outer and inner radius,
b = the length,
c = the difference between the outer and inner radius, and
y_1, and y_2 = functions of b/c (tabulated in Rosa and Grover).

This formula is accurate to better than 1% when the coil length is less than its outer diameter. For all of the control coils, a = 3.75 inches and c = 3 inches. For the side coils, b = 1 inch, y_1 = .737 and y_2 = .207, while for the top and bottom coils, b = 2 inches, y_1 = .828 and y_2 = .443.

The resistance of the coils is given by:

$$R/N^2 = 2\pi\rho_c a/\eta bc$$

where:

ρ_c = the resistivity of copper and
η = is the fill factor, (taken to be 0.7).

The quotient of the inductance and resistance per turn squared is the corner frequency of the coils. This quantity is independent of the number of turns N. Table 6.6 contains these quantities. The time constants of the control coils are shorter than those of the system instabilities, but on the same order.

Table 6.6. Control Coil Characteristics

Inductance / Turn^2 (L/N^2)	
Top and Bottom Coils	0.158 μH
Side Coils	0.183 μH
Resistance / Turn^2 (R/N^2)	
Top and Bottom Coils	4.59 μΩ
Side Coils	9.18 μΩ
Time Constant (L/R)	
Top and Bottom Coils	0.034 seconds
Side Coils	0.020 seconds

6.2.4 Amplifier Requirements

The amplifier requirements are estimated by modelling the excitation as superposed steady (DC) and sinusoidal-steady-state (AC) currents (ampere-turns). The DC current levels were taken from Tables 6.2 and 6.3 corrected for the more conservative estimate of the weight of the suspended body. The amplitude of the AC current was set equal to the DC current level. This requires that the amplifiers be able to deliver a 100% margin over the estimated DC level. The frequency of the AC current was set at 10 times the frequency which corresponds to fastest unstable time constant of the system.

The terminal voltage (per turn) required to deliver these currents (ampere turns) consists of that required to overcome the DC resistive (per turn^2) and AC impedance (also per turn^2) at the excitation frequency. The product of the DC current and voltage is the static power required for suspension. The product of the maximum instantaneous current and maximum instantaneous voltage is the rating of the power amplifier. For the case of the 12-coil LAMS, the rating must be doubled since one amplifier will drive two coils in series. Table 6.7 presents the results of the analysis. These conservative requirements were later relaxed to reduce development risk as discussed in the next section.

Table 6.7. Amplifier Requirements

	Twelve-coil LAMS			Six-coil LAMS	
Angle $\theta_{x'}$ (degrees)==>	30	60	90	30	90
Unstable Frequency (Hz)	1.3	1.5	1.5	2.5	2.1
AC Frequency (Hz)	13.2	15.2	15.5	24.6	20.6
Top Coils					
DC Excitation (A)	5,539	3,464	N/A	4,992	N/A
AC Excitation (A, pk)	5,539	3,464	N/A	4,992	N/A
Total Exc. (A, max)	11,078	6,928	N/A	9,984	N/A
DC Excitation (V)	0.025	0.016	N/A	0.023	N/A
AC Excitation (V, pk)	0.077	0.055	N/A	0.124	N/A
Total Exc. (V, max)	0.102	0.071	N/A	0.147	N/A
Static Power (W)	141	55	N/A	114	N/A
x 2	282	110	N/A	N/A	N/A
Ampl. Power Rating (VA)	1,134	490	N/A	1,468	N/A
x 2	2,267	979	N/A	N/A	N/A
Side Coils					
DC Excitation (A)	3,188	4,780	4,209	5,593	4,049
AC Excitation (A, pk)	3,188	4,780	4,209	5,593	4,049
Total Exc. (A, max)	6,377	9,560	8,417	11,186	8,098
DC Excitation (V)	0.029	0.044	0.039	0.051	0.037
AC Excitation (V, pk)	0.057	0.095	0.084	0.166	0.103
Total Exc. (V, max)	0.086	0.138	0.123	0.218	0.140
Static Power (W)	93	210	163	287	150
x 2	187	420	325	N/A	N/A
Ampl. Power Rating (VA)	547	1,324	1,035	2,437	1,136
x 2	1,095	2,647	2,069	N/A	N/A

6.2.5 Power Amplifier Selection

The power amplifiers were chosen based on the worst-case peak-virtual-power 2650 VA for the side coils in the twelve-coil configuration at $\theta_{x'} = 60°$. This value was required for a control excitation at ten times the unstable-frequency equal to the steady-state excitation level. At this virtual-power level, there are basically two candidates for the power amplifier: a linear device from Techron, Inc. of Elkhart, IN and a switched type from Copley Controls of Newton, MA. At this rating, the Techron amplifier

(Model 7570) costs $3,300 and weighs 100 lbs, while the Copley device (Model 240H) costs approximately $1000 (each amplifier shares a common input transformer and rectifier), and weighs about 20 lbs. The switching power amplifier is also extremely efficient with a worst-case dissipation of 40 watts while the linear device would dissipate kilowatts. The disadvantages of the Copley unit are three-fold: 1) it has only 1 kHz bandwidth versus 30 kHz for the Techron; 2) its output waveform is 300 volt peak-to-peak, Pulse-Width Modulated; and 3) it requires a minimum value of load inductance.

Since the bandwidth required of the current source for these control coils is about 150 Hz, the 1 kHz power amplifier bandwidth is not a problem. Also, the inductance of the control coils, when wound for these voltage levels, will be well above the 300 μHy required load inductance. Thus, the only drawback to the Copley Controls device is the high-voltage switched output. The potential problem with this waveform is that it can couple high-frequency energy into the signal leads of the position sensors, or those of other low-level signals. In addition, the angular position sensor operates on the principal of variation in mutual inductance between two large-diameter coils. The large area enclosed by these coils makes them highly susceptible to radiated fields.

Based on the potential risk of interference with proper system operation, the decision was made not to use the Model 240H power amplifier, but to use a Copley Controls Model 230H which employs internal filtering of the switched waveform. This unit is still light (25 lbs.), efficient (100 Watts maximum power dissipation), and less expensive than the linear version ($1600 per channel). Its power capability is however reduced to 2250 VA, with a continuous rating of 10 amperes. This necessitates redesigning the control coils for reduced current and reducing the required control excitation. The remaining, significantly reduced risk of coupling will be minimized by synchronizing all six power amplifiers so that there is only one switching frequency, and by physical separation of the power and signal leads to the maximum extent allowed by the

test configuration. The Model 230H has no minimum load-inductance requirement, and has a current-source bandwidth of over 10 kHz.

The complete power amplifier system consists of six Model 230H amplifiers, a common mounting plate with rectifier, filter capacitor, and reverse-energy absorbing snubber, and a three-phase 60 Hz transformer capable of 4,500 Watts continuous output.

6.3 Position Sensing Electronics Subsystem

This section describes the operation of the position sensing electronics subsystem. The subsystem consists of two major components: a driver board, which drives the position sensing coils with a low distortion sinusoid at a controlled current level, and a set of ten receiver cards, which measure the induced voltage in each of ten sense coils. In operation, the sense coils are connected in series, so that only one driver is needed. Coil reactances are canceled by resonating each coil with a capacitor in series. The remaining impedance is low, nearly resistive, and for a given sense coil depends primarily on the relative position of the shorted-turn probe-coil.

6.3.1 Driver Card

The driver card receives a 71 kHz square wave at TTL level, and generates a low distortion (ca 0.02 %) sine wave current output. The output level is sensed on the current return path by a ten ohm resistor to ground. The sensed current is rectified and used to control the output drive current at a desired value. The output current level can be varied between 10 and 100 mA peak-to-peak, using an onboard control ("Drive").

The sensed current is also used to generate a phase-synchronous square-wave output, used as the reference by the synchronous detector on each of the receiver cards. Two other controls on the driver card ("Phase" and "Symmetry") provide minor corrections of the square-wave output waveform. Two square-wave output signals are provided, in normal and inverted polarity, as required by the receiver cards. Individual outputs are HCMOS

compatible and each capable of driving a 10 mA load. In normal operation, each pair is intended to drive five of the receiver cards. Outputs should be transmitted to the receiver cards using shielded, twisted pair cable.

The driver card consists of the following:

1) **Line receiver/square-wave generator** (Z8, Z9, Z10A, Z13, VR1). The receiver (Z13) regenerates the TTL source signal while isolating the local ground from source ground, to protect from possible noise coupling. The receiver output drives a current switch (Z8), whose DC input is generated by reference VR1, and summing amplifiers Z10A and Z9 resulting in a bipolar square wave which is filtered to eliminate both high-frequency harmonics and low frequency level-correction transients.

2) **Three bandpass filters tuned to 71 kHz** (Z1-Z2, Z3-Z4, and Z5-Z6). These filter the square-wave output from the reference generator, producing a low distortion sine wave at 71 kHz. Multiple low-Q filters are used (Q = 5) in preference to a single highly selective filter, whose transient response might affect system dynamics more severely, and for which tuning would be more critical.

3) **Output driver** (Z7 and Q1-Q2). This circuit amplifies, the sinusoid, and has output capability up to 20 volts pk-pk and up to 100 mA pk-pk. A voltage amplifier is used in preference to a current driver, to allow convenient damping of the parallel resonance caused by cable capacitance and the sensor coils. Constant coil-current is obtained by automatic level correction of the voltage output using the sensed coil current, together with high output impedance at the drive frequency (71 kHz).

4) **71 kHz Output filter** (R26, R26A, R27, R27A, L1, C22, C22A). This passive tuned-circuit blocks the residual distortion at the driver output, and provides a relatively high output source impedance to the sensor coil assembly at the drive frequency, to enhance constant current operation. The filter is presently located on the driver board for convenience, and its components chosen to provide relative insensitivity to moderate values of cable capacitance (< 1 nF). If long cable runs are required (> 10 meters), it may prove desirable to locate the output filter at the sensor coil assembly.

5) **Level Correction circuitry** (Z10B and Z11). Z11 rectifies the drive current measured across resistors R43 and R43A, in the sensor coil return path. The rectified signal output is compared with the desired level at the input of integrator Z10B, whose output correction is summed into the square wave generator's input signal. The required correction range has been deliberately limited since the bandpass filter and output driver gains are well-determined. Output levels are intended to be correct to +/- 20 %, even without the level correction circuit.

6) **Square wave regenerator** (Z14, Z15, Z16) Amplifier Z14 amplifies the sensed current measured by R28/R28A summing it with an offset correction provided by the "Symmetry" control, R64. To correct for amplifier and comparator delays, a small, adjustable phase lead is provided by C36 and the "Phase" control, R60. The resulting signal is clipped (to protect Z15's input), then converted to TTL levels by comparator Z15. Z16 provides two sets of buffered output pairs, in normal and inverted sense.

It is assumed that the sense coils have been individually tuned at 71 kHz, using series capacitors, and connected to series.

1) Connect sense coil assembly to Output connector J2. Connect signal processor cards to Sync connector J3 (cards may be connected in tandem: 5 cards/output pair).

2) Power up the board, and apply 71 kHz TTL to input J1.

3) Adjust "Drive" control R32 for desired current through sense coils, using an external current probe to measure sense coil current, or measuring the voltage developed across R28/R28A (10 ohms). In general, the drive level should be adjusted so that the voltage developed across L1 substantially exceeds (100 x or more) the voltage across any one sense coil/capacitor.

4) Using an external differential amplifier (or the input stage of a receiver card) observe the voltage developed across one of the sense coil/capacitors. The observed voltage should be sinusoidal, with no visible distortion, for any setting of the probe coil position.

5) Using a dual trace oscilloscope, with matched channel time delays, observe the sense coil current on one channel, and either of the buffered (SYNC)H signals on the other. Synchronize the horizontal scan to the (SYNC)H signal for both traces. Adjust the "Symmetry" control until (SYNC)H spends equal time intervals high and low. Now adjust the "Phase" control until the transitions of (SYNC)H coincide with the zero crossings of the coil current. Verify similar waveforms on the other Sync signal outputs.

6.3.2 Receiver Card

The receiver cards have been built as printed circuit boards, one receiver channel per board. Ten cards are normally used, to accommodate the ten sense coils used for position sensing. Eight

adjustment options have been provided, three of which have been implemented as trimpot adjustments, and five as trims using selected fixed resistors. The latter are identified in *italics*.

The receiver cards measure AC voltages developed across each of the coil/capacitor combinations in the sense coil assembly. Two detector channels are provided: a full-wave averaging rectifier, which is insensitive to phase, and a synchronous detector, which measures AcosØ, where A is the average signal amplitude, and Ø the phase difference between the signal input to the detector, and the external synchronizing signal generated by the driver card and supplied to the "Sync" input.

The receiver cards are required to deal with a number of possible error sources. As noted above, the inductive reactance of each of the sense coils is canceled by resonating it with a series-connected capacitor. At resonance, the source impedance of each coil/ capacitor is quite low, consisting of series coil and capacitor losses, the induced impedance from the probe coil, and residual reactive components if the tuning is imperfect. Off resonance, the reactance can be substantial, and has the effect of emphasizing drive signal distortion components. There is also a common-mode signal at the drive frequency, which is larger for those coils near the top of the chain.

Each receiver card consists of the following:

1) **Differential Input Amplifier** (Z1A). This circuit amplifies (x10) the differential signal sensed across each coil/capacitor source, while providing about 60 dB common mode rejection. Protection diodes are provided for fault conditions in which the input signal levels exceed 15 volts. A resistor slot (R6A) and two capacitor slots (C1 and C2) have been provided for trimming low and high frequency common mode rejection.

2) **Bandpass filter** (Z1B, Z2). The bandpass filter provides additional (x3) gain at the frequency of operation, while

rejecting off-frequency noise and distortion. The filter uses a state variable active design, and includes adjustments to trim frequency (R10: "FREQ"), *and bandwidth (R 14: "BW").* The filter design is deliberately broadband, so that the dominant poles of the receiver are caused by the detector output filters. 3db bandwidth is preset to around ±4 kHz.

3) **Full Wave Rectifier and Filter** (Z3, Z4). The rectifier converts the average value of the bandpass filter output to a scaled DC value, adjustable over a 2.5:1 range by a trimpot (R31: "RGAIN"). *Additional corrections for offset are provided by trims "ROFF1" and "ROFF2". These are normally pretrimmed using fixed resistors to reduce DC offsets contributed by Z3 and Z4 to less than 1 mVolt when no signal is present.* The rectifier output is filtered to minimize ripple by a two-pole Butterworth filter (Z4A) with a cutoff frequency of approximately 1200 Hz. A voltage divider is provided at the output for load.

4) **Sync Receiver** (Z5). This comparator receives the synchronizing signal supplied to the "Sync" input by the driver card, while isolating the source ground from the local card ground. Normal and inverted sync phases are required. Normal operation uses TTL levels, however the receiver is sensitive enough to accommodate signal levels down to 1/2 volt. These may be used to reduce system noise levels. A small delay (ca 50 ns) is introduced by the comparator. This is normally compensated by adjusting the "FREQ" tuning control to maximize output at the synchronous detector.

5) **Synchronous Detector and Filter** (Z6, Z7, Z8): This is a phase sensitive demodulator. Its DC output is

proportional to AcosØ, where A is the average signal amplitude input to the demodulator, and Ø is the phase of the input relative to the square wave synchronizing signal supplied to the "Sync" input. Gain of the synchronous detector is adjusted using a trimpot (R59: "SGAIN"). *Offset trims are also provided: R47 :"SOFF1" adjusts the offset of Z7B to equal that of its opposite phase channel, Z7A, within 1/2 mV. Difference amplifier Z8A subtracts the two, eliminating the offset. R56: "SOFF2" provides offset correction for the difference amplifier and output amplifier, Z8A,B. Both offset trims normally use selected fixed resistors to reduce output offset to < 1 mV total error, when no signal is supplied to the rectifier. Use of trimpots is optional.* The rectifier output is filtered by a two-pole filter identical to that used by the full-wave rectifier. Identical output protection is also provided.

6) **5 volt regulator** (Z9): supplies regulated 5 volt power required by Z5 and Z6.

It is assumed that the driver board has been properly set up, and the sense coils have been tuned for series resonance at the 71 kHz drive frequency. As a convention, connect the inputs so that +Vin is on the side of the sense coil/capacitor pair nearer the driver output.

1) Power the board.

2) Verify output offsets: should be < 1 mV with input connector pins shorted together.

3) Verify LF common mode rejection: apply 100 Hz 10 volts pk-pk sinusoid to J1 pins 2 and 3. Observe Z1/1. 100 Hz signal should measure less than 0.1 volt pk-pk. LF CMRR

is trimmed by adjusting the balance of the input resistors. Holes for trim resistor R6A have been provided.

4) Verify HF common mode rejection: apply 71 kHz 10 volts pk-pk sinusoid to J1 pins 2 and 3. Repeat # 3 above. Holes for trim capacitors C1 and C2 have been provided, to optimize HF CMRR.

5) Adjust bandpass filter frequency: connect the Sync signal from the driver card to connector J2 "Sync". Connect J1 to its appropriate sensing coil. Apply 71 kHz drive to the driver card input. Turn "SGAIN" fully CW. Now adjust "FREQ" to maximize the synchronous detector output.

7. CONTROL SYSTEM

The controller for the superconducting LAMS was implemented on the Spirit30 DSP. This chapter documents the development of that controller, beginning with the basic modelling of the plant. The approach to exciting the control coils to obtain the desired forces and moments is presented. The heart of the control system is a set of five single-input-single-output (SISO) compensators. The implementation of these on the DSP is also presented.

7.1 Superconducting LAMS Modelling

The models described here are aimed towards quantifying the LAMS dynamics and defining a control strategy to suspend the superconducting source coil.

The LAMS geometry normally consists of twelve (12) coils arranged in a dodecahedral arrangement. A six-coil geometry consisting of the lower half of the dodecahedron, referred to here as a "Half Bowl", will be considered for the first step of the program. The discussion presented below will be with reference to this Half Bowl configuration. The arrangement of the control coils is with reference to the X,Y,Z coordinate system which is shown in Figure 7.1. The coils exhibit a symmetry for rotation around the Z axis. The coil geometry repeats every 72°. The coil numbering is as shown in the figure with coil [1] parallel to the XY plane.

The geometry is described with reference to the fixed coordinate frame (XYZ). The superconducting coil is described with reference to the X'Y'Z' i.e. the local coordinate frame. The XYZ and X'Y'Z' axes are nominally taken to be coincident. The Euler angle rotations (Θ about the Z axis and ϕ about the X' axis) which describe the orientation of the source coil are shown in Figure 7.2. A coordinate transformation (Γ) applied to the superconducting source coil geometry in the X'Y'Z' frame transforms it to the XYZ frame.

The magnet model was used to derive parameters of interest to the control system design. There are two principal items of

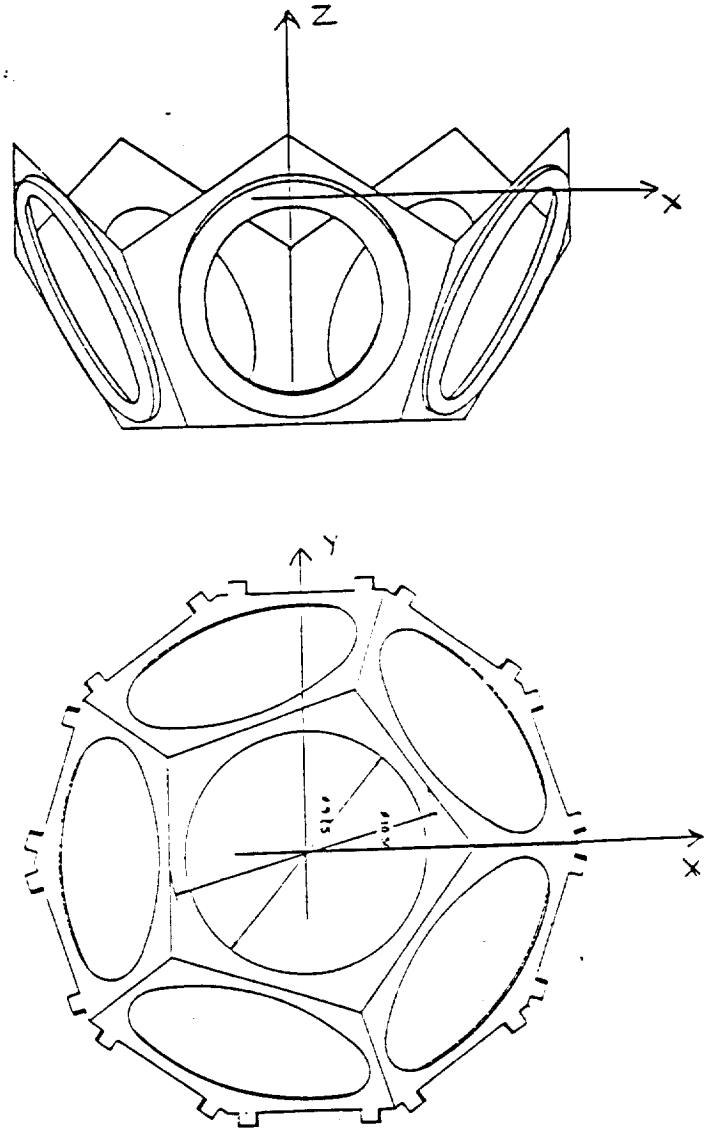

Figure 7.1. "Half Bowl Configuration

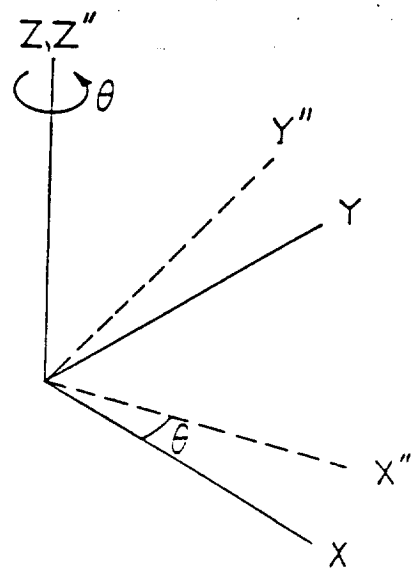

Θ rotation around the Z axis to give the intermediate axis X",Y",Z". Z and Z" remain coincident.

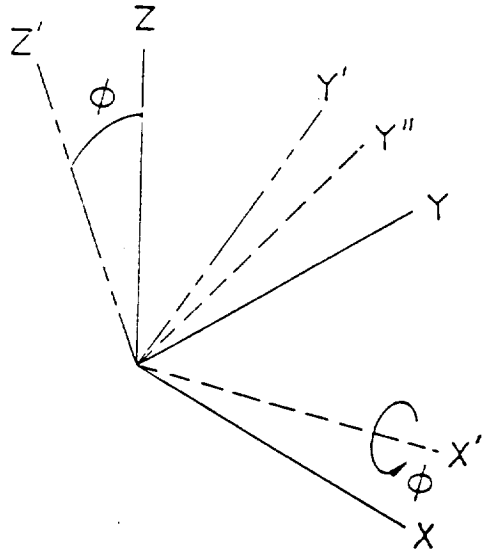

ϕ rotation around the X" axis to give the axis X',Y',Z'. X" and X' remain coincident.

Figure 7.2. Euler Angles

interest. These are the stiffness and control coefficients which are described below.

7.1.1 Stiffness Coefficients

These are defined as the coefficients relating incremental forces generated as a result of incremental displacements ($\Delta x', \Delta y', \Delta z'$) along the X'Y'Z' axes and incremental rotations ($\Delta\alpha', \Delta\gamma'$) around the X' and Y' axes of the superconducting coil.

7.1.2 Control Coefficients

These are defined as the coefficients relating the incremental forces along the X'Y'Z' axes and torques around the X' and Y' axes on the superconducting coil as a result of incremental changes in the excitations to the control coils.

The coefficients are derived with reference to the coordinate frame X'Y'Z' as the controller will operate essentially in this frame as described below. Figures 7.3(a) through 7.3(d) show the variations in the four of the stiffness coefficients ($K_{z'z'}$, $K_{x'x'}$, $K_{y'y'}$ and $K_{x'y'}$) as a function of variation in Θ from 90-270° with ϕ kept constant at 90° i.e. the superconducting coil rotates in the XY plane. The coefficient variations are shown over the range 0-180°. The stiffness coefficients at some orientation Θ and ϕ of the superconducting coil are the second derivative of the system magnetic energy (E). The energy is a function of orientation (Θ, ϕ), the control coil excitations (i_1, i_2, i_3, i_4, i_5, i_6), and the superconducting coil excitation (i_{sc}).

$$K_{z'z'} = \partial^2 E/\partial z'^2$$
$$K_{x'x'} = \partial^2 E/\partial x'^2$$
$$K_{y'y'} = \partial^2 E/\partial z'^2$$
$$K_{x'y'} = \partial(\partial E/\partial x')/\partial y'$$

The stiffness coefficients at a particular orientation were calculated with control coils excited to support the weight of the superconducting source coil in a 1g environment.

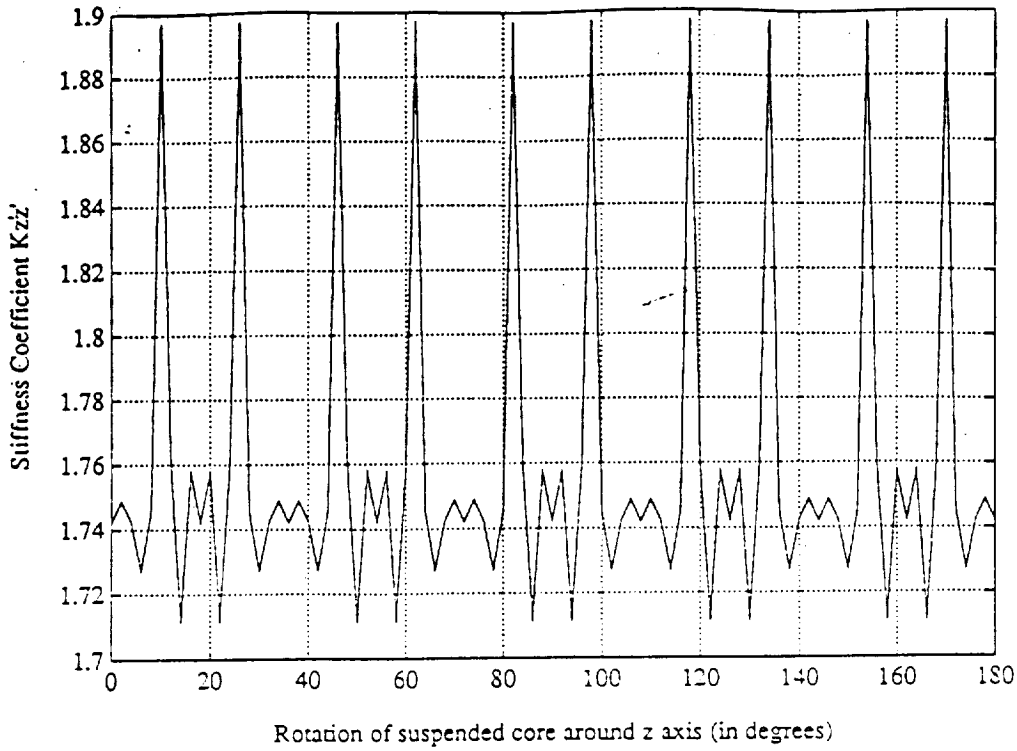

(a) Z′ Axis

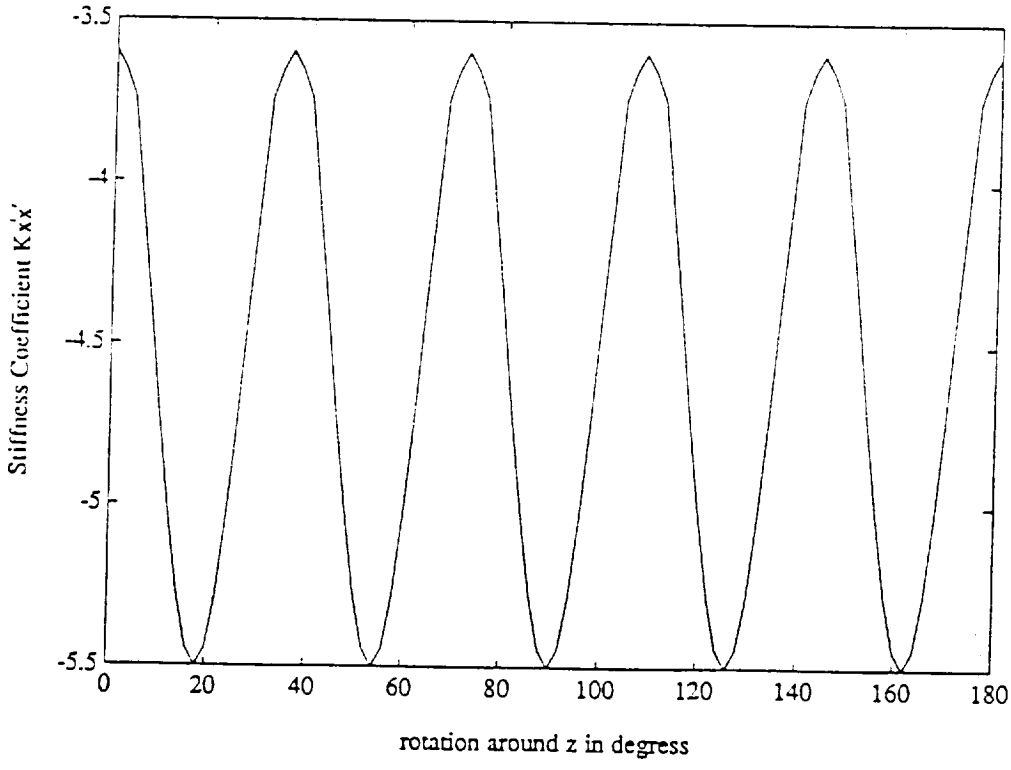

(b) X′ Axis

Figure 7.3. Stiffness Coefficients

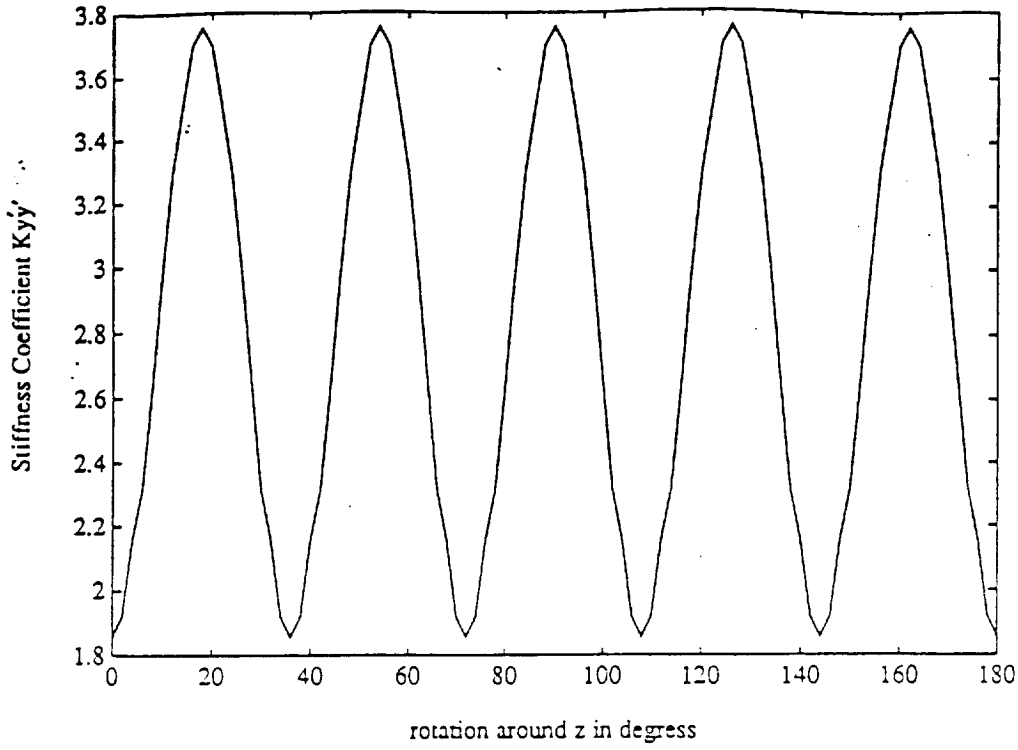

(c) Y′ Axis

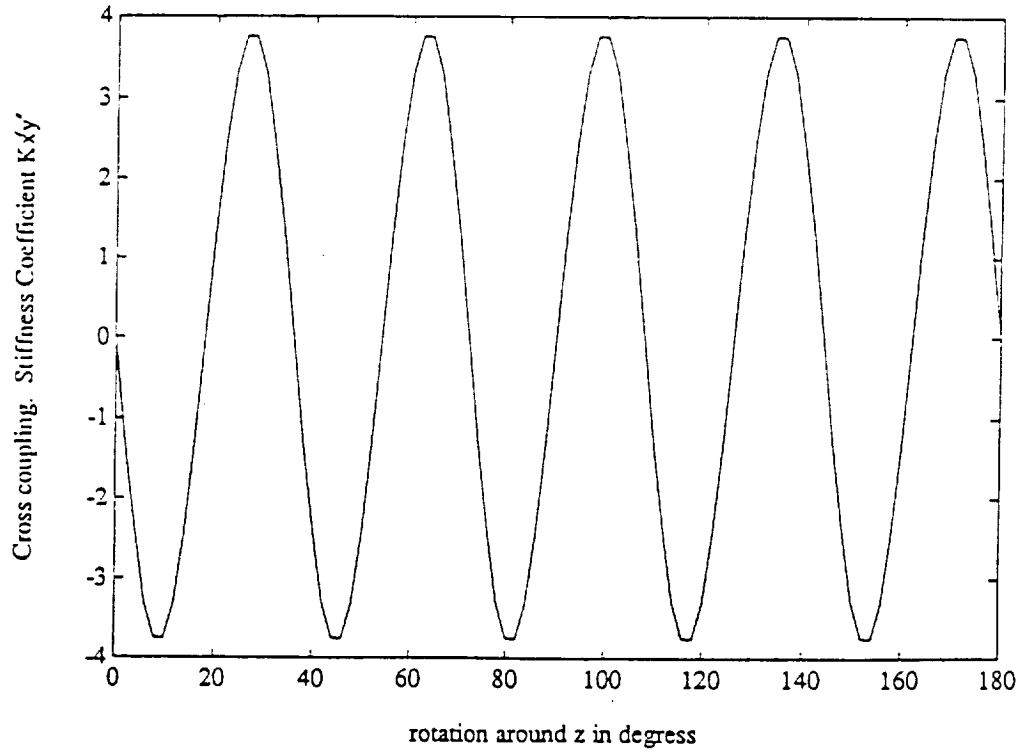

(d) X′, Y′ Cross-Axes

Figure 7.3. Stiffness Coefficients

The variations are seen to be large and nearly sinusoidal with the cross-coupling term ($K_{x'y'}$) comparable in magnitude to the direct stiffness term. The symmetry is interestingly enough 10 fold as compared to the five-fold symmetry of the coil configuration. The odd number of coils leads to doubling the symmetry in the stiffness variations. Cross-coupling terms other than $K_{x'y'}$ are small.

Figures 7.4(a) and 7.4(b) show the variations in the currents required to support the weight of the source coil ("levitation" currents) in coils [1], [2] and [3] as a function of variation in Θ from 90-270° with ϕ kept constant at 90° i.e. the superconducting coil rotates in the XY plane. The variations are all seen to be sinusoidal.

Figures 7.5(a) and 7.5(b) show the variation in the control coefficients ($K_{fx'i2}$, $K_{fx'i3}$, $K_{fy'i2}$, and $K_{fy'i3}$) for coils [2] and [3] i.e. the influence or effectiveness of coils [2] and [3] in generating incremental forces ($\Delta f_{x'}$ and $\Delta f_{y'}$) to control the orientation of the superconducting coil along the x′ and y′ axis. These control coefficients are second derivatives of the system energy (E).

$$K_{fx'i2} = \partial f_{x'}/\partial i_2 = \partial(\partial E/\partial x')/\partial i_2$$
$$K_{fx'i3} = \partial f_{x'}/\partial i_3 = \partial(\partial E/\partial x')/\partial i_3$$
$$K_{fy'i2} = \partial f_{y'}/\partial i_2 = \partial(\partial E/\partial y')/\partial i_2$$
$$K_{fy'i3} = \partial f_{y'}/\partial i_3 = \partial(\partial E/\partial y')/\partial i_3$$

where

i_2, i_3 = excitations in control coils [2] and [3].

Figure 7.6(a) shows the variation in levitation current of coils [1], [2], and [3] as a function of variation in ϕ from 0-90° with Θ kept constant at 90° i.e. the superconducting coil starts from a vertical position and rotates to end up in the XY plane. These are also seen to follow a sinusoidal variation with a discontinuity near the vertical orientation. Figure 7.6(b) shows the corresponding variation in the control coefficients ($K_{fz'i1}$,

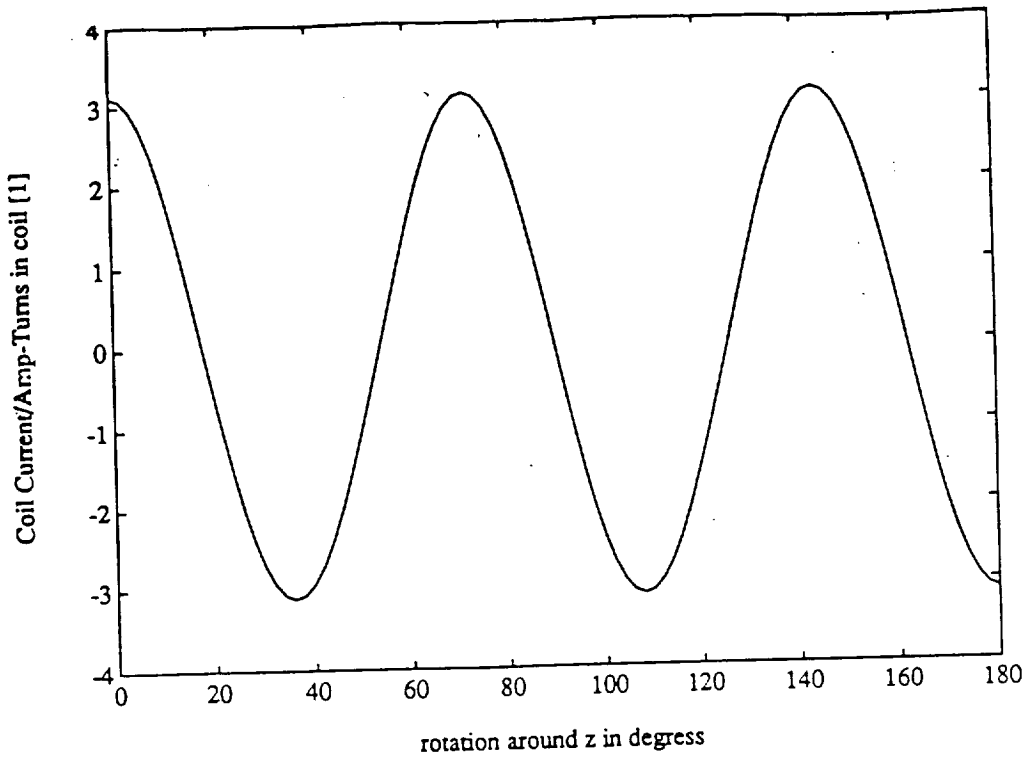

(a) Coil [1]

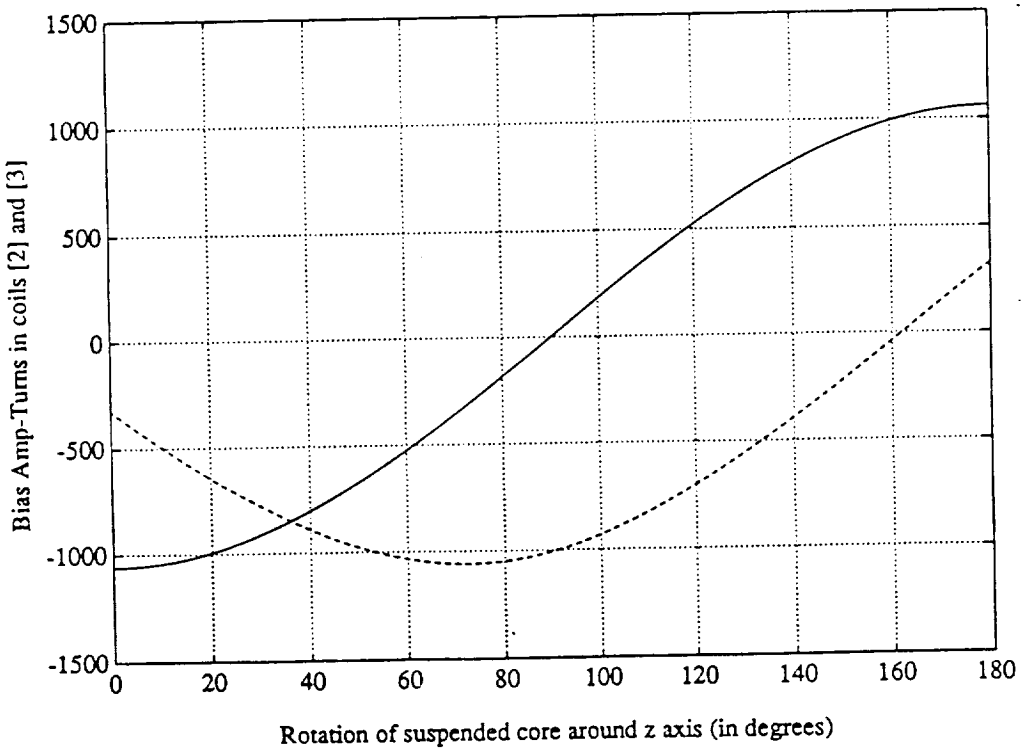

(b) Coils [2] and [3]

Figure 7.4. Levitation Currents

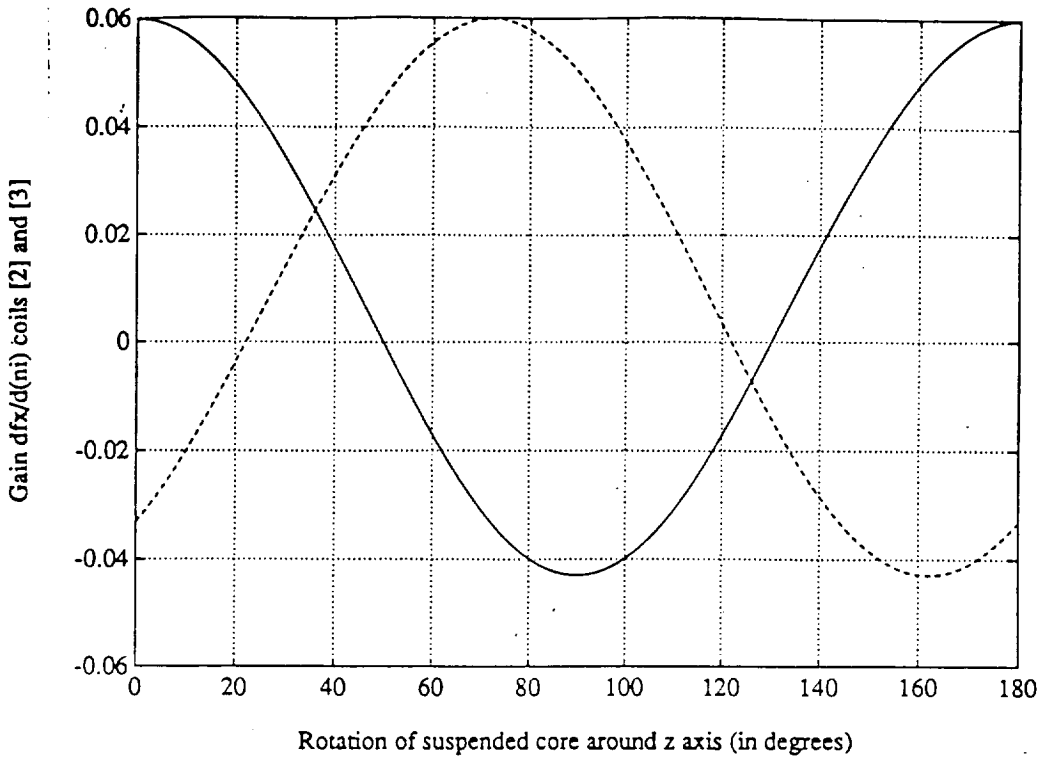

(a) X' Axis

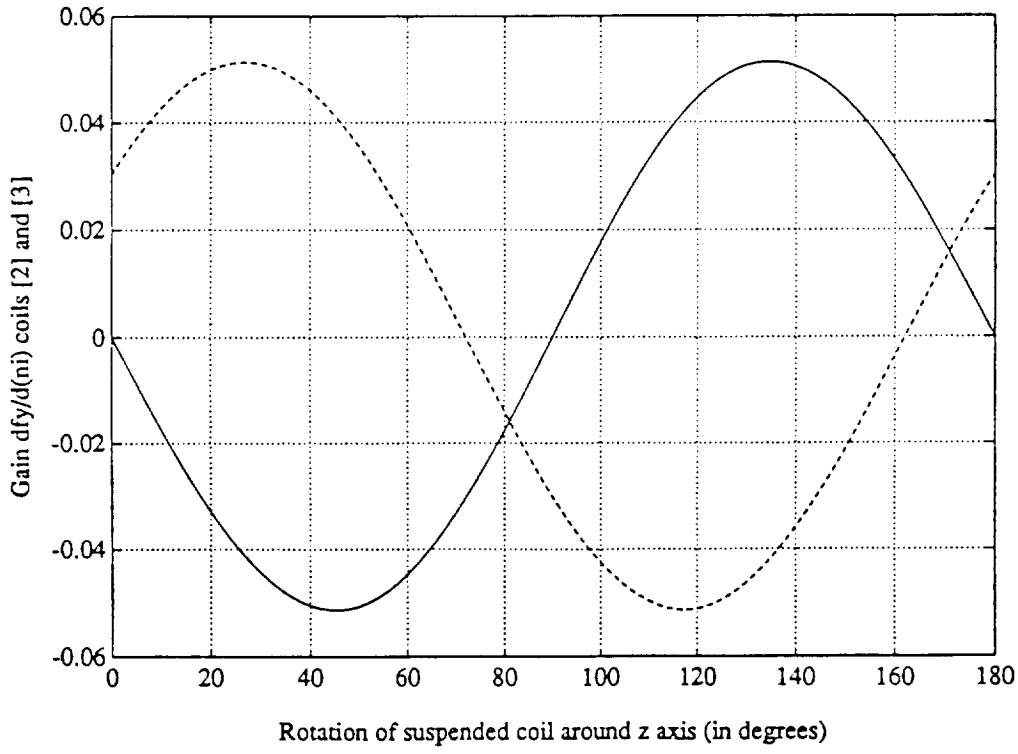

(b) Y' Axis

Figure 7.5. Control Coefficients

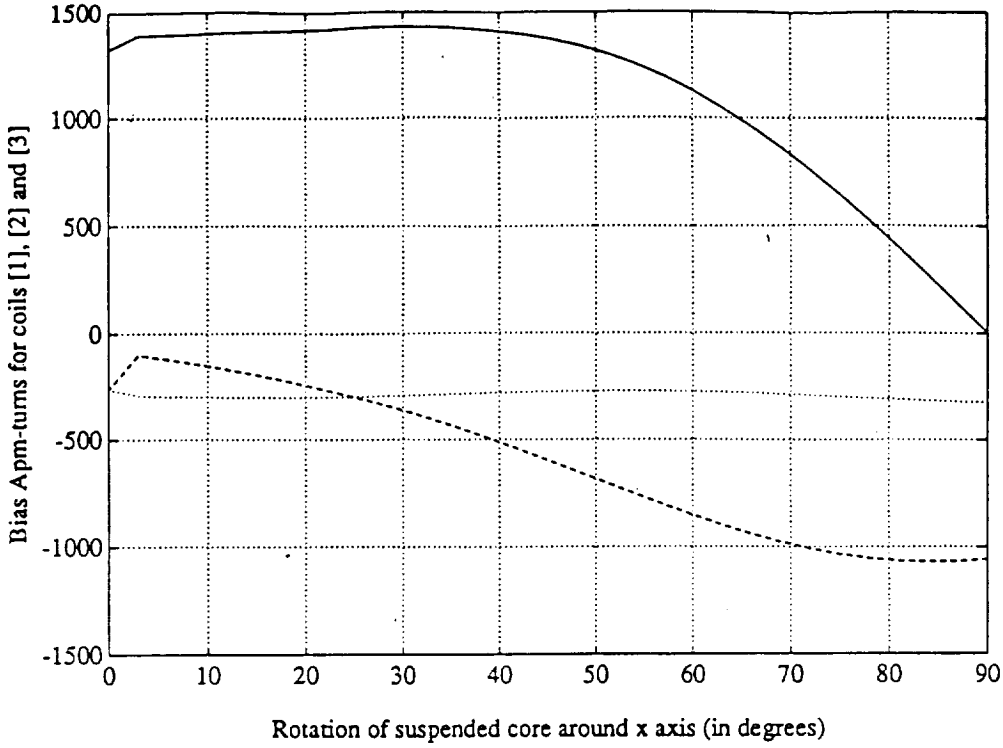

(a) Levitation Currents

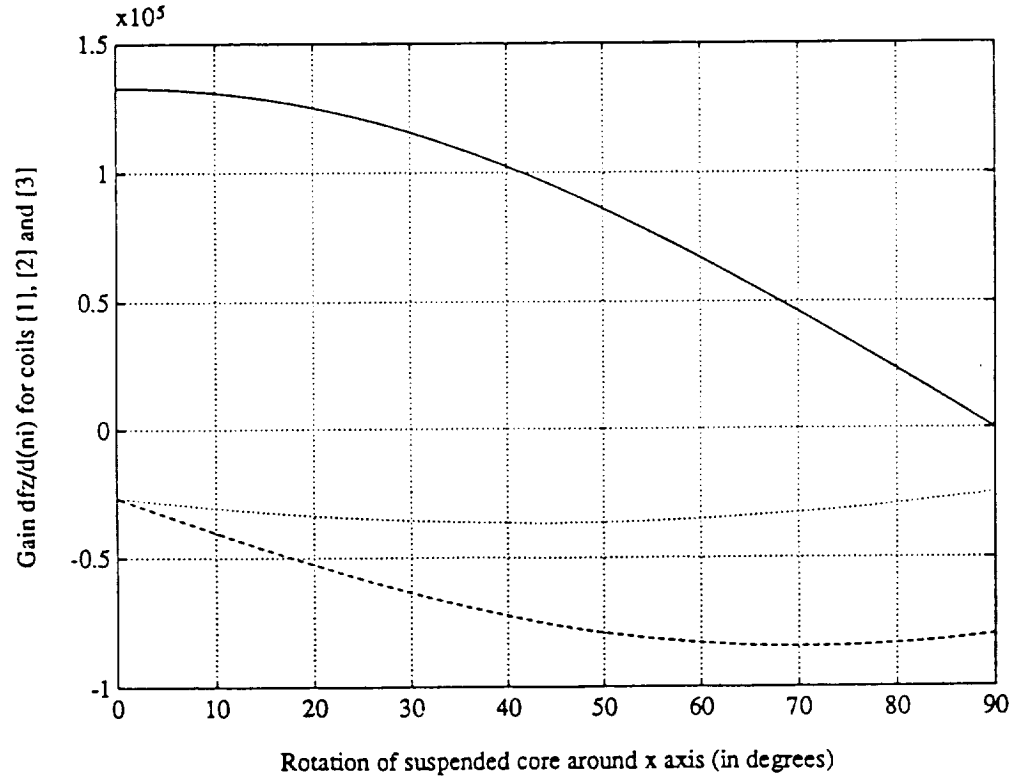

(b) Control Coefficients

Figure 7.6. Variations with X Axis Rotation

$K_{fz'12}$, $K_{fz'13}$) for coils [1], [2] and [3] i.e. the influence or effectiveness of coils [1], [2] and [3] in generating incremental forces $\Delta f_{z'}$ to control the orientation of the superconducting coil along the z' axis. These are stated below:

$$K_{fz'11} = \partial f_{z'}/\partial i_1 = \partial(\partial E/\partial z')/\partial i_1$$
$$K_{fz'12} = \partial f_{z'}/\partial i_2 = \partial(\partial E/\partial z')/\partial i_2$$
$$K_{fz'13} = \partial f_{z'}/\partial i_3 = \partial(\partial E/\partial z')/\partial i_3$$

The variations are all seen to be sinusoidal.

A control scheme regulating the incremental displacements $(\Delta x', \Delta y', \Delta z')$ along the X'Y'Z' axes and incremental rotations $(\Delta\alpha', \Delta\gamma')$ around X'Y' axes will need to take into account the variations with Θ and ϕ of the influence coefficients described above i.e. the control signals would need to be transformed to drive signals to the power amplifiers using a transformation whose terms are appropriate functions of Θ and ϕ. Two of the terms of such a transformation, referred to here as (Γ_{decoup}) are shown in Figure 7(a) and 7(b) with Θ varying from 90-270° and ϕ kept constant at 90°. These are also seen to be sinusoidal.

7.1.3 Amplifier Modelling

The amplifier model considers the interaction between the various control coils and the superconducting coil and the influence on the power rating of the amplifiers. The superconducting coil is assumed to be in a persistent mode i.e the net voltage on it is zero, then the control coil and superconducting coil currents are governed by the following differential equations.

$$\dot{I} = L^{-1} * V$$

where

$\dot{I}$ = $[\partial i_1/\partial t, \partial i_2/\partial t, \partial i_3/\partial t, \partial i_4/\partial t, \partial i_5/\partial t, \partial i_6/\partial t, \partial i_{sc}/\partial t]^T$

L = Inductance matrix

V = $[V_1, V_2, V_3, V_4, V_5, V_6, 0]^T$

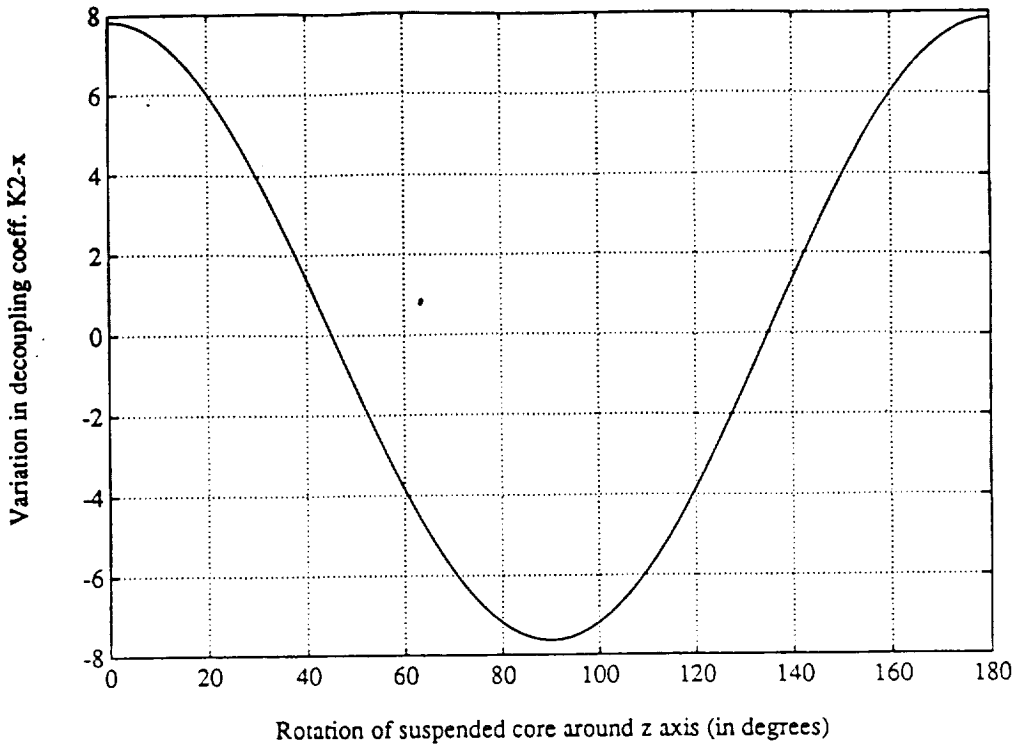

(a) Force Along X' Axis

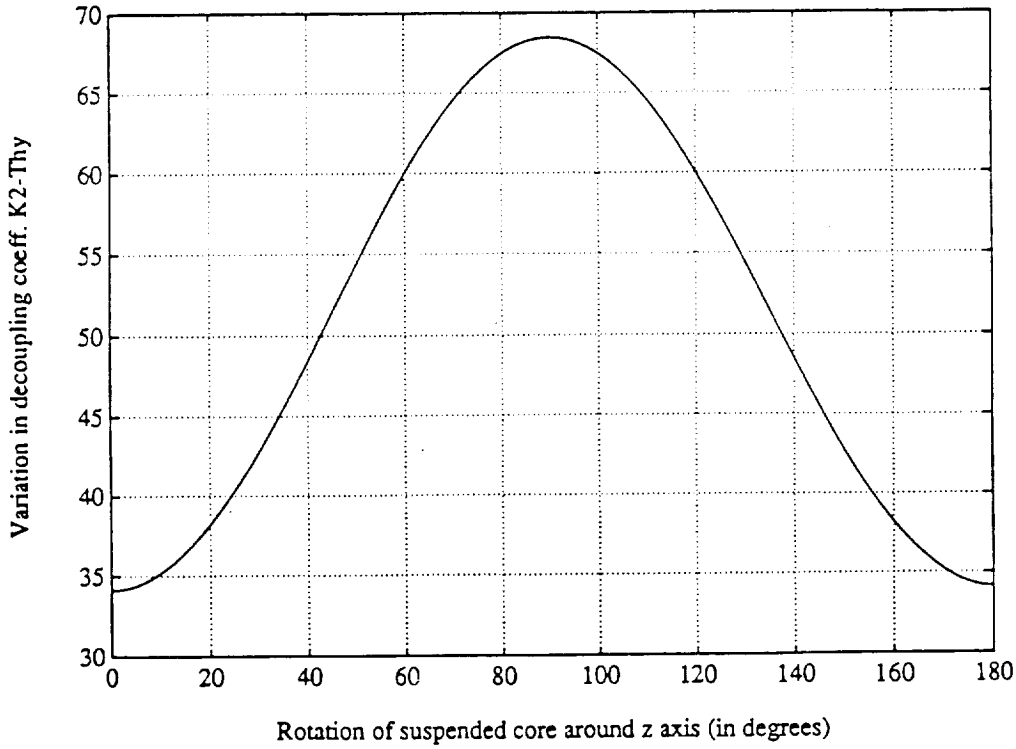

(b) Torque About Y' Axis

Figure 7.7. Decoupling Coefficients (Coil [2])

V_1-V_6 = Excitation voltages to the control coils and the net voltage on the superconducting coil is zero.

The coupling between the control coils and the superconducting coil will influence the superconducting coil current i_{sc} which in turn will influence the force current relationship.

7.2 Control Coil Excitation

The coil excitation strategy for the LAMS is described here. In order to maintain consistency in nomenclature used in describing the LAMS geometry and identifying the coil current and the superconducting core orientation for this report and for ongoing work in developing a stabilization and control strategy a naming convention is described below.

7.2.1 Coil Naming Convention

The coils are named consecutively from 1 to 12 (refer to Figure 7.8). The LAMS coil assembly rests on one of the faces of the dodecahedron. The origin of the x,y,z laboratory reference frame is at the center of the dodecahedron. The bottom most coil, i.e the one the structure is resting on is designated Coil 1. The coil diametrically opposite Coil 1 is designated Coil 7. The z axis passes through the centers of these coils. The x axis passes through Coil 2 (refer to Figure 7.8). Coil 3 is adjacent to Coil 2 going counterclockwise in the x-y plane. The coils numbering continues sequentially to Coil 6 in the bottom half of the dodecahedron. The coils in the top half of the dodecahedron are numbered with reference to the bottom half coils. Coil 8 is diametrically opposite Coil 2, Coil 9 is diametrically opposite Coil 3 and so on to Coil 12.

7.2.2 Coil Current Naming Convention and Excitation Strategy

The currents energizing the coils (designated 1-12 with current I_1 energizing Coil 1) are assumed to have two components

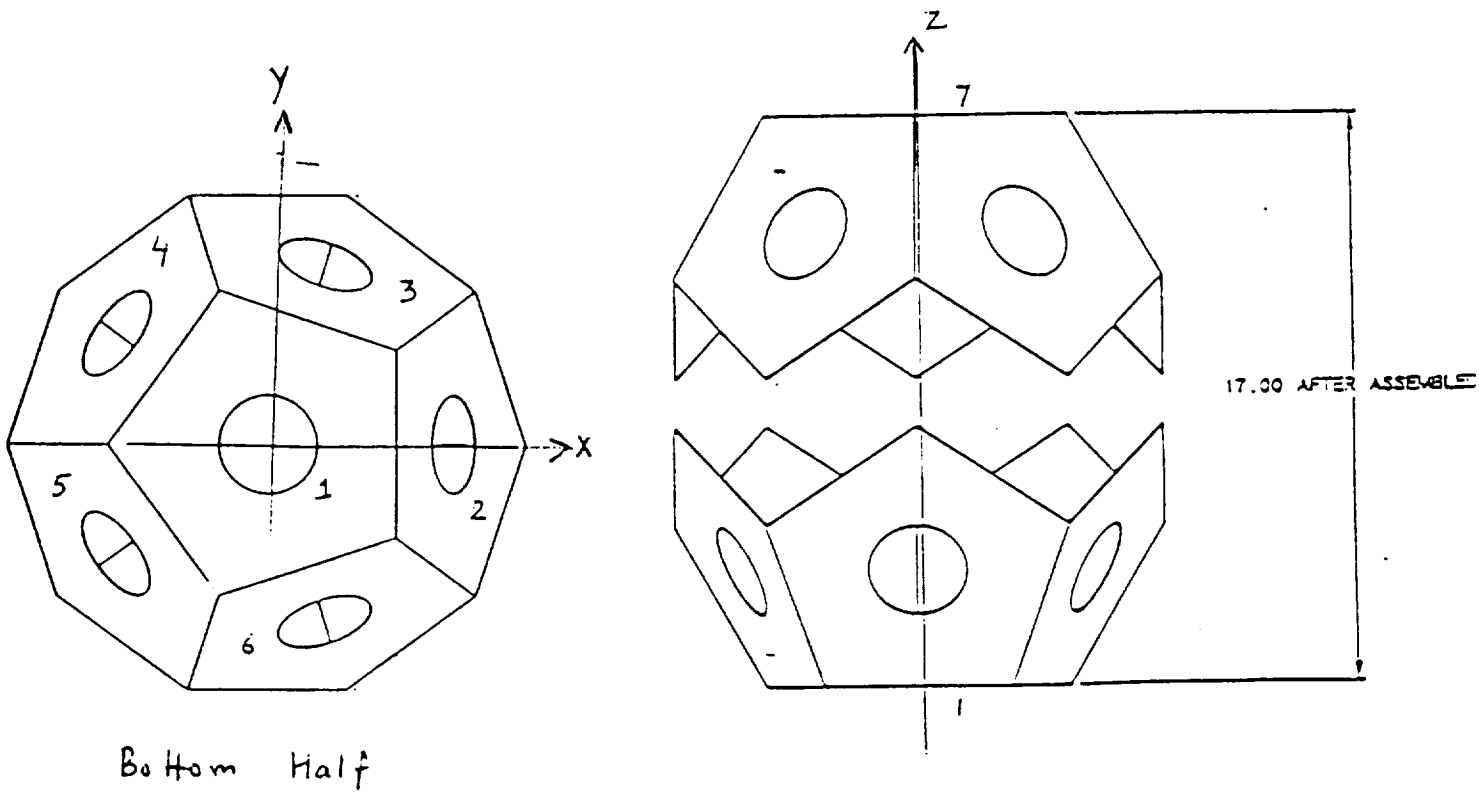

Figure 7.8. Coil Numbering

(i) one to hold up the superconducting coil in 1g, with a subscript "o" and nominally refereed to as the bias current

(ii) the second to stabilize and control the core orientation and designated Δi

Hence the currents are

$$I_1 = I_{1o} + \Delta i_1$$
$$I_2 = I_{2o} + \Delta i_2$$
$$\cdots\cdots\cdots$$
$$I_{11} = I_{11o} + \Delta i_{11}$$
$$I_{12} = I_{12o} + \Delta i_{12}$$

Nominally the bias currents will be a function of both Θ_z, and Θ_x,. Bias current calculations using the mutual inductance model developed at SatCon indicated that I_1 and I_7 are strong functions of Θ_x, and have very weak dependance on Θ_z, in 1g conditions. Currents I_{2o} to I_{11o} are strongly dependent on both Θ_z, and Θ_x,. The variation is almost sinusoidal.

The coil excitation strategy pairs the coils such that Coil "n" is paired with Coil "n + 6" where n = 1 to 6 i.e Coil 1 is paired with Coil 7 etc. The coil pairs will be connected in series. Hence $I_n = I_{n+6}$ designated here as $I_{n,n+6}$ i.e for Coil 1 and Coil 7 the common excitation current will be $I_{1,7}$. Following the above definition of dividing the excitation current into two components

$$I_{1,7} = I_{1,7o} + \Delta i_{1,7}$$
$$\cdots\cdots\cdots\cdots$$
$$I_{6,12} = I_{6,12o} + \Delta i_{6,12}$$

The coil excitation strategy will command current $I_{1,7o}$ to be a function of angle Θ_x, only. The excitation to Coil 1 and Coil 7 will not be used to stabilize the superconducting Core. Consequently $\Delta i_{1,7}$ will always be zero. Currents $I_{2,8o}$ to $I_{6,12o}$ will be commanded to be functions of Θ_z, and Θ_x,. Control currents $\Delta i_{2,8}$ to $\Delta i_{6,12}$ will be determined by the stabilization and control algorithm used.

The effect of commanding current $I_{1,7}$ to be a function of angle Θ_x, only, is illustrated in Figure 7.9, 7.10 and 7.11. With

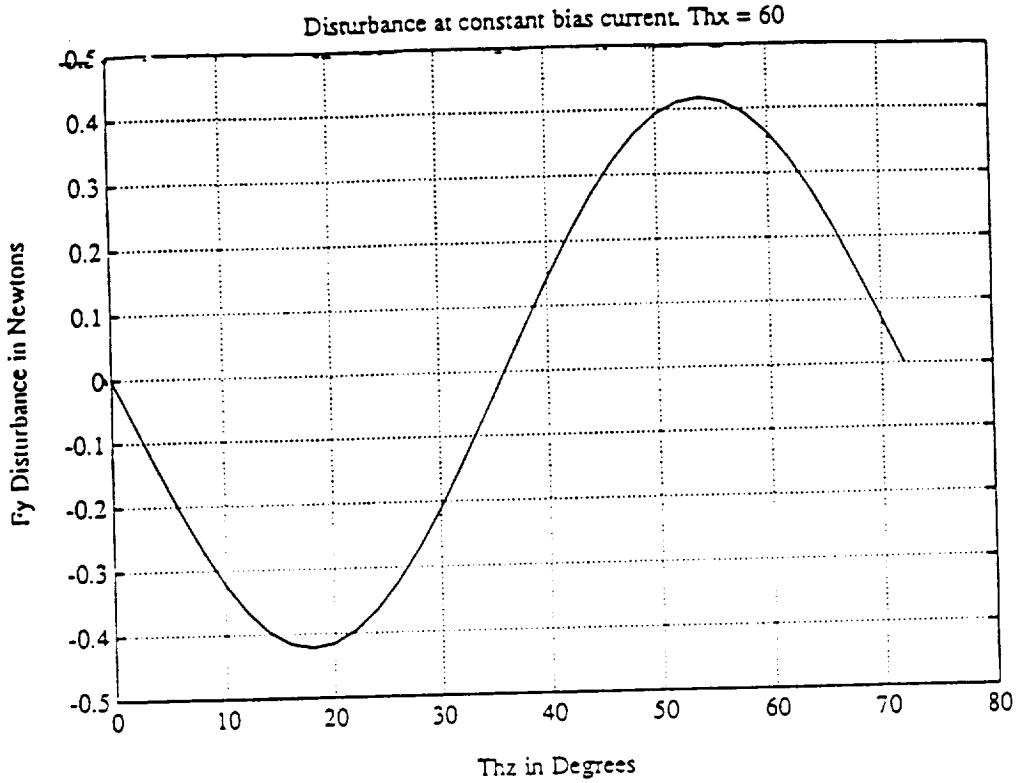

Figure 7.9. F_y Disturbance ($\theta_{x'}$ = 60°)

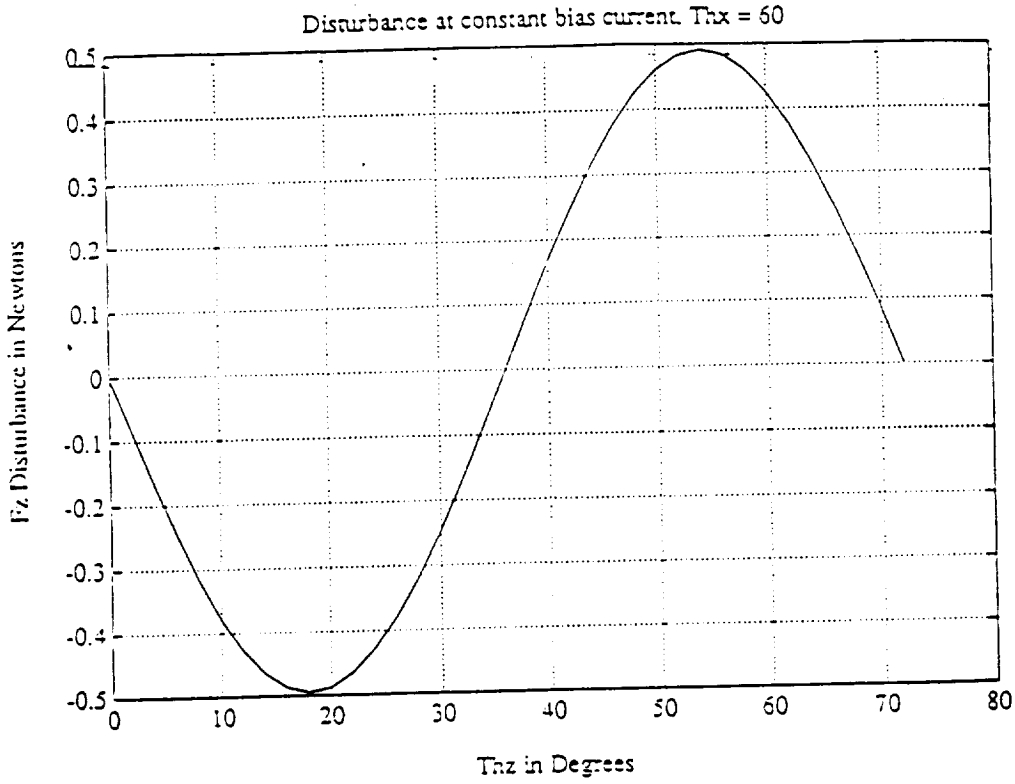

Figure 7.10. F_z Disturbance ($\theta_{x'}$ = 60°)

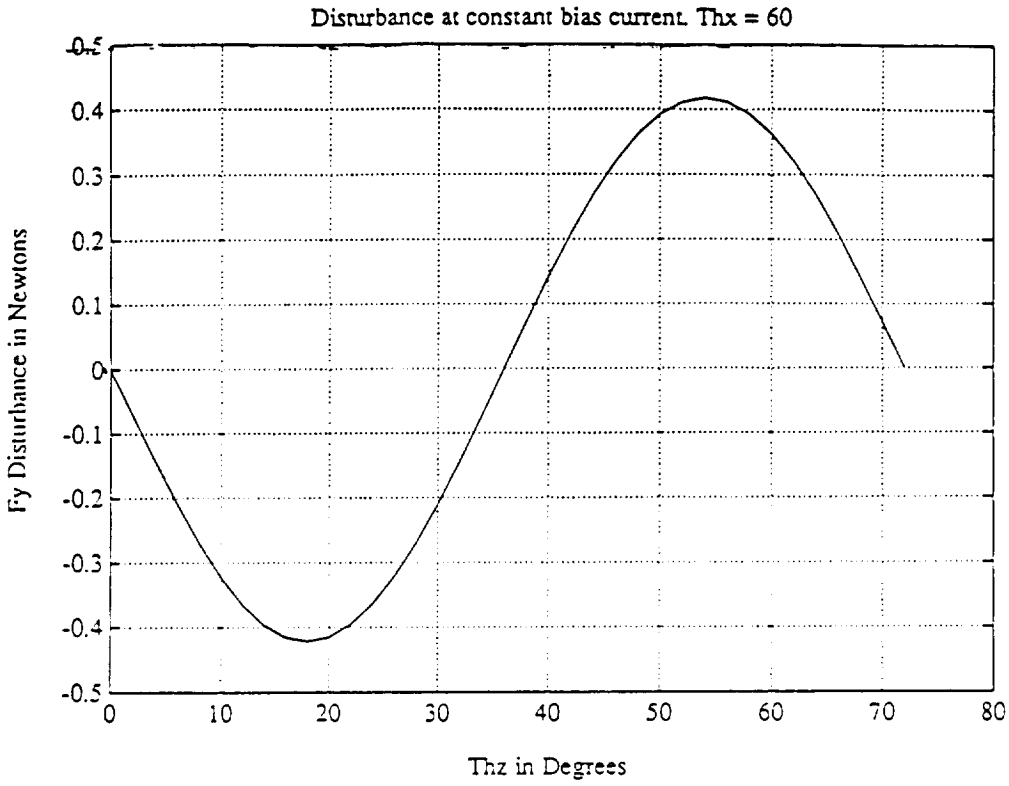

Figure 7.9. F_y Disturbance ($\theta_{x'}$ = 60°)

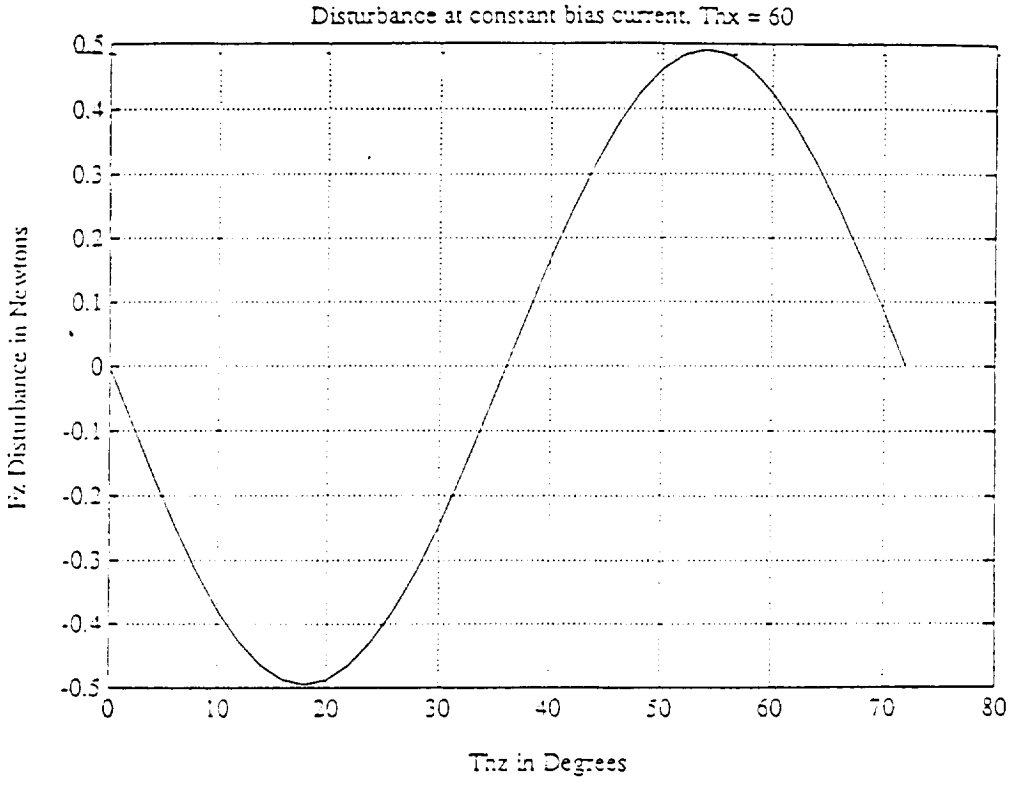

Figure 7.10. F_z Disturbance ($\theta_{x'}$ = 60°)

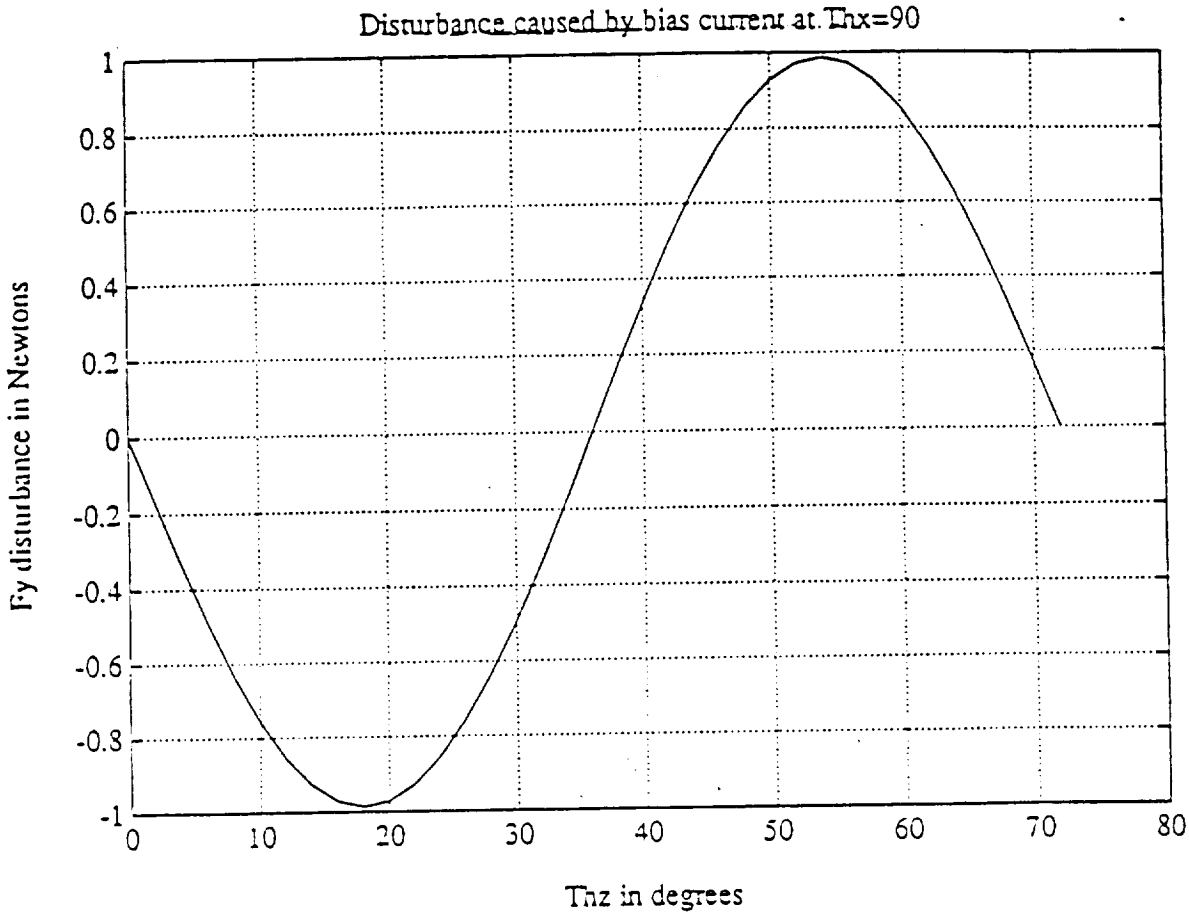

Figure 7.11. F_y Disturbance ($\theta_{x'}$ = 90°)

reference to the figures, the force variations along the z and y axis as the orientation angle $\Theta_{z'}$ is varied from 0 to 72° is a maximum of 1 Newton. The force variation is shown for 3 different values of $\Theta_{x'}$ which cover the "space" within which the core will be orientated. The 5 fold symmetry allows results over 72° to be interpreted for the full range of 360°. The force variation may be viewed as a disturbance. The calculated magnitude of this disturbance indicates it to be trivial compared to potential disturbances or uncertainties which will be introduced from sources such as errors in geometrical alignments.

The superconducting core will essentially be stabilized with reference to its local coordinate frame x',y',z'. The incremental translations and rotations namely $\Delta x'$, $\Delta y'$, $\Delta z'$, $\Delta\Theta_{x'}$, $\Delta\Theta_{y'}$ will be derived from the measurements made in the fixed coordinate frame x,y,z. The control algorithm determines the control forces and moments required to regulate $\Delta x'$, $\Delta y'$, $\Delta z'$, $\Delta\Theta_{x'}$, $\Delta\Theta_{y'}$ to zero. The 5 control forces and moments $\Delta fx'$, $\Delta fy'$, $\Delta fz'$, $\Delta M\Theta_{x'}$, $\Delta M\Theta_{y'}$ have to

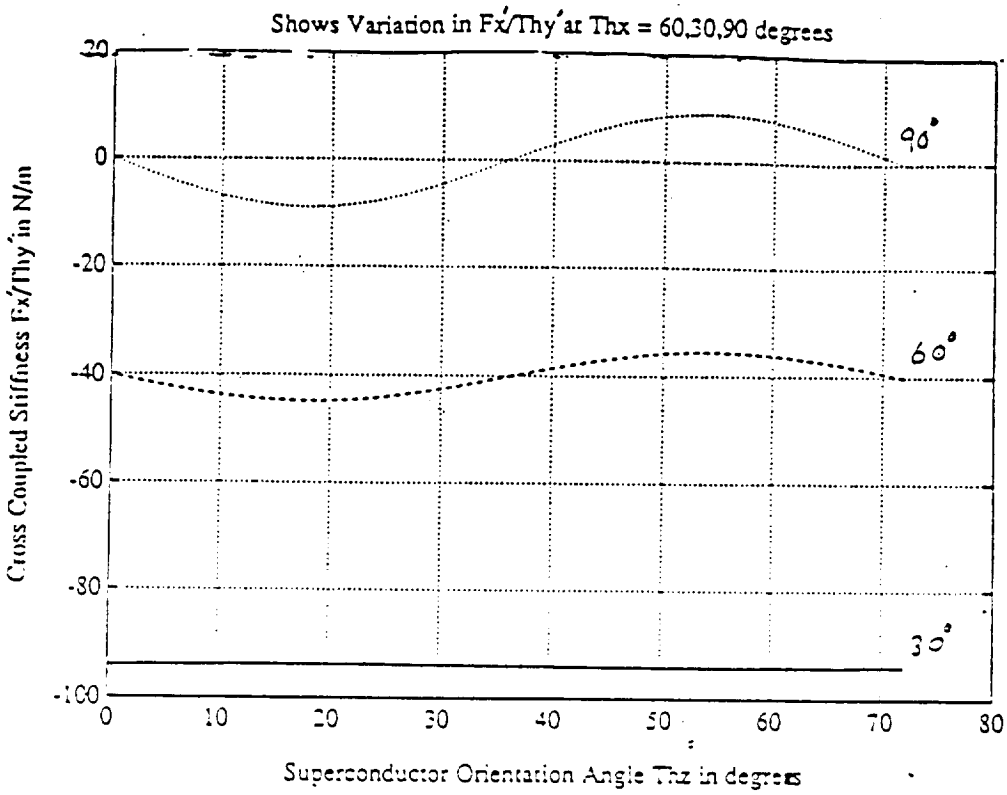

Figure 7.12. Cross-coupled Stiffness ($F_{x'}/\theta_{y'}$)

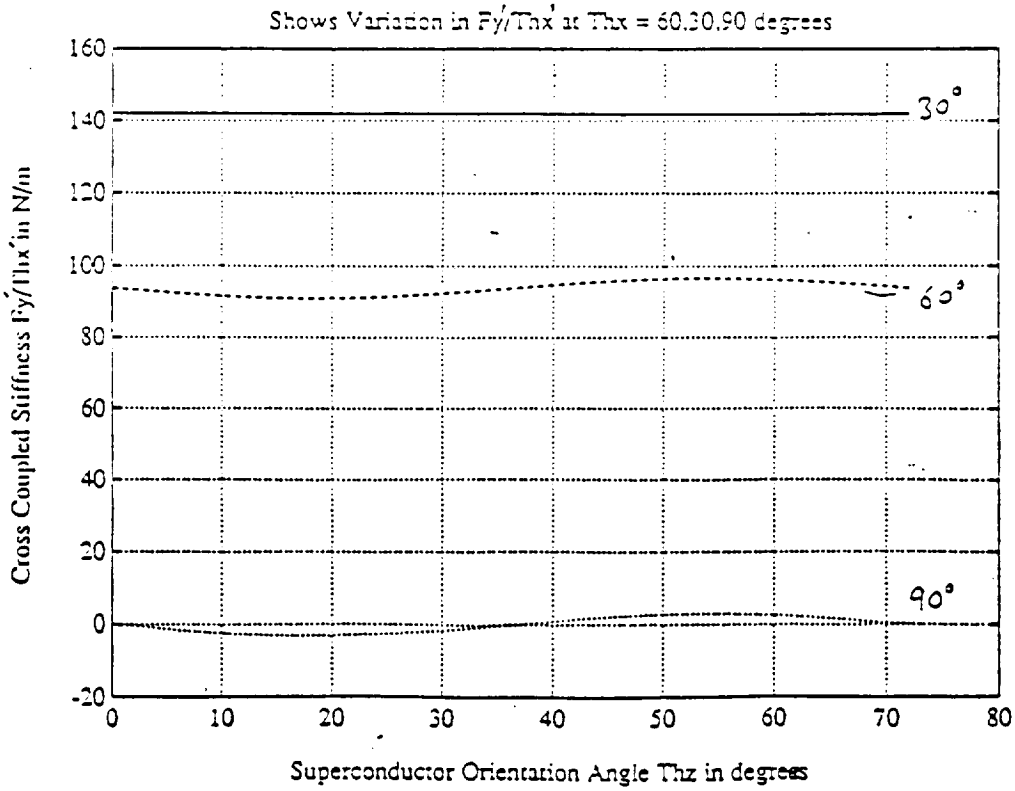

Figure 7.13. Cross-coupled Stiffness ($F_{y'}/\theta_{x'}$)

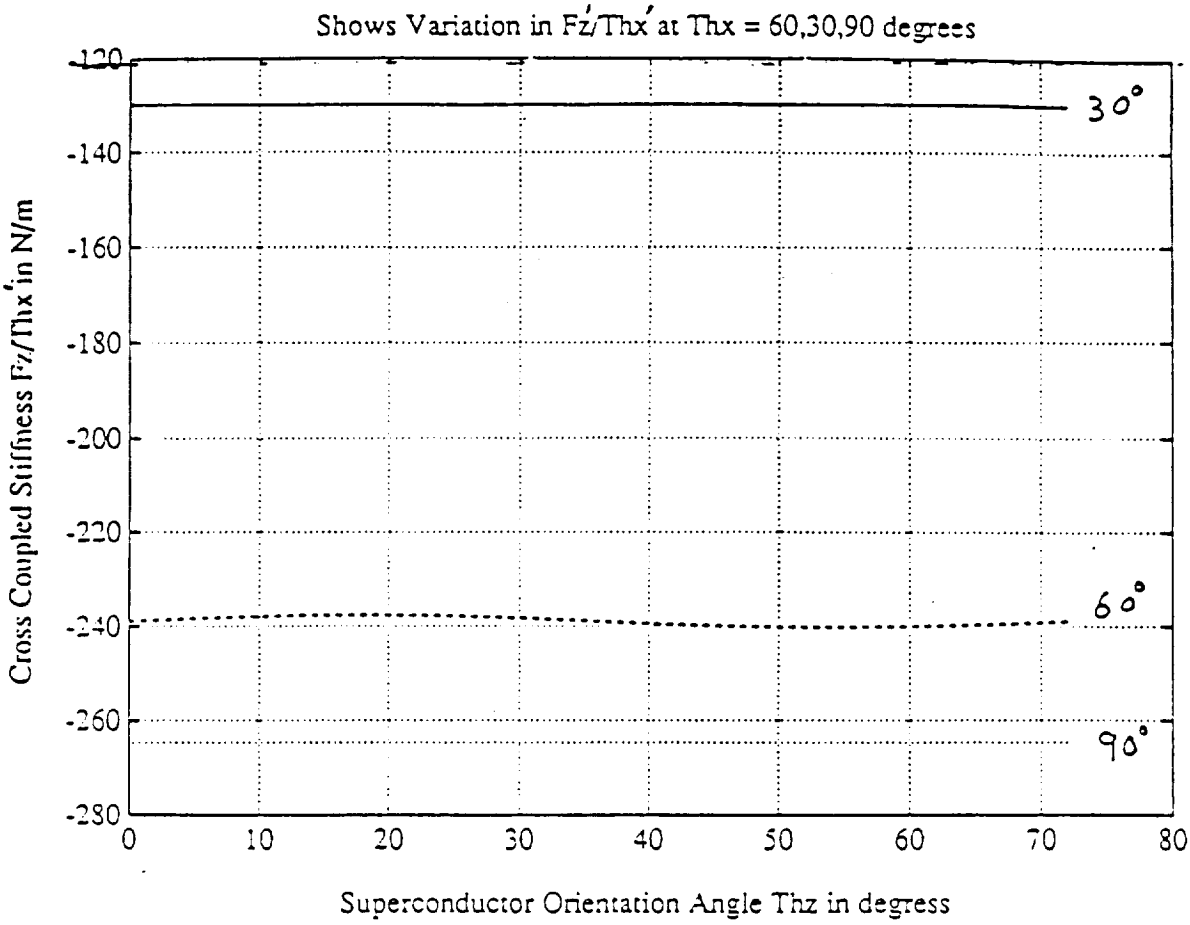

Figure 7.14. Cross-coupled Stiffness ($F_{z'}/\theta_{x'}$)

force. The controller structure is designed to accommodate both the six and twelve coil configurations. As will be described later, the difference between the two control configurations is only the size of one transformation matrix. In this report, the twelve coil configuration will be used as the baseline. Except where noted, however, the six coil configuration is the same.

An overview block diagram of the system is shown in Figure 7.15. Four major subcomponents are identified; the controller, the sensors, the power amplifiers, and the plant. The power amplifiers boost the control signal to power levels and provide current control. The current controllers are internal to the amplifier modules and provide at least one kilohertz of closed-loop current control bandwidth.

The inputs to the plant are the 12 control currents in the normal coils surrounding the superconducting source coil. The outputs of the plant are the orientation and position of the superconducting source coil. The orientation is described by the

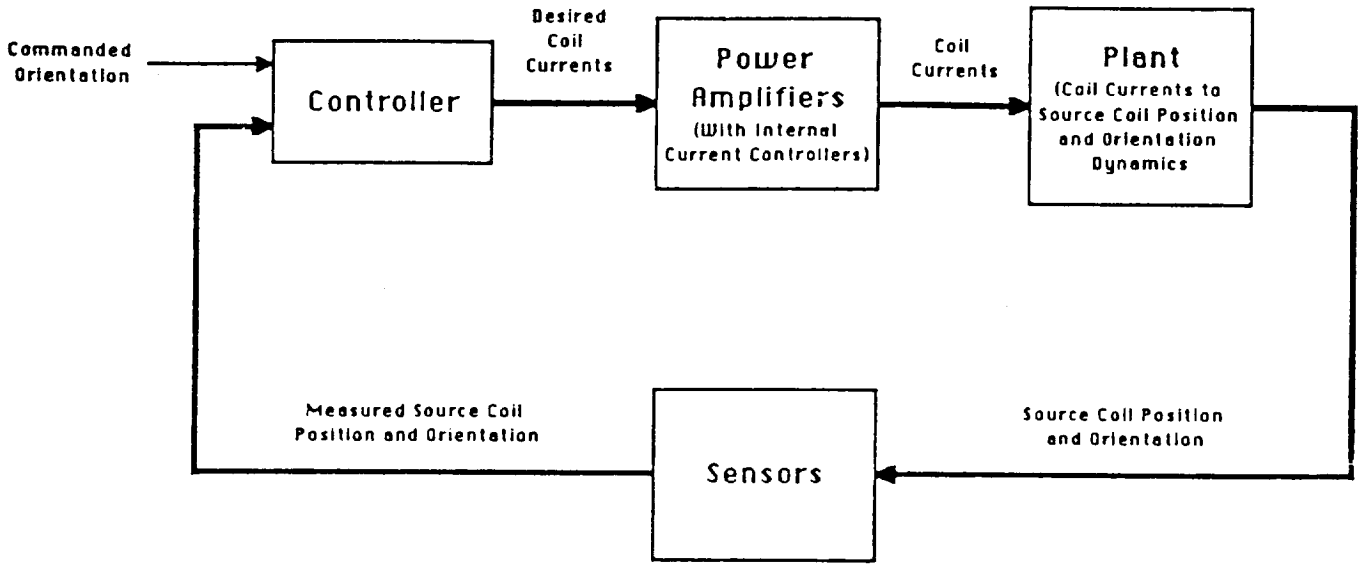

Figure 7.15. Overall System Block Diagram

rotations about the θ_z and $\theta_{x'}$ axis. The position of the superconducting source coil is described by three orthogonal displacements (x,y,z) from the nominal, centered position. The sensors measure the position and orientation, providing these measured quantities as outputs to the controller.

The controller has as inputs the five measured signals that represent the superconducting source coil orientation and position as well as two inputs for the commanded orientation. The controller uses the five measurements and two commanded signal as inputs to determine the twelve desired controller currents. The goal of the controller is to stably suspend the superconducting source coil in the presence of modelling error and sensor noise and make the superconducting source coil orientation follow the commanded orientation.

Figure 7.16 presents the same block diagram in slightly more detail. Two separate sensors system are indicated, a capacitive sensor subsystem that measures the position of the superconducting source coil and a mutual inductance sensor system that measures the orientation of the superconducting source coil. These sensor systems measure the orientation and position of the superconducting source coil relative to the stationary frame to which they are attached. The stationary frame of reference will be denoted as the "fixed-frame" in the following block diagrams.

Figure 7.16 also shows the important features of the controller that are the use of feedforward, the use of a quasi-static frame of reference, and the nonlinear force/torque to coil current transformation. As is shown knowledge of the required gravity force is used along with the feedback force to produce total desired force. This use of a "feedforward" term reduces the

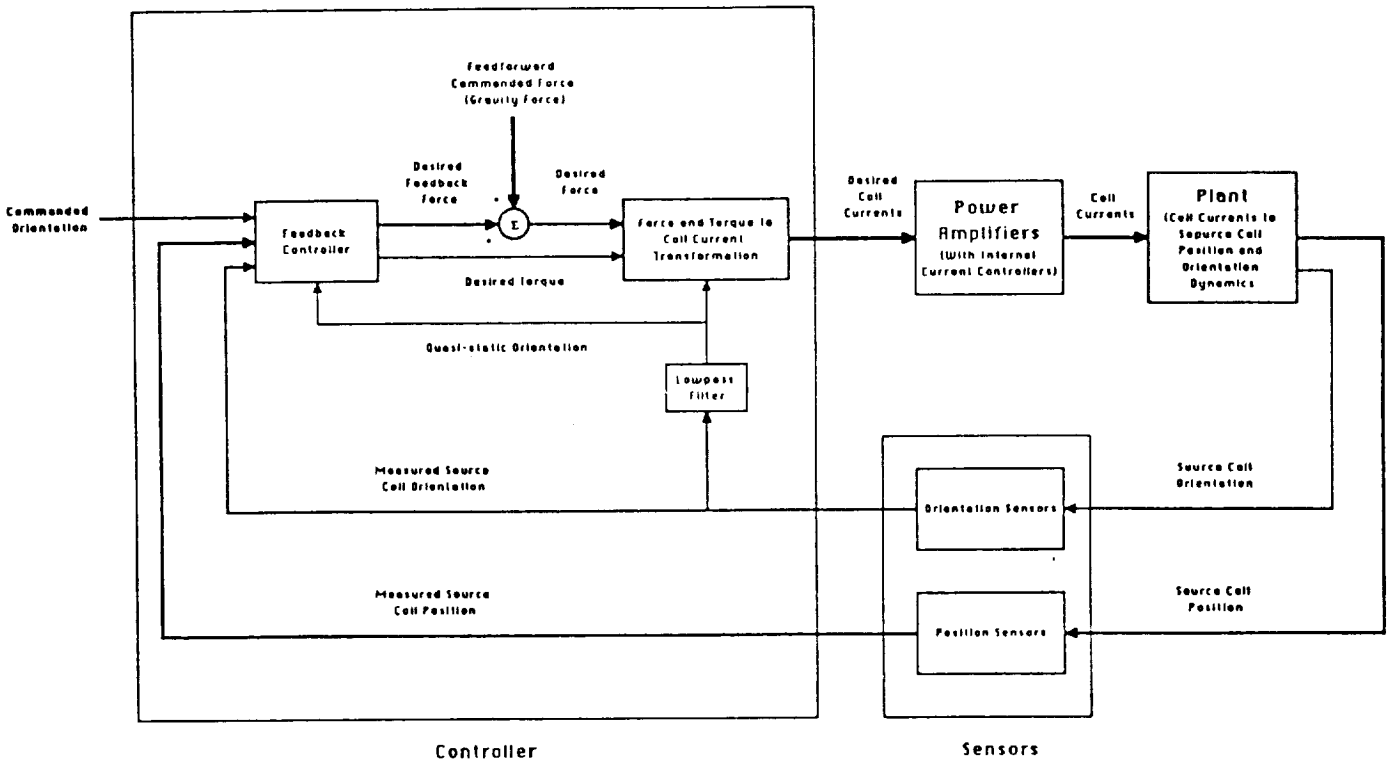

Figure 7.16. Detailed Loop Block Diagram

loading of the feedback loop and, therefore, reduces the steady-state error in position caused by the gravity force. The quasi-static frame of reference is determined by low-pass filtering the measured superconducting source coil orientation. This frame of reference is used by the feedback controller and to determine the proper transformation of desired control forces and torques into control coil currents. In steady-state, the quasi-static orientation is the same as the measured orientation. The low-pass filtering is used to reduce any orientation sensor noise.

The controller is shown in more detail in Figure 7.17, where the use of the quasi-static frame of reference is presented. As discussed above, the measured superconducting source coil orientation is low-pass filter to obtain the orientation of the quasi-static frame of reference. As shown in the block diagram, this the orientation of this quasi-static frame of reference is used to determine the transformation matrix **T** between the fixed and quasi-static frames. This transformation matrix is used to transform the measured and commanded signals from the fixed to quasi-static frame of reference. This transformation matrix is given by

$$T = \begin{bmatrix} \cos(\theta_z) & \sin(\theta_z) & 0 \\ -\sin(\theta_z)*\cos(\theta_x) & \cos(\theta_z)*\cos(\theta_x) & \sin(\theta_x) \\ \sin(\theta_z)*\sin(\theta_x) & -\cos(\theta_z)*\sin(\theta_x) & \cos(\theta_x) \end{bmatrix}$$

where θ_x and θ_z are the orientation angles of the quasi-static frame relative to the fixed frame.

As shown in Figure 7.17 the transformation matrix **T** is used to convert the measured orientation, measured position, commanded orientation, and feedforward gravity force from the fixed to the quasi-static frame. The feedback controller, therefore, operates in the quasi-static frame in which the plant dynamics do not vary as strongly as the fixed-frame. The use of the quasi-static frame, in combination with the decoupling effect of the desired force/

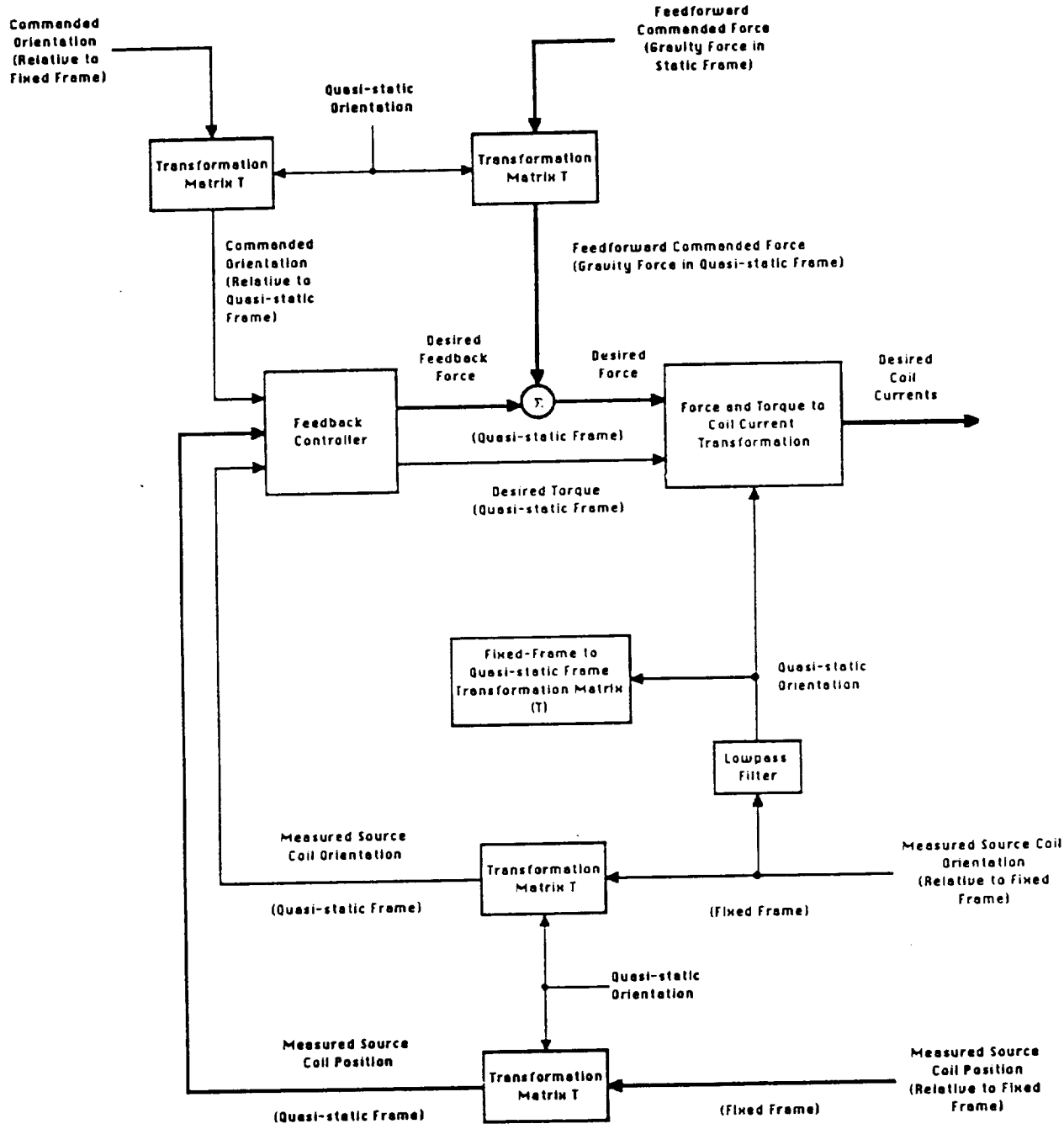

Figure 7.17. Controller Block Diagram

torque to coil current transformation provides the controller with a relatively decoupled system with which to interact. In the quasi-static or local frame, feedback controller consists of simple SISO compensators. As shown in Figure 7.18, the measured source coil orientation is compared to the commanded orientation to drive the orientation compensators. This two-input, two-output compensator is decoupled into two simple SISO lead-lag compensators on the diagonal terms. These compensators feature a decade of lead starting at 10 hz with the loop gain set to give a loop cross-over frequency of 20 hz. The resulting loop gain and phase are shown in Figure 7.19. The top graph shows the loop gain for the nominal plant and assuming a ± 30% plant gain variation. The bottom graph shows the loop gain including the effect of phase lost due to a full sampling period delay with a 500 Hz sampling rate. For the curves shown, the open loop suspension plant eigenvalues as reported in the Power Amplifier Section of are used. The orientation used with $\theta_{x'}$ of 30° gives the largest open loop

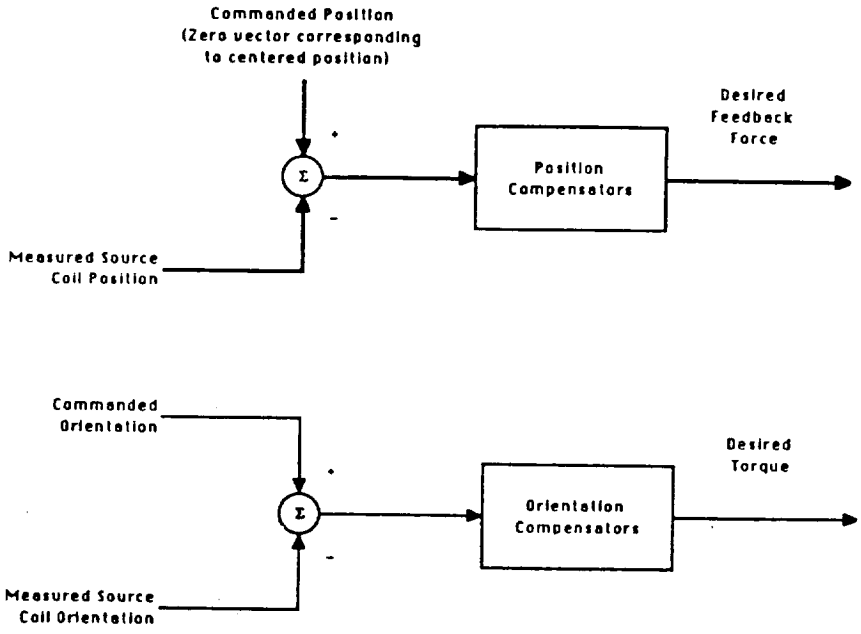

Figure 7.18. Feedback Controller

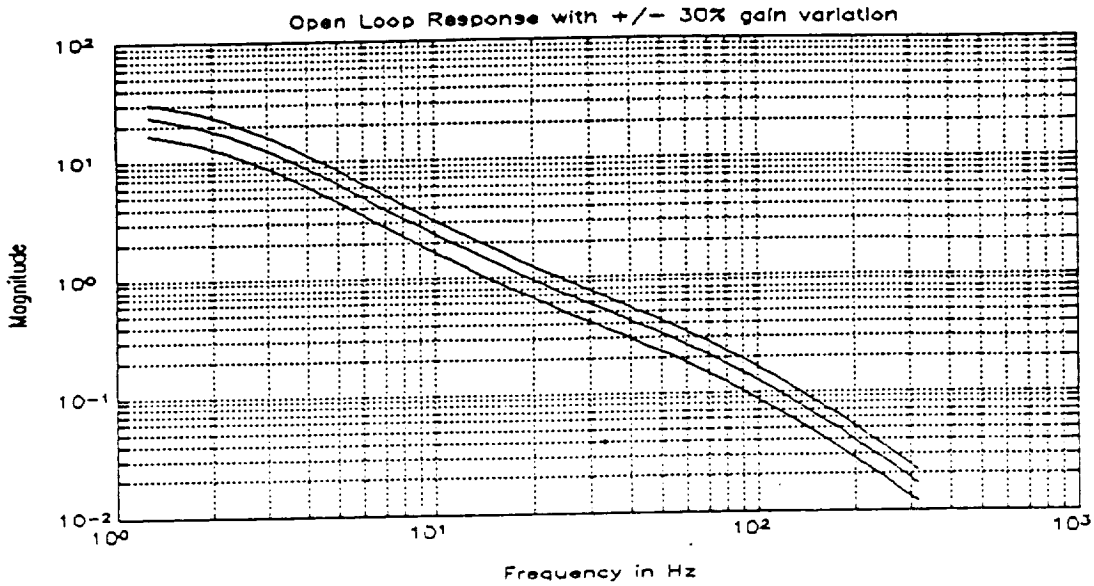

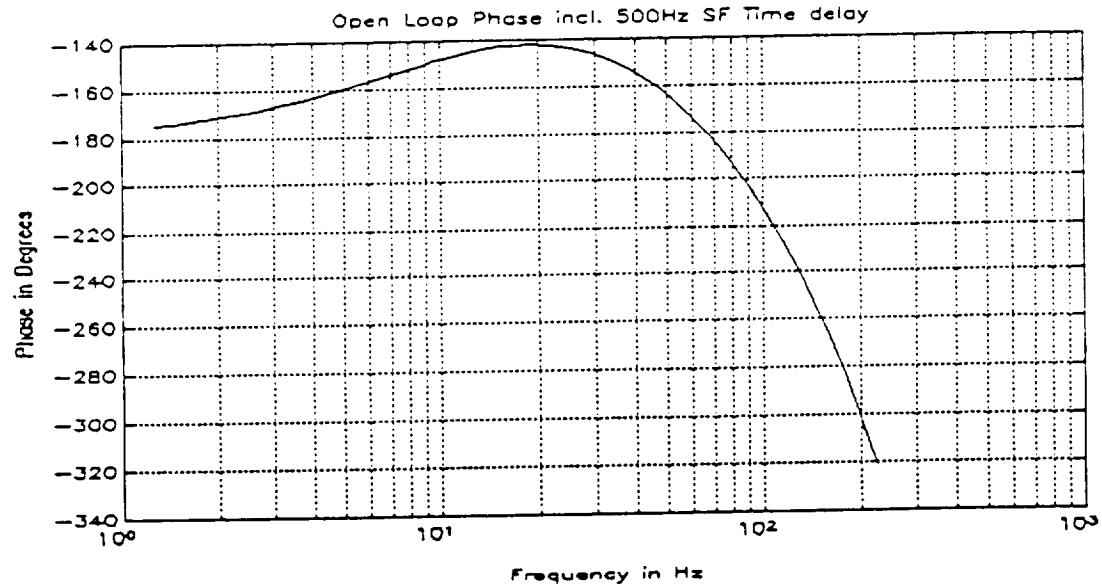

Figure 7.19. Open-loop Transfer Functions

unstable constants and was used in calculating the loop gains of Figure 7.19. Over the gain variation represented here, the phase margin is better than 35°. The closed loop bandwidth lies between 18-20 Hz. The controller design is largely insensitive to expected variations in the unstable constants over the range of motion.

The most complicated part of the of the controller is the desired force/torque to control coil current transformation or gain matrix. This gain matrix is a highly nonlinear function of the superconducting source coil orientation as represented by the orientation of the quasi-static frame. The gain matrix is found by first determining the force and torque produced on the superconducting source coil per ampere of current in each normal coil. The force and torque produced by unit currents in a specific control coil is a function of the superconducting source coil orientation. The force and torque are found for each of the 12 coil given the quasi-static orientation. These are combined to form the coil control effectiveness matrix **B**. This matrix defines the relation between the twelve control currents ($\underline{I}$) and the generalized force vector $\underline{F}$ acting on the superconducting control coil. The generalized force vector $\underline{F}$ consists of the three torques acting on the superconducting coil appended to the three forces as

$$\underline{F}^T = [f^x,\ f^y,\ f^z,\ \tau^x,\ \tau^y,\ \tau^z].$$

The coil control current vector $\underline{I}$ consists of the twelve coil control currents arranged in a vector.

The control algorithm finds the elements of the six by twelve matrix **B** by using a simplified model of the force/torque to current relation for the superconducting source coil interacting with a normal coil. Based on the work of Grover, the force and torque have been found as a function of the relative angle between the dipole moments of the superconducting source coil and the normal coil. For each normal control coil, the algorithm first determines the angle between the superconducting source coil and the normal coil. Using the simplified model, the force and torque per unit

current are determined for each coil. These forces and torques are then transformed into the quasi-static frame yielding the coil control effectiveness matrix **B**.

The coil control effectiveness matrix **B** gives the generalized force $\underline{F}$ as a function of the coil control currents $\underline{I}$. The control algorithm, of course, needs to determine the currents $\underline{I}$ given a desired generalized force $\underline{F}$. This is accomplished by finding the pseudo-inverse $\mathbf{B}'$ of the control effectiveness matrix **B**. The control currents are then found from $\underline{I} = \mathbf{B}'\underline{F}$.

7.4 Control System Implementation

The control laws for LAMS were coded in the "C" programming language. The following paragraphs briefly describe the operation of the code.

7.4.1 Main Program

Figure 7.20 describes the Main Program. After initializing variables, a recursive routine continuously recalculates the relationship between the currents in the control coils and the forces that these forces exert on the superconducting source coil. The forces are expressed in the coordinate system local to the source coil.

Two models are maintained. One model is currently considered valid (accurate) by the algorithm. The other is currently being recomputed. A Model Flag indicates which of the two is currently valid. The logical expression branch at the center of Figure 7.20 sets the Model Flag upon completion of each computation. The Model Flag is merely toggled. The Model Flag is available to the Interrupt Routine as are both of the models.

When a Halt Flag is set by the user, recomputation of the model stops and control is passed to the Shut-down Procedure.

7.4.2 Interrupt Routine

A timer interrupts the Main Program every sampling period. Control then passes to the Interrupt Routine whose Flow Chart is

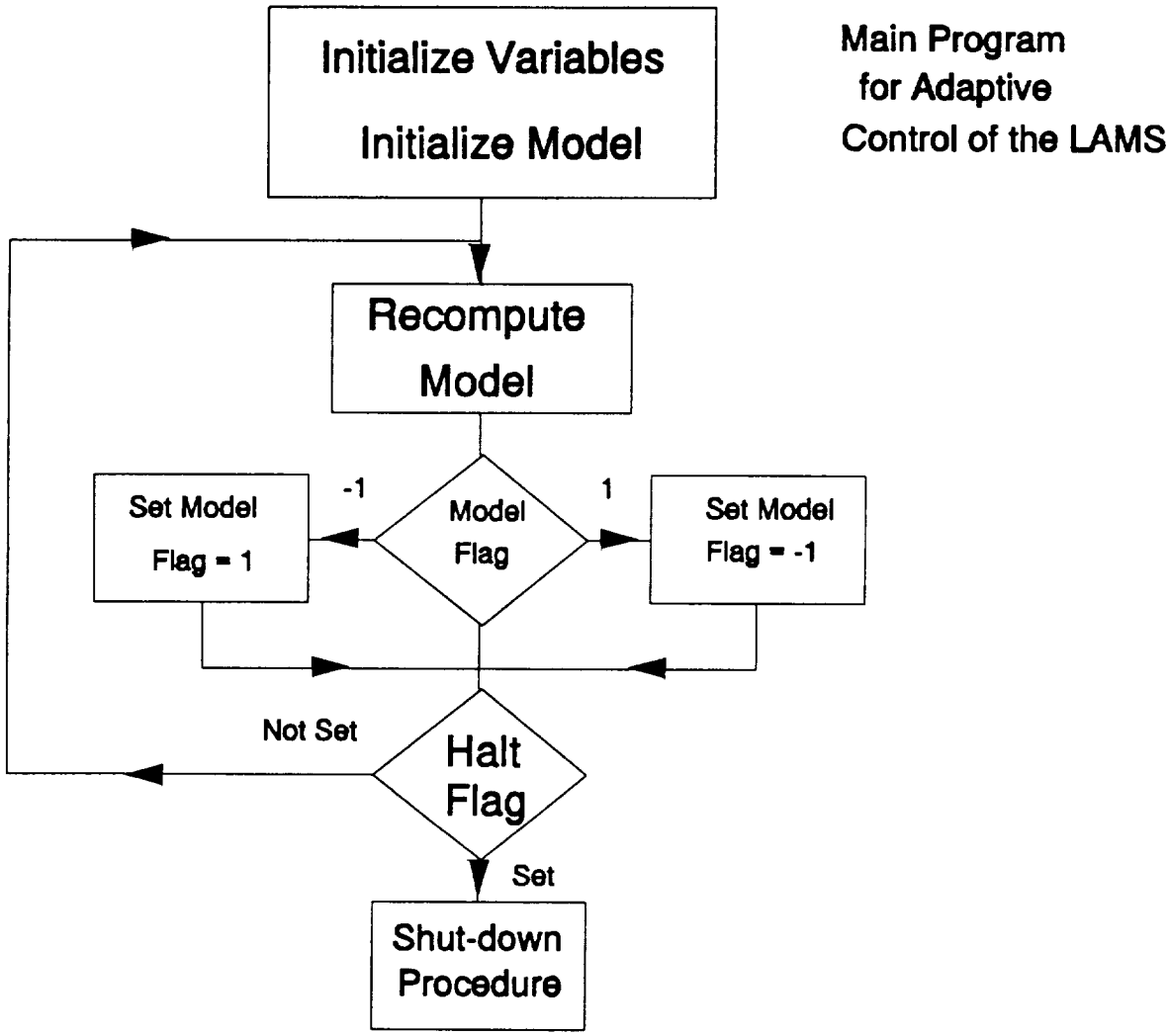

Figure 7.20. Flow Chart for Main Program

given in Figure 7.21. At the start of the Interrupt Routine, a signal is sent to the A/D cards to begin to start converting the 16 analog inputs to digital values.

The Command Buffers are then read. These contain the desired position of the source coil as defined by the desired pitch and yaw angles. Based on the value of the Model Flag, a set of pointers are set to identify the coefficients of the force/current model.

The program loops around until all the A/D conversions are complete. On completion of the A/D conversion, the values stored in the data buffers are read and the rotations and displacements of the source coil are computed. These are compared to the values read from the Command Buffers and Error Signals are created.

The Error Signals are applied as inputs to Compensation Filters. These are "C"-callable routines from the SPOX operating system. The outputs of the Compensation Filters are forces in the local coordinate system. They are added to the weight of the suspended body as expressed in the local coordinates.

The desired forces in the local coordinates are then multiplied by the inverse of the force/current relationships to provide the individual desired currents. These signals are then provided to the D/A converters which drive the power amplifiers.

Control then returns to the Main Program, where the recomputation of the model continues.

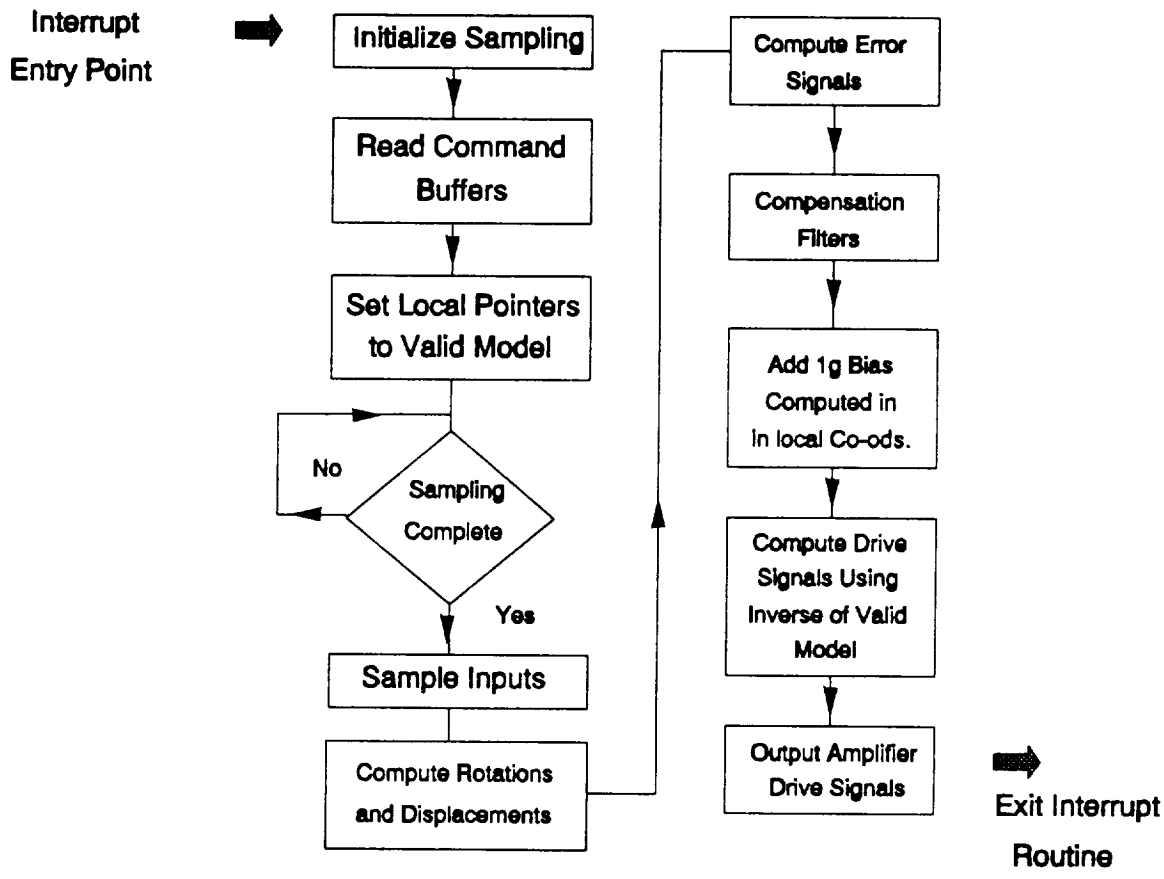

Figure 7.21. Flow Chart of Real-time Controller

THIS PAGE

INTENTIONALLY

LEFT BLANK

8. System Performance

This section presents the results of the testing of the superconducting LAMS. Following the usual development process of debugging the controller, initial tests were focussed toward demonstrating that the superconducting source coil could be suspended (supported by magnetic forces alone) and stabilized. Subsequent testing was directed toward demonstrating the gimballing capability of the superconducting LAMS.

8.1 Initial Suspension

Once the control system software was debugged and the source coil was suspended in a stable configuration, square-waves were injected into the DSP via analog inputs. These square-wave inputs represented commands for step changes in the translational position of the source coil. Using the Tektronics spectrum analyzer, the translational position response (laboratory frame) of the system along all three orthogonal axes was recorded.

8.1.1 X-Axis Step Response

Figure 8.1 shows the X-axis position response to a commanded step in X-axis position. The response is slightly underdamped. Figure 8.2 and 8.3 show the Y-axis and Z-axis position responses during the X-axis step. The Y-axis response shown in Figure 8.2 has some steady-state error due to the X-axis motion. The Z-axis response has less steady-state error, but a significant transient response to the X-axis step.

8.1.2 Y-Axis Step Response

Figure 8.4 shows the Y-axis position response to a commanded step in Y-axis position. Figures 8.5 and 8.6 show the X-axis and Z-axis responses to the Y-axis step. Except for the slight (note the expanded scale) steady-state error on the X-axis response, any coupling is on the level of the sensor noise.

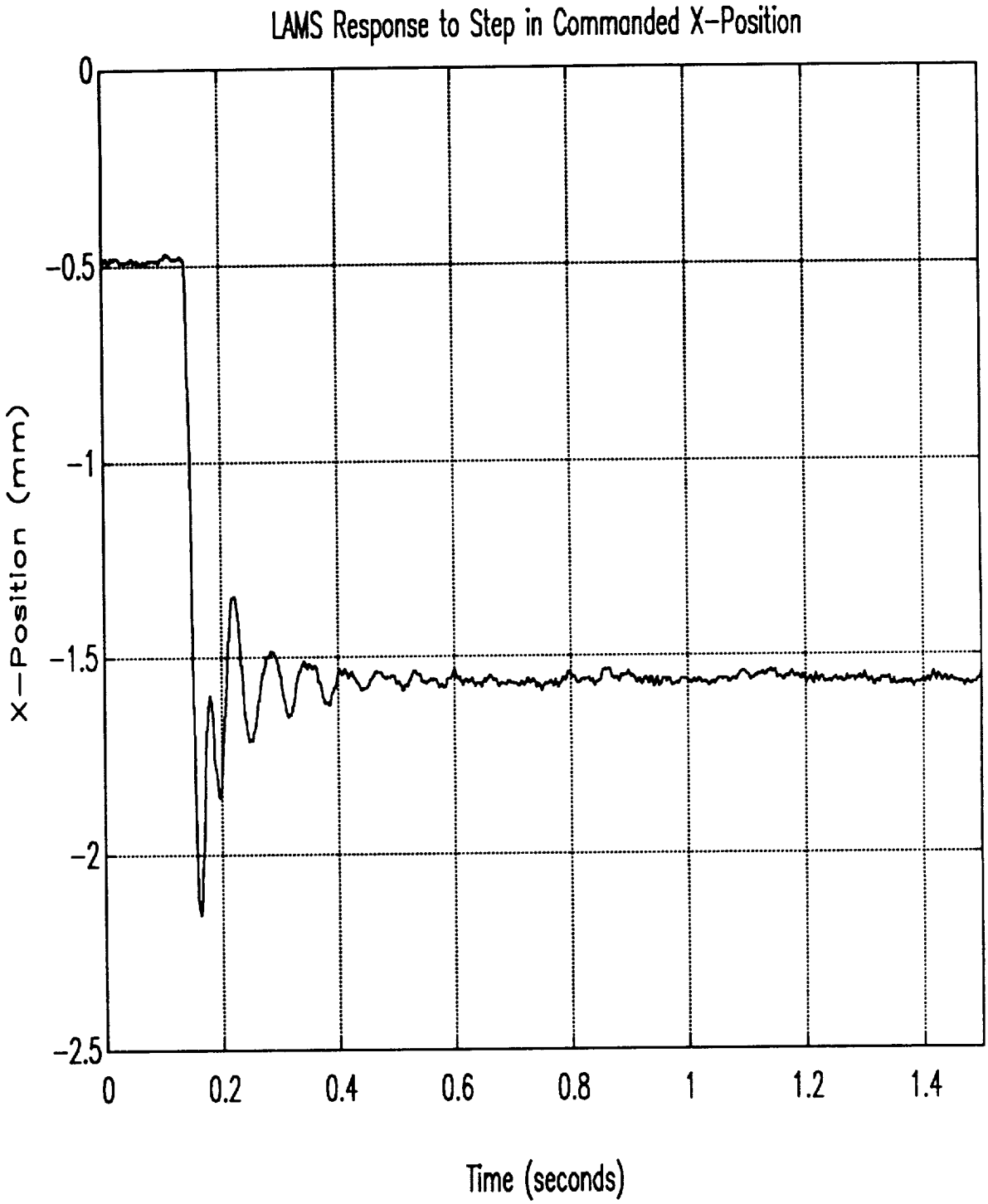

Figure 8.1. X-Axis Response to X-Axis Step

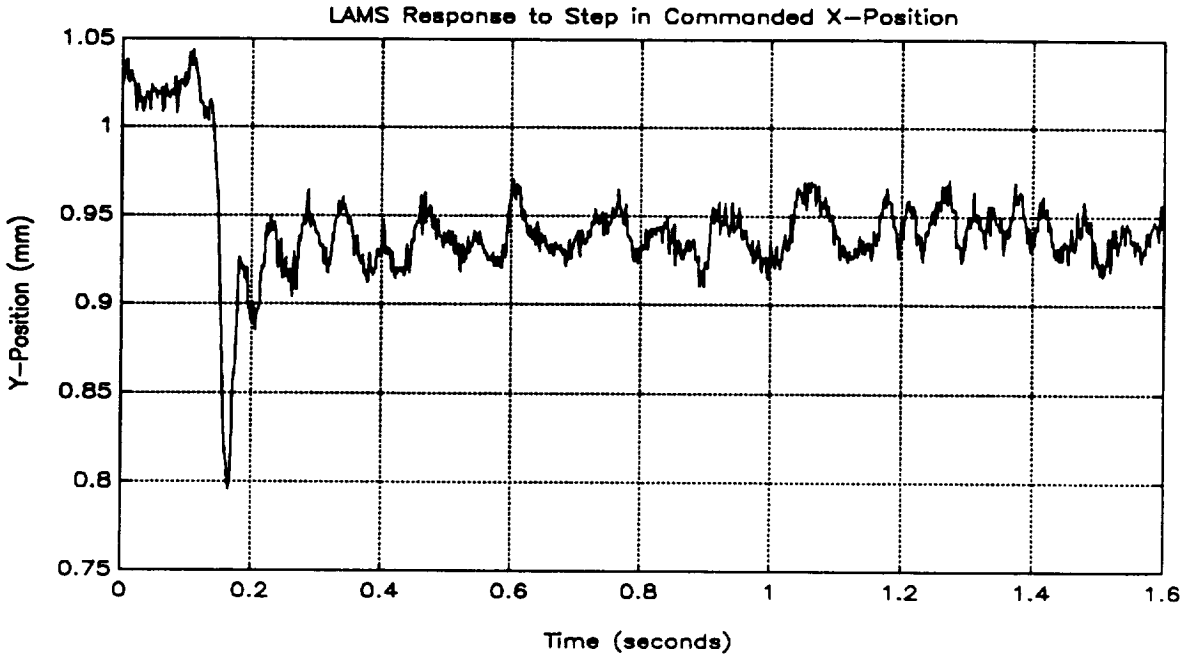

Figure 8.2. Y-Axis Response to X-Axis Step

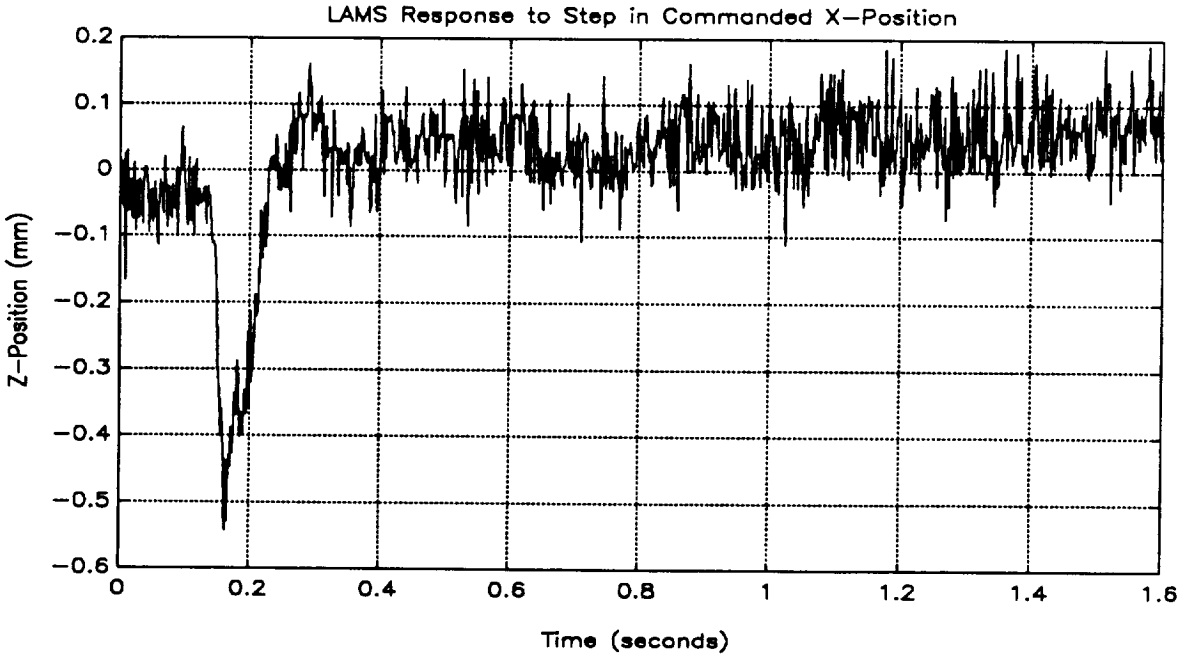

Figure 8.3. Z-Axis Response to X-Axis Step

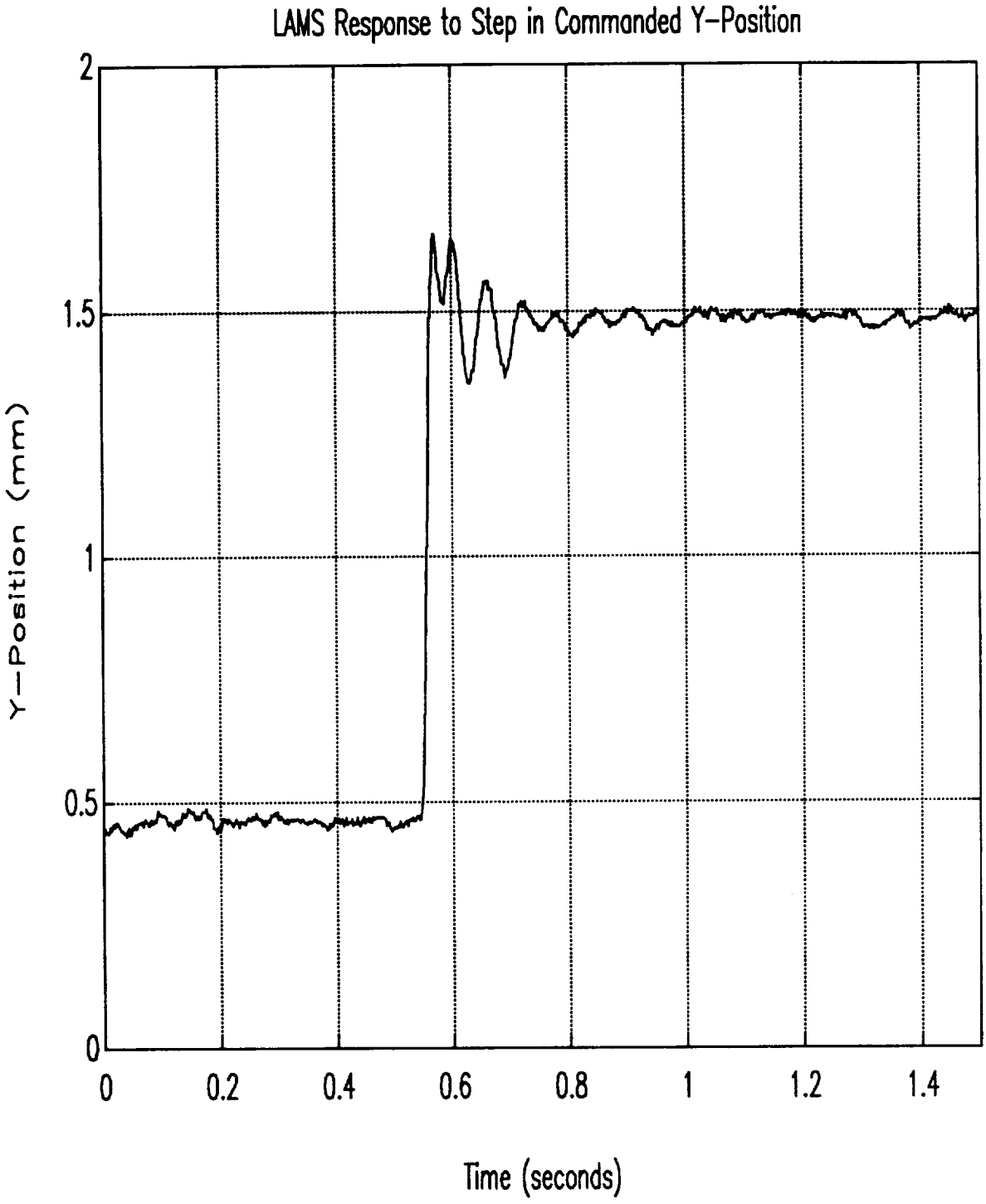

Figure 8.4. Y-Axis Response to Y-Axis Step

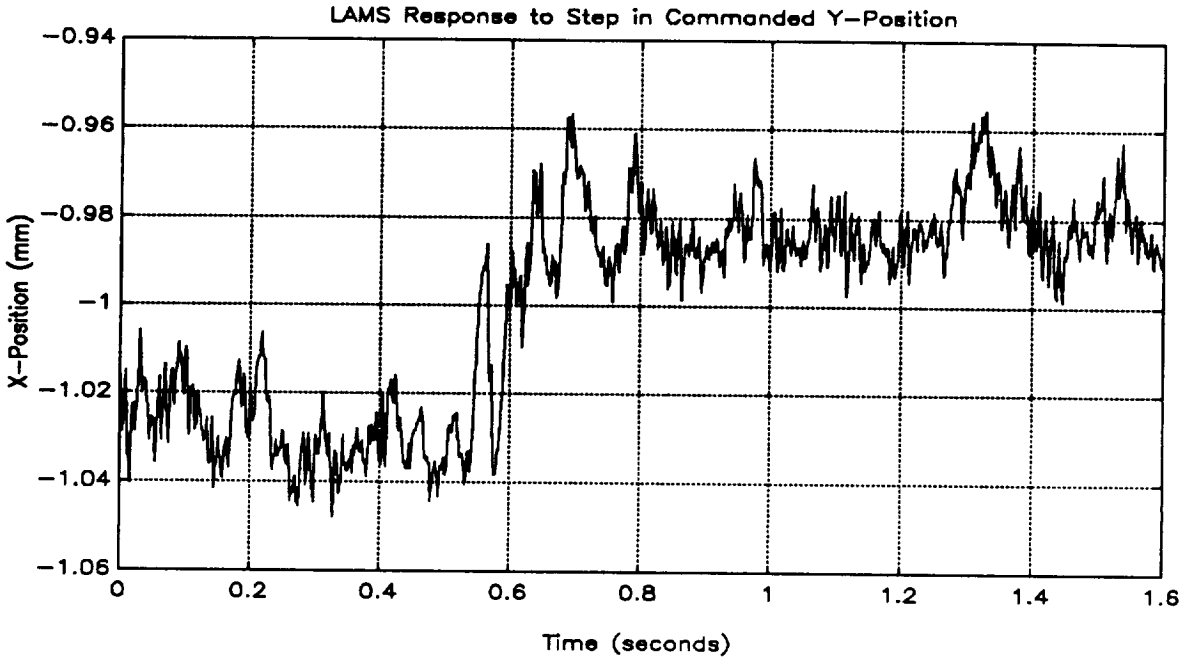

Figure 8.5. X-Axis Response to Y-Axis Step

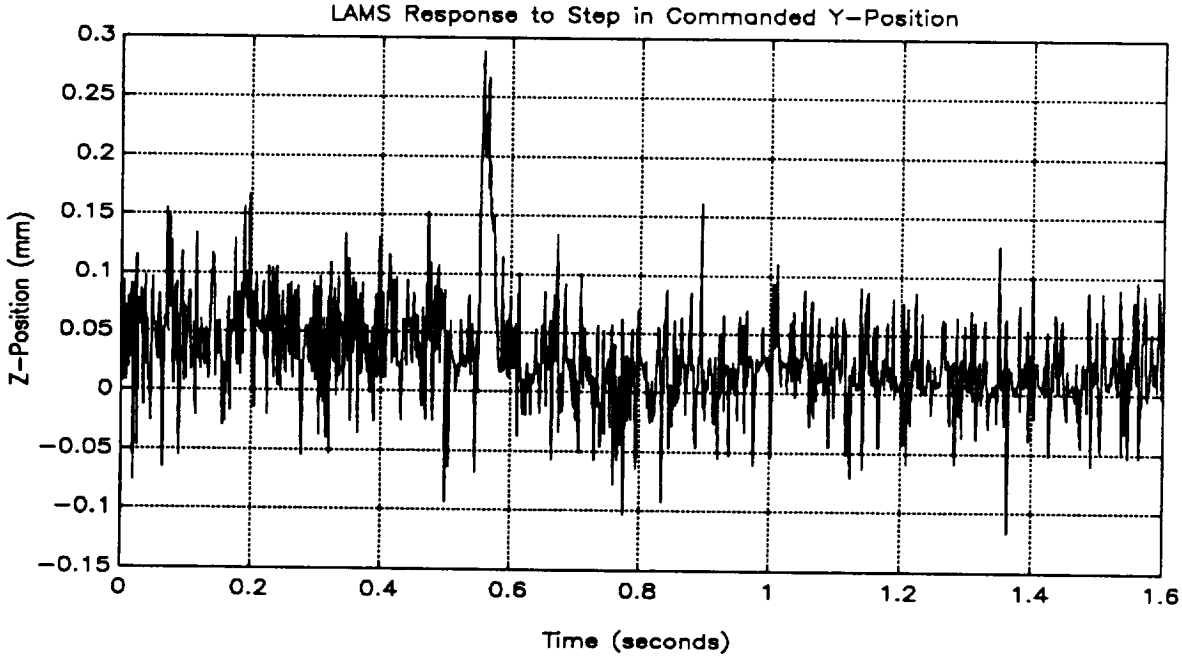

Figure 8.6. Z-Axis Response to Y-Axis Step

8.1.3 Z-Axis Step Response

Figures 8.7, 8.8, and 8.9 show the in-axis (Z-axis) and cross-axes (X-axis and Y-axis) responses to a step command along the vertical (Z) axis. There is only a second-order steady-state error in the X-axis and essentially none in the Y-axis

8.2 Gimballing

Given the role of the LAMS as both a rotor suspension and gimballing system, the angular responses of the system to commands for step changes in the Euler (gimbal) angles are of particular interest. In a manner similar to the previous section, step changes in commanded source-coil orientation were applied to the controller and the responses were evaluated.

8.2.1 Θ_z Step Response

In more conventional gimbal-system terminology, the Euler angle Θ_z would correspond to the "azimuth axis angle." Figure 8.10 shows the Θ_z response to a step change in commanded Θ_z. This is an extremely well damped response.

8.2.2 $\Theta_{x'}$ Step Response

Elevation-axis angle (actually the complement of this, declination angle) would be the analog to the $\Theta_{x'}$ Euler angle. Figure 8.11 shows the $\Theta_{x'}$ response to a step change in commanded $\Theta_{x'}$. These step responses (two are shown) are also extremely behaved.

8.2.3 Cross-axis Effects

A final effect which was measured was the angular motion about one axis in response to a step change in the other angle. Figures 8.12 and 8.13 show these responses. Except for a well-damped response in the $\Theta_{x'}$ response to the Θ_z step, the controller handles the cross-axis effects well.

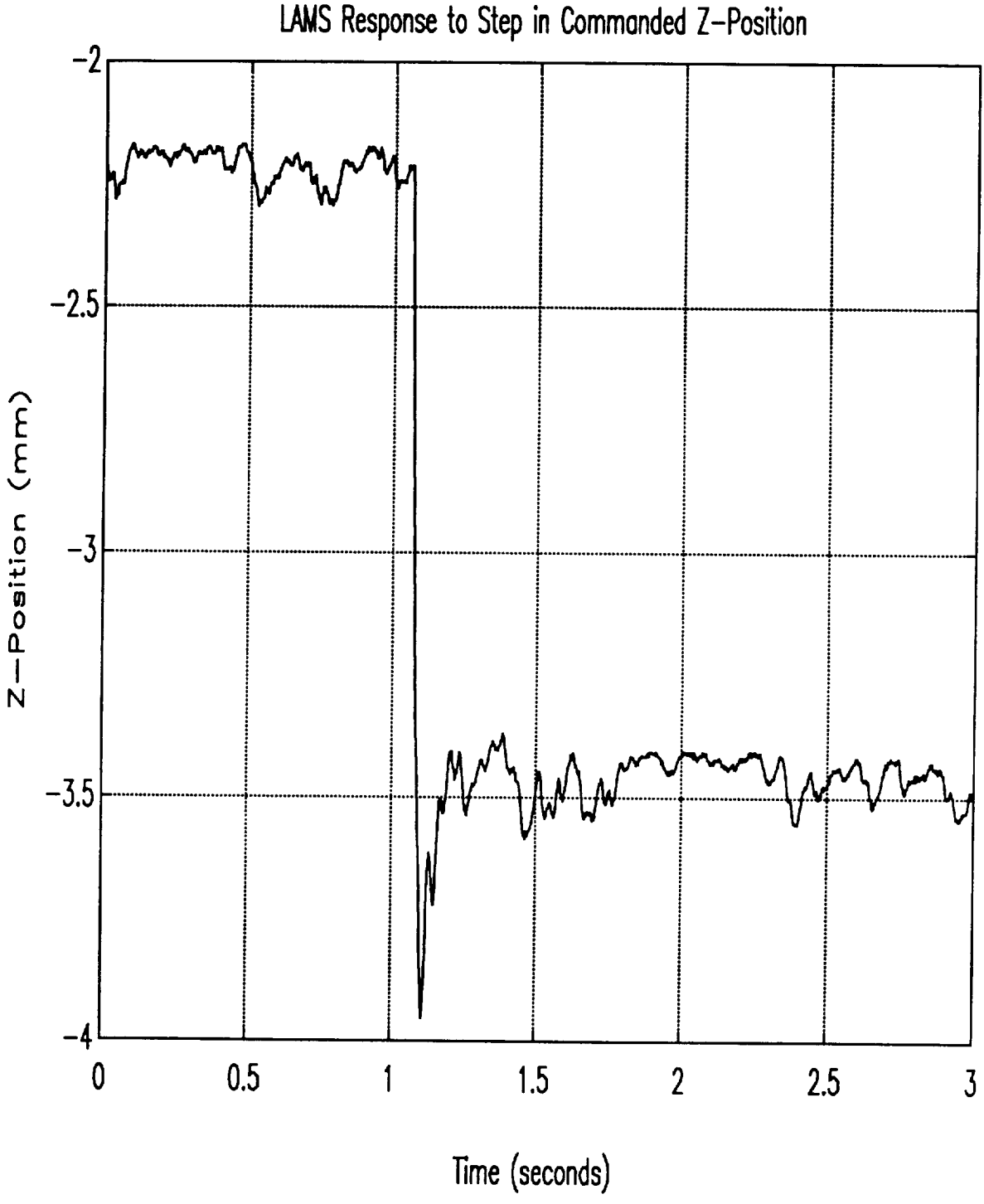

Figure 8.7. Z-Axis Response to Z-Axis Step

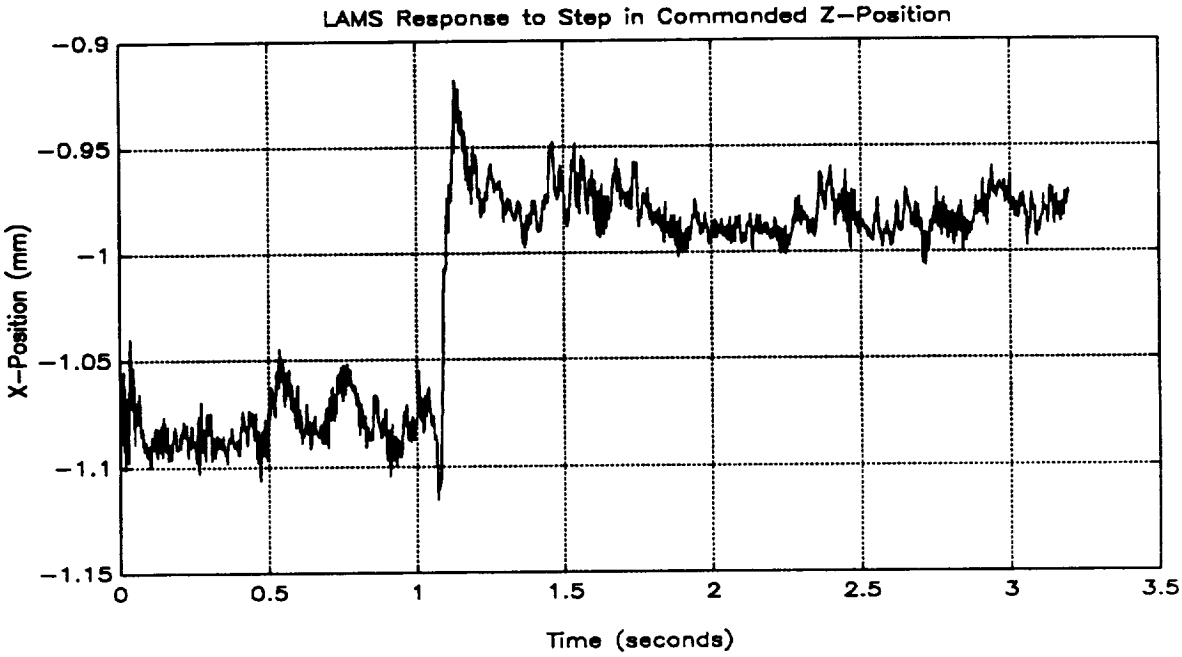

Figure 8.8. X-Axis Response to Z-Axis Step

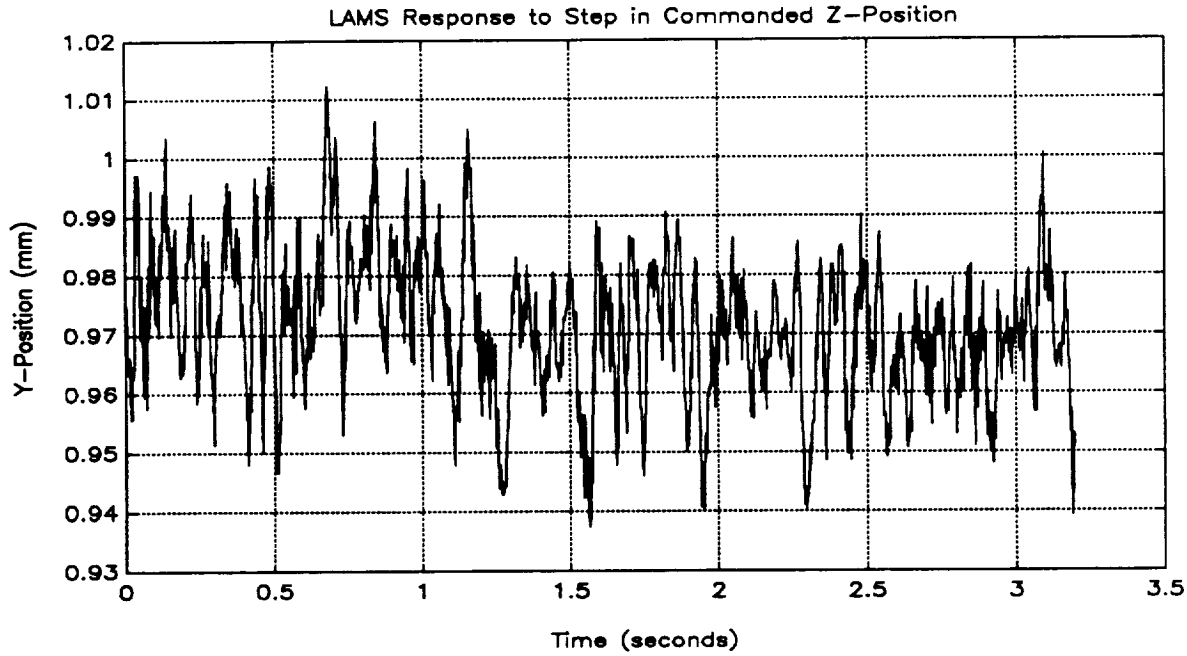

Figure 8.9. Y-Axis Response to Z-Axis Step

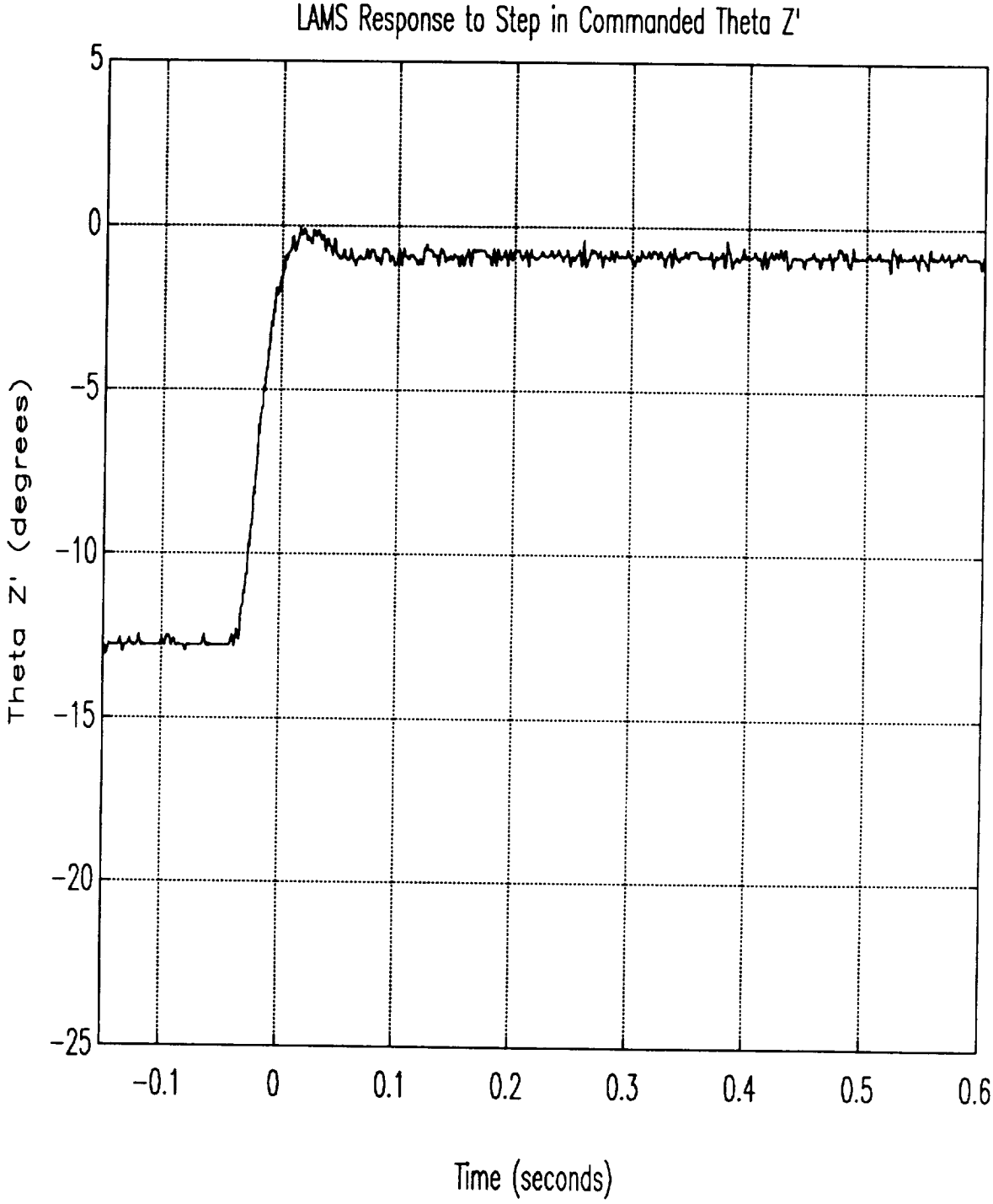

Figure 8.10. Θ_z Response to Θ_z Step

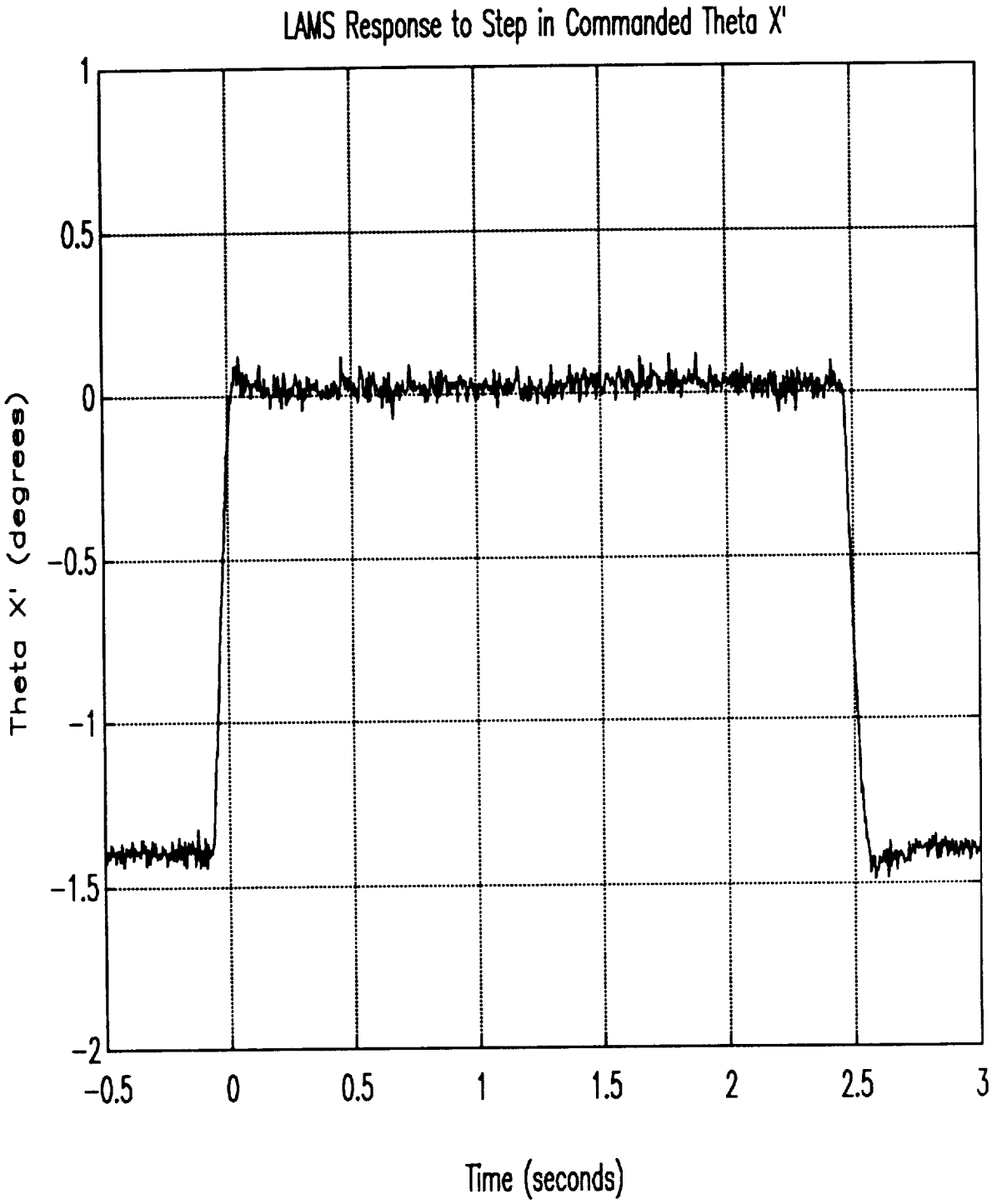

Figure 8.11. $\Theta_{x'}$ Response to $\Theta_{x'}$ Step

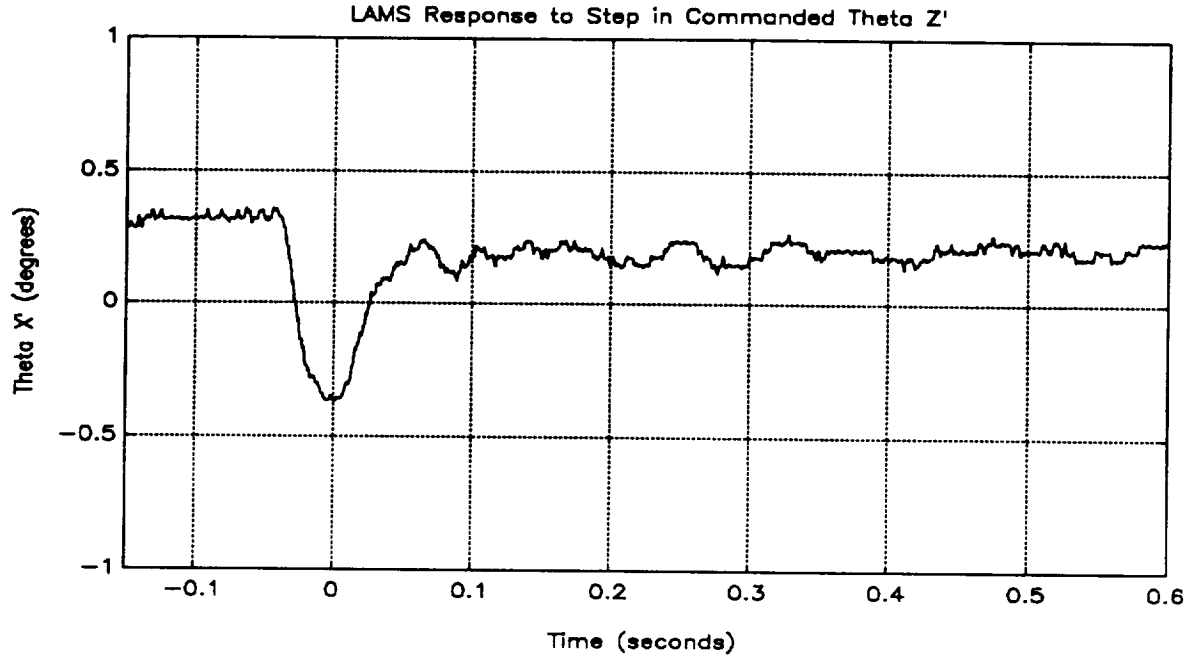

Figure 8.12. $\Theta_{x'}$ Response to Θ_z Step

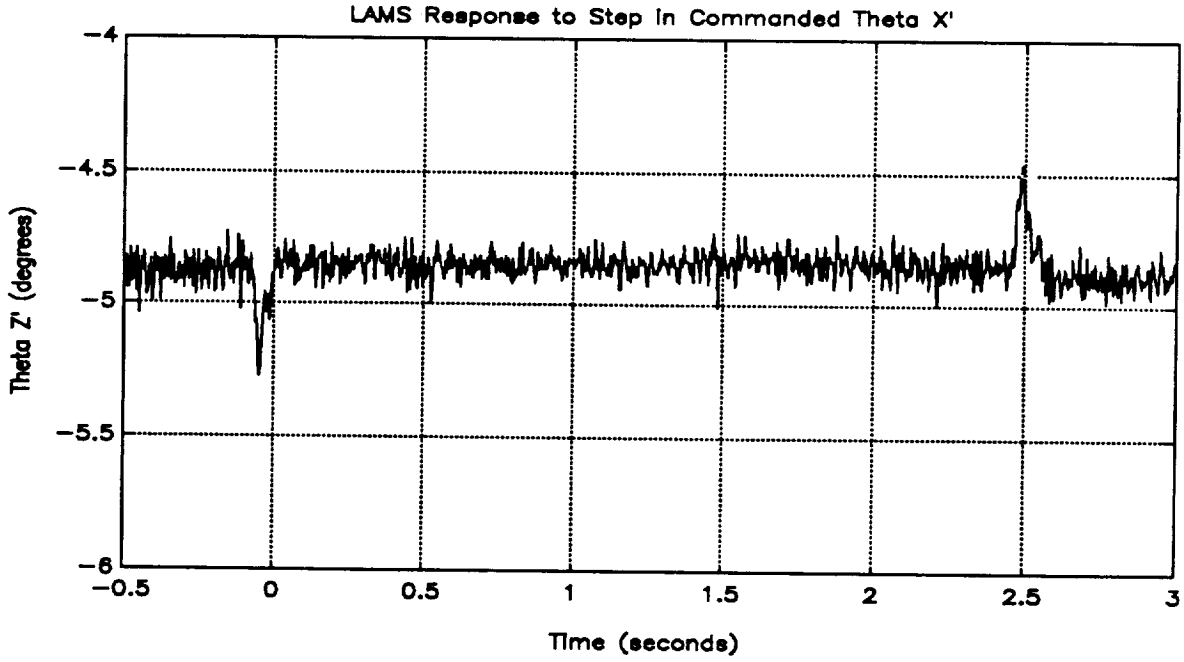

Figure 8.13. $\Theta_{z'}$ Response to Θ_x Step

THIS PAGE

INTENTIONALLY

LEFT BLANK

9. Conclusions and Recommendations for Further Work

SatCon Technology Corporation has successfully demonstrated the feasibility of suspending the source coil of the superconducting LAMS. The superconducting LAMS hardware demonstration is a substantial step forward in the development of the advanced concept control moment gyro.

9.1 Phase II Results

The Phase II results clearly demonstrated the feasibility of suspending the source coil. Gimballing (pointing the axis of the source coil) was, however, demonstrated over only a limited range.

An innovative application of the position dependence of the mutual inductance between two coils is used to sense the angular position of the suspended body of the superconducting LAMS. A set of series resonant static transmitting coils excite one or more tuned passive coils moving with the gyro. The rotational position are determined from the measured coupling between moving and fixed coils. This is achieved by correlating the mutual inductance with the angular separation between the two coils. The method (**R**esonant **M**utual **I**nductance) combines real time data obtained from the full set of transmitters which are then digitally deconvoluted to obtain position information.

The RMI system has the advantage of allowing high oscillator frequencies that are immune to internal or external electrical noise, do not respond to DC or slowly varying magnetic fields, and have no inherent limitation on precision. The system requires one or more oscillator/drivers operating at an ultrasonic carrier frequency, the sensing coils, and a demodulator circuit for each sensed coil. The resulting DC levels can be electronically summed or processed digitally in real time.

The RMI principle has great promise, but will require further development to achieve its full potential. With further development of the rotation sensing system, enhanced angular freedom should be possible.

As currently configured, the rotation sensing system has a limited angular range of about $\pm 5°$. The limitation is due to both the current software configuration and eddy-current shielding by the stainless-steel structure which supports the control coils. SatCon would like to investigate the use of alternate software and hardware in order to achieve an enhanced angular range.

9.2 Future Work

SatCon has proposed to retain the hardware in order to pursue an internal research and development (IR&D) program. SatCon is interested in making further developments on the rotation sensing system that was used in the LAMS testbed. SatCon will investigate the use of alternate software and hardware in order to achieve an enhanced angular range.

9.2.1 Software Modifications

The current software examines the output from three static transmitting coils which are in the proximity of a single passive coil. The RMI system can be readily reconfigured to examine the output of ten static transmitting coils with three passive coils. This will provide a larger active range for angular sensing. The required software changes will have to accommodate a far more complex deconvolution algorithm. The additional time required for running the software will be a primary consideration in the software development.

9.2.2 Hardware Modifications

The static transmitting coils currently operate at a frequency of 71 kHz. The thickness of the statinless steel weldment used to support the LAMS control coils is more than a skin depth, indicating that some of the electromagnetic energy radiated by the transmitting coils is not reaching the passive coils. The reduction is radiated energy reduces the range of the sensing system. The high frequency was selected to coincide with the switching frequency of the switching power amplifiers used to drive

the LAMS control coils. Lowering the tuning frequency of the transmitting coils may have a substantial impact on the performance of the sensing system.

9.3 Benefits of the Proposed Research

The proposed IR&D program will have benefits to NASA and other Government agencies as well as to SatCon.

9.3.1 Benefits to NASA

The superconducting LAMS was an experiment directed toward the development of the control technologies required to demonstrate an advanced concept CMG type of angular momentum exchange effector. The advanced concept CMG will also require a large angle capability in the angular sensing system. The proposed IR&D program will lead to the development of this capability.

9.3.2 Benefits to Other Government Agencies

The RMI sensing system will also be usable in other Government research programs. SatCon has proposed a modified RMI sensing system to the Naval Weapons Center for sensing the rotational parameters required by a free gyro seeker of a multi-spectrum guidance system. The Navy's motivation in soliciting innovative sensors for the gyros of IR seekers is improved precision in angle, rate, and phase measurements in a smaller volume than current designs.

THIS PAGE

INTENTIONALLY

LEFT BLANK

Appendix A. Mechanical Drawings of Fabricated Parts

THIS PAGE

INTENTIONALLY

LEFT BLANK

REVISIONS				
REV	DESCRIPTION	DWN	CHK	APPVL/DATE

NOTES:

1. FINISH WHERE MACHINED 63
2. REMOVE BURRS AND BREAK SHARP EDGES .020 MAX

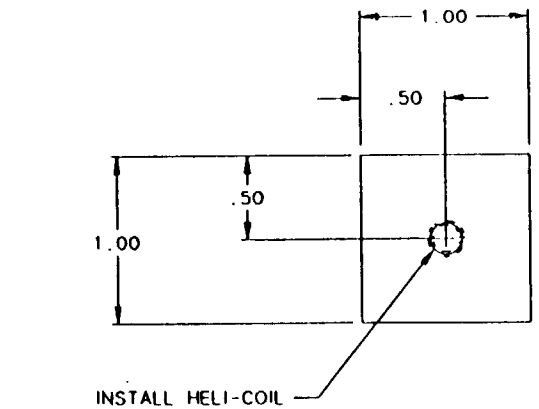

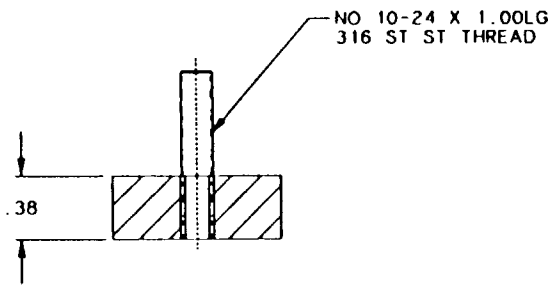

DWG. NO. 1016303 SH 1

		UNLESS OTHERWISE SPECIFIED CAPACITOR VALUES ARE IN RESISTOR VALUES ARE IN OHMS DIMENSIONS ARE IN INCHES TOLERANCE ON DECIMALS .XX ± .01 .XXX ± .005 ANGLES ± - DO NOT SCALE THIS DRAWING MATERIAL ALUM ALLOY 6061-T6	CONTRACT NO
			DRAWN K AVAKIAN 20JUL90
			CHECKED
			ENGINEER
			APPROVED
			APPROVED
			SATCON APPROVED
NEXT ASSY	USED ON		
APPLICATION			

SATCON

BRACKET, SENSOR COILS LAMS

SIZE	FSCM NO.	DRAWING NO.	REV
C		1016303	1

SCALE 4/1 SHEET 1

NOTES:

1. FINISH WHERE MACHINED 63
2. REMOVE BURRS AND BREAK SHARP EDGES .020 MAX

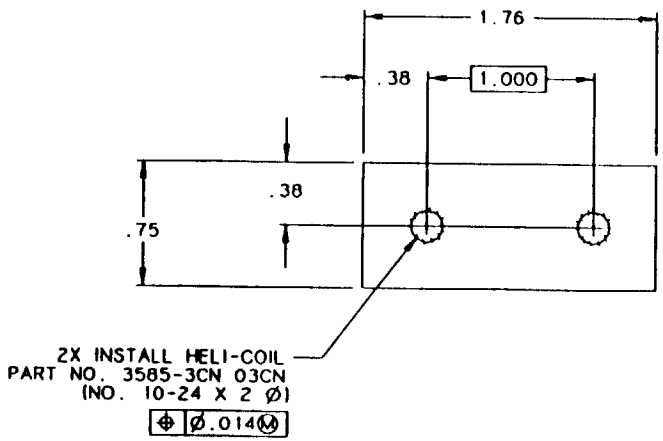

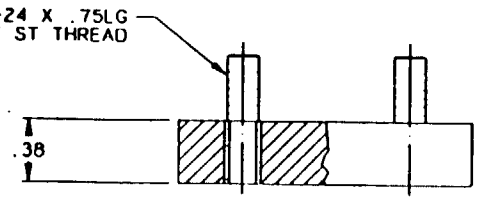

REVISIONS				
REV	DESCRIPTION	DWN	CHK	APPVL/DATE

UNLESS OTHERWISE SPECIFIED
CAPACITOR VALUES ARE IN
RESISTOR VALUES ARE IN OHMS
DIMENSIONS ARE IN INCHES
TOLERANCE ON
DECIMALS ANGLES
.XX ± .01 ± -
.XXX ± .005
DO NOT SCALE THIS DRAWING
MATERIAL
ALUM ALLOY
6061-T6

CONTRACT NO	
DRAWN K AVAKIAN	30JUL90
CHECKED	
ENGINEER	
APPROVED	
APPROVED	
SATCON APPROVED	

NEXT ASSY	USED ON
APPLICATION	

SATCON

BRACKET, SPHERE ATTACHMENT LAMS

SIZE	FSCM NO.	DRAWING NO.	REV
C		1016304	2

SCALE 2/1 SHEET 1

DWG. NO. 1016304 SH 1

176

FEB 0 1 1991

REVISIONS				
REV	DESCRIPTION	DWN	CHK	APPVL/DATE

NOTES:

1. FINISH WHERE MACHINED $\sqrt{63}$
2. REMOVE BURRS AND BREAK SHARP EDGES .020 MAX

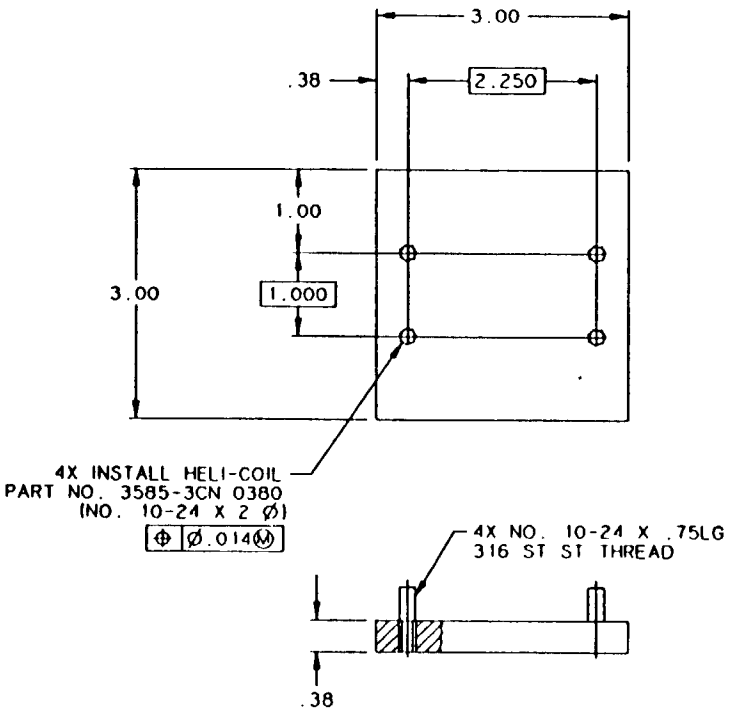

		UNLESS OTHERWISE SPECIFIED CAPACITOR VALUES ARE IN RESISTOR VALUES ARE IN OHMS DIMENSIONS ARE IN INCHES TOLERANCE ON DECIMALS .XX ± .01 .XXX ± .005 ANGLES ± - DO NOT SCALE THIS DRAWING MATERIAL ALUM ALLOY 6061-T6	CONTRACT NO	SATCON
			DRAWN K AVAKIAN 30JUL90	MOUNT, LIFTING BRACKET LAMS
			CHECKED	
			ENGINEER	
			APPROVED	
			APPROVED	
			SATCON APPROVED	
NEXT ASSY	USED ON		SIZE C	FSCM NO.
APPLICATION			DRAWING NO. 1016305	REV 2
			SCALE 1/1	SHEET 1

DWG. NO. 1016305 SH 1

1 FEB 0 1 1991

177

REVISIONS				
REV	DESCRIPTION	DWN	CHK	APPVL/DATE

NOTES:

1. FINISH WHERE MACHINED 63
2. REMOVE BURRS AND BREAK SHARP EDGES .020 MAX

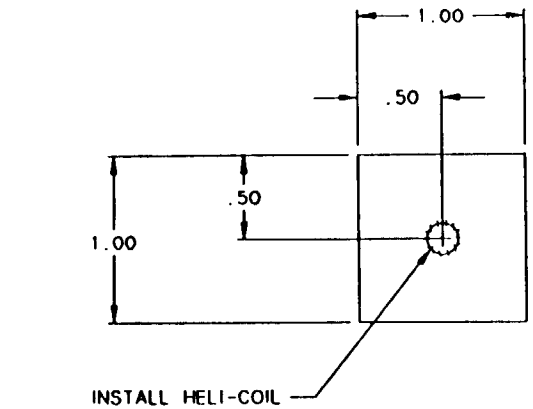

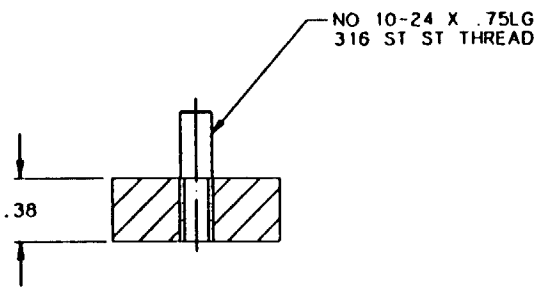

NEXT ASSY	USED ON	UNLESS OTHERWISE SPECIFIED CAPACITOR VALUES ARE IN RESISTOR VALUES ARE IN OHMS DIMENSIONS ARE IN INCHES TOLERANCE ON DECIMALS .XX ± .01 .XXX ± .005 ANGLES ± - DO NOT SCALE THIS DRAWING	CONTRACT NO	SATCON
APPLICATION		MATERIAL ALUM ALLOY 6061-T6	DRAWN R AVAKIAN 30JUL90	MOUNT, SENSOR COIL LAMS
			CHECKED	
			ENGINEER	
			APPROVED	
			APPROVED	
			SATCON APPROVED	

SIZE	FSCM NO.	DRAWING NO.	REV
C		1016306	1

SCALE 2/1 SHEET 1

1 FEB 0 1 1991

DWG. NO. 1016306 1 SH

178

NOTES:

1. MATERIAL: ST ST TYPE 304L OR EQUIV (NON-MAGNETIC)
2. REMOVE BURRS AND BREAK SHARP EDGES .02 MAX
3. FINISH WHERE MACHINED 63

REVISIONS				
REV	DESCRIPTION	DWN	CHK	APPVL/DATE
A	RELEASED PER ECR11015	KMA	DB	DB/150CT90

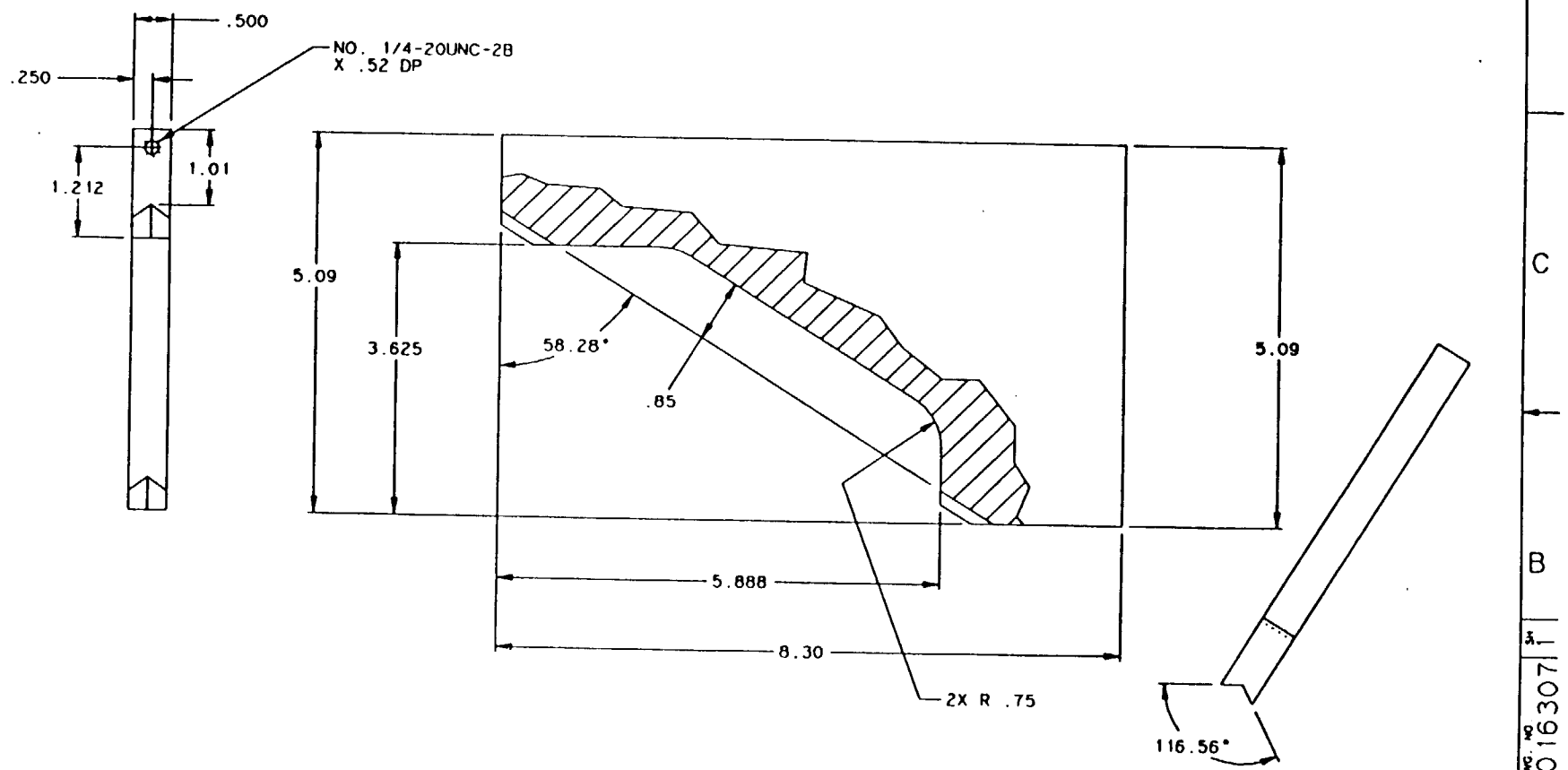

NEXT ASSY	USED ON
APPLICATION	

UNLESS OTHERWISE SPECIFIED
CAPACITOR VALUES ARE IN
RESISTOR VALUES ARE IN OHMS
DIMENSIONS ARE IN INCHES
TOLERANCE ON

DECIMALS	ANGLES
.XX ± .01	± 5°
XXX ± .005	

DO NOT SCALE THIS DRAWING

MATERIAL

SEE NOTE 1

CONTRACT NO		
DRAWN	K AVAKIAN	090CT90
CHECKED	D BUSHKO	150CT90
ENGINEER	D BUSHKO	150CT90
APPROVED	J GOLDIE	150CT90
APPROVED		
SATCON APPROVED		

SATCON

GUSSET
L.A.M.S.

SIZE	FSCM NO.	DRAWING NO.	REV
C		1016307	A

SCALE 1/1 SHEET 1

DWG. NO 1016307 SH 1

FEB 0 1 1991

179

REVISIONS				
REV	DESCRIPTION	DWN	CHK	APPVL/DATE
A	RELEASED PER ECR11015	KMA	DB	DB/15OCT90

NOTES:

1. MATERIAL: ST ST TYPE 304L OR EQUIV (NON-MAGNETIC)
2. REMOVE BURRS AND BREAK SHARP EDGES .02 MAX
3. FINISH WHERE MACHINED 63

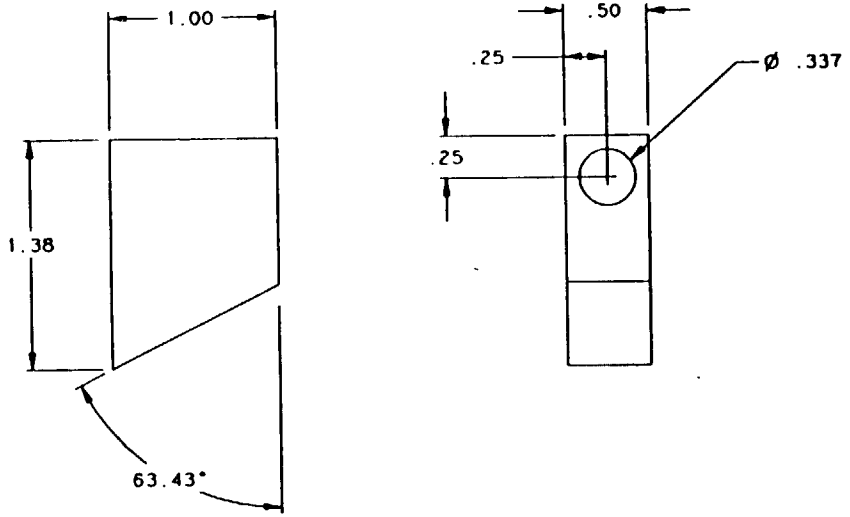

		UNLESS OTHERWISE SPECIFIED CAPACITOR VALUES ARE IN RESISTOR VALUES ARE IN OHMS DIMENSIONS ARE IN INCHES TOLERANCE ON DECIMALS .XX ± .01 XXX ± .005 ANGLES ± .5°	CONTRACT NO	SATCON	
			DRAWN K AVAKIAN 08OCT90	MOUNT - TOP HALF L.A.M.S.	
			CHECKED D BUSHKO 15OCT90		
			ENGINEER D BUSHKO 15OCT90		
		DO NOT SCALE THIS DRAWING	APPROVED J GOLDIE 15OCT90	SIZE C / FSCM NO. / DRAWING NO. 1016308 / REV A	
NEXT ASSY	USED ON	MATERIAL SEE NOTE 1	APPROVED		
APPLICATION			SATCON APPROVED	SCALE 2/1	SHEET 1

DWG. NO. 1016308 REV A

180

REVISIONS				
REV	DESCRIPTION	DWN	CHK	APPVL/DATE
A	INITIAL RELEASE PER ECR11102	KMA	DB	08/02NOV90
B	REVISED PER ECR 11121	KMA	DB	08/2 NOV90

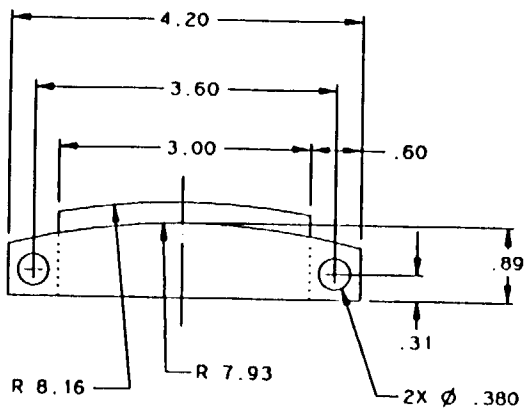

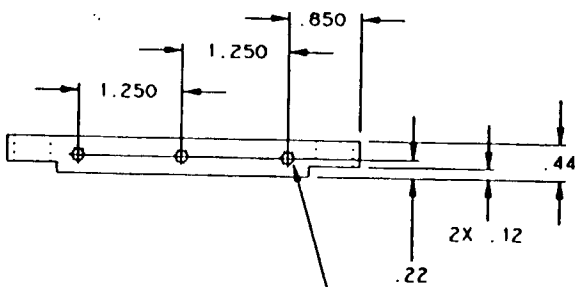

UNLESS OTHERWISE SPECIFIED
CAPACITOR VALUES ARE IN
RESISTOR VALUES ARE IN OHMS
DIMENSIONS ARE IN INCHES
TOLERANCE ON
DECIMALS .XX ± .01 .XXX ± .005
ANGLES ± -

DO NOT SCALE THIS DRAWING

MATERIAL
PHENOLIC
GRADE CE OR LE

NEXT ASSY	USED ON
APPLICATION	

CONTRACT NO.		
DRAWN	K AVAKIAN	31OCT90
CHECKED	D BUSHKO	02NOV90
ENGINEER	D BUSHKO	02NOV90
APPROVED		
APPROVED		
SATCON APPROVED		

SATCON

MOUNT, SPHERE-
TOP HALF
L.A.M.S.

SIZE	FSCM NO.	DRAWING NO.	REV
C		1016309	B

SCALE 1/1 SHEET 1

DWG NO 1016309 1 SH

FEB 0 1 1991

181

REVISIONS				
REV	DESCRIPTION	DWN	CHK	APPVL/DATE
A	INITIAL RELEASE PER ECR11102	KMA	DB	08/02NOV90
B	REVISED PER ECR 21121	KMA	DB	08/2 NOV90

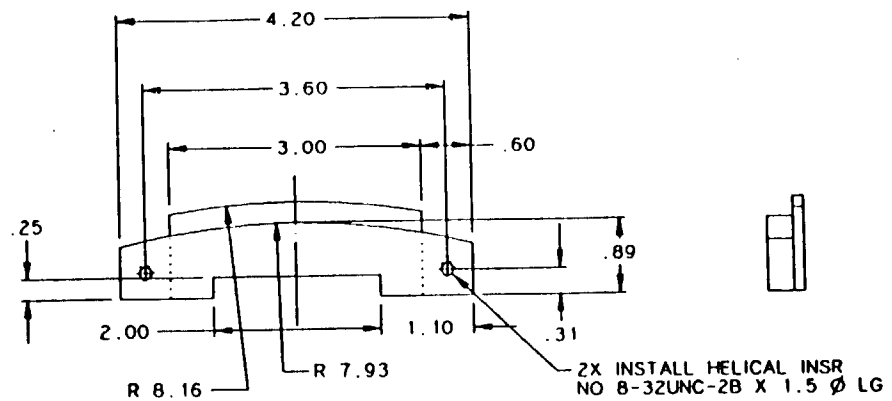

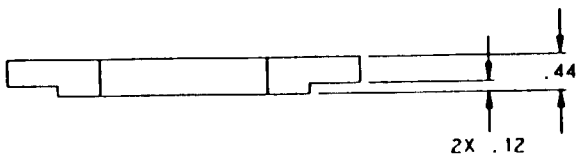

182

DWG. NO 1016310 REV B

NEXT ASSY	USED ON
APPLICATION	

UNLESS OTHERWISE SPECIFIED
CAPACITOR VALUES ARE IN
RESISTOR VALUES ARE IN OHMS
DIMENSIONS ARE IN INCHES
TOLERANCE ON

DECIMALS	ANGLES
.XX ± .01	± -
.XXX ± .005	

DO NOT SCALE THIS DRAWING

MATERIAL
PHENOLIC
GRADE CE OR LE

CONTRACT NO.		
DRAWN	K AVAKIAN	31OCT90
CHECKED	D BUSHKO	02NOV90
ENGINEER	D BUSHKO	02NOV90
APPROVED		
APPROVED		
SATCON APPROVED		

SATCON

MOUNT, SPHERE-
BOTTOM HALF
L.A.M.S.

SIZE	FSCM NO.	DRAWING NO.	REV
C		1016310	B

SCALE 1/1 SHEET 1

FEB 0 1 1991

NOTES:

1. FINISH WHERE MACHINED 63
2. REMOVE BURRS AND BREAK SHARP EDGES .015 MAX

REVISIONS				
REV	DESCRIPTION	DWN	CHK	APPVL/DATE
A	INITIAL RELEASE PER ECR11102	KMA	DB	02/02NOV90

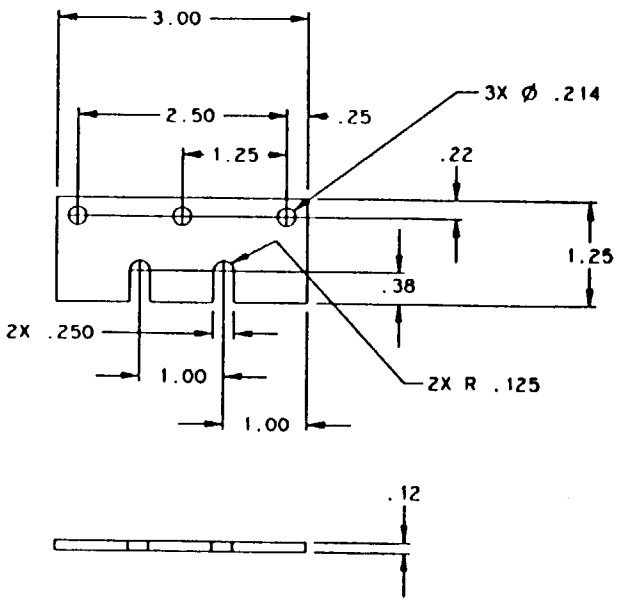

NEXT ASSY	USED ON	UNLESS OTHERWISE SPECIFIED CAPACITOR VALUES ARE IN RESISTOR VALUES ARE IN OHMS DIMENSIONS ARE IN INCHES TOLERANCE ON DECIMALS .XX ± .01 .XXX ± .005 ANGLES ± -	CONTRACT NO	SATCON
APPLICATION		DO NOT SCALE THIS DRAWING	DRAWN K AVAKIAN 02NOV90	BRACKET, SPHERE MOUNT TOP L.A.M.S.
		MATERIAL ST ST TYPE 303 (NON-MAGNETIC)	CHECKED D BUSHKO 02NOV90	
			ENGINEER D BUSHKO 02NOV90	
			APPROVED	
			APPROVED	
			SATCON APPROVED	

SIZE	FSCM NO.	DRAWING NO.	REV
C		1016311	A
SCALE 1/1		SHEET 1	

DWG NO 1016311 REV A

FEB 0 1 1991

183

REV	DESCRIPTION	DRN	CHK	APPVD & DATE
A	INITIAL RELEASE PER ECR 11102	KVALDS		

NOTES:

1. OUTER SPHERICAL RADIUS TO BE SPHERICAL TO WITHIN ±.010
2. OUTER SPHERICAL RADIUS TO BE FINISHED TO 63
3. OUTER SPHERICAL RADIUS TO BE MATCHED WITH OUTER SPHERICAL RADIUS OF PART NO. 1016406 TO WITHIN ± .010

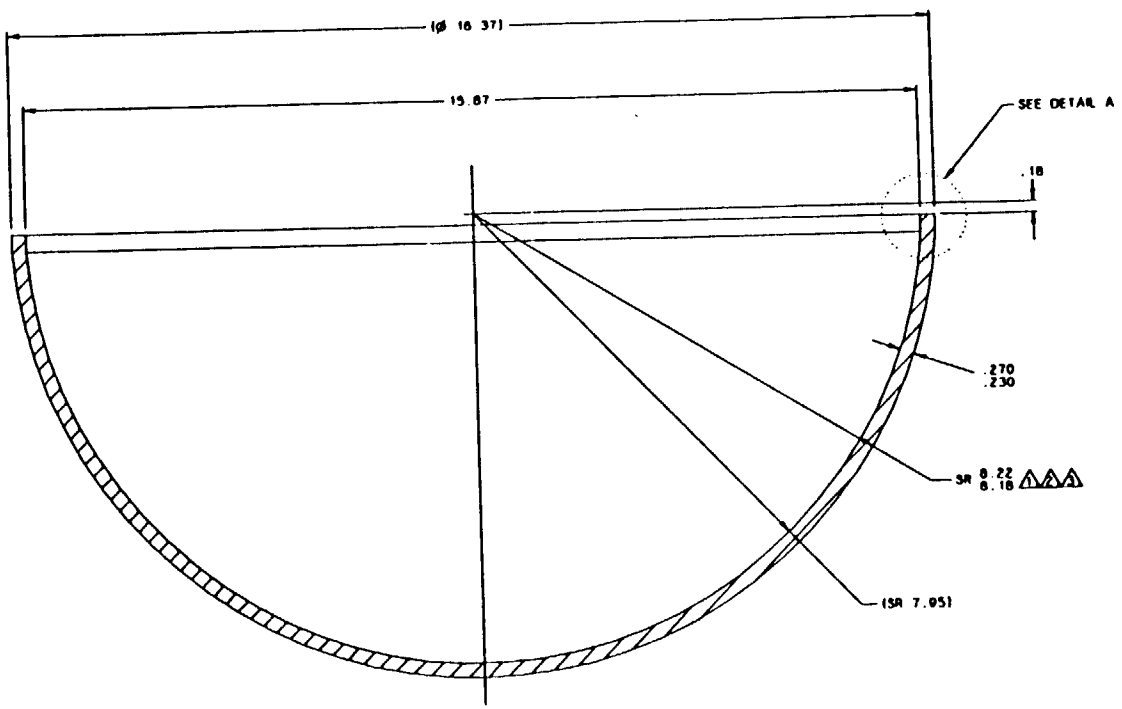

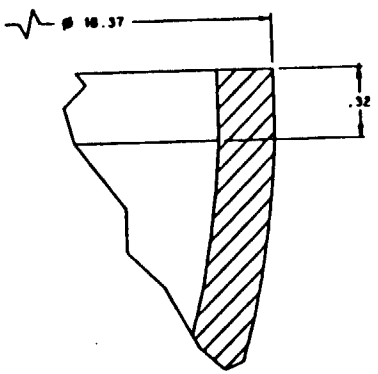

DETAIL A
SCALE: 4/1

PART NO. 1016405-001
SEE PL

NEXT ASSY	USED ON
APPLICATION	

ROYALSTAT R83

SATCON

SPHERE, BOTTOM
LAMS

SIZE	FSCM NO	DRAWING NO.	REV
D		1016405	A

SCALE 1 SHEET 1

1016405

FEB 0 1 1991

NOTES:

1. OUTER SPHERICAL RADIUS TO BE SPHERICAL TO WITHIN ±.010
2. OUTER SPHERICAL RADIUS TO BE FINISHED TO 63
3. OUTER SPHERICAL RADIUS TO BE MATCHED WITH OUTER SPHERICAL RADIUS OF PART NO. 1016405 TO WITHIN ±.010

REV	DESCRIPTION	DRN	CHK	APPVD & DATE
A	INITIAL RELEASE PER ECR 11102	KWA	DB	

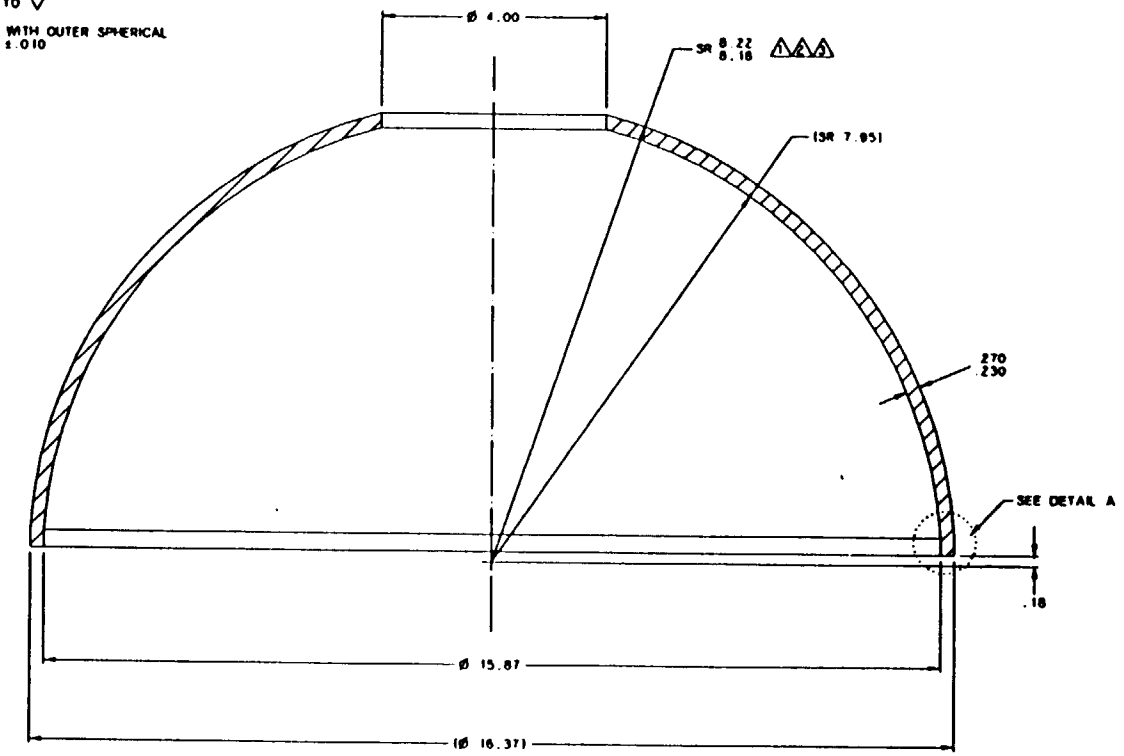

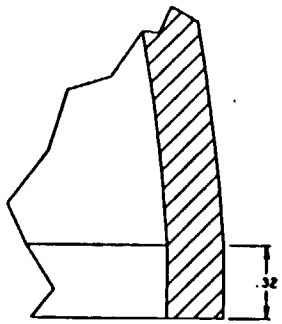

DETAIL A
SCALE: 4/1

NEXT ASSY	USED ON	LAMS	
APPLICATION		ROYALSTAT R83	

SATCON

SPHERE, TOP
LAMS

SIZE	FSCM NO	DRAWING NO.	REV
D		1016406	A
SCALE 1		SHEET 1	

185

1016406 A

FEB 0 1 1991

NOTES:
1. REMOVE FEATHER EDGES .020 MAX
2. FINISH ALL OVER 63

REV	DESCRIPTION	DWN	CHK	APPD	DATE
A	INITIAL RELEASE PER ECR23105	KWADB			

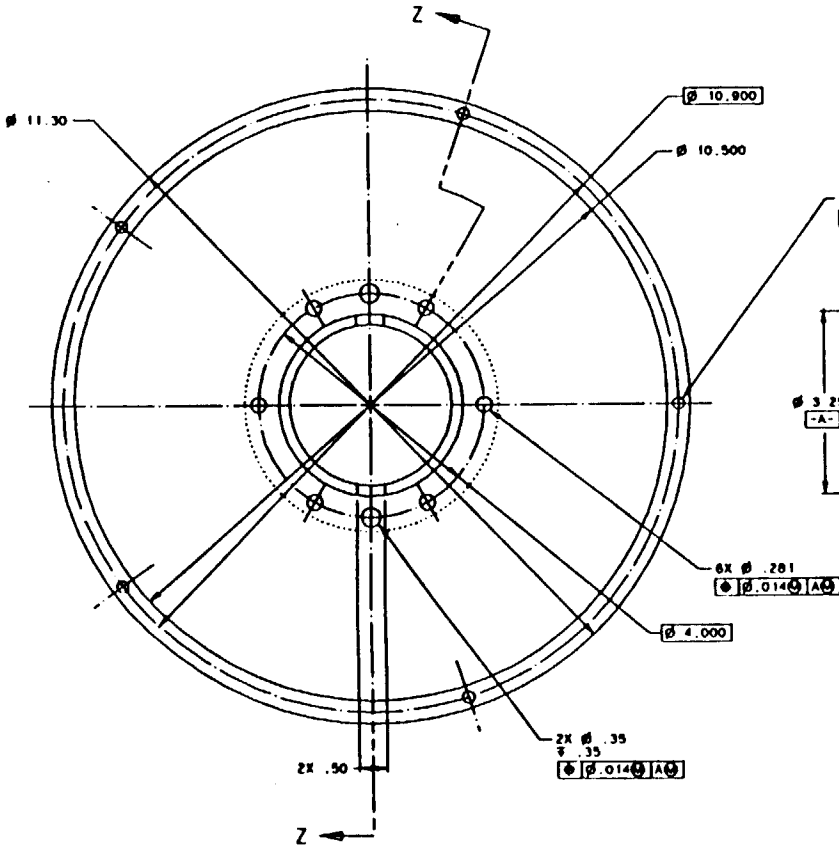

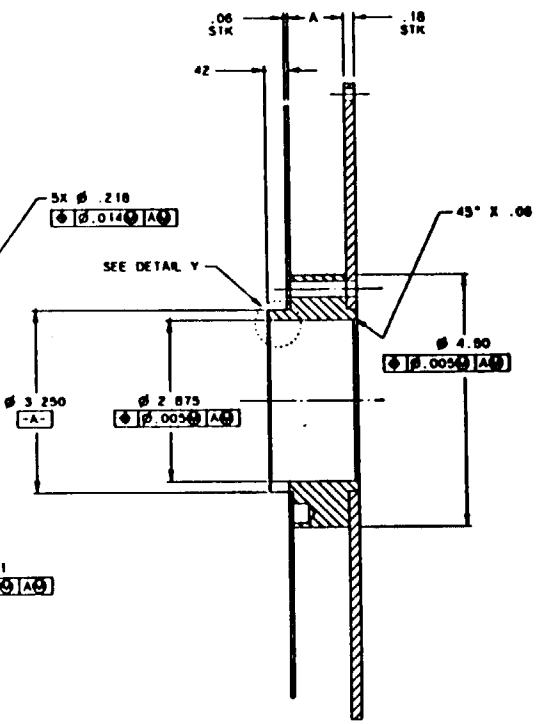

SECTION Z-Z

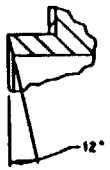

DETAIL Y
SCALE 2/1

TABULATION		
PART NO.	DIM A	REQD
1016413-001	1.010-.990	3
1016413-002	2.010-1.990	1

PART NO. 1016413 - SEE TABLE
SEE PL

NEXT ASSY	LAMS		
APPLICATION	USED ON	0-10 OR EQUIV	

BOBBIN- CONTROL COIL SENSOR MOUNT LAMS

SIZE	FSCM NO	DRAWING NO.	REV
D		1016413	A

SCALE 1/1 SHEET 1

1016413 F1

FEB 0 1 1991

NOTES:
1. REMOVE FEATHER EDGES .020 MAX
2. FINISH ALL OVER 63

REV	DESCRIPTION	DRN	CHK	APPD & DATE
A	INITIAL RELEASE PER23105	KWA	DB	

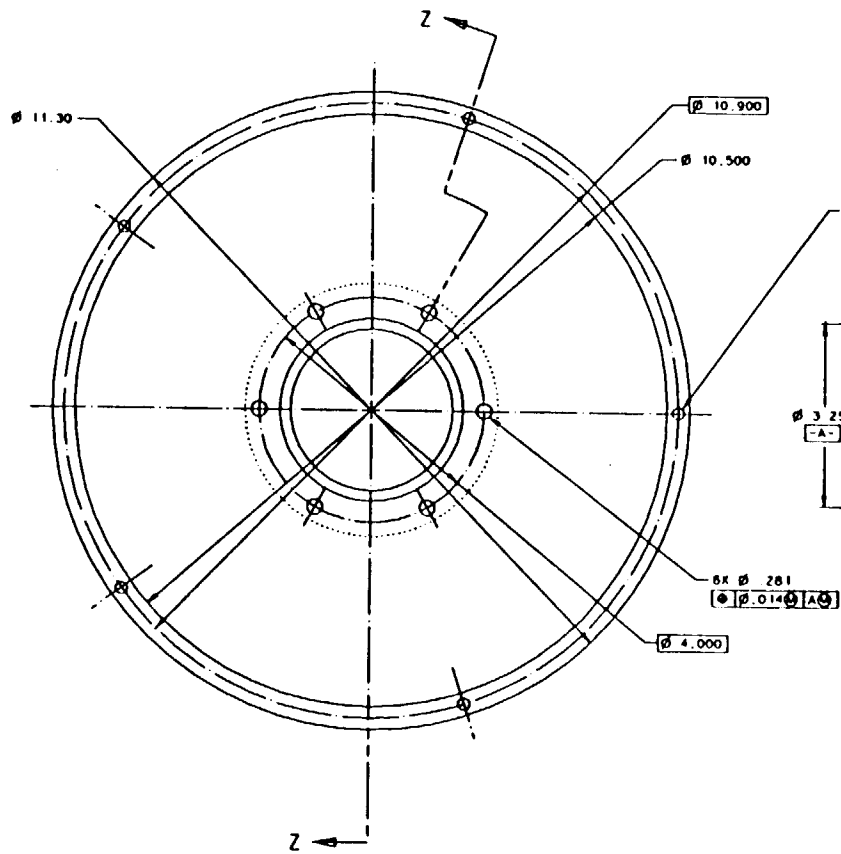

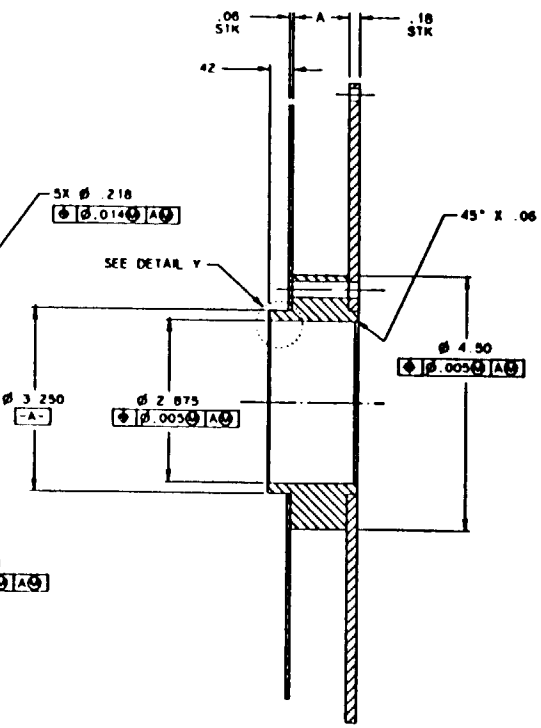

SECTION Z-Z

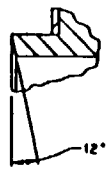

DETAIL Y
SCALE: 2/1

TABULATION		
PART NO.	DIM A	REQD
1016414-001	1.010-.990	5
1016414-002	2.010-1.990	1

PART NO.1016414-SEE TABLE
SEE PL

				SATCON
				BOBBIN- CONTROL COIL LAMS
				SIZE D / FSCM NO / DRAWING NO. 1016414 / REV A
				SCALE 1/1 / SHEET 1
NEXT ASSY	LAMS			
APPLICATION	USED ON	G-10 OR EQUIV		

1016414 A

187

FEB 0 1 1991

REVISIONS			
REV	DESCRIPTION	DRWN	APPVD
A	INITIAL RELEASE PER ECR 13107		

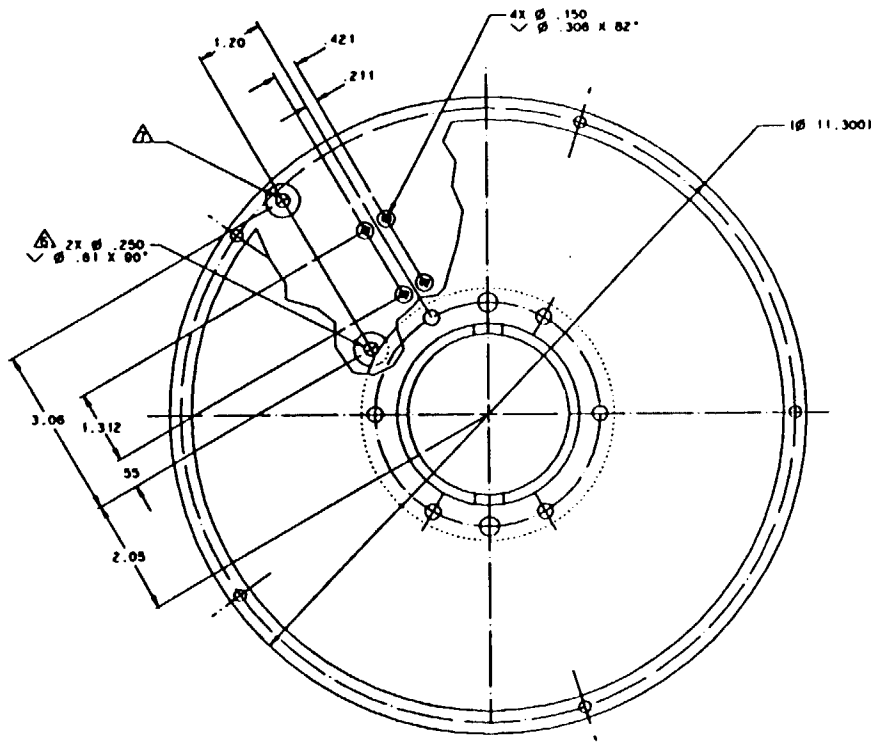

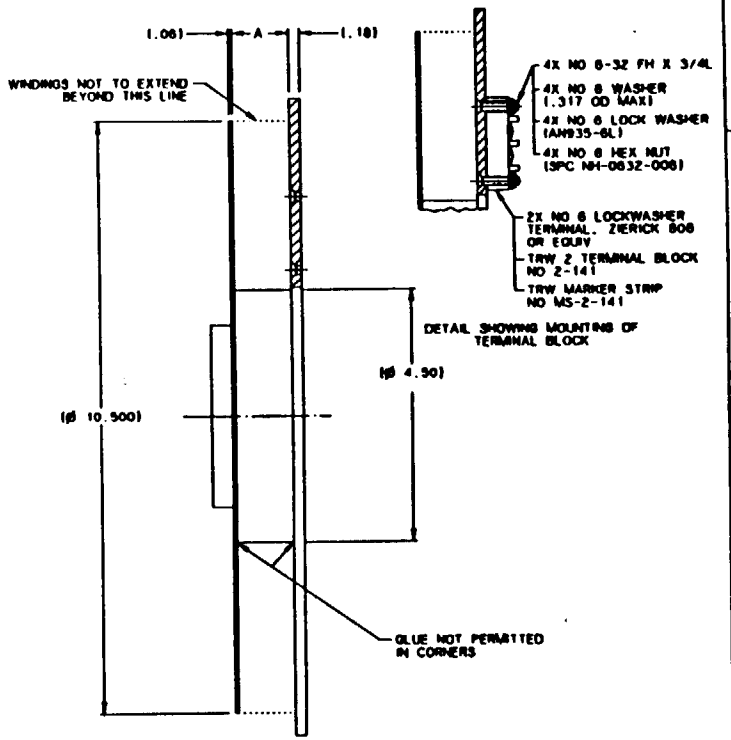

NOTES:

1. REMOVE FEATHER EDGES .020 MAX
2. THE 2 .00 IN COIL SHOULD BE AS IDENTICAL AS POSSIBLE TO PART NO 1016416-002 AND THE 5 1.00 IN COILS SHOULD BE AS IDENTICAL AS POSSIBLE TO THE 5 1.00 IN COILS PART NO 1016415-001
3. THE SIDES OF THE BOBBIN MUST BE SUPPORTED DURING WINDING AND CURING
4. EACH LAYER SHALL BE COATED WITH DOLPH BC-346A VARNISH AND WHEN COMPLETE, AN EQUIVALANT VARNISH MAY BE USED. FEATURES ARE "NO ASSEMBLY RUSH" BAKE CURED, MIN. CLASS 200. COMPATIBILITY WITH WITH ML FILM MAGNET WIRE INSULATION. CHECK WITH SATCON IF YOU DOUBT EQUIVALENCE
5. MIN. MAGNET WIRE BEND RADII 5 WIRE DIAMETERS (FILM FAILURE)

⚠ START OF WIRE TO BEGIN AT THIS LOCATION, WIND IN A CLOCKWISE DIRECTION

⚠ FINISH OF WIRE TO END AT THIS LOCATION

TABULATION

PART NO	DIM A	REQD	WIRE SIZE	TURNS/LAYER	NO. OF LAYERS	NO. OF TURNS
1016415-001	1.00	5	NO. 15 HAL FILM	16	44	704
1016415-002	2.00	1	NO. 12 HAL FILM	23	32	736

PART NO. 1016415 - SEE TABLE

SEE PL ———

	LAMS		
NEXT ASSY	USED ON		
APPLICATION			

1016413-001
1016413-002

SATCON

BOBBIN- CONTROL COIL SENSOR MOUNT MODIFIED, LAMS

SIZE	FSCM NO	DRAWING NO.	REV
D		1016415	A

SCALE 1/1 SHEET 1

1016415 A

FEB 0 1 1991

REV	DESCRIPTION	DRN	CHK	APPR. DATE
A	INITIAL RELEASE PER ECR 13107	MMA	LAD	

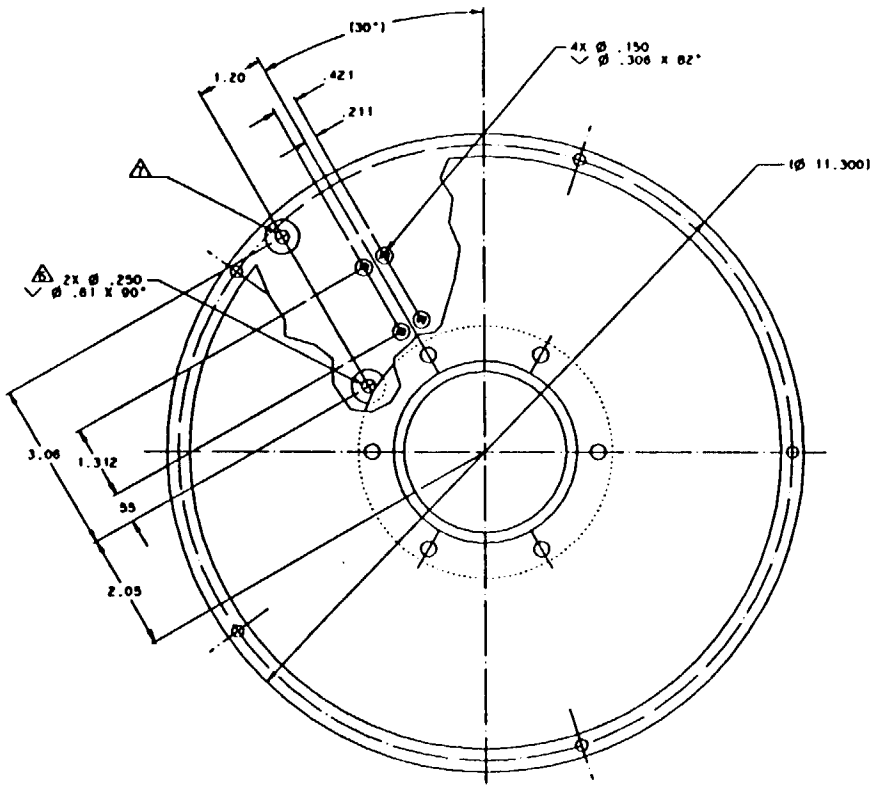

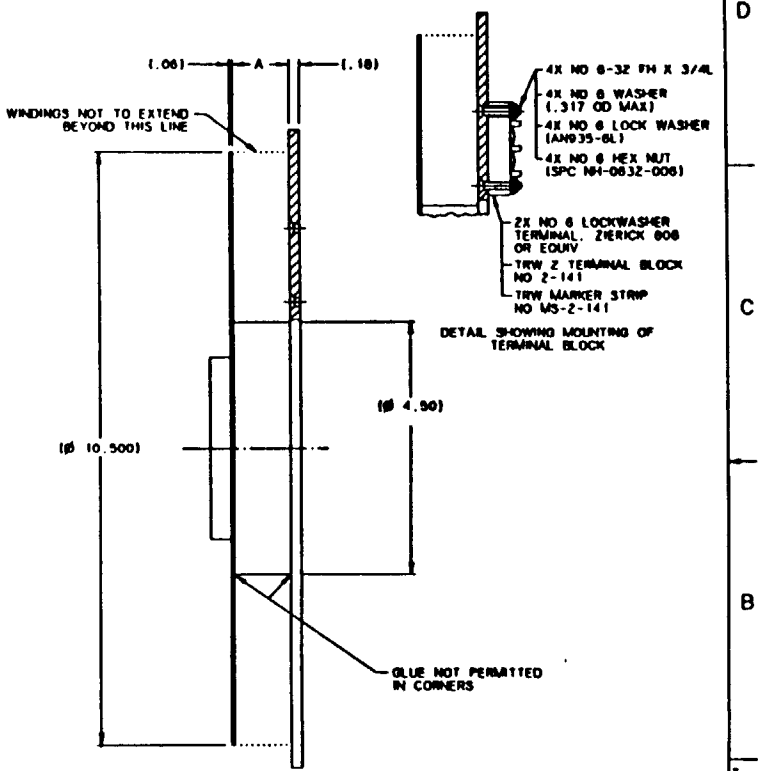

NOTES:

1. REMOVE FEATHER EDGES .020 MAX
2. THE 2 00 IN COIL SHOULD BE AS IDENTICAL AS POSSIBLE TO PART NO 1016415-002 AND THE 5 1.00 IN COILS SHOULD BE AS IDENTICAL AS POSSIBLE TO THE 5 1.00 IN COILS PART NO 1016415-001
3. THE SIDES OF THE BOBBIN MUST BE SUPPORTED DURING WINDING AND CURING
4. EACH LAYER SHALL BE COATED WITH DOLPH BC-346A VARNISH AND WHEN COMPLETE, AN EQUIVALENT VARNISH MAY BE USED. FEATURES ARE 'NO ASSEMBLY RUSH' BAKE CURED, MIN. CLASS 200. COMPATIBILITY WITH WITH ML FILM MAGNET WIRE INSULATION. CHECK WITH SATCON IF YOU DOUBT EQUIVALENCE
5. MIN. MAGNET WIRE BEND RADII 5 WIRE DIAMETERS (FILM FAILURE)

(A) START OF WIRE TO BEGIN AT THIS LOCATION. WIND IN A CLOCKWISE DIRECTION

(A) FINISH OF WIRE TO END AT THIS LOCATION

TABULATION

PART NO.	DIM A	REQD	WIRE SIZE	TURNS/LAYER	NO. OF LAYERS	NO. OF TURNS
1016416-001	1.00	5	NO. 15 HML FILM	18	44	764
1016416-002	2.00	1	NO. 12 HML FILM	23	32	736

PART NO.1016416 - SEE TABLE
SEE PL ———

		LAMS	
NEXT ASSY	USED ON		
APPLICATION			

1016414-001
1016414-002

SATCON

BOBBIN- CONTROL COIL MODIFIED LAMS

SIZE	FSCM NO	DRAWING NO.	REV
D		1016416	A

SCALE 1/1 SHEET 1

1016416 11 A

189

FEB 0 1 1991

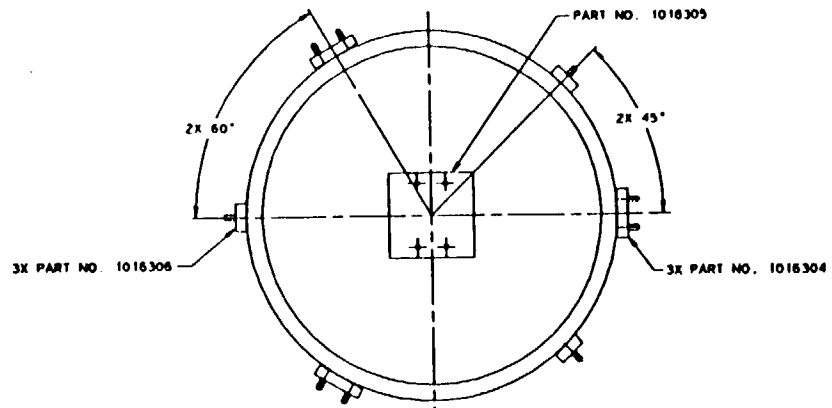

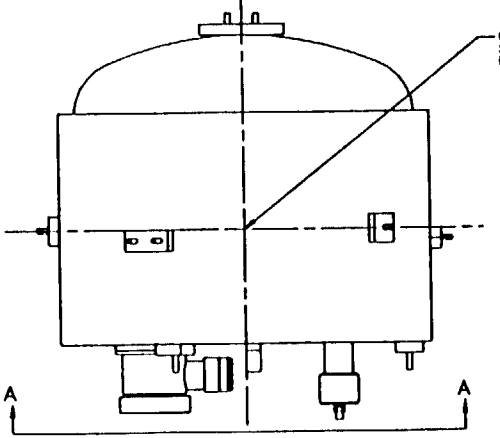

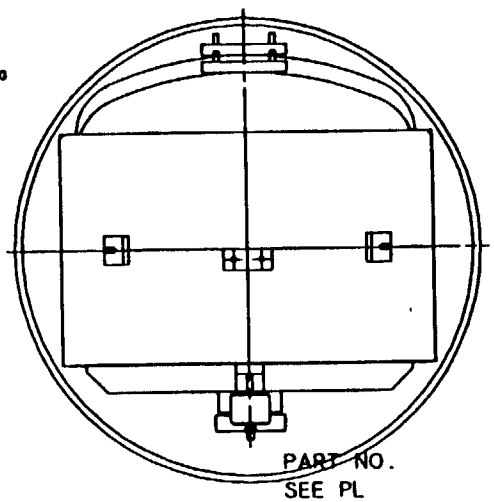

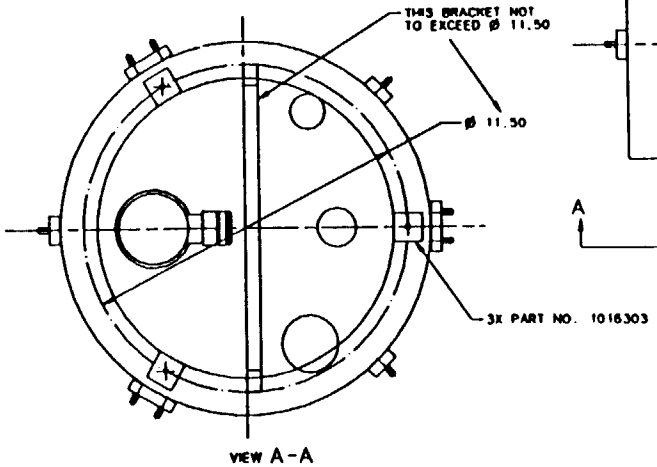

			SATCON
			BRACKET WELDMENT DEWAR LAMS
			SIZE D · DRAWING NO. 1016417 · REV 2
			SCALE 1/2 · SHEET 1
NEXT ASSY	USED ON	LAMS	
APPLICATION			

190

1016417

FEB 0 1 1991

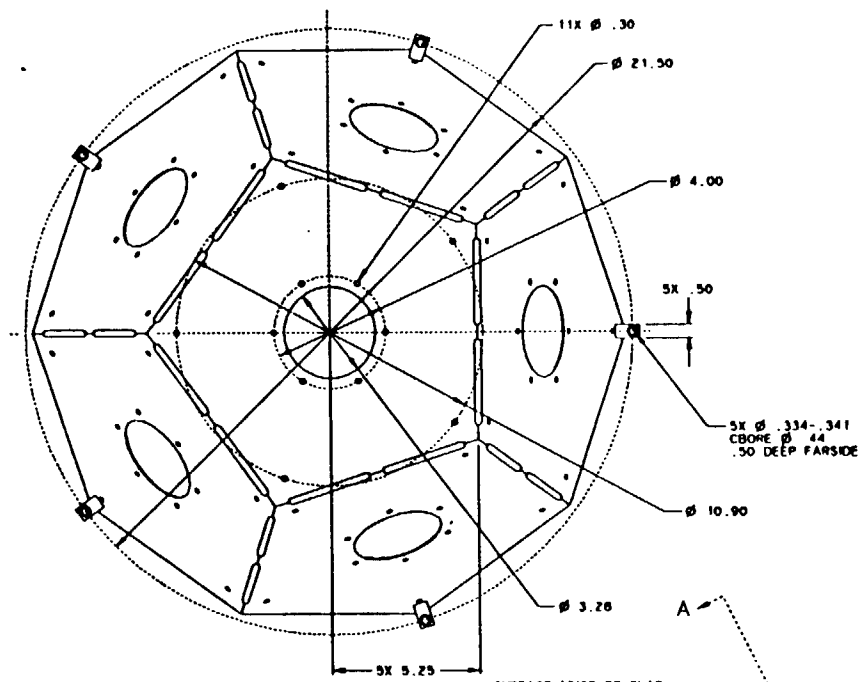

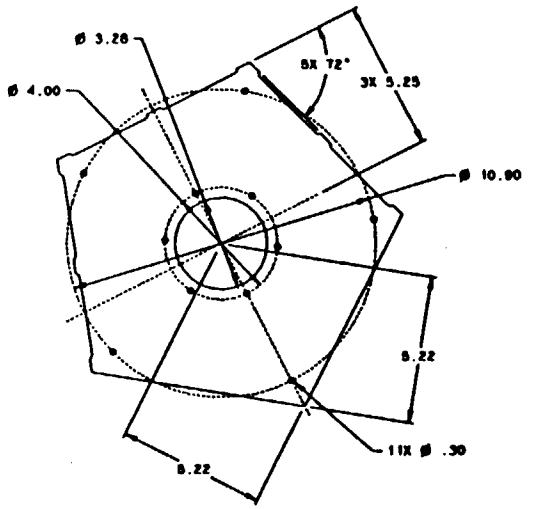

VIEW A-A
5 PLACES

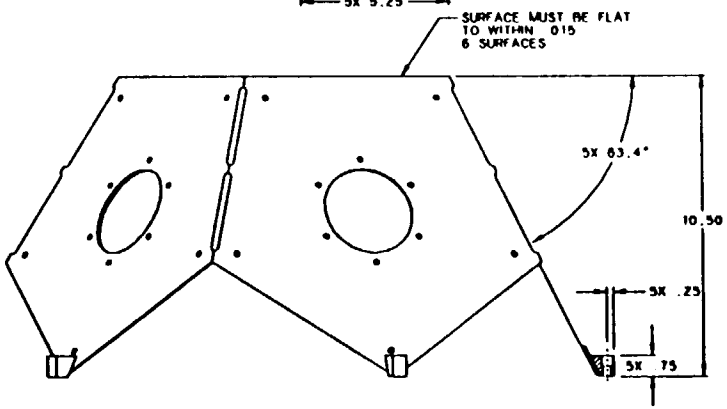

PART NO. 1016418-001
SEE PL ———

NEXT ASSY	USED ON
APPLICATION	

51 ST TYPE 303
OR EQUIV

SATCON

SHELL, UPPER-
CONTROL COIL
L A M S

SIZE	FSCM NO	DRAWING NO	REV
D		1016418	2

SCALE 1/2 SHEET 1

1016418

FEB 0 1 1991

REV	DESCRIPTION	DRAWN	CHK'D	APPR'D & DATE
A	INITIAL RELEASE PER ECN 1015	KWARD		

NOTES:

1. MATERIAL: S1 ST TYPE 304L OR EQUIV 10 GA(.135 THK NON-MAGNETIC)
2. ALL OPPOSING OUTER SURFACES MUST BE PARALLEL TO WITHIN .030

.135

SECTION C-C

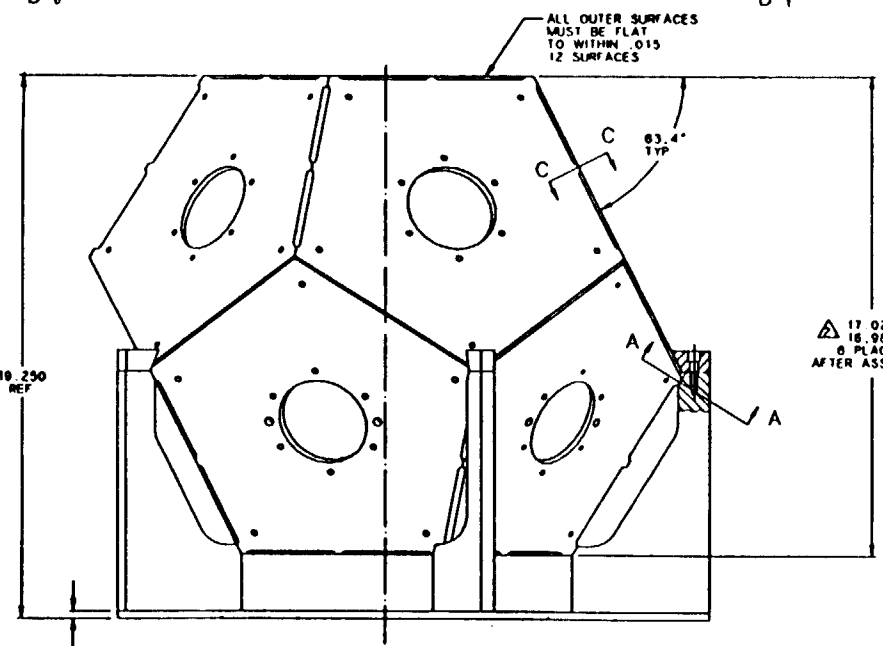

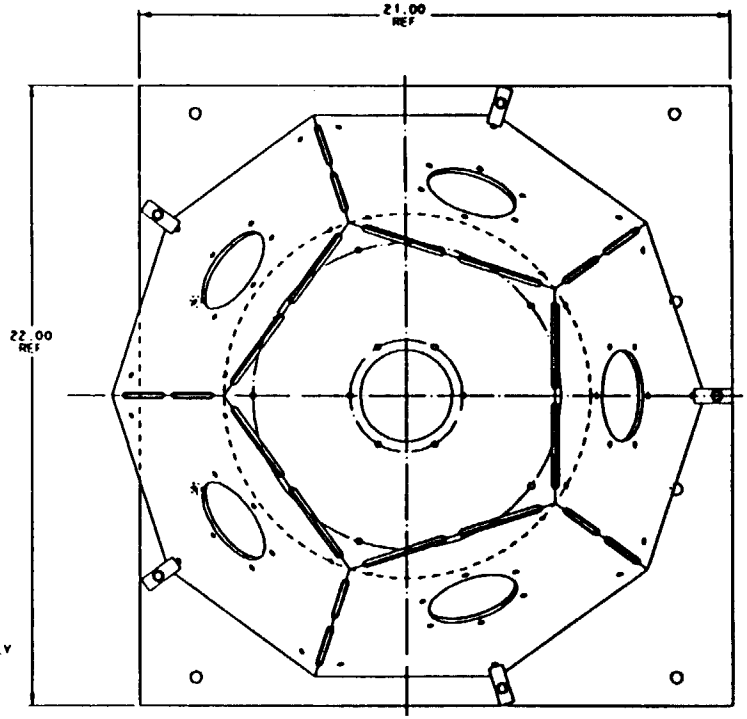

VIEW B-B

SECTION A-A

PART NO. 1016419-001
SEE PL _____

NEXT ASSY	USED ON
APPLICATION	

SEE NOTE 1

SATCON

ASSEMBLY-
COIL SUPPORT
L.A.M.S.

SIZE	FSCM NO.	DRAWING NO.	REV
D		1016419	A

SCALE 1/2 SHEET 1

1016419

192

C-3

FEB 0 1 1991

NOTES:

⚠ MATERIAL: ST ST TYPE 304L OR EQUIV
10 GA(.135 THK NON-MAGNETIC)

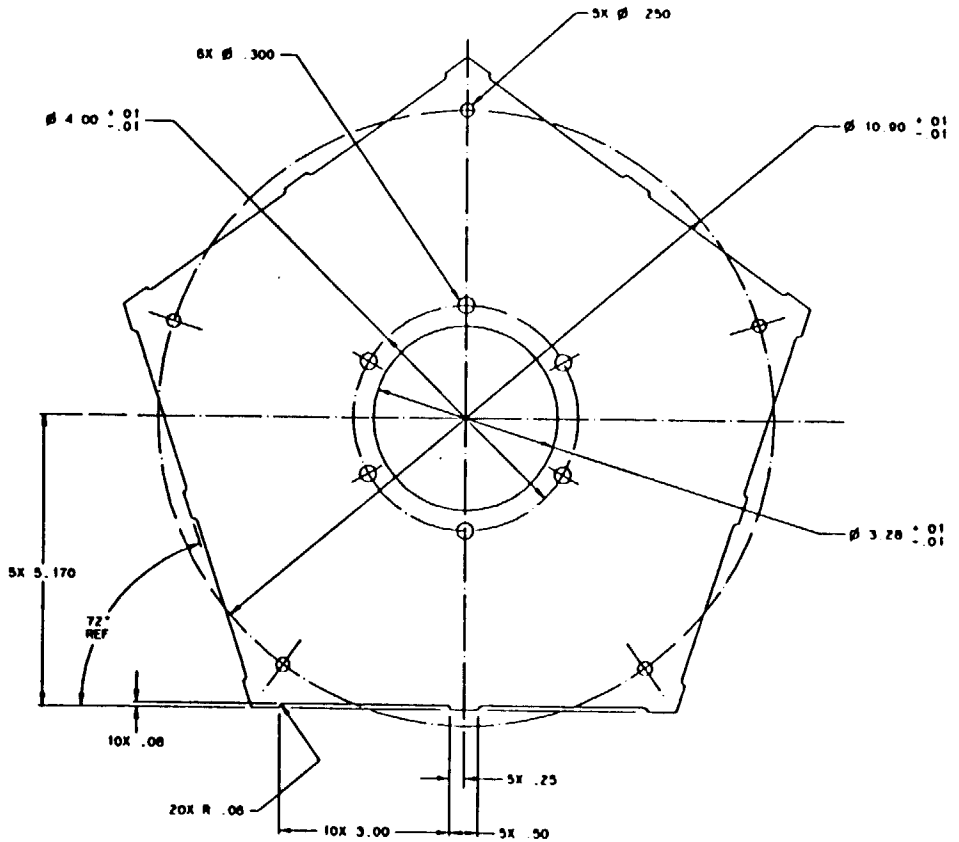

REV	DESCRIPTION	DRN	CHK	APPR & DATE
A	INITIAL RELEASE PER ECR11015	KMADD		

PART NO. 1016421-001
SEE PL _____

NEXT ASSY	USED ON	SEE NOTE ⚠	
APPLICATION			

SATCON

PENTAGON-
UPPER
L.A.M.S.

SIZE	FSCM NO	DRAWING NO.	REV
D		1016421	A

SCALE 1/1 SHEET 1

193

1016421 A

FEB 0 1 1991

REVISIONS			
REV	DESCRIPTION	DRWN	APPD
A	INITIAL RELEASE PER ECR 11015	KVADO	

NOTES:

⚠ MATERIAL: S1 ST TYPE 304L OR EQUIV
10 GA(.135 THK NON-MAGNETIC)

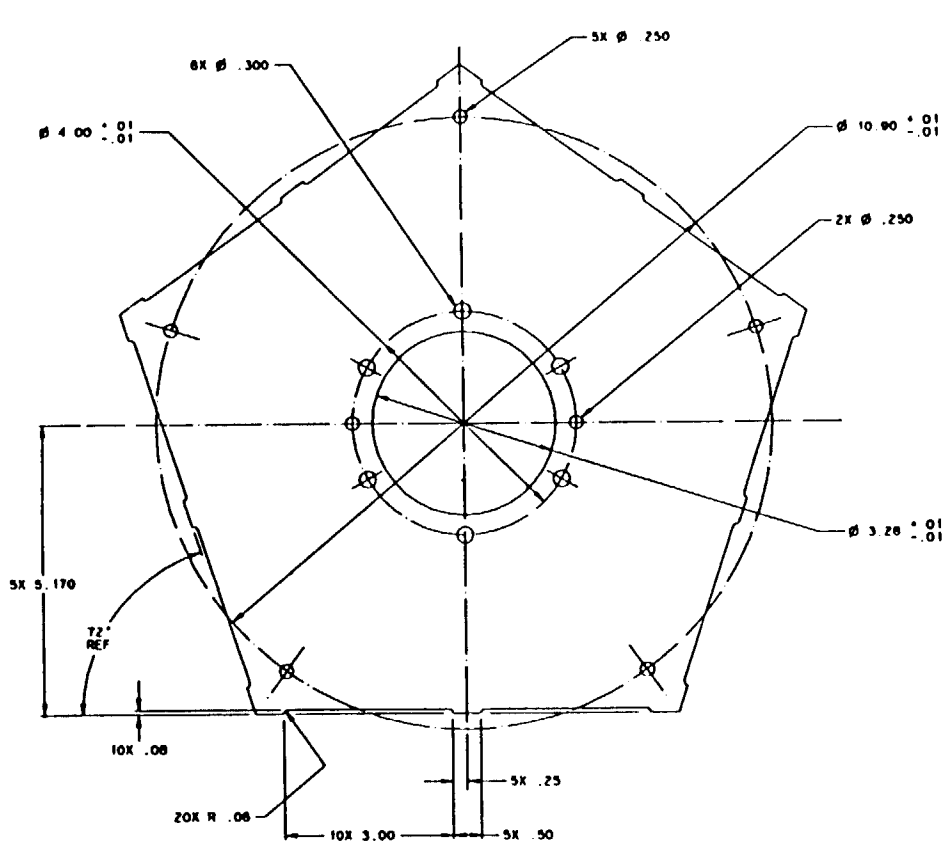

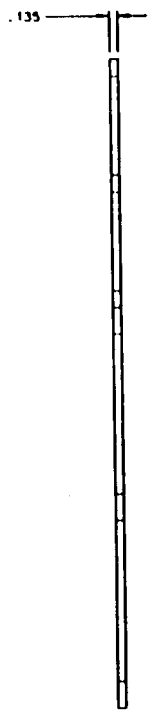

PART NO. 1016422-001
SEE PL _____

NEXT ASSY	USED ON		
APPLICATION			

SEE NOTE ⚠

SATCON

PENTAGON-
LOWER
L.A.M.S.

SIZE	FSCM NO	DRAWING NO	REV
D		1016422	A

SCALE 1/1 SHEET 1

FEB 0 1 1991

NOTES:

1. MATERIAL: ST ST TYPE 304L OR EQUIV 10 GA(135 THK NON-MAGNETIC)
2. REMOVE BURRS AND BREAK SHARP EDGES .02 MAX
3. FINISH WHERE MACHINED 63

REV	DESCRIPTION	DRN	CHK	APPR/DATE
A	INITIAL RELEASE PER ECR 11015	KVADD		

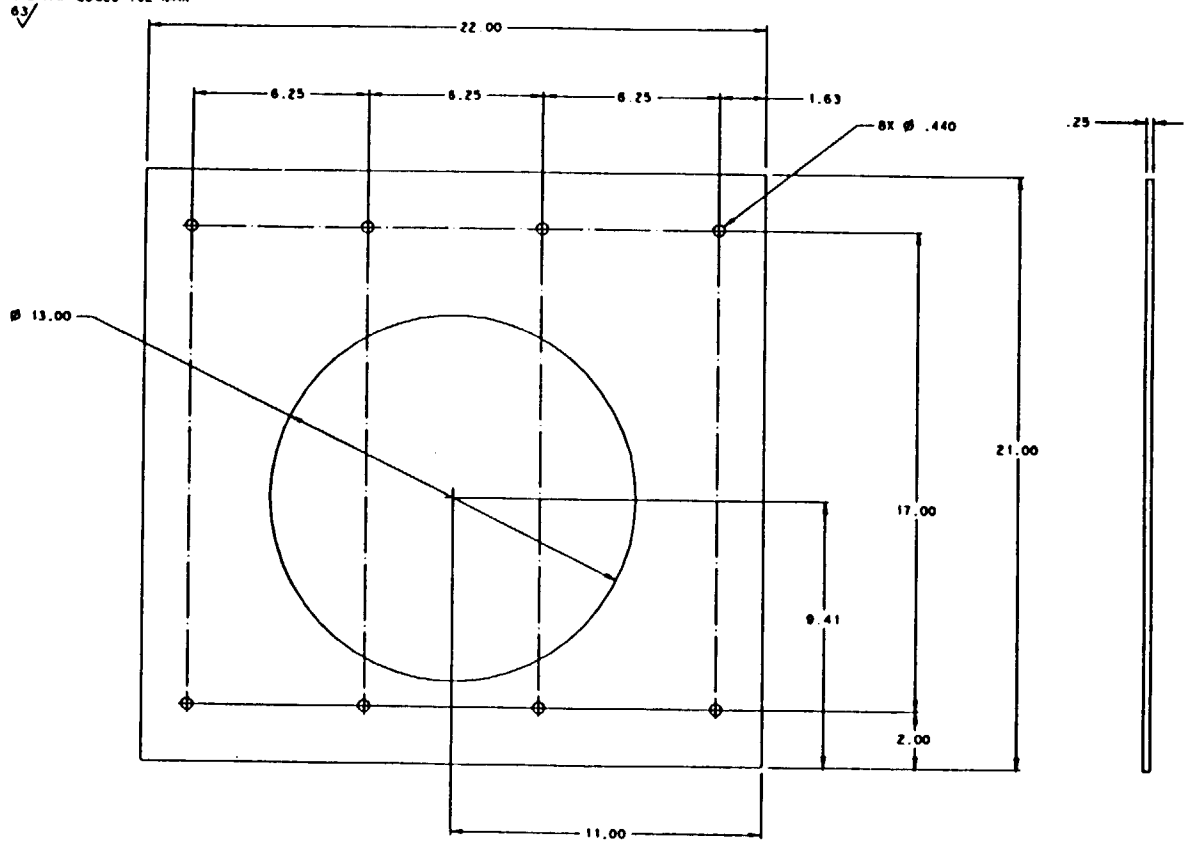

PART NO. 1016423-001
SEE PL

NEXT ASSY	USED ON
APPLICATION	

SEE NOTE 1

SATCON

BASE-
L.A.M.S.

SIZE	FSCM NO	DRAWING NO	REV
D		1016423	A

SCALE 1/2 SHEET 1

1016423 A

195

FEB 0 1 1991

REVISIONS				
REV	DESCRIPTION	DRN	CHK	APPVD & DATE
A	INITIAL RELEASE PER ECR 11015	KWADE		

NOTES:

⚠ MATERIAL: ST ST TYPE 304L OR EQUIV
10 GA(.135 THK NON-MAGNETIC)

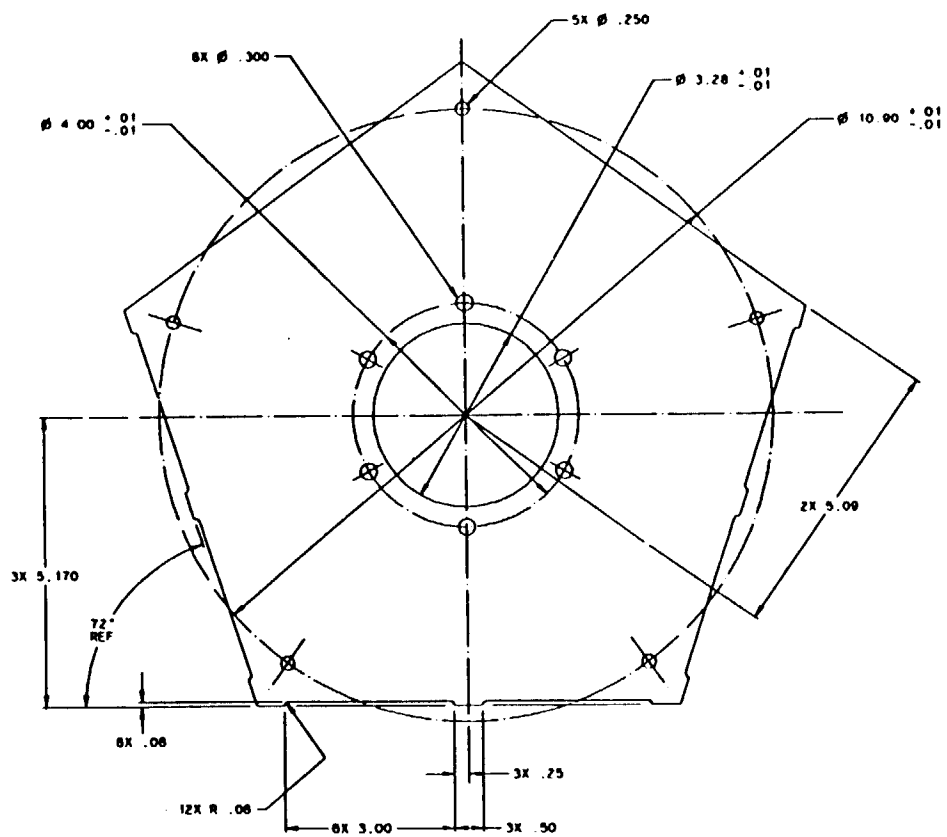

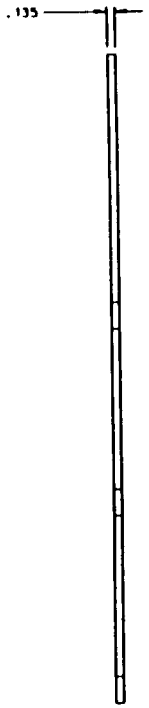

PART NO. 1016424-001
SEE PL _____

NEXT ASSY	USED ON		
APPLICATION			

SEE NOTE ⚠

SATCON

PENTAGON-
UPPER. SIDES
L.A.M.S.

SIZE	FSCM NO	DRAWING NO.	REV
D		1016424	A

SCALE 1/1 SHEET 1

DWG # 1016424 REV A

196

FEB 0 1 1991

NOTES:

⚠ MATERIAL: S1 ST TYPE 304L OR EQUIV
10 GA(.135 THK NON-MAGNETIC)

REVISIONS				
REV	DESCRIPTION	DRWN	CHK	APPVD DATE
A	INITIAL RELEASE PER ECR11015	KVANDE		

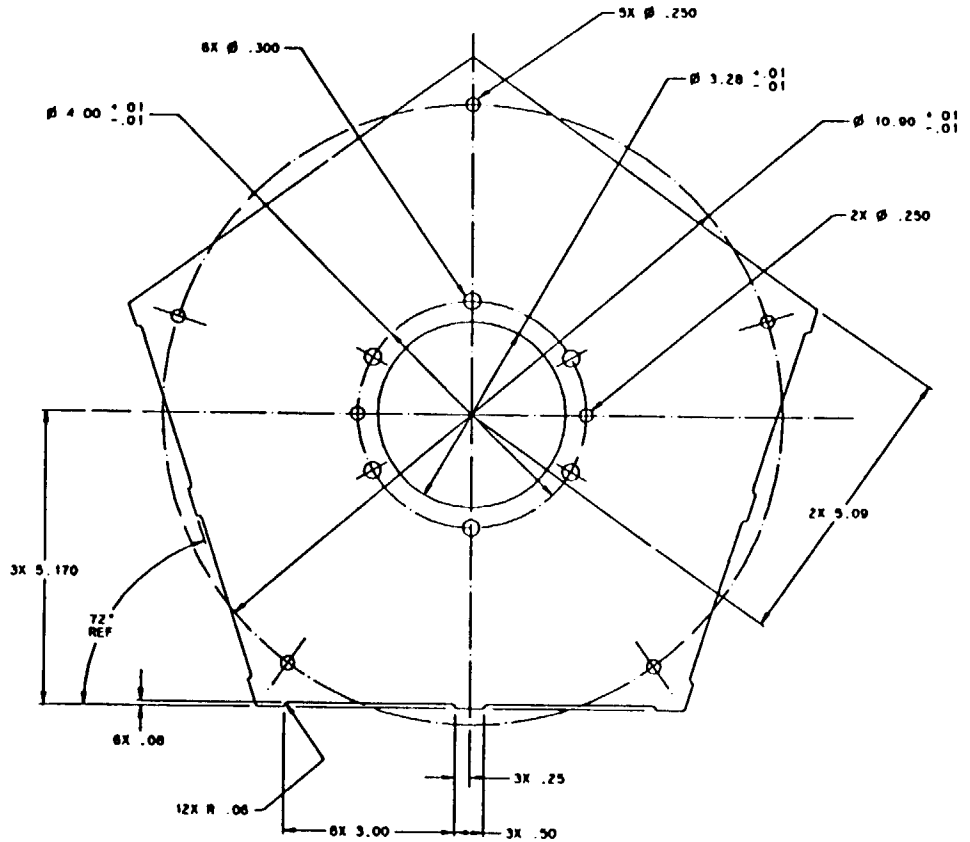

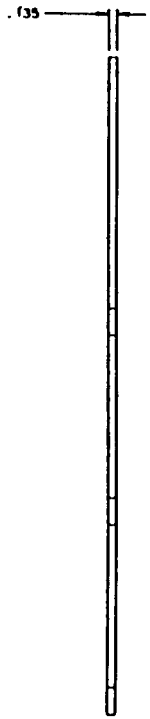

PART NO. 1016425-001
SEE PL _____

NEXT ASSY	USED ON			
APPLICATION		SEE NOTE ⚠		

SATCON

PENTAGON-
LOWER. SIDES
L.A.M.S.

SIZE	FSCM NO	DRAWING NO.	REV
D		1016425	A

SCALE 1/1 SHEET 1

1016425 A

FEB 0 1 1991

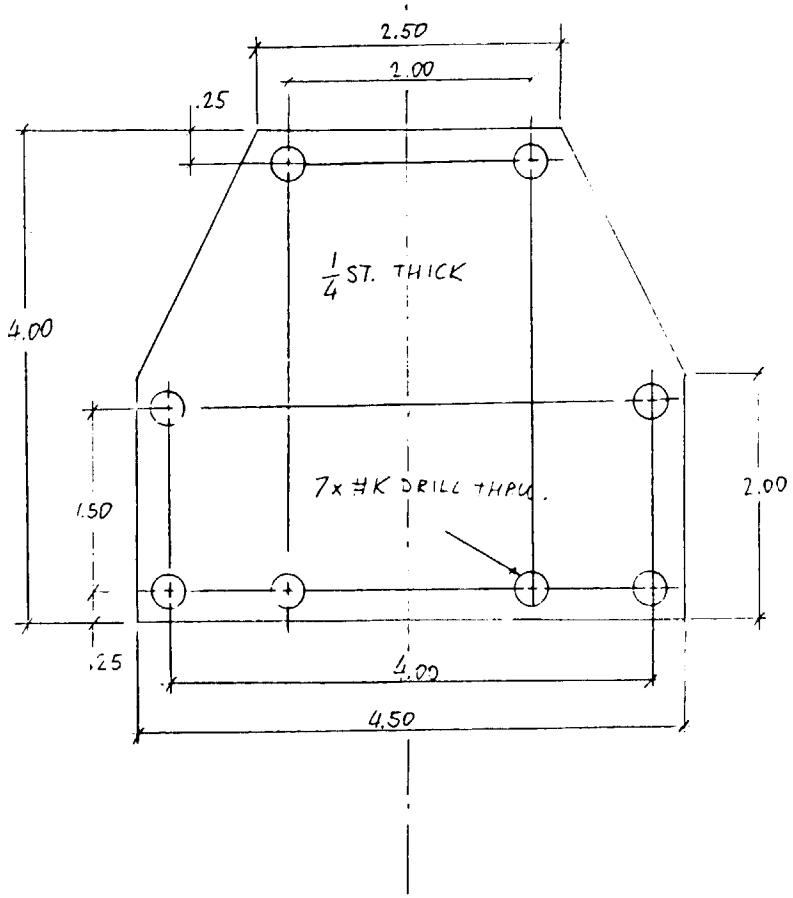

(9)
ALUM.
(3) REQ'D

38

198

PLATE, UPPER		
SCALE: 1/1 DATE:	APPROVED BY	DRAWN BY D. BUSHKO
MATL: ALUM		DRAWING NUMBER 1016-601

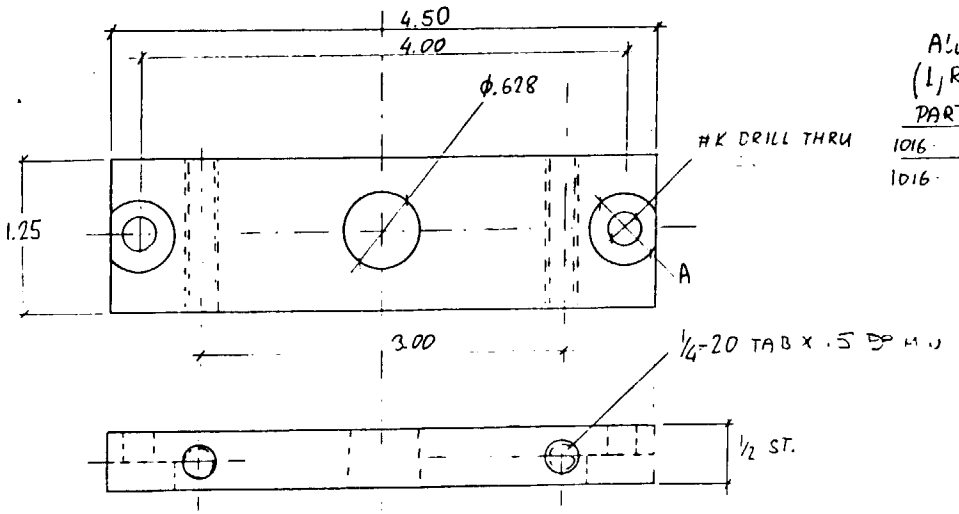

Alum.
(1) REQ'D

PART#	A
1016	ϕ.437
1016	ϕ.687

} C.BORE .25 DEEP

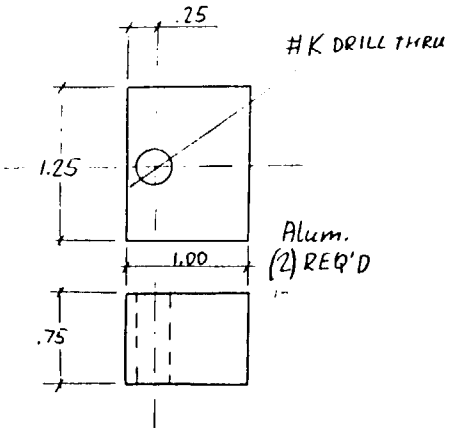

Alum.
(2) REQ'D

Assembly

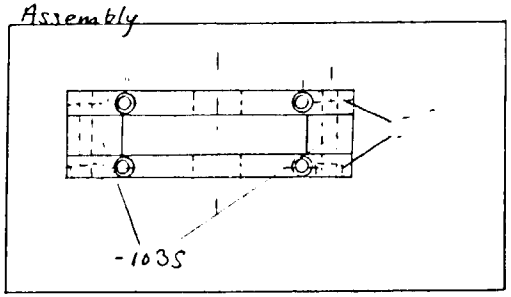

PULLEY SUPPORT-TOP RAIL LEFT

SCALE: 1/1	APPROVED BY	DRAWN BY: BOSHKO
DATE:		
		DRAWING NUMBER: 1016-602

199

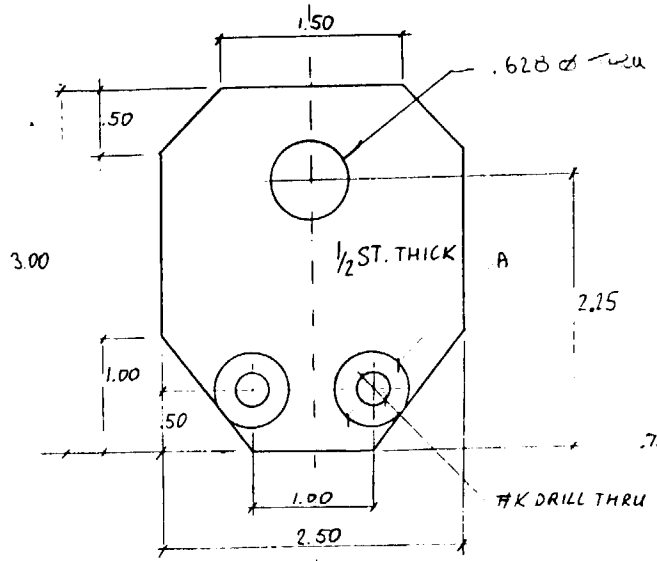

Alum.
(1) REQ'D

PART #	A
1016	ø.437
1016	ø.687

} C. BORE .25 DEEP

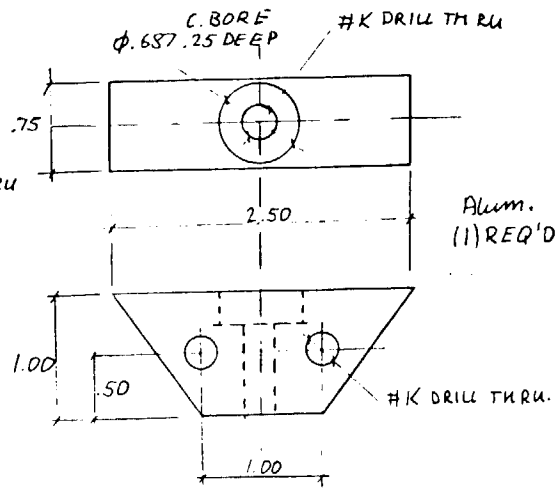

Alum.
(1) REQ'D

PULLEY SUPPORT - HOOK END

SCALE: 1/1	APPROVED BY:	DRAWN BY BUSHKO
DATE:		REVISED
		DRAWING NUMBER 1016-603

200

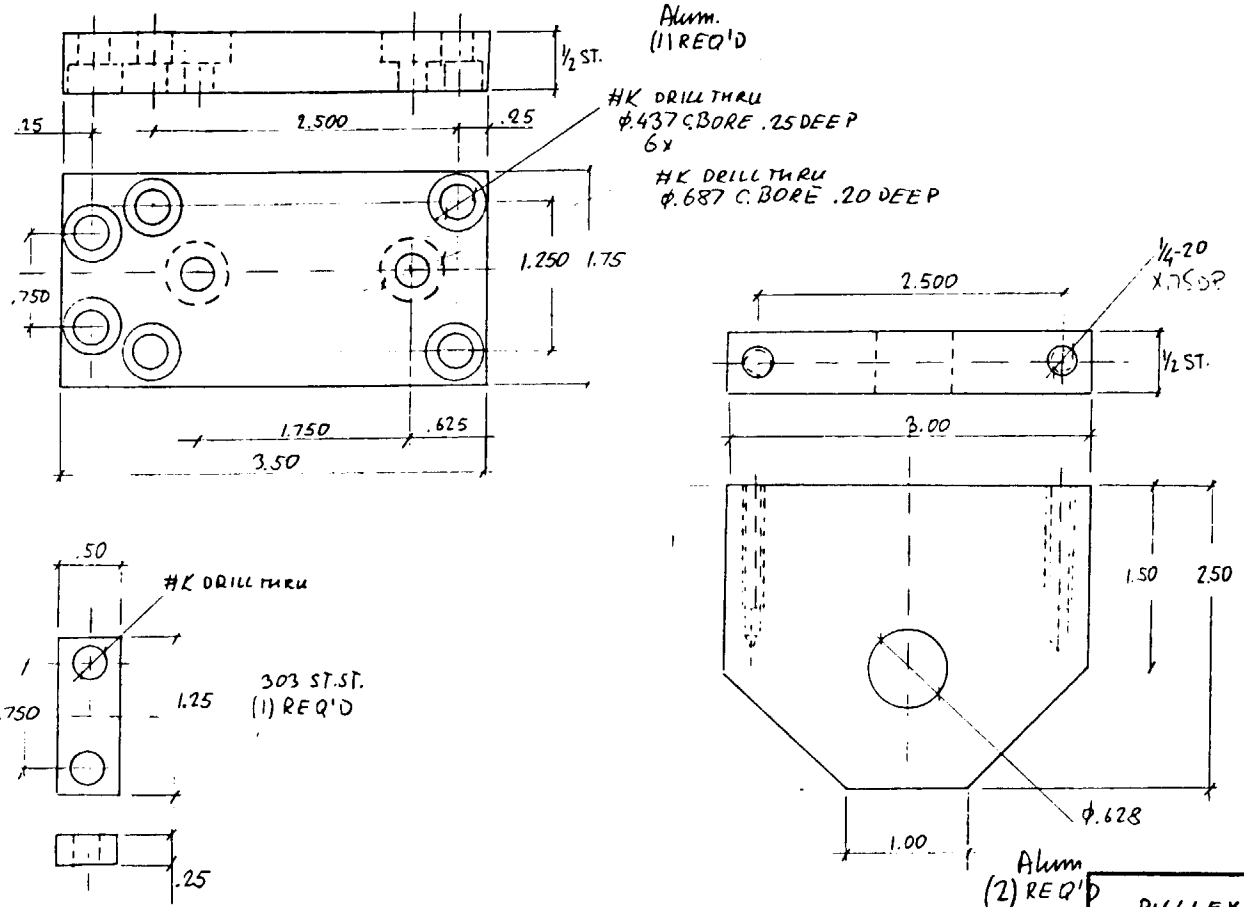

PULLEY SUPPORT – TOP RAIL CENTRAL

SCALE: 1/1	APPROVED BY:	DRAWN BY BUSHKO
DATE:		REVISED
		DRAWING NUMBER 1016-604

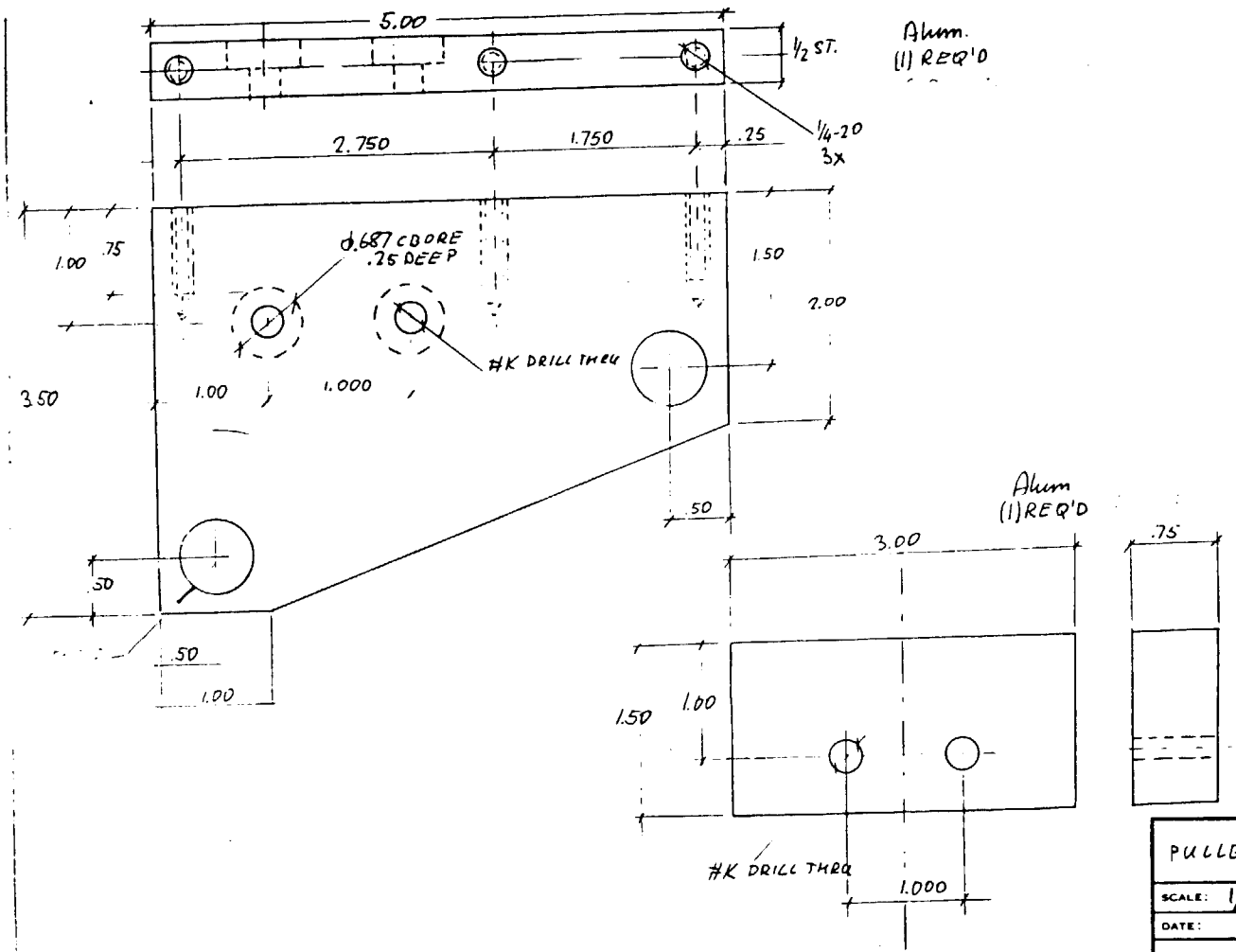

PULLEY SUPPORT - TOP RAIL RIGHT(1)

SCALE: 1/1	APPROVED BY:	DRAWN BY BUSHKO
DATE:		REVISED
		DRAWING NUMBER 1016-605

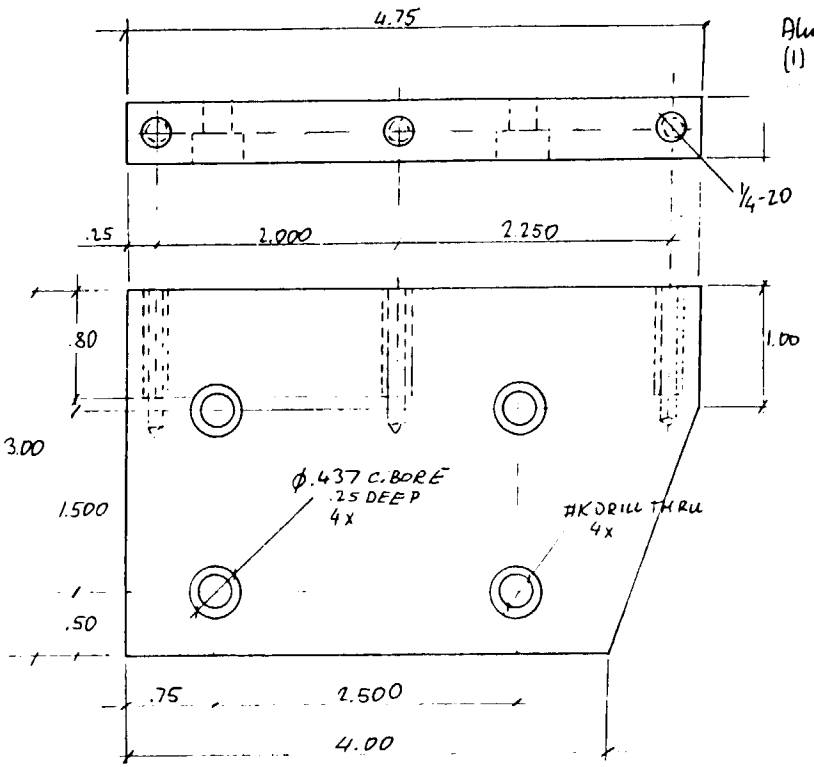

PULLEY SUPPORT - TOP RAIL RIGHT (2)

SCALE: 1/1	APPROVED BY:	DRAWN BY BOSHKO
DATE:		REVISED
		DRAWING NUMBER 1016-606

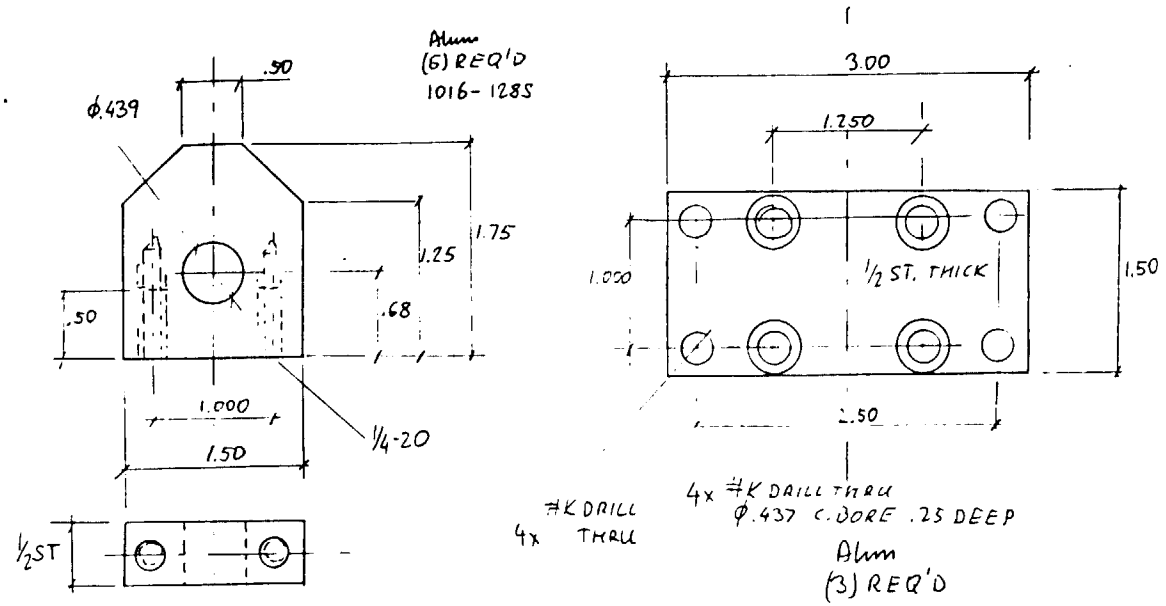

PULLEY SUPPORT - ROPE END		
SCALE: 1/1	APPROVED BY:	DRAWN BY BUSHKO
DATE:		REVISED
		DRAWING NUMBER 1016-607

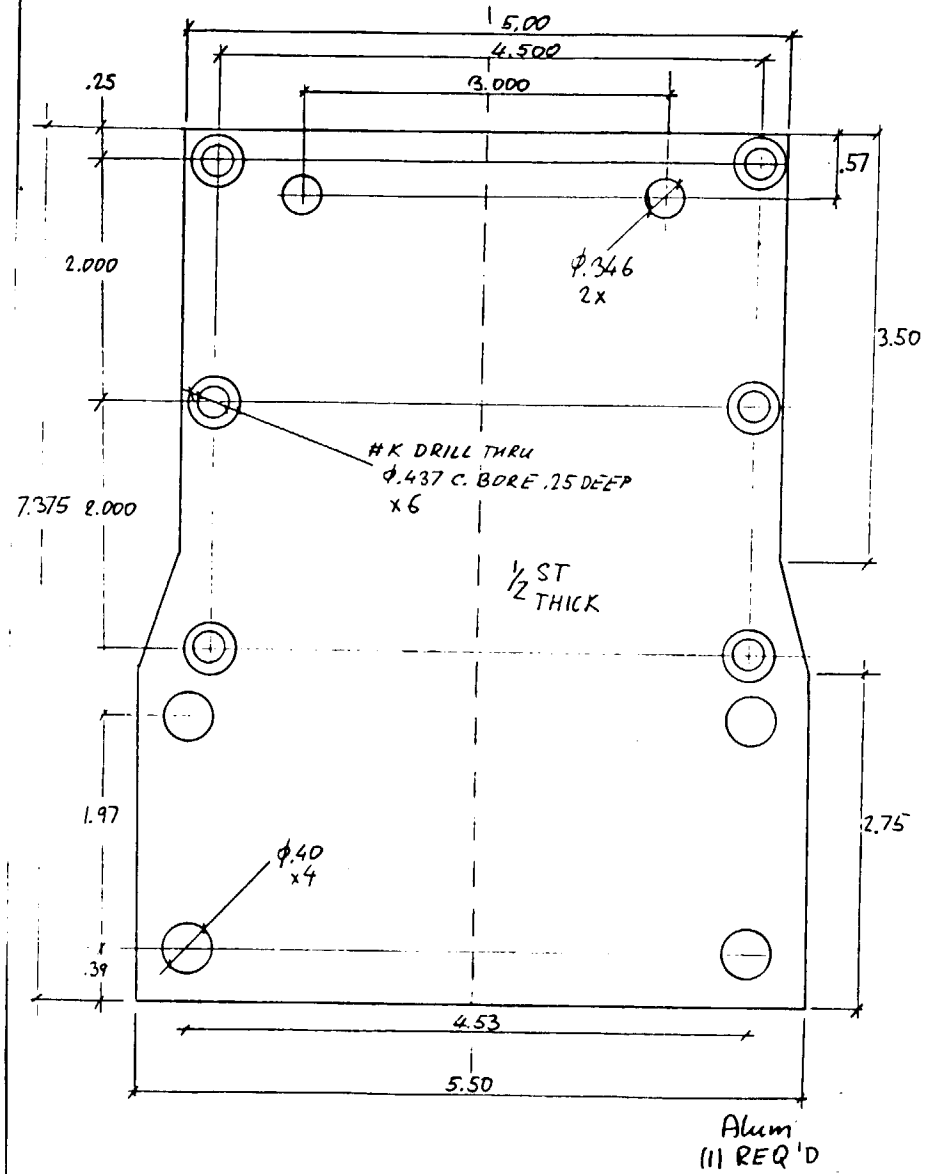

REDUCER'S BASE - TOP			
SCALE: 1/1	APPROVED BY:	DRAWN BY BUSHKO	
DATE:		REVISED	
		DRAWING NUMBER 1016-608	

11 X 17 PRINTED ON NO. 1000H CLEARPRINT ®

Alum
(3) REQ'D

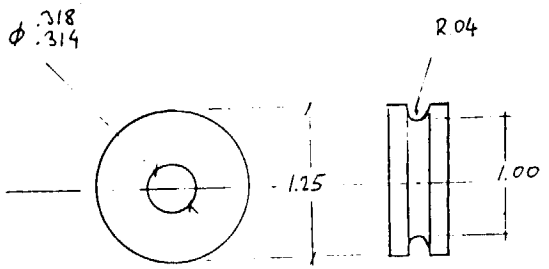

PULLEY - SMALL			
SCALE: 1/1	APPROVED BY:	DRAWN BY BUSHKO	
DATE:		REVISED	
		DRAWING NUMBER 1016-609	

206

ORIGINAL PAGE IS
OF POOR QUALITY

C.R. Steel
(2) REQ'D

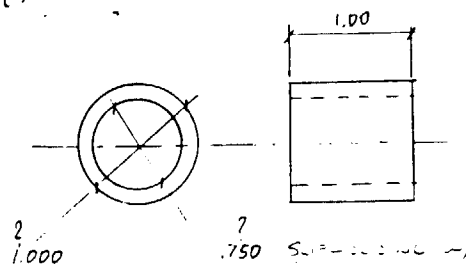

C.R. Steel.
(1) REQ'D

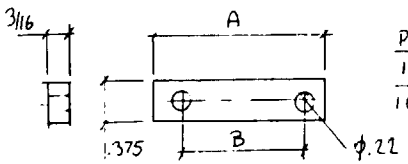

PART #	A	B
1016	1.35	1.00
1016	1.10	.750

BUSHING / SPACER

SCALE: 1/1	APPROVED BY:	DRAWN BY BUSHK
DATE:		REVISED
		DRAWING NUMBER 1016-610

Alum.
(5) REQ'D

.4997 +.000 -.0001

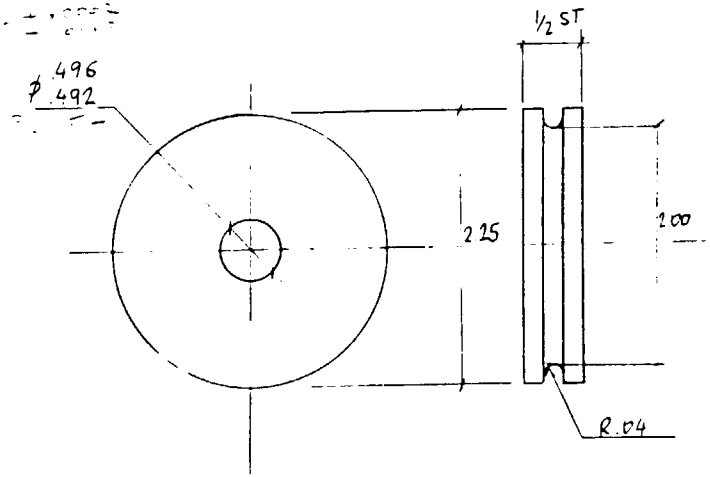

PULLEY-BIG		
SCALE: 1/1	APPROVED BY:	DRAWN BY BUSHKO
DATE:		REVISED
		DRAWING NUMBER 1016-611

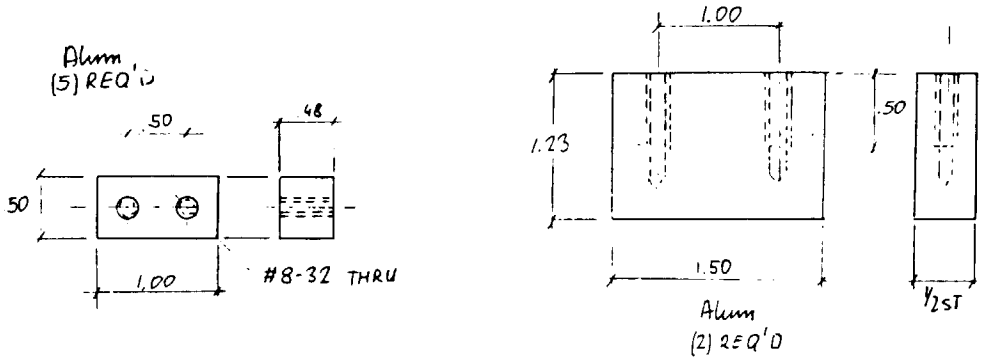

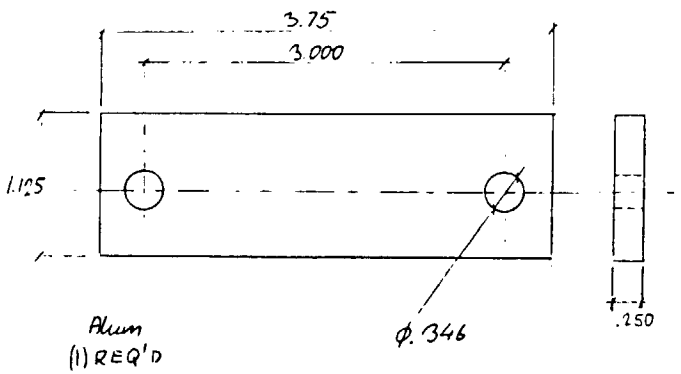

ROPE POSITIONERS		
SCALE: 1/1	APPROVED BY:	DRAWN BY BUSHKO
DATE:		REVISED
		DRAWING NUMBER 1016-612

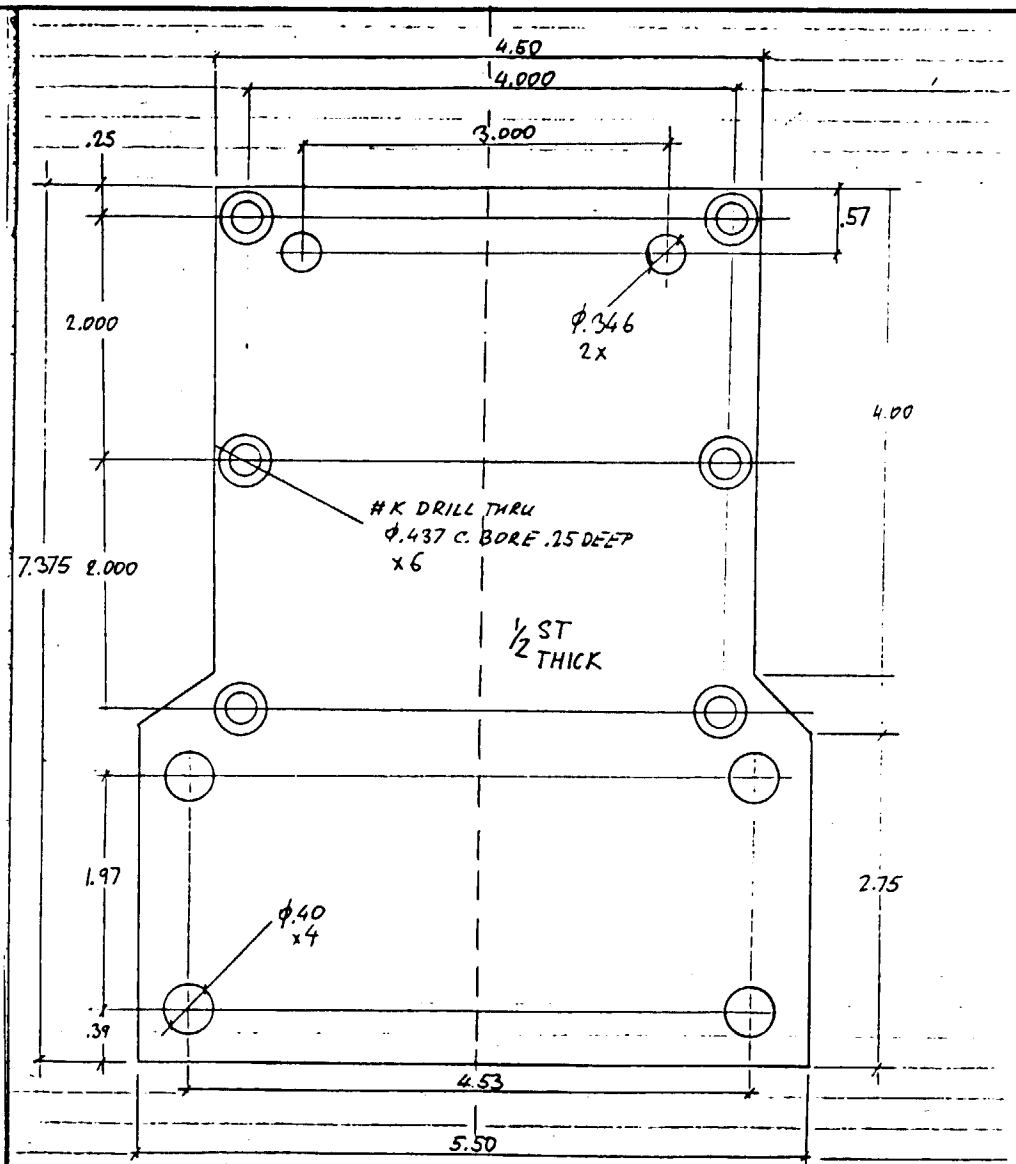

Alum
(1) REQ'D

REDUCER'S BASE-LOWER		
SCALE: 1/1	APPROVED BY:	DRAWN BY BUSHKO
DATE:		REVISED
		DRAWING NUMBER 1016-613

Appendix B. Electrical Schematics

THIS PAGE

INTENTIONALLY

LEFT BLANK

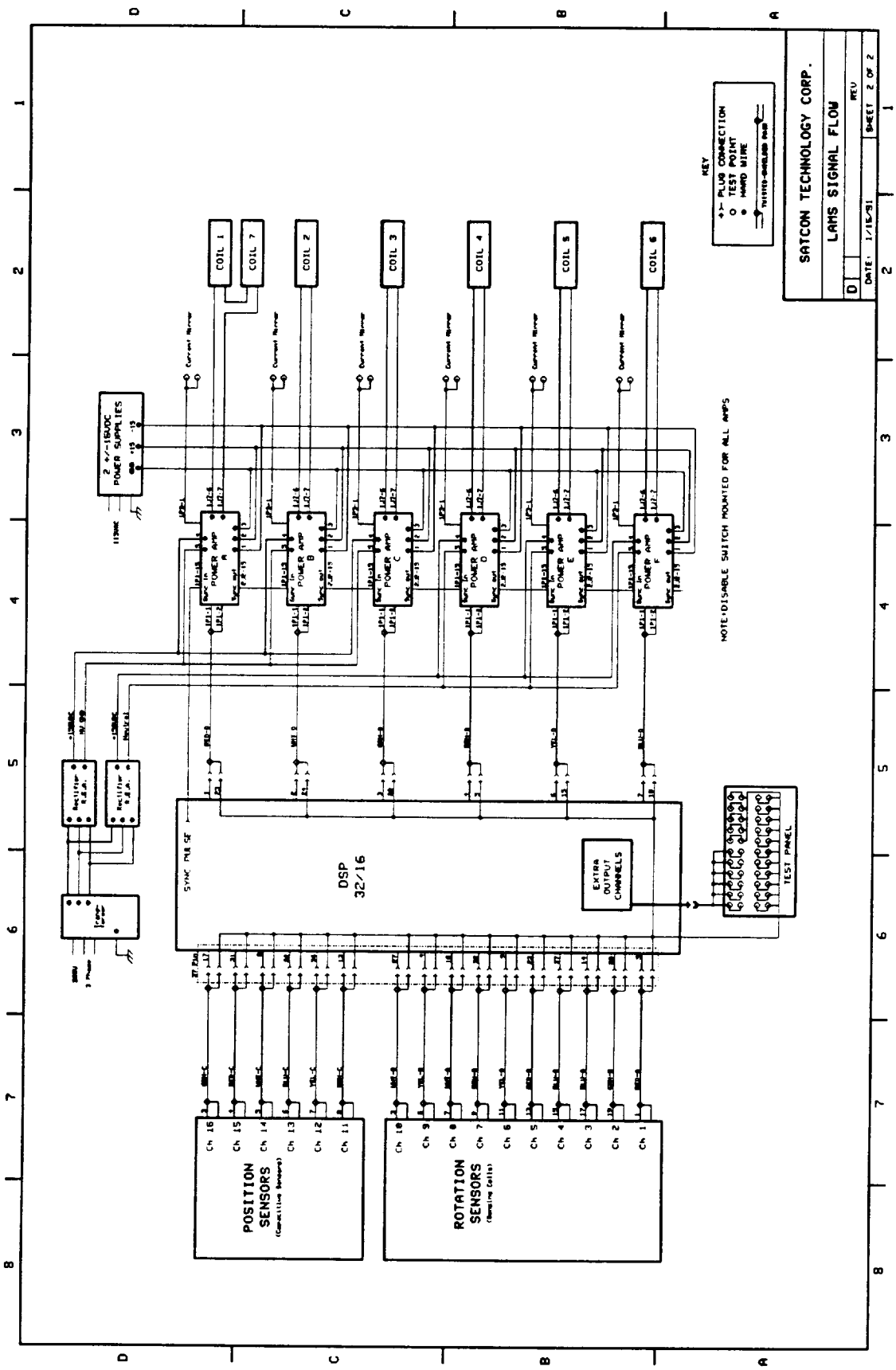

PRECEDING PAGE BLANK NOT FILMED

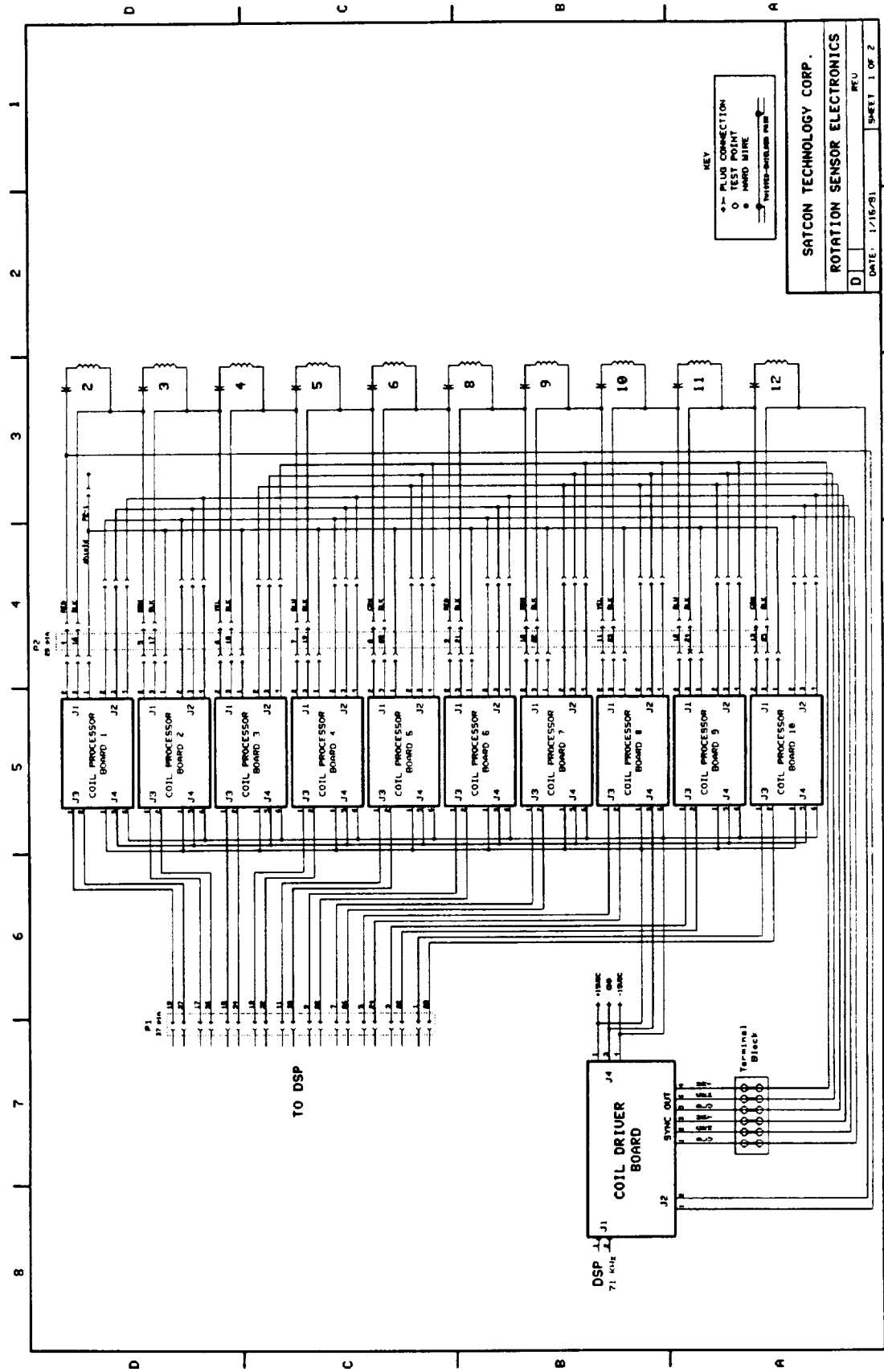
SATCON TECHNOLOGY CORP.
ROTATION SENSOR ELECTRONICS
DATE: 1/16/91
SHEET 1 OF 2
KEY
PLUG CONNECTION
TEST POINT
HARD WIRE
COIL PROCESSOR BOARD 1
COIL PROCESSOR BOARD 2
COIL PROCESSOR BOARD 3
COIL PROCESSOR BOARD 4
COIL PROCESSOR BOARD 5
COIL PROCESSOR BOARD 6
COIL PROCESSOR BOARD 7
COIL PROCESSOR BOARD 8
COIL PROCESSOR BOARD 9
COIL PROCESSOR BOARD 10
COIL DRIVER BOARD
TO DSP
DSP
Terminal Block

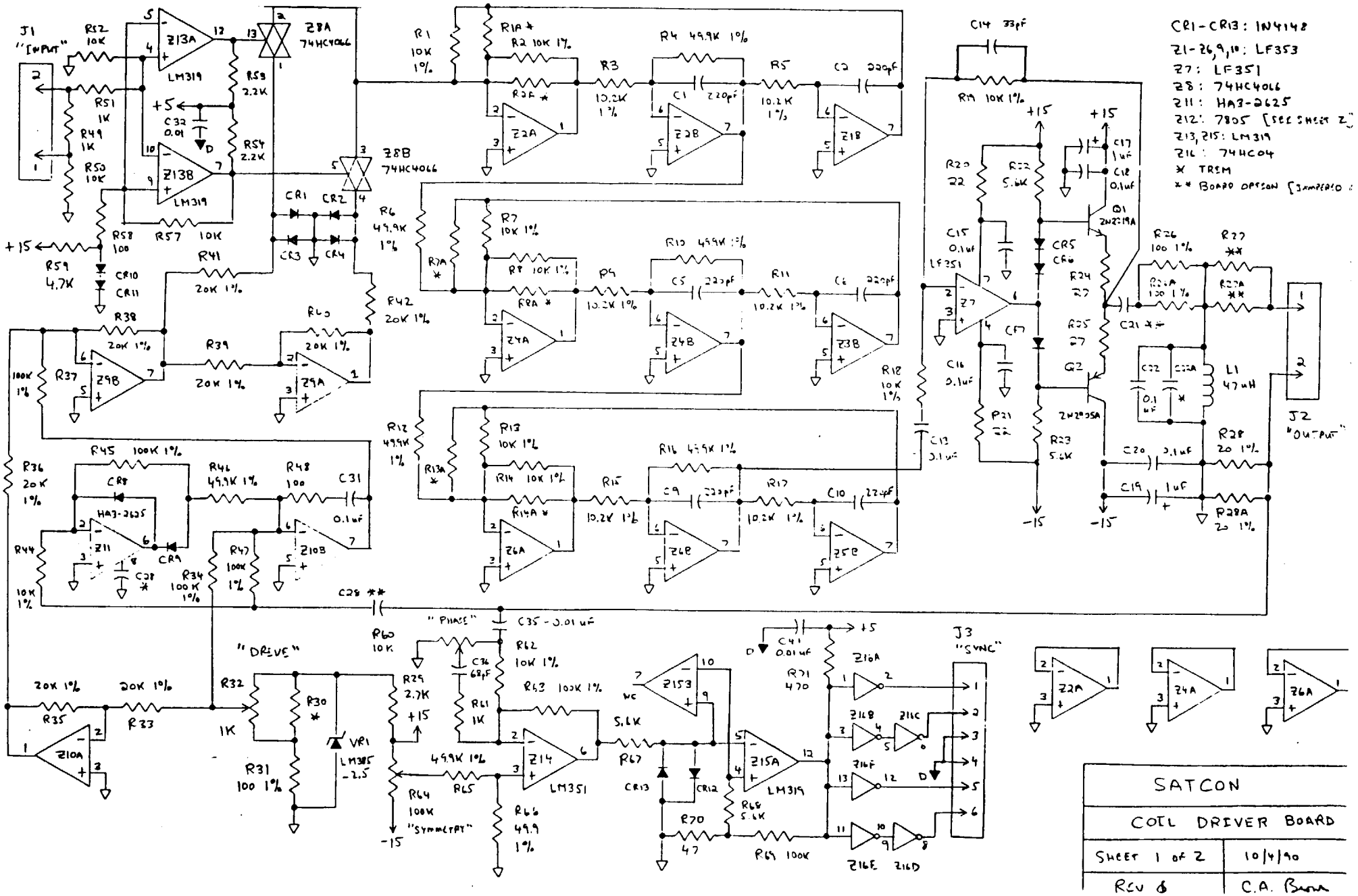
CR1-CR13: 1N4148
Z1-Z6,9,10: LF353
Z7: LF351
Z8: 74HC4066
Z11: HA3-2625
Z12: 7805 [SEE SHEET 2]
Z13, Z15: LM319
Z16: 74HC04
* TRIM
** BOARD OPTION [JUMPERED]
J1 "INPUT"
J2 "OUTPUT"
J3 "SYNC"
"DRIVE"
"PHASE"
"SYMMETRY"
SATCON
COIL DRIVER BOARD
SHEET 1 OF 2
10/4/90
REV 0
C.A. Brown

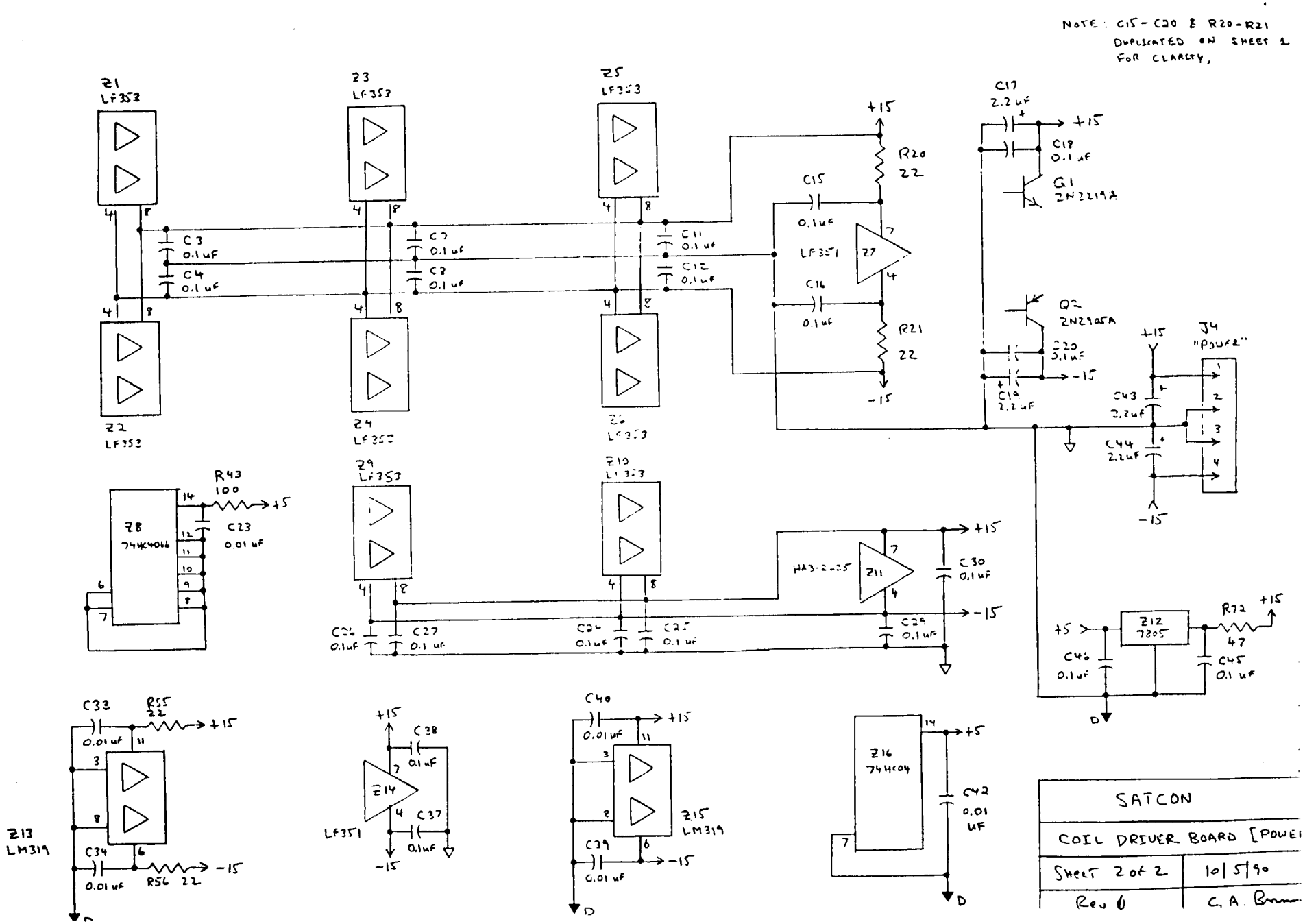

SATCON	
COIL DRIVER BOARD [POWE	
SHEET 2 of 2	10/5/90
Rev 0	C. A. B

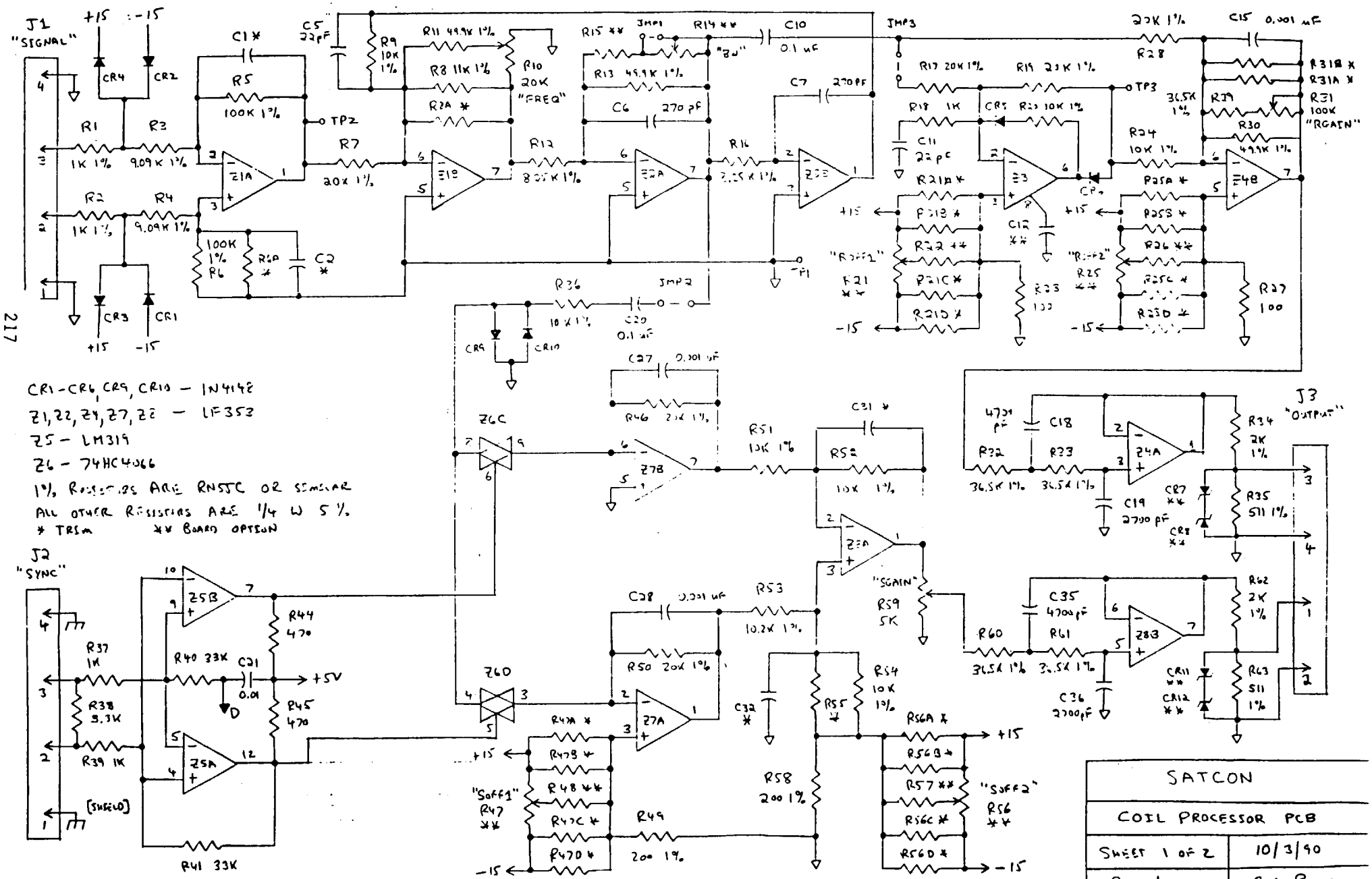

SATCON	
COIL PROCESSOR PCB	
SHEET 1 OF 2	10/3/90
Rev 0	C. A Brown

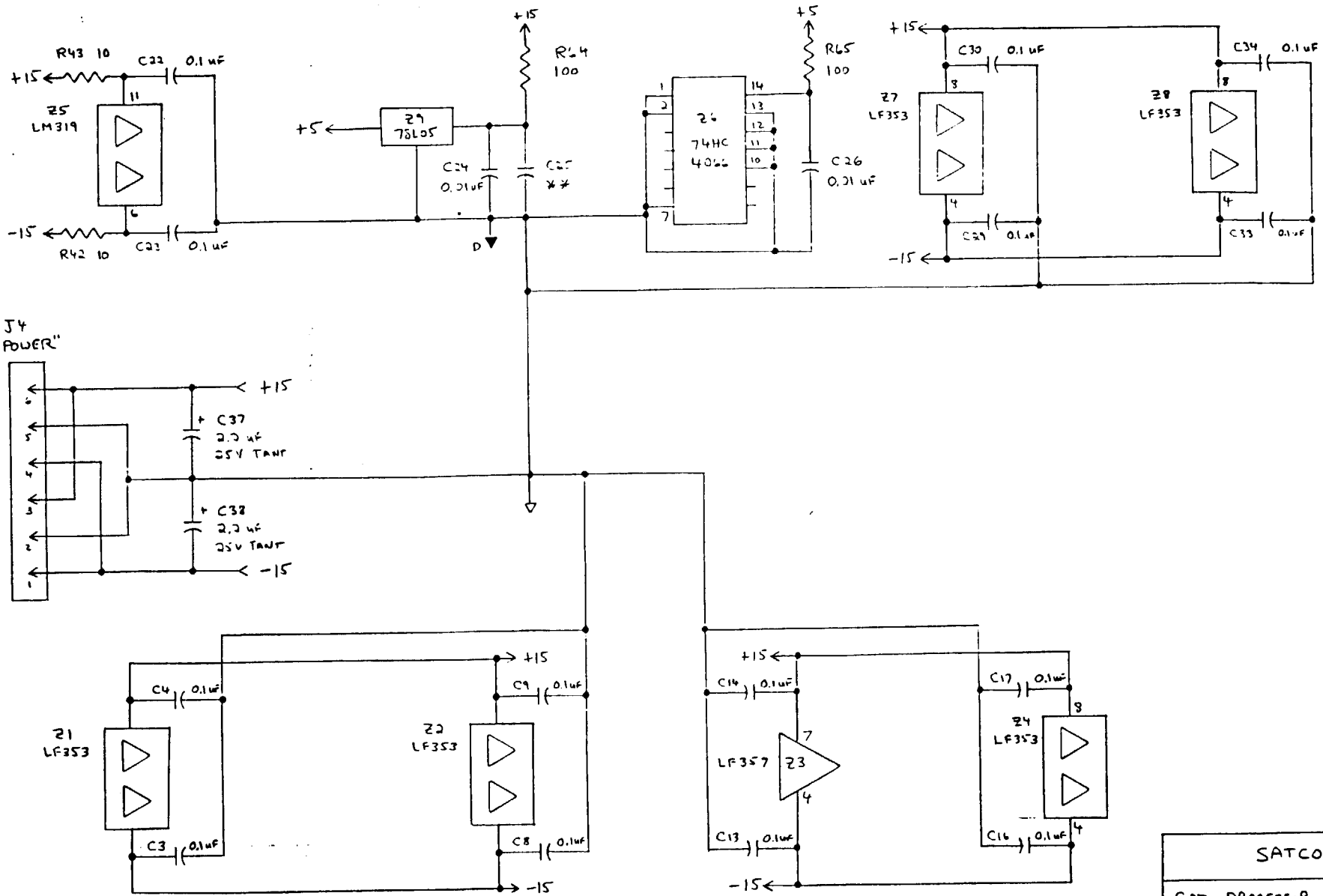

SATCON	
COIL PROCESSOR PCB [POWER]	
SHEET 2 OF 2	10/4/90
D. V. H.	C. A. Rum

Appendix C. Operating Manual for Superconducting Magnet

THIS PAGE

INTENTIONALLY

LEFT BLANK

OPERATING INSTRUCTION MANUAL
FOR
SUPERCONDUCTING MAGNET SYSTEM

DESIGNED AND MANUFACTURED
FOR
SATCON TECHNOLOGY CORP.
CAMBRIDGE, MA 02139
PURCHASE ORDER # 0158

BY
CRYOMAGNETICS, INCORPORATED
P. O. BOX 548
739 EMORY VALLEY ROAD
OAK RIDGE, TENNESSEE 37831-0548
(615) 482-9551

WARNING: DO NOT ATTEMPT TO OPERATE THIS EQUIPMENT BEFORE THOROUGHLY READING THESE OPERATING INSTRUCTIONS.

TABLE OF CONTENTS

LIST OF TABLES

LIST OF FIGURES

1.0 INTRODUCTION

The purpose of this operating instruction manual is to familiarize the equipment user with the following:

a) System Design Specifications

b) System Description

c) System Operating Procedures

d) System Safety Precautions

UNDER NO CIRCUMSTANCE SHOULD THIS SUPERCONDUCTING MAGNET/CRYOSTAT SYSTEM BE OPERATED BY PERSONNEL WHO HAVE NOT FIRST READ THIS INSTRUCTION MANUAL IN ITS ENTIRETY.

2.0 SYSTEM DESIGN SPECIFICATIONS

This superconducting magnet system was specifically designed in accordance with the following requirements. Any use of applications of this equipment outside of these design parameters is neither intended nor recommended.

TABLE 2-1 SYSTEM DESIGN SPECIFICATIONS

A.	Superconducting Magnet	Custom Solenoid
	Manufacturer	Cryomagnetics, Inc.
	Model	Custom
	Rated Central Field	80 kilogauss at 4.2K
	Rated Operating Current (8.0 tesla)	47.1 amperes
	Total Inductance	15 henries
	Superconductor	Twisted Multi-filamentary NbTi/Cu
	Fabrication	Epoxy impregnated to prevent training
	Quench Protection	Adiabatic protection using Cu matrix and diodes
	Persistence	Persistent switch installed on magnet. Switch heater operating current: 55 mA
B.	Cryostat	1 each
	Manufacturer	Precision Cryogenic Systems
	Model	Custom
C.	Vapor-Cooled Current Leads	1 pair
	Manufacturer	M-100 breakaway
D.	Liquid Helium Level Sensor	1 each
	Manufacturer	20 cm active length 22 cm overall length
E.	Liquid Helium Level Meter	1 each
	Manufacturer	Cryomagnetics, Inc.
	Model	12 (calibrated for Item D above)
F.	Magnet Power Supply	1 each
	Manufacturer	Cryomagnetics, Inc.
	Model	IPS-100

G. Temperature Sensor and Monitor..... 1 each
Manufacturer..... Cryomagnetics, Inc.
Model..... 70

H. Helium Transfer Line..... 1 each
Manufacturer..... Precision Cryogenic Systems
Model..... Custom

3.0 SYSTEM DESCRIPTION

This superconducting magnet system consists of the following elements which will be discussed individually:

a) Superconducting Magnet

b) Cryostat

c) Helium Level Meter and Sensor

d) IPS-100 Power Supply

e) Persistent Switch and Heater Supply System

f) Magnet Support Assembly

g) Temperature Sensor and Monitor

h) Electrical Connections

3.1 Superconducting Magnet

The custom designed 8.0 tesla at 4.2K superconducting magnet is optimized for 0.5% homogeneity over a 1 cm diameter spherical volume. The magnet has been thoroughly tested by Cryomagnetics. The final test results are indicated in Table 3-1.

The superconducting magnet was built using twisted multifilamentary NbTi wire in a copper matrix. The coil is completely epoxy impregnated to prevent training. The copper matrix used in the wire acts as a form of quench protection along with diodes.

TABLE 3-1

Magnet Specifications
Satcon Technology Corp.
September 13,1990

Rated Central Field	80 kilogauss at 4.2K
Maximum Test Field	84.4 kilogauss at 4.2K
Rated Current (80 kilogauss)	47.1 amperes
Inductance	15.0 henries
Homogeneity	+/- 0.5% over 1 cm DSV
Field to Current Ratio	1699.6 gauss/ampere
Charging Voltage	1 volts
Persistent Switch Heater Current	55 milliamperes

3.2 Cryostat

The cryostat is a Precision Cryogenic Systems,Inc. custom design. The cryostat uses an all aluminum and fiberglass design. A drawing of the dewar is attached (Figure 3.1).

3.3 Helium_Level_Meter_and_Sensor

The dewar contains a liquid helium level sensor 20 cm long (active). All electrical connections to this sensor are found on the 19-pin connector on top of the dewar.

The control system contains a Cryomagnetics' Model 12 helium level meter for use with the installed sensor. The meter will give a negative reading while the dewar is above 4.2 Kelvin. It has been calibrated at the factory to be compatible with the installed sensor, but the recalibration procedure is easy and is outlined in the instruction manual which is appended to this manual.

3.4 Magnet_Power_System

The magnet power supply consists of a Cryomagnetics' Model IPS-100 power supply and all required protection devices, cables, and interconnecting hardware.

The IPS-100 power supply is cable of providing +5 to -5 volts at 0-100 amperes. Detailed instructions can be found in the IPS-100 manual.

3.5 Persistent_Switch_and_Heater_Supply_System

The superconducting magnet has a persistent switch installed. The IPS-100 has two heater supplies either one can be

used.

3.6 Temperature Sensor and Monitor

The magnet has a PT-100 platium temperature sensor mounted on the bottom end flange. This is very usefull during the system cooldown. Because the sensor is magnetoresistive the readout will read high when the magnet is charged. The reading is only accurate when the magnet is at zero field. The readout is Model 70. The manual is appended to this manual.

3.7 Electrical Connections

The pin designations for the 19 pin connector are found in Table 3-2. This connector contains all electrical contacts to the magnet and system monitoring components within the liquid helium vessel.

TABLE 3-2

WIRING DIAGRAM

19 PIN CONNECTOR	CONTROL CABLE WIRING	ELECTRICAL CONNECTIONS
A	ORANGE	I+ TEMPERATURE SENSOR
B	RED/BLACK	I- TEMPERATURE SENSOR
C	VIOLET	V+ TEMPERATURE SENSOR
D	WHITE/BLUE	V- TEMPERATURE SENSOR
E	WHITE	PERSISTENT SWITCH HEATER
F	WHITE/YELLOW	PERSISTENT SWITCH HEATER
G	WHITE/RED	I+ HELIUM LEVEL SENSOR
H	WHITE/GREEN	I- HELIUM LEVEL SENSOR
J	RED	V-,I- HELIUM LEVEL SENSOR
K	RED/GREEN	I+ HELIUM LEVEL SENSOR
L	TAN	V+ HELIUM LEVEL SENSOR
M	PINK	V-,I- HELIUM LEVEL SENSOR
N	BROWN	
P	GREEN	
R	BLACK	
S	YELLOW	
T	WHITE/BLACK	
U	RED/YELLOW	
V	BLUE	

4.0 MAGNET SYSTEM OPERATING PROCEDURES

The Cryomagnetics, Inc. superconducting magnet/cryostat system will give many years of trouble free rewarding service, if the proper operating instructions as contained in this manual are followed.

4.1 Preparation for Cooldown

Most dewars are shipped with the vacuum space evacuated and should not need evacuating. This is a result of the final testing at the factory, and it helps ensure a clean vacuum space. If the system needs evacuating the following procedure should be followed. This is best done with a good pumping station (e.g. a cold - trapped rotary/diffusion pumping station) capable of bringing the ultimate pressure down to approximately 10^{-5} Torr. Any inserts with independent vacuum jackets must also be evacuated at this time. An engineering drawing showing the details of your system is enclosed for your reference.

Every vacuum jacket is protected against cold leaks with a pressure relief valve which will vent any pressure that exceeds 2 to 4 psig. This pressure relief is usually located on the evacuation valve or the side of the dewar.

The evacuation valves supplied for the dewar and insert vacuums (optional) are mostly of the bellows sealed type. After evacuating the jacket, the valve should be firmly closed, but care should be exercised to avoid damaging the seat with too much pressure.

When evacuation of the (dewar or insert) jacket is initiated, always be sure that the pressure on the pump side of the evacuation valve is lower than the jacket pressure. This is done to avoid drawing oil vapor from the pump into the vacuum jacket. Thus, one should not pump the vacuum jacket while liquid helium is in the dewar, since liquid helium will usually cryopump to a lower pressure (10^{-5} Torr or less) than the pumping station in use.

CAUTION: NEVER PUMP ON THE HELIUM RESERVOIR UNLESS THE DEWAR IS UNDER VACUUM. THIS COULD RESULT IN MAJOR DAMAGE (COLLAPSE) TO THE DEWAR AND THE ENCLOSED MAGNET.

4.2 Cooldown Procedure

1) General

Before introducing any liquid cryogens into the dewar, check carefully for water in both the nitrogen and helium reservoirs. This is particularly important for dewars with an open nitrogen reservoir, due to condensation on the walls during warm up from a previous run. If not removed, this water will freeze upon cooling, and could cause severe damage to the dewar, magnet and any cryostat insert.

If possible, one should evacuate the helium reservoir (with the dewar jacket under vacuum - see last caution) in order to remove all the air, and then back fill with helium gas. Similar procedures will also be necessary for any cryostat inserts present in the system. Such procedures will be described in the enclosed description for the insert (e.g. "SuperVaritemp" System Operation). In either case,

one should at least purge the helium space thoroughly with helium gas, and isolate it with one-way valves (e.g. pressure relief) to prevent air from entering back into this space.

2) Liquid_Nitrogen_Transfer

(a) Nitrogen Reservoir

The nitrogen reservoir should now be filled with liquid nitrogen. If an automatic device is supplied, check the instructions for this device. Otherwise, maintain a steady flow of liquid into the reservoir, but not so fast that a large spattering occurs. It is always advisable to maintain the liquid nitrogen level as high as possible, since the efficiency of some dewars will decrease rapidly when the nitrogen level drops far below the top of the reservoir. Open nitrogen reservoirs should always have a cover flange (usually an aluminum/styrofoam flange is supplied) on top of the reservoir. This will reduce consumption of liquid nitrogen as well as the amount of condensation build-up around the top of the dewar.

(b) Helium Reservoir

It is very important to cool the helium reservoir, the magnet and any cryostat insert to as close to liquid nitrogen temperature as possible. This must be done to conserve the amount of liquid helium necessary for final cooldown to 4.2K. This can be done in one of two ways.

The first method involves direct transfer of liquid nitrogen into the helium reservoir. This is the faster

method, and could take from one to several hours to cool the magnet/cryostat assembly to 77K. The temperature may be monitored by a thermometer inside the reservoir, or judged by the amount, or lack of boiling, of the liquid nitrogen. When cooled, the helium reservoir must be emptied completely by either blowing or siphoning the liquid nitrogen out.

CAUTION: REMOVE ALL LIQUID NITROGEN FROM THE HELIUM RESERVOIR PRIOR TO TRANSFERRING HELIUM.

The helium reservoir should be evacuated and back filled with gaseous helium. The pressure inside the helium reservoir must drop to about one Torr. Should the pressure remain higher (about 90 Torr), this may indicate the presence of liquid (or frozen) nitrogen in the helium reservoir. The blowing (or siphoning) and pumping procedure should be repeated to ensure that all the nitrogen has been replaced by helium (gas).

The second method of cooling the helium reservoir (and its contents) to nitrogen temperature is to fill the nitrogen reservoir with liquid nitrogen, while maintaining an overpressure of helium gas in the helium reservoir. A combination of radiational and conductive cooling will eventually cool the helium reservoir close to nitrogen temperatures. This process will take at least overnight, and possibly up to several days (in bigger units) for the helium reservoir/magnet/insert to cool down. If an over pressure of helium gas is not used, one should seal the reservoir (after purging it with helium gas) with a one way

valve to prevent air from entering when the temperature (and the pressure) of the helium reservoir drops.

For either of the two methods above, any cryostat insert in the helium reservoir must be at least thoroughly purged with helium gas.

3) Liquid Helium Transfer

In many cases, a liquid helium transfer line is supplied with the system, with a built-in "initial fill" adapter in the helium reservoir. The purpose of such an adapter is to bring the liquid helium entry point below the magnet during the initial helium fill or your system may have a straight access to the bottom of the dewar. On the cool-down the transfer line should go to the bottom for a efficient transfer. The transfer should start at a steady slow rate in order to make full use of the cooling power of the cold helium vapor as it rises and escapes through the helium vent tube(s). This rate should be maintained for at least 5-10 minutes, and the temperature inside the reservoir monitored carefully (if this option is included). When the temperature inside the reservoir drops to approximately 10K, the liquid helium transfer rate should be increased, and the helium level monitored through any supplied level probe. The amount of liquid helium needed will be a function of the size of the reservoir, the coil, as well as the efficiency of the transfer. About five liquid helium liters, plus one liter per five pounds of magnet is required to cool the reservoir and magnet from 77 to 4.2K. This, along with the

overall capacity of the helium reservoir, should offer a rough figure for the amount of liquid helium required for initial cooldown.

When the helium reservoir is full, all entrances into the reservoir should be sealed, except for the vapor cooled high current magnet leads. This will cause the dewar boil-off to vent through the leads, thereby intercepting most of the heat load that such leads bring into the helium reservoir. This is particularly important when large currents are passing through the leads. Also a small relief on the top plate should be venting at the same time as the current leads, this cools the neck of the dewar. These relief valves are adjustable so that both valves can be set to vent at the same time (see adjustment instructions amended to manual).

It is good procedure to maintain the liquid helium level above the coil at all times. This is absolutely necessary when a current is passing through the superconducting coil in order to prevent a magnet quench and possible damage to the coil. With this in mind, any subsequent liquid helium transfers should be made above the level of the remaining liquid in the helium reservoir. This can be done without the initial fill line (if supplied), or simply by keeping the tip of the transfer line above the remaining liquid.

4.3 Superconducting Magnet Operation

1) General Precautions

During the operation of any superconducting magnet system, certain hazards to the operator and the equipment exist, and should be noted. The following precautions should therefore be taken before any attempt is made to charge the magnet:

Remove (or tie down) any objects (tools, screws, etc.) that could be magnetized and attracted to the magnet when the field is turned on. Also remove any personal articles such as watches or credit cards that could be affected by intense magnetic fields. This is particularly important in large coils and units with a room temperature bore.

Make absolutely sure that the liquid helium level is above the superconducting coil before the field is turned on, and throughout the whole time that current is passing through the coil. Failure to do so may result in a magnet quench (sudden loss of field associated with the coils going "normal") that could damage the coil. Also, any quench relief (usually located at the helium reservoir pumping arm or on the top plate) should be checked for proper operation, in order to protect the dewar and operator in the unlikely event of a magnet quench.

Exercise extreme care when handling the power circuit for the magnet. In particular, never disconnect the power supply from the circuit while it is providing a current to the magnet. A lethal voltage can immediately develop at the terminal being disconnected. This is due to the large change in flux and associated large emf that can develop when a sudden interruption of the current (and magnetic field) occurs. The proper procedure for handling the magnet power circuit will be detailed below.

2) Charging the Magnet

The following procedure assumes that only a magnet power supply is provided with the system, and that a low resistance standard shunt (e.g. 100 ampere, 100 millivolt) is connected in series with the power supply/magnet circuit. The shunt enables accurate monitoring of the current in the circuit by monitoring the voltage across this shunt. When a programmer (or a programmable power supply) is also provided, check the enclosed manual for any modification in the charging procedure.

1) Check the enclosed magnet specifications and note the rated field, the rated current at that field and the recommended charging voltage. Also check whether a persistent current switch is supplied at the coil. Never exceed the rated current indicated in these specifications. In rare cases one current may be rated at 4.2K, and a higher one at lower temperatures.

2) Make all the necessary electrical connections according to the enclosed pin wiring diagrams. These could include the persistent switch heater, magnet voltage taps, magnet current, etc., in addition to the main magnet leads and any other sweep or secondary coils supplied. Particular importance should be given to the higher current magnet circuit, where any loose contacts could result in dangerous overheating during the current flow.

3) Make certain that the liquid helium level is above the superconducting coil, and preferably up to its highest recommended level.

4) Make certain that the helium reservoir is vented through the vapor cooled high current magnet leads. This flow should be

periodically checked throughout the experiment to ensure proper cooling of these leads.

5) Turn the persistent switch heater power supply on, to change the persistent switch to its "normal" mode (if the system includes such a switch).

6) Close the line switch for the magnet power supply, with both the current and voltage limits set at zero.

7) Set the current limit to a value equal or less than the rated magnet current. This is best done by initially shorting the high current cables before attaching them to the magnet leads on top of the cryostat. The current limit can now be set to any desired value, and the position of the (current) indicator noted for later reference. Thus, the same current limit can be set after the power supply is connected to the magnet leads.

8) Start charging the superconducting coil be setting the voltage limit to the recommended charging voltage. The current will now start to increase at a rate determined by the charging voltage, in inductance of the coil, the lead resistance, the (protective) diode (across the output terminals of the power supply) voltage, and any additional diodes' voltage that might be supplied as part of an (optional) energy absorber. Systems with a programmable power supply, or an electronic programmer will have an accompanying manual that describes the charging procedure to be followed.

9) Once the current limit is reached, the voltage across the magnet will approach zero. Fine adjustments of the current may then be slowly made to obtain a precise magnet current (and

field).

10) For magnets with a persistent current switch, the switch heater power supply may now be turned off to bring the switch to its superconducting mode. The current in the coil will now flow in a closed (superconducting) loop, and the current passing through the magnet leads may now be reduced to zero in order to eliminate Joule heating in those leads. This is done by ramping the supply's output current down to zero and switching the power supply off. The current in the leads will drop to zero. Do not change the setting on the current limit and do not disconnect the power supply from the circuit unless removable current leads where provided with the system (see section 4-4).

If the persistent switch needs to be turned back to its "normal" state (e.g. for changing the field), the magnet power supply should first be turned back on (if it was turned off), and the power supply's output current should be set back to its original value (if it was ramped down). With the current limit unchanged, the last current that flowed through the circuit should once again pass through the leads. Only at this point should the persistent switch heater power supply be switched on to change the persistent switch back to its "normal" mode. This interrupts the closed superconducting loop in the coil, and brings back the power supply and magnet leads into the same circuit as the coil.

11) To reduce the field to any level below the operating level, one can very slowly reduce the current limit in order to avoid a magnet quench. The voltage across the coil will reverse

its polarity due to the back emf of the coil.

An alternate method is to switch the power supply to ramp down and observe the current decay in the circuit. This can be followed by a slow decrease in the current limit to the approximate value desired, then a resetting of the ramp to UP. The power supply will then ramp UP to the new current limit and stop.

12) To discharge the coil, the power supply should be ramped down to zero. The voltage across the coil will once again reverse polarity during the discharge, and the current will decay to zero.

CAUTION: DO NOT DISCONNECT THE POWER SUPPLY FROM THE CIRCUIT AS LONG AS ANY CURRENT IS FLOWING. A LETHAL VOLTAGE CAN OTHERWISE DEVELOP AT THE TERMINAL BEING DISCONNECTED.

13) Once the current drops to zero, all power supplies can be turned off (not disconnected), and the system allowed to warm up gradually to room temperature. Should the power supply have to be disconnected from the circuit while the coil is superconducting (with the current apparently zero), a low resistance shunt should be connected across the magnet high current terminals before disconnecting the leads. This shunt must be kept in place until the coil turns "normal". Once the coil is "normal", it is then quite safe to disconnect the power supply or cables from the circuit. Any safety pressure relief valves should be kept in position to allow venting of the cryogen gases as the dewar warms up, and prevent any air or moisture from condensing inside the dewar.

4.4 Removable Current Lead Operation

If it is desired to retract the current leads to reduce the LHe boil-off rate and your system has retractable current leads installed, the following procedure should be used. CURRENT LEAD RETRACTION CAN BE VERY DANGEROUS!! GREAT CAUTION SHOULD ALWAYS BE USED DUE TO THE POSSIBILITY OF POTENTIALLY LETHAL VOLTAGES OCCURRING. ALWAYS USE A 30 KV INSULATED TOOL FOR RETRACTING THE LEADS. NEVER TOUCH THE LEADS WITH BARE HANDS.

Step 1. Check to be sure that NO CURRENT is flowing in the power cables leading to the magnet.

Step 2. Check to be sure that the voltage across the voltage taps of the magnet are at ZERO volts indicating persistent mode operation.

Step 3. Using a 30 KV insulated tool, retract the power leads straight up by first loosening the brass nut on the current lead mount fitting. Be careful not to bend the current leads.

NOTE: If you feel it is necessary to disconnect the power cables from the current leads to avoid bending them, be sure you mark the polarities of the power supply cables and the current leads since you will have to hook them back up the same way later. Hooking the leads up backwards later on and then trying it discharge the superconducting magnet can cause the magnet to quench.

Step 4. With the current leads retracted, retighten the brass nut to hold the leads in the retracted position.

Step 5. When reinserting the current leads to discharge the magnet, loosen the brass nut and insert them slowly. Remember,

they have been retracted up into the warm gas and must cool to helium temperature. Inserting them too quickly may induce a quench. Be sure the leads seat tightly into their connectors within the cryostat and good electrical contact is made. Be sure gas flow through the leads is present.

4.5 Troubleshooting

All power supplies and other electronic components supplied as part of your superconducting magnet/cryostat system have their accompanying manuals. The operator should always refer to these manuals for proper operating procedures, and in case of any difficulties with these parts.

Should any difficulty arise with the dewar or superconducting coil supplied, it is recommended that you contact Cryomagnetics before any repair work is undertaken. In addition to the description of the difficulty, it is always helpful to obtain the model and serial number of the system in question.

5.0 SYSTEM SAFETY PRECAUTIONS

CAUTION:

5.1 NEVER DISCONNECT THE CURRENT LEADS WHEN THE MAGNET IS CHARGED A POTENTIAL FATAL VOLTAGE (KILOVOLTS) WILL OCCUR THAT CAN CAUSE SEVERE INJURY OR DEATH.

5.2 NEVER TOUCH THE CURRENT LEADS WHILE THE MAGNET IS ENERGIZED. ALWAYS USE A 30 KV INSULATED TOOL.

5.3 NEVER OPERATE THE MAGNET WITH INSUFFICIENT LIQUID HELIUM LEVEL.

5.4 NEVER OPERATE THE VAPOR COOLED CURRENT LEADS WITHOUT HELIUM GAS FLOWING.

6.0 LIMITED WARRANTY POLICY

Cryomagnetics warrants its products to be free from defects in materials and workmanship. This warranty shall be effective for one year after the date of shipment from Cryomagnetics. Cryomagnetics reserves the right to elect to repair, replace, or give credit for the purchase price of any product subject to warranty adjustment. Return of all products for warranty adjustment shall be FOB Oak Ridge, Tennessee, and must have prior authorization for such return from an authorized Cryomagnetics' representative.

This warranty shall not apply to any product which has been determined by Cryomagnetics' inspection to have become defective due to abuse, mishandling, accident, alteration, improper installation or other causes. Cryomagnetics products are designed for use by knowledgeable, competent technical personnel.

In any event, the liability of Cryomagnetics, Incorporated is strictly limited to the purchase price of the equipment supplied by Cryomagnetics. Cryomagnetics, Inc. shall not assume liability for any consequential damages associated with use or misuse of its equipment.

VAPOR-COOLED CURRENT LEADS

CAUTION:

When soldering bus bars to the bottom of the lead care should be taken to just melt 60/40 solder. If the temperature reaches approximately 430° the solder inside the lead will melt damaging the lead (closing the gas vent holes).

CAUTION:

The vapor-cooled lead must always have helium gas flowing during operation. If the gas flow is cut off the lead will possibly be destroyed.

WARNING:

Cryomagnetics vapor-cooled current leads have been optimized for minimum boil off performance.

The stainless steel case is very thin walled.

Be certain that you observe the following practice:

1) Do NOT overtighten the compression nut on the mounting fitting. It has been designed to seal when just finger tight.

2) Be careful when inserting or retracting the lead. It may be bent easily.

739 EMORY VALLEY ROAD
OAK RIDGE, TN
MAILING ADDRESS
P.O. BOX 548 OAK RIDGE, TN 37831-0548
TELEPHONE 615-482-9551
TELEX 883-945
FAX 615-483-5891

VAPOR-COOLED CURRENT LEADS

LIMITED WARRANTY

Cryomagnetics Vapor-Cooled Magnet Current Leads are protected by a one year limited warranty for defects in materials and workmanship. The warranty period begins on the date of shipment to the customer. All warranty repairs or replacements are F.O.B. Oak Ridge, Tennessee USA.

WARNING: All models of Cryomagnetics Vapor-Cooled Magnet Current Leads are warranteed for DC-current use only, and only up to the rated current maximum of the particular model. No warranty is given or implied for damage or failure due to loss of helium gas counterflow through the current lead, or for pulsed current or over-current operation.

LIMITATION OF LIABILITY

It is a condition of all product sales by Cryomagnetics that the Company shall not accept liability for coincidental damages to personnel, equipment, or facilities due to use or failure of any Cryomagnetics product. Cryomagnetics liability for use of its products is strictly limited to the amount of the total purchase price of each product, F.O.B. Oak Ridge, Tennessee USA.

739 EMORY VALLEY ROAD
OAK RIDGE, TN
MAILING ADDRESS
P.O. BOX 548 OAK RIDGE, TN 37831-0548
TELEPHONE 615-482-9551
TELEX 883-945
FAX 615-483-5891

OPERATING INSTRUCTION MANUAL

FOR

MODEL 12 DIGITAL LIQUID HELIUM LEVEL METER

WARNING: DO NOT ATTEMPT TO OPERATE THIS EQUIPMENT BEFORE YOU HAVE THOROUGHLY READ THIS INSTRUCTION MANUAL.

INNOVATION AND EXCELLENCE IN CRYOMAGNETICS

739 EMORY VALLEY ROAD
OAK RIDGE, TN
MAILING ADDRESS
P.O BOX 548 OAK RIDGE TN 37831-0548

TELEPHONE 615-482-9551
TELEX 855945

MODEL 12 DIGITAL LIQUID HELIUM LEVEL METER

The Model 12 Digital Liquid Helium Level Meter provides simplicity with all new, state-of-the-art digital circuitry and level sensor design at an affordable price. Its features have been tailored for general purpose laboratory applications.

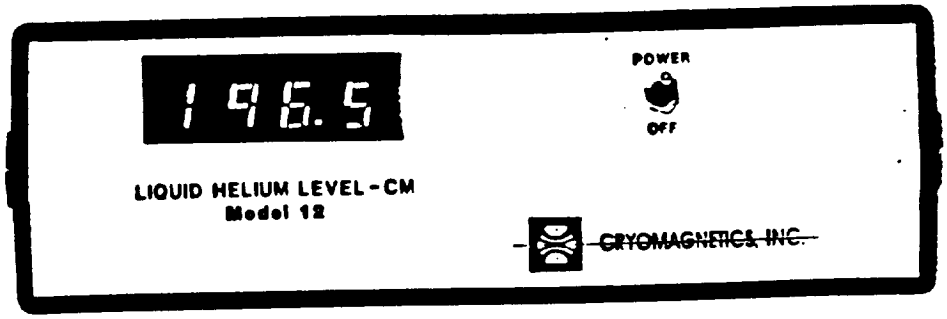

FEATURES

- ✱ 0.4 inch high, 3½ digit LED readout
- ✱ Readout calibrated in centimeters, 1 mm resolution, 0.5% linearity
- ✱ Single level sensor operation, 1 cm to 200 cm active sensing length
- ✱ Low liquid helium loss 3-wire sensor
- ✱ Easy rear panel calibration adjustment
- ✱ Plug-in sensor connector
- ✱ Rugged, lightweight construction
- ✱ Tilt stand

OTHER SPECIFICATIONS

Overall Dimensions ..... 15.9 cm x 6.35 cm x 20.5 cm
Weight ..... 1.25 kg
Input Power ... 120/220 Vac ±10%, 50-60 Hz

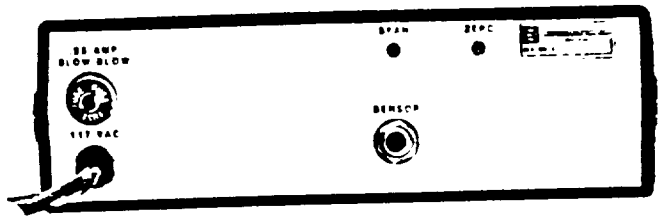

Rear View Model 12

PRICE

Model 12 Digital Liquid Helium Level Meter, without sensor $285/each
Optional Adjustable Analog BNC 1 mV/cm Output on Rear Panel ..... Add. $15
Panel Mount, Single Unit, 3.5 inch (8.9 cm) high, 19 inch (48.2 cm) wide ..... Add. $55
Panel Mount, Two Units, Side-By-Side, 3.5 inch (8.9 cm) high, 19 inch (48.2 cm) wide ..... Add. $85

*All prices are FOB Oak Ridge, Tennessee
Prices subject to change without notice

CRYOMAGNETICS, INC.
INNOVATION AND EXCELLENCE IN CRYOMAGNETICS
P.O. BOX 548
OAK RIDGE, TN USA
37831
TELEPHONE 615-482-9551
TELEX 823545

OPERATING INSTRUCTIONS

MODEL 12 DIGITAL LIQUID HELIUM LEVEL METER

1.0 INTRODUCTION

The Model 12 provides simplicity with all new state-of-the-art digital circuitry. It is easy to install, calibrate, and operate. It is designed to operate Cryomagnetics Models 2D, 3D, and 4D superconducting liquid helium level sensors.

2.0 INSTALLATION AND OPERATION

The Model 12 is delivered to you fully tested and ready to operate. If you have specified the active length of the level sensor to be used, the Model 12 will also be delivered to you fully calibrated.

Unless otherwise specified, the Model 12 will be delivered for use with 120 VAC ±10%, 50-60 Hz input power. The unit can be supplied for operation on 220 VAC ±10%, 50-60 Hz input. It can also be easily rewired for one or the other input by you. Procedures are given below for implementing an input voltage change.

2.1 Procedure for Change of Input Voltage

In order to change the input voltage, it is only necessary to remove the instrument cover and change two wire connections on the power transformer primary as shown below.

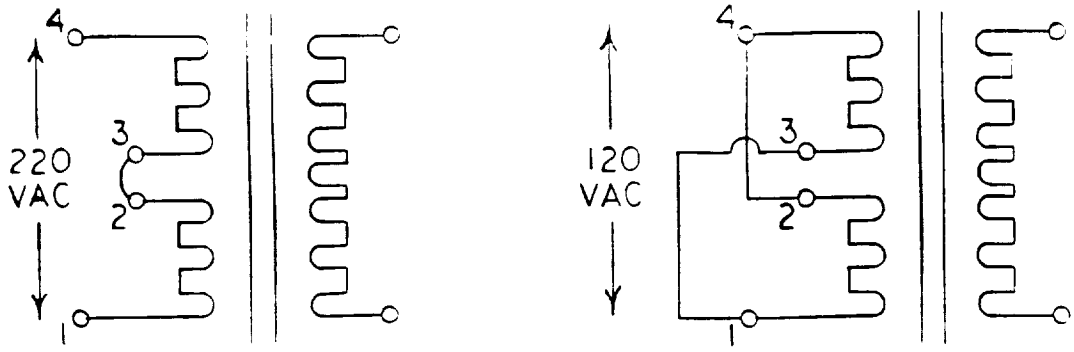

Transformer

*NOTE: ALWAYS DISCONNECT POWER CORD BEFORE REMOVING COVER.

2.2 Sensor Wiring

Cryomagnetics level sensors have only three (3) #30 AWG lead wires for sensor hookup.

Level Sensor Wire Color Code

Red	I+	Pin A
Black	I-	Pin B
Blue	V+	Pin D

The sensor and male connector which plug into the rear panel of the Model 12 are provided with pigtail leads. The interconnecting cable between the room temperature envelope of the dewar and the level meter is not provided by Cryomagnetics. Cable wire sizes for various distances between the Model 12 and dewar are tabluated below.

Distance Bewteen Model 12 and Dewar	Recommended Cable Wire Size
Up to 12 feet	#18 AWG
12 to 50 feet	#16 AWG
50 to 100 feet	#14 AWG

Unshielded three-conductor cable may be used where no significant use of SCR-controlled equipment or intense electrostatic field sources are present. Otherwise, it is recommended that shielded three-conductor cable be used.

2.3 Model 12 Calibration

The Model 12 can be easily calibrated for use with different active length level sensors. The ZERO and SPAN can be adjusted at the rear panel without removing the instrument cover. The SPAN should always be adjusted before adjusting ZERO.

2.3.1. Procedure for Span Adjustment

1) POWER OFF
2) Remove the male sensor connector from the rear panel of the Model 12
3) Switch POWER ON on the Model 12 front panel
4) Adjust the SPAN adjustment on the rear panel with a

screwdriver until the readout reads the sensor active length either in centimeters or inches (inches optional)

5) POWER OFF

6) Reconnect sensor to the Model 12

WHEN OPERATING THE SENSOR OUTSIDE THE DEWAR AT ROOM TEMPERATURE, THE READOUT WILL INDICATE A NEGATIVE NUMBER, THE VALUE OF WHICH DEPENDS ON THE SENSOR ACTIVE LENGTH.

2.3.2 Procedure for Off-Set Adjustment for High Connecting Lead Resistance

For applications wherein resistive hook-up wire is employed within the cryostat between the sensor leads and the electrical connector on the room temperature envelope of the cryostat, or for applications wherein extremely long cabling distances between the level meter and cryostat are involved, it is very easy to perform the following off-set adjustment:

1) Before connecting cable to rear panel of the level meter, measure the total resistance between the I- (Black) cable lead at the meter connector male and the I- (Black) lead at the top of the sensor. Make this measurement with all lead resistances in the circuit.
2) Divide the measured resistance by 4.15 Ohm/cm.
3) Switch POWER ON on the level meter front panel.
4) Adjust the SPAN adjustment on the rear panel with a screwdriver until the readout reads a number which is the total of the sensor active length plus the number resulting from the calculation in Step 2 above. The meter will now be offset for connecting lead resistance.

5) POWER OFF

6) Reconnect the sensor cable to the rear panel of the meter. Now, with the sensor completely immersed in liquid helium in the cryostat, the readout should read the full sensor active length with the level meter POWER ON.

2.3.3 Procedure for Zero Set

1) POWER OFF

2) Remove the male sensor connector from the rear panel of the Model 12

3) Insert a load resistor between V+ (Blue) and I- (Black) Short I+ (Red) to V+. The resistance of the load resistor should be 4.15 Ohm per centimeter active length of the sensor.

CAUTION: Be sure that adequate power rating of resistor is used for sensor current of 65 mA.

4) Switch POWER ON on the Model 12 Front Panel.

5) Adjust the ZERO adjustment on the rear panel with a screwdriver until the readout reads 000.0

6) POWER OFF

7) Remove load resistor and reconnect sensor to the Model 12.

Generally, once zero has been set, it will not be necessary to reset when changing sensor active lengths.

3.0 TROUBLE SHOOTING

For any problems or questions not discussed herein, please contact Cryomagnetics for prompt assistance.

4.0 LIMITED WARRANTY

All Cryomagnetics products are protected by a one year limited warranty for defects in materials and workmanship. The warranty period begins on the date of

shipment to the customer. All warranty repairs or replacements are FOB, Oak Ridge, Tennessee.

WARNING: Any alteration of or tampering with the Model 12 circuitry or level sensor by the customer automatically voids the warranty.

5.0 LIMITATION OF LIABILITY

It is a condition of all product sales by Cryomagnetics that the Company shall not accept liability for coincidental damages to personnel or equipment or facilities due to use of Cryomagnetics products. Cryomagnetics liability for use of its products is strictly limited to the amount of the total purchase price, FOB Oak Ridge, Tennessee.

CRYOMAGNETICS, INC.

OPERATING INSTRUCTION AND MAINTENANCE MANUAL

FOR

IPS 20/50/100 MAGNET POWER SYSTEMS

CAUTION: DO NOT ATTEMPT TO OPERATE THIS EQUIPMENT
BEFORE THOROUGHLY READING THIS MANUAL.

739 EMORY VALLEY ROAD
OAK RIDGE TN
MAILING ADDRESS
P O BOX 548 OAK RIDGE TN 37831-0548
TELEPHONE 615-482-9551

INNOVATION AND EXCELLENCE IN CRYOMAGNETICS

TABLE OF CONTENTS

LIST OF FIGURES

LIST OF TABLES

1.0 GENERAL INFORMATION

1.1 Introduction

Cryomagnetics, Incorporated superconducting magnet power systems are designed to provide stable and efficient energizing, discharging, and controlling of highly inductive loads common to superconductive magnet systems. The IPS (Integrated Power System) series combines the functions of Sweep Generator, High Current Power Supply, Energy Absorber, Quench Protection, Persistent Switch Heater Power Supplies, and System Monitoring Electronics into a single, compact, extremely versatile instrument. Advanced circuit design, and construction and calibration techniques enable the IPS power supply to generate reliably stable output currents with excellent low noise specifications. In addition, the IPS power supplies all contain Cryomagnetics' proprietary quench detection circuitry which automatically and smoothly shuts off the power supply if a sudden load error is sensed.

1.2 Description

The three models of IPS power supplies described in this manual all use fully transistorized series-type power regulation. They are linear supplies which utilize a very low noise triac preregulator for high efficiency, excellent regulation, and low ripple. All supplies come with full 19 inch standard width rack-mountable cabinets and are suitable for either rack or bench top use.

The IPS power supplies provide a multitude of features including:

1.2a Current Monitor

A 4½ digit LED display is provided to indicate operating current, charge rate, or the preset current limit in amperes and amperes/second.

1.2b Voltage Monitor

A 3½ digit LED display is provided to indicate the power supply's

output voltage, actual magnet voltage, or the preset voltage limit in volts. Displaying of the actual magnet voltage requires that a pair of voltage taps be connected from the magnet's power leads in the dewar to the rear panel terminal strip on the supply.

1.2c Preset Current Limit

The Current Limit is set on a front panel 10-turn lockable dial between zero and the full scale output of the supply. The limit setting can be displayed before affecting the supply's output. When the supply reaches current limit, a front-panel LED is illuminated indicating that the output current is stable.

1.2d Preset Charge Rate

The Charge Rate for the magnet is set on a lockable 10-turn dial between zero and 1.000 amperes per second. The rate is valid for both the charge and discharge of the magnet. The rate can be displayed and precisely set using the current monitor display.

1.2e Fast Ramp

The Fast Ramp capability allows the user to override the preset charge rate with a faster (10 a/s) ramp. This feature lets the operator quickly bring the supply back to zero current after putting the magnet in persistent mode; or to quickly return the supply's current back to the current limit when coming out of persistent mode.

1.2f Preset Voltage Limit

The Voltage Limit of the supply is set on a front panel 10-turn lockable dial between zero and 5 volts. The voltage limit is used to prevent overvoltage on the magnet. The voltage limit set is valid for both positive and negative output levels (i.e. charging and discharging the magnet). The limit setting can be displayed before affecting the supply's output. When the supply reaches its voltage limit, a front

panel LED is illuminated.

1.2g Energy Absorbing

All supplies contain built-in energy absorbing capabilites to allow the supply to efficiently discharge the energy stored in a magnet. The supply is capable of absorbing energy at up to -5 volts at its full rated current. Output current from the supply is always between zero and + full scale current at +5 to -5 volts (2 quadrant operation). A current reversing switch is available to provide full four (4) quadrant operation. The energy absorber has a built-in automatic thermal shut-down as a safety precaution.

1.2h Quench Protection

Both the superconducting magnet and the IPS power supply are protected from over-voltage damage due to magnet quench through the use of SCR crowbars. The built-in SCR's trip to "short" the supply's output if a voltage of more than 15 volts (+ or -) is detected at the supply's output.

1.2i Quench Detection

Cryomagnetics' proprietary quench detection and automatic shut-down is built into all IPS power supplies. This circuitry monitors the supply's load (superconducting magnet) and is sensitive to sudden changes in this load. If a load change is detected, the supply is smoothly and quickly returned to zero output current. The supply is disabled from ramping back up until the detection circuitry is reset via a rear panel pushbutton switch. A LED is used to indicate that the quench detector has tripped. The quench detector (error detect) can be disabled for use in "noisy" load environments.

1.2j Remote Control

All front and rear panel functions can be remotely controlled via a terminal strip including current limit, voltage limit, charge rate, up/pause/down ramp control, error detect reset, and persistent switch heater supplies. In addition, the terminal strip provides the user with output signals such as operating current, current limit LED status, voltage limit LED status, and quench detection circuitry status. A complete RS-232C/IEEE-488 controller is available as an option.

1.2k Persistent Switch Heater Power Supplies

Two Persistent Switch Heater Power Supplies are built-in to allow multiple magnets to be powered from a single supply (not available on IPS-20).

1.3 Specifications

	IPS-20	IPS-50	IPS-100
OUTPUT POWER RATING	0-20 AMPS. ±5 VOLTS	0-50 AMPS. ±5 VOLTS	0-100 AMPS. ±5 VOLTS
POWER CONSUMPTION	110/115V, 4A*	200/230V, 6A**	200/230V, 12**
OUTPUT CURRENT SETTABILITY	BETTER THAN 0.1%		
OUTPUT CURRENT STABILITY	<0.005% per hour		
RIPPLE AND NOISE (RESISTIVE LOAD)	<100 mA p/p		
LINE REGULATION	0.005%		
LOAD REGULATION	0.05%		
CURRENT MONITOR	0.10 V/A		
EXTERNAL PROGRAMMING	CURRENT LIMIT: 0.10V/A VOLTAGE LIMIT: 1.00V/V UP/PAUSE/DOWN: +5V/0V (TTL COMPATIBLE)		CHARGE RATE: 10.0V/(A/S)
SWITCH HEATER OUTPUT	N/A	2 EACH, 0-100 mA	2 EACH, 0-100 mA
SWEEP RATE	0.010 — 1.000 A/S		
COOLING	FORCED-AIR WITH OVER-TEMPERATURE SHUTDOWN ON TRANSISTOR BANK		
CABINET DIMENSIONS	19" W X 5.187" H X 14.25" D	19" W X 8.75" H X 20" D	19" W X 8.75" H X 20" D
WEIGHT	30 LBS (13.6 kG)	90 LBS (40.9 kG)	110 LBS. (50.0 kG)

*200/230V, 2A AVAILABLE

**110/115V AVAILABLE (multiply current by 2)

1.4 Options

Cryomagnetics manufactures a full line of related support devices for superconducting magnet power systems.

1.4a Helium Vapor-Cooled Current Leads

Introducing high currents to a cryogenic environment can cause high heat loads on a system's cryogens. Cryomagnetics manufactures current leads which utilize the cold helium off-gas from a system to cool the high current power leads. These leads are optimized to introduce a minimal heat load into the cryostat. Installation of the leads is simple and retractable accessories are available for ultra low loss systems. Standard designs are optimized for currents up to 3000 amperes.

1.4b Computer Interface Module (CIM)

Cryomagnetics' CIM can be used to control virtually all functions on the IPS power supplies through standard RS-232C or IEEE-488 (GPIB) computer interfaces. Both interfaces are provided. The CIM is extremely versatile in that it can also be used to monitor and/or control other functions in the user's system. In particular, the CIM provides 8 analog ports which can be user defined as inputs or outputs. These analog ports have a +10 to -10 volt range with 13 bit resolution. In addition, the CIM has 18 binary ports which are TTL compatible. The CIM can be configured to take data locally and store it in its 3500 sample memory.

1.4c Current Reversing Switch

Cryomagnetics' Current Reversing Switch provides the user with safe reversing of power supply high current leads. The instrument is safety interlocked to prevent switching of the power leads unless zero

current is present in them. The CRS is protected against power failure and quenches also. The CRS can be remotely controlled either, through the user's circuitry or through Cryomagnetics' Computer Interface Module (1.4b above).

2.0 INSTALLATION

The IPS power supply has been shipped ready for permanent installation or bench top use. It is only necessary to connect the instrument to a power source and it is ready to operate.

2.1 Initial Inspection

Before shipment, this instrument was inspected and found to be free of mechanical and electrical defects. A rigorous check-out, calibration, and burn-in procedure is followed on all supplies.

As the supply is unpacked, inspect it for any damage that may have occurred in transit. Save all packing materials until the inspection and turn-on check-out procedures have been completed. If damage is found during inspection, file a claim with the carrier immediately. Also notify Cryomagnetics as soon as possible.

Initial inspection should include verifications that all knobs and switches operate properly and are undamaged. Also, the cabinet and panels should be checked and free of scratches and dents.

2.2 Location and Cooling

All IPS power supplies are fan cooled and must be installed with sufficient space for cooling air to flow freely through them. The IPS power supplies have two exhaust ports exiting the rear of the supplies and two air inlet ports on the sides. All exhaust ports and inlet ports should have free access to air with a minimum of direct recirculation. the supplies should be used in an area where the ambient air temeprature at the inlet does not exceed 50°C.

Rack mounting of the instrument is available on the front panel. Due to the weight of the instruments, it is suggested that bottom support in the form of a tray be provided for the supply to eliminate the chance of

bending the front panel of the supply or cabinet.

2.3 Input Power Requirements

Input power cords for the supply are provided with the instrument. Standard power connections call for 110/115 VAC single phase power for the IPS-20 and 200/230 VAC single phase power for the IPS-50 and IPS-100. The IPS-20 can be modified for 200/230 VAC use and the IPS-50/100 can be modified for 110/115 VAC use. Consult the factory if this change is necessary. Additional input power requirements are detailed in section 1.3.

2.4 Repackaging for Shipment

To insure safe shipment of the instrument, it is recommended that the original package designed for the instrument be saved and reused. The instrument should be wrapped with plastic and then inserted into the box with the foam protection in place. A tag should be attached to the instrument with the serial number of the instrument and the owner's name and phone number on it. A brief description of the problem with the instrument should accompany the supply if it is being returned for repair.

3.0 OPERATING INSTRUCTIONS

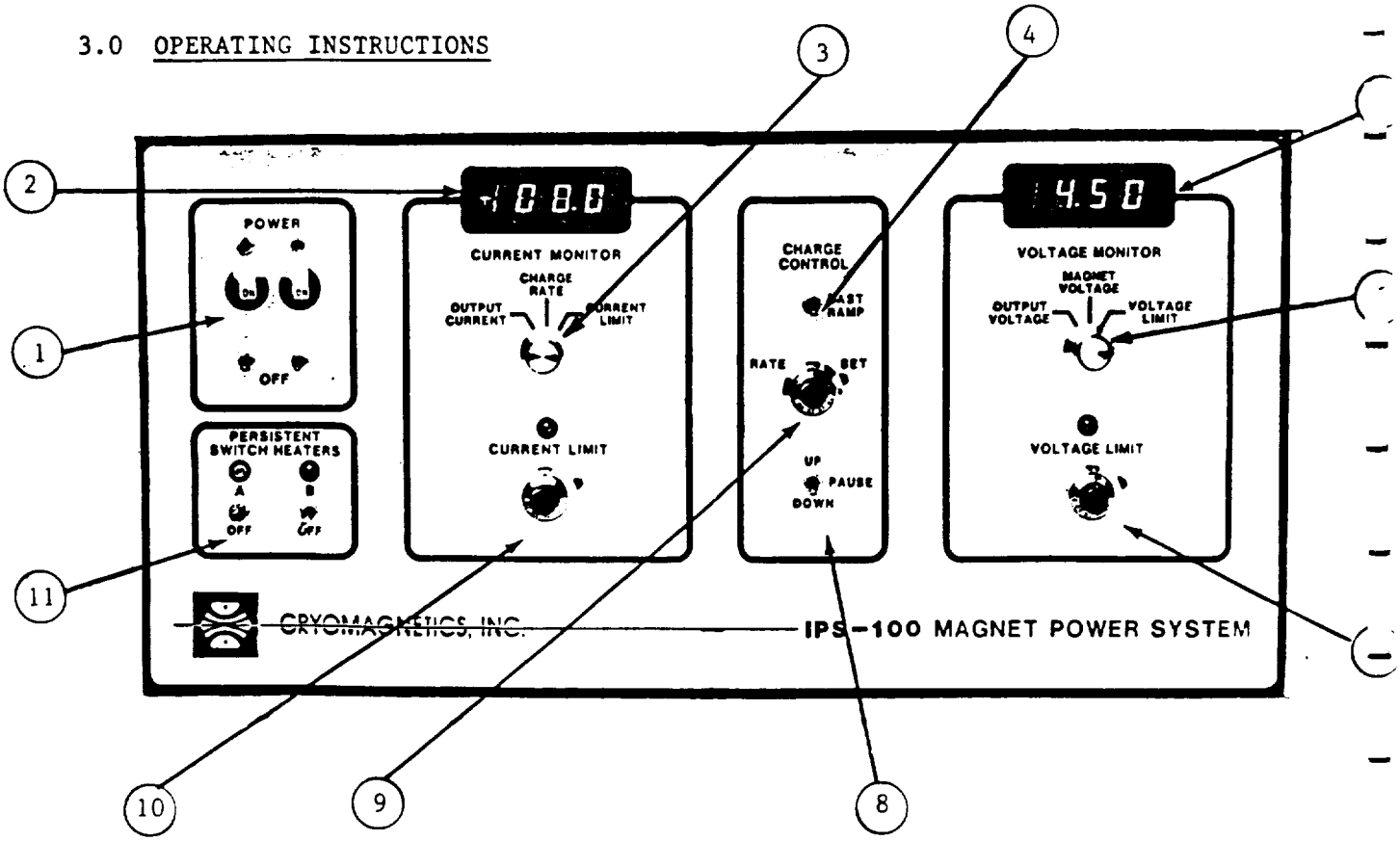

FIGURE 3-1. Front Panel Controls and Displays

The following operating procedures should be observed in order to insure safe and trouble-free performance from the IPS power supply. It is recommended that this section be thoroughly read prior to actually operating the supply.

3.1 Turn-on and Checkout Procedure

The following steps describe use of the front and rear panel controls and indicators detailed in Figures 3-1 and 3-2. These steps provide an initial check of the supply's operational capabilities as well as familiarizing the user with the controls. The procedure does not require the use of the magnet.

3.1a With the POWER OFF and the supply unplugged, connect a short across the output terminals of the supply (19). This short can be either directly on the back of the supply or at the end of the power cables.

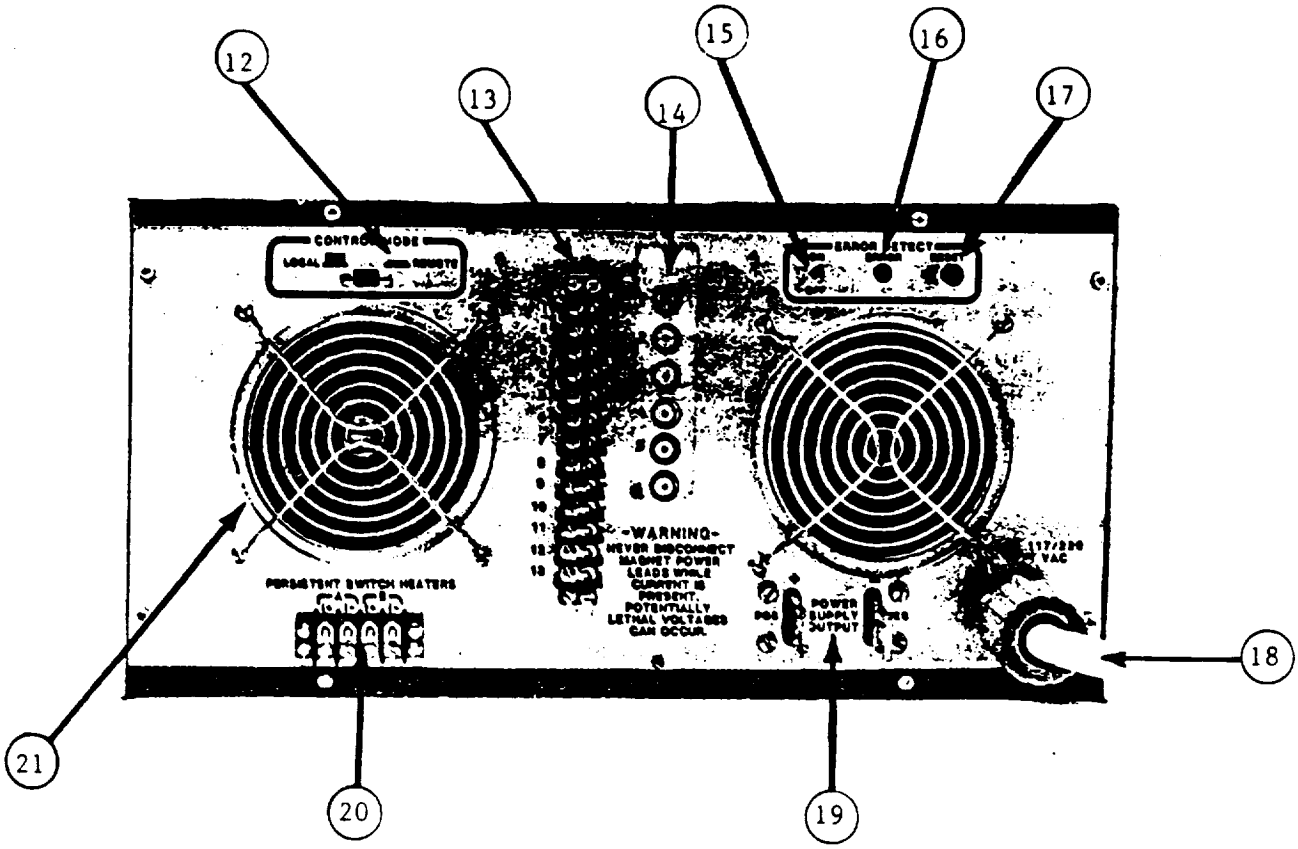

FIGURE 3-2. Rear Panel Controls and Displays

3.1b Plug the supply into the appropriate power source using the provided line cord (18).

3.1c Set the front panel charge control switch (8) to the DOWN position. Turn the Current Limit dial (10), Rate Set dial (9), and Voltage Limit dial (7) to full scale (full clockwise).

3.1d Set the Current Monitor Selector Switch (3) to display Current Limit and the Voltage Monitor Selector Switch (6) to display Voltage Limit.

3.1e Turn off both Persistent Switch Heaters (11).

3.1f Make sure that rear panel Control Mode switch (12) is set to LOCAL and the Error Detect switch (15) is ON.

3.1g POWER ON the supply using the front panel circuit breaker switch (1). The Current Monitor display should read approximately 101.0 amperes and the Voltage Monitor display should read approximately

5.30 volts. These are the preset limit settings for the supply. Check to see that the Current Limit dial (10) changes the Current Monitor display. Likewise check that the Voltage Limit dial (7) changes the Voltage Monitor display. Return the Limit dials (10) and (7) to the full clockwise position. The instrument has been calibrated such that the LED displays represent the current settings for the limits. The number indicated on the dials (10) and (7) should not be used.

3.1h Switch the Current Monitor Selector Switch (3) to display Charge Rate. The display should read approximately -1.000 amperes per second. Turn the Rate Set dial (9) to check that the displayed charge rate varies. Return the Rate dial to the full clockwise position.

3.1i Switch the Voltage Monitor Selector Switch (6) to display Magnet Voltage. The display should indicate 0.00 volts.

3.1j Switch the Voltage Monitor Selector Switch (6) to display Output Voltage. Again the display should indicate 0.00 volts.

3.1k Switch the Current Monitor Selector Switch (3) to display the supply's Output Current. The Current Limit has been preset to about 100 amps, the Voltage Limit preset to 5.30 volts, and the Charge Rate at one (1) ampere per second.

3.1l Switch the Charge Control (8) to the UP position and see that the current begins to rise at 1 ampere per second. If the current does not rise, check the Error Detect LED (16) for illumination. If the LED is on, press the RESET switch (17) and release it to extinguish the LED. The current should now rise. Eventually, a small voltage will appear on the voltage monitor corresponding to the IR drop across the "shorted" output. Verify that the PAUSE and DOWN positions of the

Charge Control Switch (8) operate properly.

3.1m When the supply reaches Current Limit (100 amperes), verify that the Current Limit LED illuminates. Switch the Charge Control to the DOWN position.

3.1n While the current is ramping down, switch up and hold the FAST RAMP switch (4). Notice that the current decreases much more rapidly. Release the switch and see that the rate returns to 1 ampere per second. Verify that the FAST RAMP works properly when the Charge Control Switch (8) is in the UP position as well.

3.1o Return the supply to zero (0) current. Connect an ammeter between I+ and I- on Persistent Switch Heater output "A" on the rear panel of the supply (20). Switch ON Persistent Switch Heater A on the front panel (11) and check that the LED associated with it illuminates. Check that the current through the ammeter is about 50 mA. This current can be adjusted between 0 and 100 mA using a potentiometer internal to the supply (see section 5.2, Calibration). Switch OFF Persistent Switch Heater A and repeat the procedure using I+ and I- on Heater B.

This completes the preliminary checkout procedure for the supply.

3.2 Normal (LOCAL) Operating Mode

The LOCAL Operating mode is the mode in which the user operates the supply via the front and rear panel knobs and switches. The user should be fully familiar with the controls of the supply before attempting to operate it with a magnet. It is recommended that the learning procedures be performed with the rear panel output terminals shorted until he/she is comfortable with the supply. Only then should it be attached to the magnet. This should minimize the chance of an accidental quench.

3.2a Setting the Limits

The Output Current Limit and Voltage Limit Settings are straight

forward on the IPS supplies. The limits can be easily set and displayed prior to affecting the output of the supply. Current Limit is set according to the magnetic field desired, while Voltage Limit is set as a protective measure. Under normal operating conditions the Voltage Limit should not be reached. A smooth linear ramp of a magnet is achieved by maintaining the output voltage of the supply below the Voltage Limit setting.

Maximum stability and minimum drift performance of the supply is obtained when the supply is ramped up to the Current Limit and left in the UP mode.

* * * IMPORTANT * * *

IT IS A FAIRLY COMMON HABIT OF USERS TO RAMP THE SUPPLY UP TO THE DESIRED CURRENT LIMIT AND THEN TO SWITCH THE SUPPLY TO "PAUSE". THIS SHOULD NOT BE DONE!! THE POWER SUPPLY CAN DRIFT SOME WHEN PLACED IN THE "PAUSE" MODE FOR EXTENDED PERIODS OF TIME - POSSIBLY RESULTING IN AN EVENTUAL QUENCH. TO ACHIEVE MINIMUM DRIFT OF THE SUPPLY AND TO INSURE THAT THE CURRENT LIMIT IS NEVER EXCEEDED, THE SUPPLY SHOULD BE LEFT IN THE "UP" MODE AGAINST THE CURRENT LIMIT.

* * * * * * * * * * * *

3.2b Setting the Charge Rate

The Charge Rate for Cryomagnetics' Power Supplies are set directly in amperes per second. If one knows the inductance (L) of their magnet, this makes the charge rate very easy to set. Using the equation $\frac{di}{dt} = \frac{V}{L}$ one can easily compute the desired rate for their particular magnet. In this equation, di=amperes, dt=seconds, V=volts and L=henries. Thus $\frac{di}{dt}$ is specified in ampere/second - the same units used by the power supply.

For example, if the user has a 9.80 henry magnet and wishes to charge it at 2.00 volts, they could compute

$$\frac{di}{dt} = \frac{2.00}{9.80} = 0.204 \text{ amperes/second}$$

One would then set the Current Monitor Selector switch (3) to display Charge Rate and would adjust the Rate Set dial (9) until 0.204 is displayed. This Charge Rate will be valid for both the charge and discharge of the magnet.

3.2c Ramp UP/PAUSE/DOWN and FAST RAMP

The Charge Control switches for the power system are used for ramping the power supply's current up and down. Under normal operating conditions where a superconducting magnet load is attached to the supply, the Charge Rate setting determined in section 3.2b will be used. During times when the supply is being used on a resistive or shorted load, the preset Charge Rate can be over-ridden using the FAST RAMP switch. An example of the proper use of the UP/PAUSE/DOWN and FAST RAMP switches would be the following:

Assume the 9.8 henry superconducting magnet described in section 3.2B is attached to the power supply. The user would first check that the Charge Control switch is in the ramp DOWN position. Then the power to the supply would be turned ON. The user would verify that the Charge Rate is set to 0.204 amperes per second and that the proper Current Limit setting has been entered. Assuming the magnet's persistent switch heater was connected to Persistent Switch Heater Supply A, this heater would be turned ON. After a few seconds for the switch to warm, the Charge Control Switch would be switched to the ramp UP position. The current from the supply would begin to increase at 0.204 amperes per second and the user

would verify that 2.00 volts appears across the magnet terminals.

When Current Limit is reached, the Current Limit LED will illuminate and the voltage across the magnet will be seen to drop to zero indicating a stable output current. The Persistent Switch Heater Supply A would then be switched OFF.

After a few seconds for the switch to cool, the user would switch the Charge Control switch to the ramp DOWN position. The power supply's current will begin to decrease at -0.204 amperes per second. The voltage across the magnet would then be checked to ensure that it is still zero volts (indicating that the magnet is, indeed, locked in persistent mode).

* * * IMPORTANT * * *

ONE SHOULD ALWAYS VERIFY THAT THE MAGNET IS IN PERSISTENT MODE BEFORE USING THE FAST RAMP SWITCH TO BRING DOWN THE POWER SUPPLY CURRENT. IF THE MAGNET IS NOT IN PERSISTENT MODE WHEN THE FAST RAMP IS PRESSED A QUENCH MAY RESULT DUE TO THE SUPPLY ATTEMPTING TO DISCHARGE THE MAGNET TOO QUICKLY!

* * * * * * * * * * * *

Since the supply is effectively operating with a short as a load now, the supply can be quickly returned to zero current by pressing the FAST RAMP switch and holding it. Likewise, when one is ready to remove the magnet from persistent mode operation, the supply can be ramped quickly back up to Current Limit using the FAST RAMP switch and then the Persistent Switch Heater Supply A turned ON.

3.2d ERROR (Quench) DETECTOR

The Error Detector built into the IPS supply is a proprietary circuit that monitors the output current of the supply and watches for

sudden changes. In general, these changes indicate that a quench is occurring. If a quench or load error occurs, the Error Detect circuitry quickly and smoothly shuts down the power supply so that the user's persistent switch and/or quench protection devices are not destroyed by the power supply's attempts to maintain current in its leads.

There are two cases where one could encounter incompatibilities between the Error Detect circuitry and their magnet system. The first potential problem lies in the fact that some magnets have extremely fast quench protection devices across their input leads. If this is the case, it is possible for a quench to go undetected by the Error Detect circuit. This problem is actually fairly rare; however, due to the fact that the Error Detect circuit is very sensitive.

Another potential concern with the Error Detect system is the possibility of a false trigger when a noisy load is placed on the supply. Most superconducting magnets are relatively quiet though, and this problem is usually encountered when a rapidly varying resistive load is on the supply.

Due to the fact that the Error Detector can have potential faults, it can be disabled should the user desire it, simply by switching the Error Detect switch to the OFF position.

3.3 REMOTE Operating Mode

The REMOTE Operating Mode is the mode in which the user operates the supply via rear panel connections to the supply rather than using the front panel controls. When the supply is placed in the REMOTE mode, almost all front panel controls are disabled. It is left to the user to generate the appropriate electrical signals to control the supply's

* Voltage Limit
* Current Limit

* Charge Rate

* Ramp UP/PAUSE/DOWN

* Fast Ramp

* Persistent Switch Heaters

All of these functions must be controlled when in the REMOTE mode and the correct signal levels must be maintained. GREAT CARE MUST BE TAKEN NOT TO EXCEED THE RATED VALUES OF INPUT SIGNAL LEVELS OR ELSE UNSTABLE CONDITIONS WITHIN THE SUPPLY MAY OCCUR WHICH COULD POTENTIALLY HARM THE SUPPLY AND/OR QUENCH THE MAGNET.

3.3a REMOTE RAMP UP/PAUSE/DOWN and FAST RAMP

Remote control of the front panel Charge Control switches is provided through terminals 2, 3 and 10 on the rear panel terminal strip of the supply. These three pins are compatible with standard Transistor-Transistor Logic (TTL) or can be driven by any other signal between zero (0) and five (+5) volts. A logic diagram indicating the functions of these three input lines is shown in Figure 3-3. A logic 0 corresponds to a ≤ 0.8 volt input and a logic 1 corresponds to a $\geq +3.5$ volt input. Absolute maximum allowable voltages are 0 and +5 volts respectively.

(10) FAST RAMP = 0

(3) RAMP UP \ (2) RAMP DOWN	0	1
0	PAUSE	RAMP DOWN
1	RAMP UP	PAUSE

(10) FAST RAMP = 1

(3) RAMP UP \ (2) RAMP DOWN	0	1
0	PAUSE	FAST RAMP DOWN
1	FAST RAMP UP	PAUSE

FIGURE 3-3 REMOTE Mode Charge Control Logic Diagram

All three input lines are disabled when the supply is operated in the LOCAL mode.

3.3b Persistent Switch Heaters

Persistent Switch Heaters A and B can be remotely operated using terminals 5 and 4 (respectively) on the rear panel terminal strip. These lines also require TTL logic levels to operate (0 to +5 volts) as do the Charge Control inputs. When using the persistent switch heater supplies while in the remote mode, one must leave the front panel switches for the heaters in the up or ON position. If the front panel switches are OFF, terminals 5 and 4 have no effect. When the supply is in the LOCAL mode terminals 5 and 4 are disabled.

3.3c Error Detect Enable/Reset and Status

The rear panel Error (Quench) Detect Circuitry can be enabled, disabled, and reset using terminal 6 on the rear panel of the supply when in the REMOTE Operating Mode. This input is TTL (0 to +5 volts) compatible. When terminal 6 is held low ($\leq$ 0.8 volts) the quench detector is enabled. When the terminal is high($\geq$ 3.5 volts) the detector is disabled. If the error detector trips, it is reset by bringing terminal 6 high and then back low again. The status of the quench detector is provided on terminal 9 of the rear panel terminal strip. If this pin is at a logic high, it is an indication that the quench detector has tripped. If terminal 9 is at a logic low, it is an indication that the quench detector is currently reset or disabled.

3.3d Voltage and Current Limit Status

The status of the Voltage and Current Limit LED's on the front panel of the supply can be monitored through terminals 7 and 8 (respectively) on the rear panel terminal strip. These terminals are TTL compatible outputs from the supply. A logic high indicates the corresponding limit has been reached, while a logic low indicates the limit has not been reached.

3.3e Magnet Voltage Monitoring

Inputs to the IPS power supply are provided for the user to attach a pair of voltage taps from the magnet. In most cases, these taps are attached to the magnet's current leads as close to the magnet as possible so that the voltage read does not include the resistive voltage drop associated with the system's power leads.

CONNECTION OF THE VOLTAGE TAPS TO THE POWER SUPPLY IS NOT REQUIRED FOR PROPER OPERATION OF THE SUPPLY. IT IS SIMPLY A CONVENIENCE FEATURE ON THE SUPPLY.

Standard practice calls for the voltage taps from the magnet to be made using a twisted pair of ~ 30 gauge teflon insulated wire. The wires should be attached to the rear panel of the IPS supply at terminals 15 and 16 of the terminal strip. These are differential inputs with a 10 kOhm resistance to the system's ground. Terminal 15 is the positive input and 16 is negative.

A fully buffered and ground referenced signal indicating the magnet voltage is made available to the user through BNC (3) on the rear panel of the supply. One (1) volt across the magnet voltage tap inputs yields a one (1) volt output on BNC (3).

THE DIFFERENTIAL INPUTS ON TERMINAL 15 AND 16 SHOULD NOT BE EXPOSED TO MORE THAN ±20 VOLTS FOR EXTENDED PERIODS OF TIME. THE ANALOG OUTPUT VOLTAGE AT BNC (3) HAS A RANGE OF ±14 VOLTS.

The Magnet Voltage Tap Inputs 15 and 16 and the analog magnet voltage output signal at BNC (3) remain valid whether the supply is in the LOCAL or REMOTE mode.

3.3f Power Supply Current Monitoring

The output current from the power supply can be monitored with more precision than the 3½ digit display provides using a digital volt-

meter attached to the rear panel of the supply. BNC (1) provides the user with a signal corresponding to 1.000 volt out for each 10.00 amperes in the supply's leads. For instance, if an IPS-100 is sourcing 73.52 amperes, BNC (1) will provide a 7.352 volt signal. The Current Monitor Output BNC (1) has a range of 0 to +10.250 volts and remains active whether the supply is in the LOCAL or REMOTE mode.

3.3g Power Supply Voltage Monitoring

A fully buffered and ground referenced signal indicating the voltage across the output terminals of the supply is provided at BNC (2) on the rear panel. The signal on BNC (2) has a one (1) volt per volt ratio and a range of -5.5 to +5.5 volts. Positive voltage indicates the supply is sourcing power while negative voltage is an indication that the supply is absorbing power. The Power Supply Voltage signal on BNC (2) remains active whether the supply is in the LOCAL or REMOTE mode.

3.3h REMOTE Current Limit Setting

When the supply is placed into the REMOTE mode, it is left to the user to supply a stable signal to the supply for use as its Current Limit Setting. This voltage must be input to the supply through BNC (4) on its rear panel. Like the Power Supply Current Monitor Output (BNC (1) and section 3.3f above), the Current Limit Setting read by the supply has a 1.000 volt equals 10.00 amperes ratio. For instance if one wished to set the Current Limit on an IPS-50 to 36.25 amperes, a 3.635 volt signal would be placed on BNC (4). All IPS supplies (IPS-20/50/100) use the same ratio for this input.

GREAT CARE SHOULD BE TAKEN NOT TO EXCEED THE LIMITS FOR THE VOLTAGE ON BNC (4) FOR ANY PARTICULAR SUPPLY. THESE LIMITS ARE:

SUPPLY	MINIMUM VOLTAGE	MAXIMUM VOLTAGE
IPS-20	0.000 VOLTS	+ 2.05 VOLTS
IPS-50	0.000 VOLTS	+ 5.10 VOLTS
IPS-100	0.000 VOLTS	+10.25 VOLTS

NOTICE THAT IT IS ESSENTIAL THAT NEGATIVE VOLTAGES NEVER BE APPLIED TO BNC (4) - NEGATIVE VOLTAGES CAN CAUSE INSTABILITIES WITHIN THE SUPPLY RESULTING IN HIGH CURRENTS!

The stability of the output current of the supply when in Current Limit is directly a function of the stability of the user's voltage source. If the voltage source drifts 0.1% over an hour, so will the output current from the supply. A very stable voltage source should be used for generation of the Current Limit signal. The Current Limit setting on BNC (4) is disabled when in the LOCAL mode.

3.3i REMOTE Voltage Limit Setting

When the supply is placed into the REMOTE mode, it is left to the user to supply a stable signal to the supply for use as its Voltage Limit Setting. This voltage must be input to the supply through BNC (5) on its rear panel. The Voltage Limit Setting read by the supply has a 1.00 volt per volt ratio -i.e. if 2.00 volts is applied to BNC (5), the supply will have a 2.00 Volt Voltage Limit. This Current Limit setting will be valid for both the Charge and Discharge cycles of the supply. In other words, when one begins to discharge the magnet, a -2.00 volt Voltage Limit is assumed by the supply even though +2.00 volts is present on BNC (5).

NEGATIVE VOLTAGES SHOULD NEVER BE SUPPLIED TO BNC (5) - INSTABILITIES WITHIN THE SUPPLY MAY RESULT!

All IPS supplies have the same minimum and maximum ratings for the signals input to BNC (5):

SUPPLY	MINIMUM VOLTAGE	MAXIMUM VOLTAGE
IPS-20/50/100	0.00 VOLTS	+5.50 VOLTS

The Voltage Limit Setting on BNC (5) is disabled when in the LOCAL mode.

3.3j REMOTE Charge Rate Setting

When the supply is placed into the REMOTE mode, it is left to the user to supply a stable signal to the supply for use as its Charge Rate Setting. This voltage must be input to the supply through BNC (6) on its rear panel. The Charge Rate setting read by the supply uses a 1 volt equals 0.100 amperes per second ratio - i.e. if 3.000 volts is placed on BNC (6), a 0.300 ampere per second Charge and Discharge Rate will be used by the supply. This Charge Rate Setting will be valid for both the Charge and Discharge cycles of the supply. In other words, when one begins to Discharge the magnet, a -0.300 ampere per second Discharge Rate is assumed by the supply even though +3.00 volts is present on BNC (6).

NEGATIVE VOLTAGES SHOULD NEVER BY SUPPLIED TO BNC (6) - INSTABILITIES WITHIN THE SUPPLY MAY RESULT!

All IPS supplies have the same minimum and maximum ratings for the signals input to BNC (6).

SUPPLY	MINIMUM VOLTAGE	MAXIMUM VOLTAGE
IPS-20/50/100	0.000 VOLTS	+10.25 VOLTS

The Charge Rate Setting on BNC (6) is disabled when in the LOCAL mode.

3.3k Summary of REMOTE Mode

Table 3-1 summarizes the signals that can be input to the supply on its rear panel. Essential signals for a minimum of operation in REMOTE mode are:

Function	Terminal Strip or BNC Connector Number
Digital Ground	TS 1
Ramp DOWN	TS 2
Ramp UP	TS 3
Current Limit	BNC (4)
Voltage Limit	BNC (5)
Charge Rate	BNC (6)

Other inputs and outputs detailed in Table 3-1 and in the preceeding text are optional and can be added according to the user's needs.

3.4 Persistent Switch Heater Supplies

Two Persistent Switch Heater Supplies are built into the IPS-50 and IPS-100. No supplies are available on the IPS-20 but they are available from Cryomagnetics as a separate instrument if they are required for the magnet system. The following explanation pertains only to the IPS-50 and IPS-100 power supplies.

The persistent switch heaters for the supply are labelled A and B. The supplies are set up as independently operable constant current sources. Two supplies are provided so multiple coils can be powered from a single IPS supply. Current outputs for the supplies are found on a four (4) terminal strip under the exhaust port on the rear panel of the supplies. The current can be adjusted using the procedure outlined in section 5.1 Calibration Procedures. The currents can be independently set to any current between 0 and 100 mA. The front panel LED's associated with the heater supplies will illuminate when the supply is ON and when current flow is present in the

TABLE 3-1 SUMMARY OF REAR PANEL CONNECTIONS

TERMINAL STRIP (TS) OR BNC CONNECTOR NUMBER	IPS INPUT OR OUTPUT	FUNCTION	RANGE	ENABLED OR DISABLED WHI IN LOCAL MOI
TS 1	COMMON	DIGITAL GROUND		ENABLED
TS 2	INPUT	RAMP DOWN	0 TO +5V (TTL)	DISABLED
TS 3	INPUT	RAMP UP	0 TO +5V (TTL)	DISABLED
TS 4	INPUT	PERSISTENT SWITCH HEATER B	0 TO +5V (TTL)	DISABLED
TS 5	INPUT	PERSISTENT SWITCH HEATER A	0 TO +5V (TTL)	DISABLED
TS 6	INPUT	ERROR DETECT ENABLE/RESET	0 TO +5V (TTL)	DISABLED
TS 7	OUTPUT	VOLTAGE LIMIT STATUS	0 TO +5V (TTL)	ENABLED
TS 8	OUTPUT	CURRENT LIMIT STATUS	0 TO +5V (TTL)	ENABLED
TS 9	OUTPUT	ERROR DETECT STATUS	0 TO +5V (TTL)	ENABLED
TS 10	INPUT	FAST RAMP	0 TO +5V (TTL)	DISABLED
TS 15	INPUT	+ MAGNET VOLTAGE TAP	+20V TO -20V DIFFERENTIAL INPUT	ENABLED
TS 16	INPUT	- MAGNET VOLTAGE TAP		ENABLED
BNC (1)	OUTPUT	CURRENT MONITOR	0 TO +10.25V	ENABLED
BNC (2)	OUTPUT	POWER SUPPLY VOLTAGE MONITOR	-5.5V TO +5.5V	ENABLED
BNC (3)	OUTPUT	MAGNET VOLTAGE MONITOR	-14V TO +14V	ENABLED
BNC (4)	INPUT	CURRENT LIMIT	0 TO +2.05V FOR IPS-20 0 TO +5.10V FOR IPS-50 0 TO +10.25V FOR IPS-100	DISABLED
BNC (5)	INPUT	VOLTAGE LIMIT	0 TO +5V	DISABLED
BNC (6)	INPUT	CHARGE RATE	0 TO +10V	DISABLED

NOTES: 1) TS 12-14 ARE NOT USED OR CONNECTED TO ANY POINT WITHIN THE POWER SUPPLY.

2) BOTH THE ANALOG AND DIGITAL GROUNDS PROVIDED ON THE TERMINAL STRIP ARE ISOLATED FROM THE CABINET GROUND OF THE SUPPLY. THE ANALOG AND DIGITAL GROUNDS ARE COMMON WITH THE POSITIVE (+) OUTPUT POWER TERMINAL OF THE SUPPLY.

3) TS 11 IS AN OUTPUT WITH A +5 REFERENCE VOLTAGE ON IT.

* * * CAUTION * * *

DO NOT CONNECT THE CABINET (LINE CORD) GROUND OF THE POWER SUPPLY TO THE ANALOG OR DIGITAL GROUNDS FOUND ON THE REAR PANEL OF THE SUPPLY. HIGH CURRENTS MAY RESULT. THE CABINET (LINE) GROUND IS ISOLATED FROM ALL POWER SUPPLY SIGNALS.

* * * * * * * * * * *

heater. If the LED does not illuminate when the supply is turned ON, it is an indication that there is an open circuit somewhere in the heater line.

When the persistent switch heater supplies are being operated by REMOTE control, the front panel switches must be in the ON position.

3.5 Connecting the Magnet

It is usually a good idea to check out the power supply with the output shorted prior to connecting the magnet. This will insure proper operation of the supply with no chance of harming or quenching the magnet.

Connecting the magnet is a straightforward procedure. It is recommended that the proper size cables be used corresponding to the length and current at which they will be operating. Helium vapor-cooled current leads are recommended to efficiently introduce the high currents to the cryogenic environment with a minimum of heat load.

* * * IMPORTANT * * *

ALWAYS CONNECT THE POWER LEADS SECURELY TO BOTH THE MAGNET AND THE POWER SUPPLY WHILE THE SUPPLY IS TURNED OFF. NEVER DISCONNECT THE POWER LEADS FROM THE MAGNET UNLESS YOU ARE ABSOLUTELY CERTAIN THAT NO CURRENT IS FLOWING IN THEM. POTENTIALLY FATAL VOLTAGES CAN OCCUR IN THE EVENT OF A QUENCH ALONG WITH PERSISTENT SWITCH AND QUENCH PROTECTION SHUNT FAILURES ON THE MAGNET!

* * * * * * * * * * * * *

4.0 PRINCIPLE OF OPERATION

The IPS series of superconducting magnet power supplies are triac preregulated linear supplies providing exceptionally low ripple and noise along with excellent stability specifications. Many features have been built into the supply to provide ease and versatility in the operation of the supply. A block diagram of the supply is shown in Figure 4-1. The following sections will briefly explain the principles behind the supply's operation.

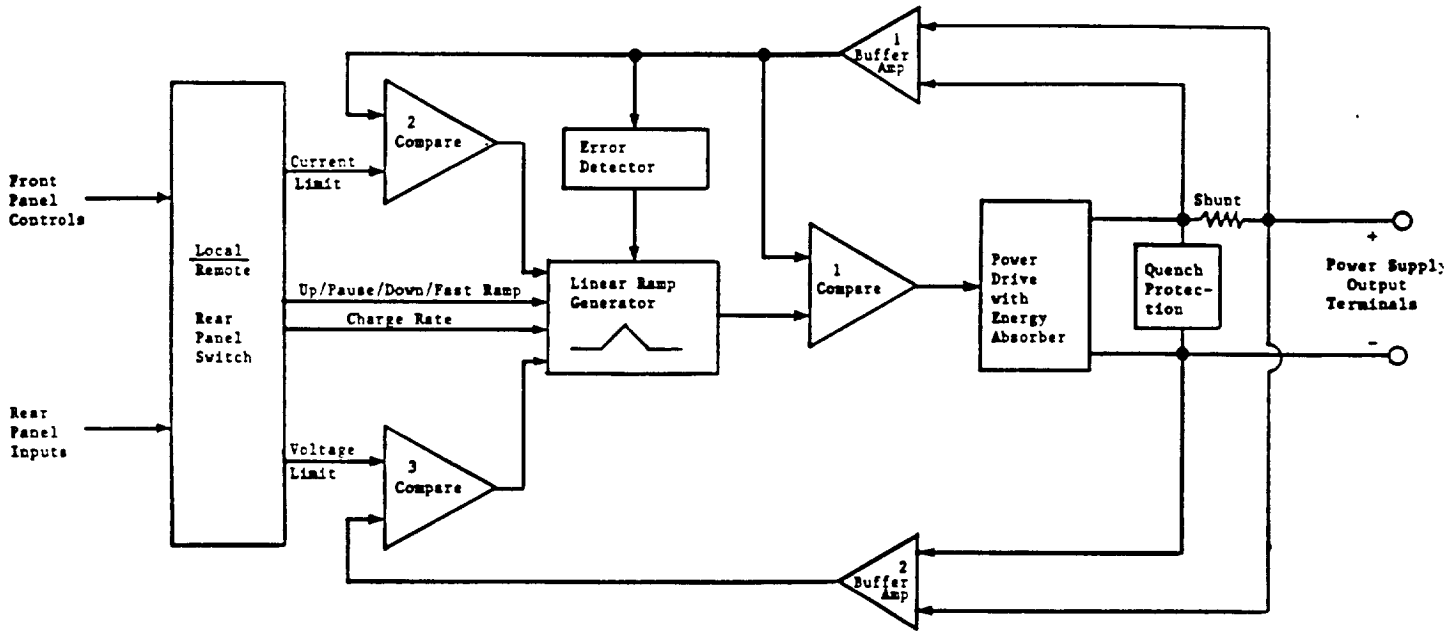

FIGURE 4-1 Integrated Power System Block Diagram

4.1 Ramp Generator

At the heart of the IPS supply's control system lies a precision analog Ramp Generator. This circuit is essentially a precision integrator used as a reference for the output current of the supply. As one can see in Figure 4-1, the Ramp Generator has several inputs and only one output. The output

is an analog signal which is proportional to the output current of the supply. If the output of the Ramp Generator is at 2.37 volts, the supply will (through the feedback loop consisting of Comparator 1, the Power Drive, and Buffer Amplifier 1) be outputting 23.7000 amperes.

The multitude of inputs to the Ramp Generator are required since many different system parameters can effect the output current. For instance, when Current Limit is reached, the Ramp must be stopped so that Current Limit is not exceeded. Likewise, the Voltage Limit must be able to stop the Ramp and the Error (Quench) Detector must not only stop the Ramp but must cause it to return to zero and be disabled.

4.2 Power Section

The Power Section of the IPS Supply consists of a triac preregulator, power transformer, full wave bridge rectifier, and a transistor pass-bank. A block diagram of the Power Section is shown in Figure 4-2. This is a common arrangement for power supplies and has been optimized to provide a high degree of regulation and minimum ripple and noise. A multiple transistor pass-bank is responsible for most of the regulation in the system. The Control Signal driving the pass-bank is generated by Comparator 1 in Figure 4-1.

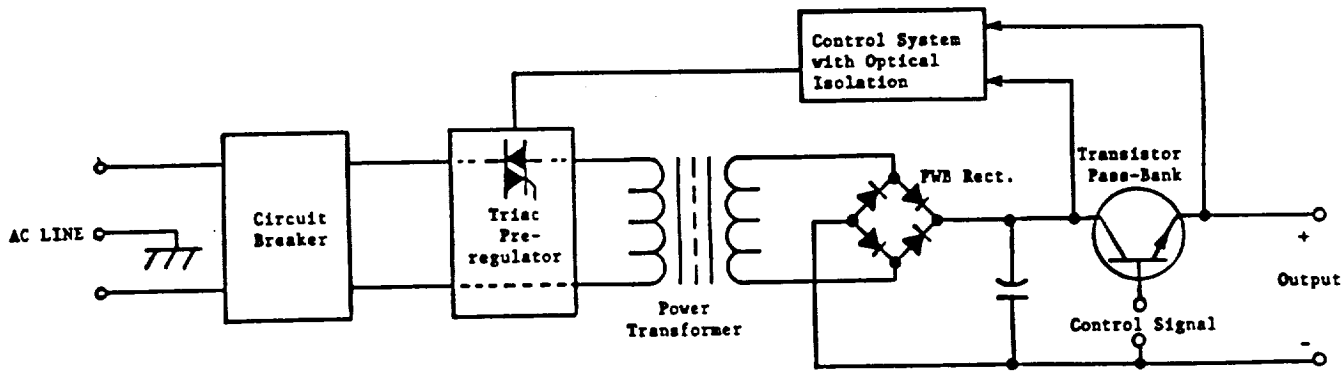

FIGURE 4-2 Simplified Power System Block Diagram

A high degree of RF shielding is built into the IPS supply to minimize the noise passed through the supply to its output and to minimize the noise reflected back into the power line. The low noise specifications of the IPS are some of the best specifications available. The Control System within the Power Section is used to control the turn-on time of the triac in the pre-regulator. The Control System monitors the power being dissipated in the pass-bank and directs the triac to deliver only the required amount of power for optimum regulation. Without this Control System the transistor pass-bank would have to be prohibitively large to constantly dissipate large amounts of energy. The Control System makes the IPS extremely power efficient.

4.3 Energy Absorbing

The Energy Absorbing capabilities of the IPS reflect back to the transistor pass-bank in the Power Section. When a magnet is being discharged, it tries to dump energy back into the supply - in particular, back into the pass-bank. The IPS power supply is designed such that the pass-bank is capable of absorbing considerable power. The supply is fully able to absorb 5 volts at its maximum rated current without any problems in the pass-bank. The Control System used to drive the triac preregulator is greatly responsible for this ability to absorb energy.

The transistor pass-bank of the IPS supply is equipped with an emergency thermal shut-down system that shuts the power system and pass transistors down in the event they are overheated. The only case where the supply may be overheated causing this shut-down would be if the airflow through the supply were too hot or blocked off from free flow. Neither the IPS nor the superconducting magnet will be damaged by this thermal shut-down.

4.4 Quench Protection

Quench Protection of the IPS supply and the magnet is provided not only through the Error Detector but also through the use of SCR crowbar circuits on

the supply's output. If a voltage of higher than +15 volts or lower than -15 volts is detected at the supply's output, the appropriate SCR will be turned ON effectively shorting the output terminals of the supply with a diode. This system works very well to eliminate the possibility of having high voltages appear across the magnet or supply. The SCR crowbar circuits are self-powered so the supply and magnet are protected even when the supply's power is shut OFF.

5.0 MAINTENANCE

Upon receipt of the IPS power supply, the performance and initial check-out procedures detailed in section 3.1 should be followed. If a problem is encountered during this procedure or during the normal operation of the supply, proceed to the Troubleshooting Section (5.2) of this manual. Once the supply is operating properly, it is ready for recalibration (if necessary) according to section 5.1. Before re-connecting the magnet or other load to the power supply, check again that all problems have been resolved and repeat the routine described in section 3.1. Before attempting any calibration procedures on the supply, turn the supply ON and allow a 30 minute warm-up and stabilization period.

5.1 Calibration Procedures

The following adjustments are available to calibrate the IPS supply should it ever become necessary. The IPS is fully burned-in, tested, and precision calibrated when it leaves the factory. If problems arise during calibration of the instrument, consult Cryomagnetics for assistance.

To access the calibration potentiometers in the IPS supply it is necessary to place the IPS supply on a bench with the front panel toward you. Remove the two screws holding the top cover of the supply in place. These screws are at the top of the supply on the rear panel. Carefully slide the top cover of the supply back revealing the main circuit board cover plate. Do not completely remove the cover plate as this will expose dangerous high current components and will impair the temperature stability of the supply by altering the airflow in the cabinet.

The main circuit board cover plate is clearly marked as to the location of all adjustment potentiometers for the system. The following descriptions define the effects of each potentiometer. If you are uncertain about which potentiometer to adjust, ask Cryomagnetics for assistance (preferably before trying).

Potentiometer	Function
P1	CURRENT ZERO OFFSET - this adjustment will trim the output current from the supply to 0.000 amperes when the Charge Control switch is in the DOWN position and has ramped down as far as it will go. An external resistive shunt and precision digital voltmeter may be required for adjustment.
P2	REMOTE MODE CURRENT LIMIT FULL SCALE CAL - this adjustment allows the user to put the proper full scale voltage into BNC (4) while in the REMOTE Mode, and to adjust the resulting output current to precisely full rated current. E.G., for an IPS-50, 5.000 volts would be placed on BNC (4) and P2 would be adjusted until precisely 50.000 amperes is output by the supply. Adjustment may require a precision voltage source, external resistive shunt and a precision digital voltmeter.
P3	CURRENT DISPLAY FULL SCALE CAL - this adjustment allows the current displayed on the front panel of the IPS to be matched to the actual output current of the supply at the full rated current of the supply. Adjustment requires a resistive shunt and precision digital voltmeter.
P4	REMOTE CURRENT MONITOR FULL SCALE CAL - this adjustment allows the precise matching of the actual output current from the supply to the output voltage at BNC (1) at the full rated current of the supply. Adjustment requires a resistive shunt and preferrably two precision digital voltmeters.
P5	REMOTE CURRENT MONITOR ZERO CAL - this adjustment allows the precise matching of the actual output current from the supply to the output voltage at BNC (1) at zero (or near zero) currents. Adjustment should be made with approximately 0.500 amperes being sourced by the supply. Adjustment requires a resistive shunt and preferably two precision digital voltmeters.
P6	RAMP TIMING CAL - this adjustment allows the timing of the internal ramp in the IPS to be precisely set. An iterative process is usually used wherein a timing cycle of several minutes is allowed for the system to ramp and this potentiometer is adjusted until the appropriate change in output current is detected.
P7	RAMP RATE DISPLAY CAL - this adjustment allows the Ramp Rate displayed on the front panel of the IPS supply to be matched at its top end such that 10.00 volts input at BNC (6) displays a charge rate of 1.000 amperes per second.

TABLE 5-1 Calibration Description

Potentiometer	Function
P8	IPS DISPLAY REFERENCE - this adjustment is used to set the reference voltage for the front panel displays to precisely 1.000 volts. This reference voltage is found on Pin 36 of both the 40 pin chips near the front of the circuit board.
P9	CURRENT LIMIT FULL SCALE DISPLAY CAL - this adjustment allows the full scale Current Limit displayed by the IPS to be precisely matched to the actual Current Limit current achieved. A resistive shunt and a precision digital voltmeter is required.
P10	-10 VOLT REFERENCE CAL - A precision voltage source is used to generate a highly stable +10 volt reference on the circuit board. The board also requires a closely matched -10 volt stable reference. This adjustment allows that +10 volt reference and the -10 volt reference to be matched to better than 1 mV. A precision digital voltmeter is required.
P11	CURRENT LIMIT ZERO OFFSET CAL - this adjustment allows the precise zero (or near zero) current matching of the Current Limit setting to the actual Current Limit achieved. The adjustment is set by entering a Current Limit setting on the front panel potentiometer of about 0.5 amperes. This adjustment is then set such that the actual output current during Current Limit matches the Current Limit setting. A resistive shunt and precision digital voltmeter are required.
P13	REMOTE MODE CURRENT LIMIT ZERO CAL - this adjustment allows the user to put a near zero voltage into BNC (4) while in the REMOTE mode, and to adjust the resulting output current to the proper value. This adjustment is similar to adjustment P2 except that it is set near zero rather than at full scale.
P14	PERSISTENT SWITCH HEATER B CURRENT CAL - allows the output current to persistent switch heater B to be set between zero and 100 mA.
P15	PERSISTENT SWITCH HEATER A CURRENT CAL - allows the output current to persistent switch heater A to be set between zero and 100 mA.

TABLE 5-1 Calibration Description (Continued)

6.0 CRYOMAGNETICS LIMITED WARRANTY POLICY

Cryomagnetics warrants its products to be free from defects in materials and workmanship. This warranty shall be effective for one (1) year after the date of shipment from Cryomagnetics. Cryomagnetics reserves the right to elect to repair, replace, or give credit for the purchase price of any product subject to warranty adjustment. Return of all products for warranty adjustment shall be FOB Oak Ridge, Tennessee, and must have prior authorization for such return from an authorized Cryomagnetics representative.

This warranty shall not apply to any product which has been determined by Cryomagnetics inspection to have become defective due to abuse, mishandling, accident, alteration, improper installation or other causes. Cryomagnetics products are designed for use by knowledgeable, competent technical personnel.

In any event, the liability of Cryomagnetics, Inc. is strictly limited to the purchase price of the equipment supplied by Cryomagnetics, Inc. Cryomagnetics shall not assume liability for any consequential damages associated with use or misuse of its equipment.

CRYOMAGNETICS, INC.

OPERATING INSTRUCTION MANUAL

FOR

MODEL 70 DIGITAL LINEARIZING CRYOTHERMOMETER

WARNING: DO NOT ATTEMPT TO OPERATE THIS EQUIPMENT BEFORE YOU HAVE THOROUGHLY READ THIS INSTRUCTION MANUAL.

INNOVATION AND EXCELLENCE IN CRYOMAGNETICS

739 EMORY VALLEY ROAD
OAK RIDGE, TN
MAILING ADDRESS
P.O BOX 548 OAK RIDGE, TN 37831-0548

TELEPHONE 615-482-9551
TELEX 883-9.

MODEL 70 LINEARIZING CRYOTHERMOMETER

The Model 70 Linearizing Cryothermometer provides versatile temperature monitoring capabilities at a budget-minded price. It incorporates microprocessor-based circuitry to linearize platinum resistance temperature sensors (RTD's) and display temperature with a resolution of 1 kelvin (above 15K) with an absolute accuracy of ±2 kelvin. The Model 70 is ideal for monitoring cool-down of superconducting magnets and other cryogenic systems that require moderate accuracy. The following features are standard:

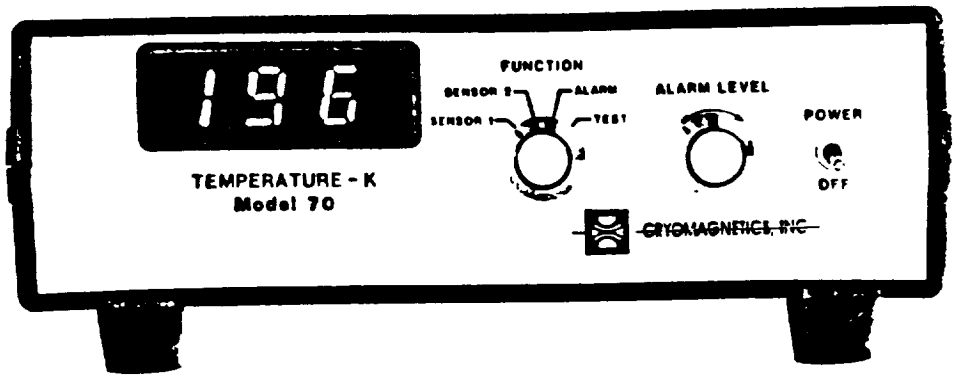

FEATURES

- ✱ Absolute accuracy of ±2K between 15K and 400K
- ✱ Readout calibrated in kelvin with 1K resolution between 15K and 400K - linearized using internal microprocessor
- ✱ 0.4 inch high, 3 digit LED readout
- ✱ Switch selectable operation of 2 level sensors
- ✱ Alarm set point continuously variable, 4K to 400K
- ✱ SPDT 5 amp relay alarm output
- ✱ Display alarm indicator
- ✱ Easy rear panel calibration adjustment
- ✱ Rear panel BNC recorder output of sensor voltage
- ✱ Plug-in sensor connectors
- ✱ Rugged, lightweight construction

OTHER SPECIFICATIONS

Overall Dimensions ..... 15.9 cm x 6.35 cm x 20.5 cm x
Weight ..... 1.36 kg
Input Power ... 120/220 Vac ±10%, 50-60 Hz

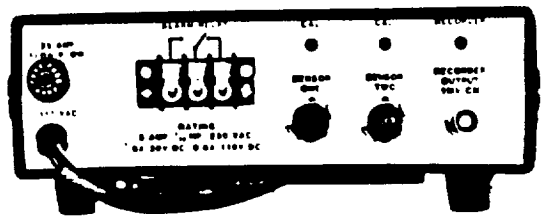

Rear View Model 70

Please consult factory for price and delivery information on both the Model 70 and calibrated sensors.

CRYOMAGNETICS, INC.
INNOVATION AND EXCELLENCE IN CRYOMAGNETICS
P. O. BOX 548
OAK RIDGE, TN USA
37831-0548
TELEPHONE
615-482-9551
TELEX 891-565

OPERATING INSTRUCTIONS

MODEL 70 DIGITAL LINEARIZING CRYOTHERMOMETER

1.0 INTRODUCTION

The Model 70 Cryogenic Thermometer is a microprocessor-based temperature monitor which utilizes inexpensive platinum resistor temperature sensors (RTD's) as its sensing element. Platinum RTD's are fairly linear devices in the 100K-500K temperature range. However, below 100K the devices become very non-linear. The built-in microprocessor in the Model 70 is used to correct for this non-linearity to provide an overall accuracy of ±2K between 15K and 400K with 1K resolution. The Model 70 is easy to install, calibrate, and operate. It is designed to operate Cryomagnetics Model PT100 platinum resistor temperature sensors.

2.0 INSTALLATION AND OPERATION

The Model 70 is delivered to you fully tested and ready to operate. If you ordered temperature sensors to accompany the instrument, it will also be delivered to you fully calibrated.

Unless otherwise specified, the Model 70 will be delivered for use with 120 VAC ±10%, 50-60 Hz input power. The unit can be supplied for operation on 220 VAC ±10%, 50-60 Hz input. It can also be easily rewired for one or the other input by you. Procedures are given below for implementing an input voltage change.

2.1 Procedure for Change of Input Voltage

In order to change the input voltage, it is only necessary to remove the instrument cover and change two wire connections on the power transformer primary as shown below.

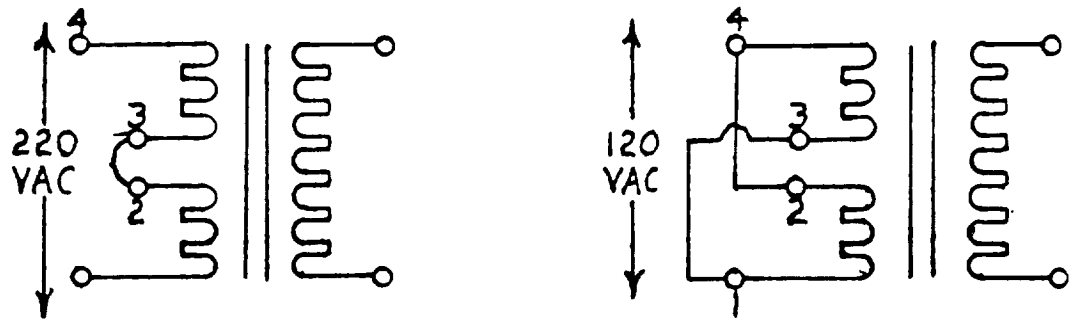

Transformer

*NOTE: ALWAYS DISCONNECT POWER CORD BEFORE REMOVING COVER.

2.2 Sensor Wiring

Cryomagnetics Model 70 utilizes PT100 temperature sensors connected in a four-wire sensing arrangement. A 5th wire can be connected as a shield if the sensors are to be located long distances from the instrument or if they will be in a "noisy" environment.

The rear panel of the Model 70 has two sensor input connectors. Replacement connectors are part number 126-1083 (Male) and 126-1085 (Female)

available through Cryomagnetics, Amphenol, and others. Connector wiring is shown below:

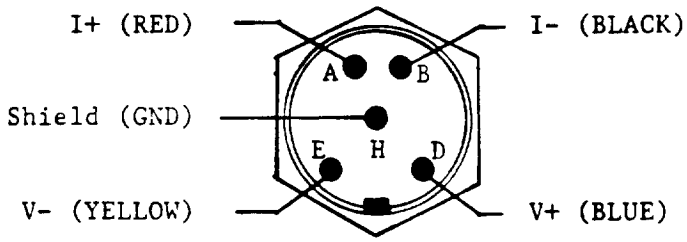

The interconnecting leads between the cryostat/dewar and the Model 70 should be of the appropriate size. The following table illustrates possible hook-up conditions:

Distance Between Model 70 and Dewar	Recommended Cable Wire Size
Up to 5 meters	#18 AWG
5 to 20 meters	#16 AWG
20 to 50 meters	#14 AWG

Unshielded four-conductor cable may be used where no significant use of SCR-controlled equipment or intense electrostatic field sources are present. Otherwise, it is recommended that shielded four-conductor cable be used with the shield grounded at pin H on the connector.

2.3 Calibration

The Model 70 comes fully factory calibrated and ready to use. In the event that recalibration ever becomes necessary, the procedure is very simple.

2.3.1 Procedures for Calibration of a New Sensor

1) Connect the sensor to Sensor One or Sensor Two on the rear panel of the Model 70.
2) Power on.
3) Set the FUNCTION selector switch on the front panel to the appropriate sensor position.

4) Insert the sensor into a liquid helium bath at 4K.

5) Adjust the appropriate "CAL" trim-potentiometer on the rear panel of the Model 70 until the display reads 004 kelvin.

The Model 70 is now completely calibrated to the new sensor for all temperatures between 4K and 400K.

2.3.2 Procedure for Test Position Calibration

The Model 70 has a built-in reference resistor that is activated when the front panel selector switch is put into the TEST position. This reference resistor has a value that directly corresponds to 273K (0 C). When the Model 70 is switched to the test position, the display should read 273K. If this is slightly off, the following recalibration procedure should be used.

1) Turn the Model 70 upside down and set it on a stable surface.

2) With the POWER OFF and the Model 70 UNPLUGGED remove the two screws which hold the bottom of the cabinet on. Do not remove the screws that hold the "legs" or "bail" of the instrument.

3) Remove the bottom of the instrument carefully to reveal the main circuit board.

4) Locate the calibration potentiometer on the circuit board. It can be found between the display and the FUNCTION selector switch.

5) Set the FUNCTION selector switch to the TEST position.

6) Plug in the Model 70 and POWER ON while being sure not to touch any internal electronics.

7) Using a small, insulated screwdriver, adjust the potentiometer located in (4) above until the display reads 273K.

8) POWER OFF and UNPLUG the instrument.

9) Reinstall the bottom cover and recalibrate the temperature sensors as described in section 2.3.1 if required.

The Model 70 is now fully calibrated.

2.4 Sensor Voltage Output

The Sensor Voltage output gives the user a partially corrected voltage proportional to temperature. The voltage at this output scales with temperature as is shown in Table 2.1. Notice that the voltage is not linearized, but has been normalized (compensated) to provide consistent voltage from room temperature to 4K.

TABLE 2.1

TYPICAL TEMPERATURE SENSOR CALIBRATION CHART

T (Kelvin)	V (Volts)	T (Kelvin)	V (Volts)	T (Kelvin)	V (Volts)
300	1.105	190	.670	77.2	.201
290	1.068	180	.630	70	.170
280	1.027	170	.590	60	.130
273	1.000	160	.548	50	.093
270	.988	150	.507	40	.0612
260	.949	140	.466	30	.038
250	.909	130	.425	25	.0283
240	.870	120	.385	20	.0217
230	.830	110	.342	15	.0183
220	.790	100	.300	10	.0165
210	.751	90	.258	4.2	.01552
200	.712	80	.213		

2.5 Alarm Relay

The Model 70 has a built-in Alarm Relay that can be used to generate audible alarms or control signals when the temperature exceeds a predetermined

point. The set point for the alarm can be adjusted using a screwdriver at the front panel "ALARM LEVEL" potentiometer. When setting the alarm level, set the front panel FUNCTION selector switch to ALARM to display the alarm trip point.

The alarm circuitry within the Model 70 continuously monitors only the selected sensor (1 or 2). If the FUNCTION selector is set to SENSOR 1, the alarm circuits monitor and react to sensor 1. Likewise if SENSOR 2 is selected, the alarm reacts to sensor 2.

The user has full access to the alarm relay contacts via a rear panel terminal strip on the Model 70.

3.0 TROUBLE SHOOTING

Symptom	Possible Cause
Blanked Display	Overrange was detected at sensor voltage inputs. Possibly caused by improper sensor hook-up or temperature over 510K detected. Check sensor connections.
Display Reads 888	Negative voltage was detected at sensor voltage inputs. Possibly caused by sensor voltage taps being reversed. See section 2.2 for proper sensor wiring or check sensor connections.
Display Reads 002 and does not change as sensor temperature changes	Voltage detected at sensor voltage was between 0V and +10mV. Check sensor connections. Possibly due to a short between leads at the sensor.
Other	Consult factory.

4.0 LIMITED WARRANTY POLICY

Cryomagnetics warrants its products to be free from defects in materials and workmanship. This warranty shall be effective for one (1) year after the date of shipment from Cryomagnetics. Cryomagnetics reserves the right to elect to repair, replace, or give credit for the purchase price of any product subject to warranty adjustment. Return of all products for warranty adjustment shall be FOB Oak Ridge, Tennessee, and must have prior authorization for such return from an authorized Cryomagnetics representative.

This warranty shall not apply to any product which has been determined by Cryomagnetics inspection to have become defective due to abuse, mishandling, accident, alteration, improper installation or other causes. Cryomagnetics products are designed for use by knowledgeable, competent technical personnel.

In any event, the liability of Cryomagnetics, Incorporated is strictly limited to the purchase price of the equipment supplied by Cryomagnetics, Incorporated. Cryomagnetics shall not assume liability for any consequential damages associated with use or misuse of its equipment.

FIGURE 3-1

RELIEF VALVE PRESSURE ADJUSTMENT

"CA" & "CPA" Series Relief Valves
Cracking Pressure Adjustment Instructions

1. Insert standard hex key wrench into locking screw. ("CA" and "4CPA" use 5/32" wrench; "8CPA" uses 5/16" wrench.)
2. Break locking screw by turning counterclockwise until wrench slides into adjusting screw.
3. Turn both screws to reach desired cracking pressure. (Turning clockwise increases opening pressure.)
4. Retract wrench into locking screw.
5. Lock against adjusting screw by turning clockwise.

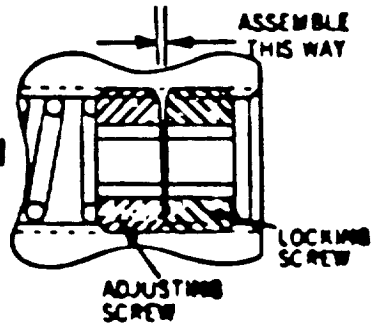

THIS PAGE

INTENTIONALLY

LEFT BLANK

Appendix D. Operating Manual for Superconducting LAMS

THIS PAGE

INTENTIONALLY

LEFT BLANK

LAMS Superconductor Charging and Discharging Procedures

Topics Covered

Cool to LN
Fill with LN for overnite temp soak-in
LHe fill
Current Charging
Current Discharging

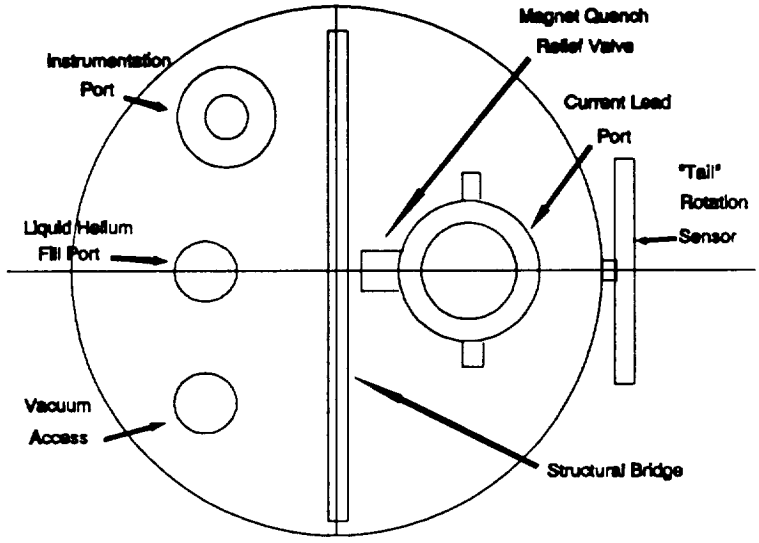

Figure 1 Underside Dewar Ports.

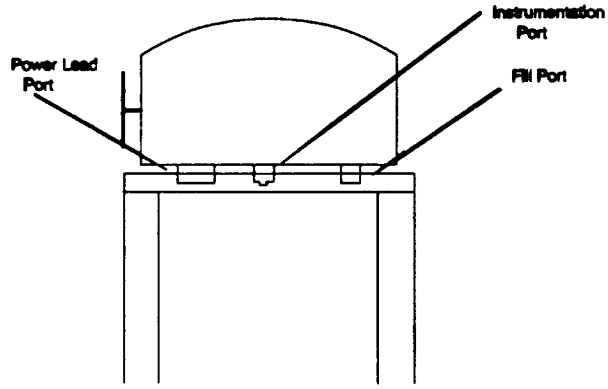

Figure 2 Dewar on Test Stand.

Coldown to LN Temperature

Configuration (Figure 3):

Lower sphere removed

Magnet dewar mounted and aligned with studs on service stand

Baffle in place in current lead port

Screw-on plug for LHe fill port removed

Barbed brass fitting with male pipe thread mounted onto current lead port so as to permit INPUT flow

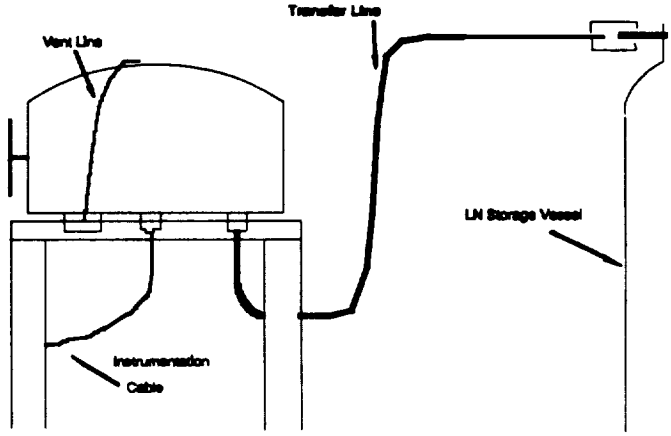

Figure 3 Liquid Nitrogen Fill.

Tygon tubing from regulated helium gas bottle connected to barbed fitting and flow gas at about 2 psi for a few minutes to purge dewar

He transfer line connected to LN storage vessel at long end (LHe source end) via 3/8" ID tygon tube 2.5" long or equivalent (The shorter tube reduces heat transfer from room across wall limits area susceptible to stress shattering)

Instrumentation cable connected to instrumentation port on magnet dewar

Safety glasses on operator

Magnet temperature gage electronics "on"

Operation:

PURGE - Purge magnet with helium gas by connecting gas tube (1/8" tygon) to flexible surgical tubing connected to power lead port. Pressure on gauge is < 4-5 psi. Three to four minutes of purging is sufficient. Maintain a low flow of He gas while transfer tube is cooled down.

TRANSFER LINE COOLDOWN - Start LN cooldown of transfer tube by opening storage tank valve to start flow. Since transfer tube aperature is very restricted at dewar end, flow is conductance limited. Opening the valve more than ~1/4 to ~1/2 turn will have

little effect on flow but subject the operator to greater risk if tygon connector ruptures.

The tube is sufficiently cool when liquid spurts out at dewar end. (About 5 minutes max for room temperature transfer line with 20 psi of tank pressure)

PREPARE DEWAR - While transfer tube is cooling, turn off He gas flow to magnet dewar, disconnect gas tube from power lead port, install one-way check valve to allow OUTFLOW from dewar, and route latex surgical tubing from barbed end to top of dewar to keep cold gas away from O-ring seals. (Until dewar reaches 77° K, the current lead port can remain completely open to speed heat transfer)

For initial cooldown stages it may be necessary to temporarily prop open quench disc.

CONNECT TRANSFER TUBE - Wipe dewar end of transfer tube - now spraying LN from its tip -with cloth to remove frost cap and quickly insert transfer tube into fill port minimizing time for air to diffuse into magnet dewar or frosting of tip.

Screw down transfer line knurled nut for finger tight seal.

COOLDOWN - Open storage vessel drain valve up to 1/2 turn if it has been partially closed.

Watch dewar temperature decrease on electronic sensor. 77-78° is indication for LN temperature. Cooldown time to 77° K is 1 1/4 hours for ~20 psi head on storage tank and unobstructed flow with good vacuum in dewar and transfer line.

Fill with or add LN

Configuration (Figure 3):

Magnet dewar pre-cooled to LN temperature

At current lead port:

Replace one-way check valve so as to allow OUTFLOW from dewar.

1" relief can be propped during initial stages of fill

Use latex surgical tubing to route exiting gas away from O-ring seal at base of dewar.

Thermal baffle should be screwed down tightly enough for reasonable seal. (Less thermal leakage minimizes buildup of frost which inhibits unscrewing the knurled nut.)

At fill port:

Cooled transfer line screwed tightly in place.

Thermal baffle plug in place at current lead port

One-way check valve at current lead port removed for first stages of fil

Magnet dewar temperature gage reads 77-78° K.

Safety glasses on operator

Thermal gloves available

Operation:

FILLING - Continue to let LN flow from storage vessel with up to 1/2 turn (with commercial 220 liter tanks). Fill time once 77 Kelvins is reached is about 60 minutes.

Slow filling can result from obstructed flow or degraded dewar vacuum.

The He level meter can be used to approximate LN fill. It reads negatively above LHe temperatures but increases from -1.9 to -.8 for a full LN dewar.

If He is to be filled immediately, do not fill completely with LN. Try about 5-10 min of filling after cooldown and then let dewar remain at LN for one hour or so to cool down core of magnet.

For complete LN fill, wait till liquid spurts out of current lead

port at vent tube, then shut down flow, remove transfer tube from magnet dewar and reset relief valve if propped. With a good vacuum in dewar, LN should last more than 60 hours.

TERMINATE FILL - Quickly unscrew the transfer line from the dewar fill port and insert the fill port plug

Surgical tubing on barbed fitting at current lead port to direct cold gas away from O-rings

Re-install one-way valve oriented to prevent inward passage of air

LHe Fill with Dewar Temperature at LN

Configuration (Figure 4):

Magnet dewar internally at 77-78° with some residual LN

Current port plugged with thermal baffle (or lead connector)

Fill port plugged with extension

Helium gas available at end of tube which can be connected to barbed fitting on one-way valve at current lead port.

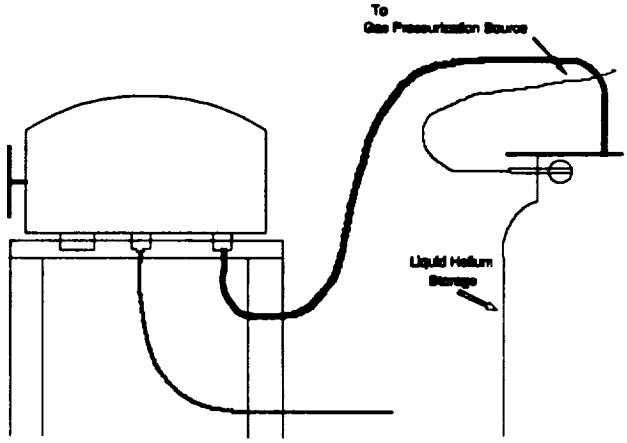

Figure 4 Liquid Helium Filling.

Operation:

SOME STEPS IN THIS PROCEDURE MUST BE DONE VERY CAREFULLY TO AVOID LATTER PLUGGING OF THE LHe FILL PATH.

IN PARTICULAR LN FREEZES AT ABOUT 10° K LOWER THAN ITS BOILING TEMPERATURE. IT IS POSSIBLE TO FREEZE A BOTTOM LAYER OF LN BY TRANSFERRING LHe TOO SOON AFTER THE LN IS "PURGED".

WAITING FOR A FEW MINUTES AFTER LN PURGING TILL DEWAR GAGE TEMPERATURE RISES A FEW DEGREES ABOUT 77° K WILL ELIMINATE THIS POSSIBILITY.

PURGING LN - Purge LN from magnet dewar. (This is accomplished by forcing He gas into current lead port with fill port uncapped. The resulting pressure above the LN bath forces liquid from the bottom up into the extending fill tube over the 'U' and out the fill port. Helium is used to reduce the possibility of freezing LN when LHe is introduced.)

Orient the current port check valve to allow incoming gas flow and connect He gas source tube. Flow with about 2 to 4 psi on gas bottle gage should be enough to force liquid out fill port. When liquid flow stops, reduce helium gas pressure but keep some flow. This should be coordinated with cooldown of transfer to minimize LHe loss.

(If the current leads are in place, measuring resistance across the magnet will act as indication of magnet temperature. The additional heat loss through the leads, make this generally undesirable if the temperature sensor is operable.)

While LN is draining, flow LN through transfer line until nitrogen as liquid comes from dewar end of tube. This should requires less

than about five minutes and should be started when the LN drain from the dewar is mostly complete.

The LN cooled transfer line should then be purged with warm helium gas to remove any frost.

The pressure build up in the LHe storage vessel should be released, and the cooled LN temperature transfer line inserted into the smaller compression fitting (cajon) and sealed against by tightening the knurled nut. At first, the boiloff pressure buildup from the transfer tube insertion will be enough to force out cold helium gas. Pressurization from the helium gas bottle may be necessary to mantain pressure but do not exceed 4 psi. It is more efficient to force helium at low pressure at first. Continue until LHe spatters from the transfer tube output end. With proper coordination, the magnet dewar purge of LN should just be completed.

Once the purged magnet dewar has WARMED A FEW DEGREES ABOVE LN TEMPERATURE, the output end of the transfer tube should be wiped for frost and inserted into the magnet dewar fill port while maintaining LHe flow. During the cooldown from LN temperature, a moderate flow is more efficient. The temperature inside the dewar is monitored with the supplied temperature sensor. The cooldown time to LHe is about fifteen minutes and the fill rate of about 2.5 cm/minute. Note the temperature gage resolution degrades near 4.2 Kelvins (±3 Kelvins).

Once full (19.9 cm on the level gage with magnet current = 0), the transfer tube can be left in while current is run up although this results in some additional loss rate. It is more efficient to fill to about 10 cm and reduce pressure while charging the magnet.

Current Charging

Configuration (Figure 5):

Magnet dewar on stand filled with LHe. Loss rate is greater with current leads connected, so level should be at least 8 cm.

Top half of sphere in place if levitation is planned

LHe transfer line connected to dewar fill port to provide refill capability during charging and other handling operations

Dewar temperature gage and level sensor active

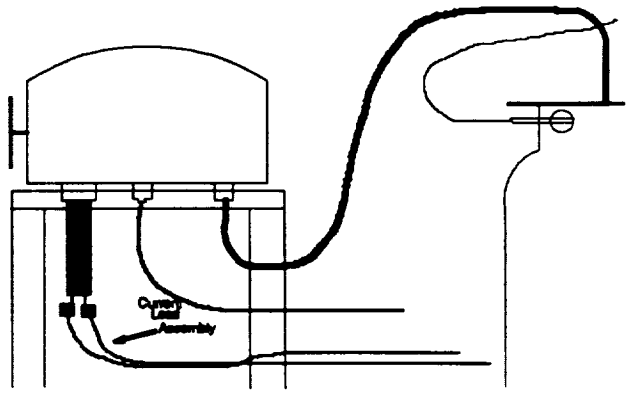

Figure 5 Charging and Discharging of Magnet.

Magnet power supply connected to line power line.

Shorting cable available

Safety glasses and thermal/High Voltage gloves on operator.

Operation:

POWER SUPPLY PREPARATION - Test power supply for proper operation by short circuiting output leads and operating current limits and controlled ramp.

CURRENT LEAD PREPARATION - With power supply current at zero and shorting leads across the current lead flags, connect wire leads to current lead plug noting polarity:

Remove power lead baffle.

Orient and insert lead assembly (with polarity noted) force Engage each lead in turn into corresponnding banana plug. The force required is about 20 # and the dewar should be bolted to support stand.

To check for positive electrical connection, one cable can be disconnected at lead or power supply and resistance of magnet probed with Ohmmeter.

(Note: the fabricator supplied knurled nut for retaining the current lead assembly has been removed to eliminate the inevitable freeze up from condensation. The effort required defrost the assembly with heat gun - usually magnetic - with

a fully charged magnet was considered more inconvenient and less of a risk than the possibility of a lead falling out.)

Remove shorting leads.

CHARGING - Set the power supply to the desired current limit (typically less than 0.07 A/s), a voltage limit of less than 1.2 v, and turn on the persistent switch heater. Use the slow ramp setting to bring current to desired limit (About 10 minutes to 45 A).

At this point the magnetic field energy is about 15 kJoules and it is possible to induce dangerous HV across the current leads.

DISCONNECTION - Once the magnet is charged, the persistent switch heater is shut down (wait about 10 seconds) and the power supply current can be removed using "fast ramp". Operating in the persistent mode removes the possibility of a spark down in case a lead becomes disconnected.

THE FOLLOWING STEP CAN BE DANGEROUS IF DONE INCORRECTLY

The current leads should be removed to minimize the extra heat load. Gently rotating and pulling each lead works well against the frozen condensation.

The power supply should be kept switched "ON" so that the persistent magnet currect can be transferred into the power supply smoothly without excessive voltage transients.

TO MINIMIZE OVERALL HELIUM LOSS, IT IS IMPORTANT TO KEEP CURRENT LEADS IN PLACE FOR AS SHORT A TIME AS POSSIBLE

The thermal baffle plug should be inserted and screwed down for a good seal.

LHe should be refilled to the desired level, the transfer tube disconnected from the fill port and the fill plug installed, and the instrumentation connector removed.

The dewar is now ready for final assembly and suspension.

Current Discharging or Current Change

Configuration (Figure 5):

Current charged magnet dewar with lower sphere removed locked in place on service stand

Instrumentation cable connected and instruments active

Current lead assembly connected to power supply with polarity orientation noted

Current lead assembly should be warmed to at least room temperature to maximize working time

If persistent mode operation is to continue, LHe transfer line should be prepared (cooled down) for LHe transfer

Safety goggles on operator(s)

Thermal or high voltage gloves available

Operation:

Observe level of remaining LHe, If < 6-7 cm, LHe should be added first to reduce possibility of quench

It will generally be necessary to melt the frost around the knurled nut holdling the baffle plug at the current lead port. A 1.5 kw heat gun will have sufficient power.

CAUTION IS REQUIRED TO HANDLE THE MAGNETIZABLE GUN IN THE HIGH FIELD GRADIENTS NEAR THE DEWAR.

The power supply should be "ON" with the current limit preset to the persistent current.

Power supply current should be zero.

Persistent switch heater should be "OFF".
Once the current lead baffle plug is removed, the current lead assembly should be positioned with the proper polarity orientation.

Operator should wear thermal or if possible high voltage insulating gloves.

THE FOLLOWING STEPS CAN BE DANGEROUS IF DONE INCORRECTLY

Each individual lead should be retracted and the assembly pushed upward properly aligned.

Each lead in turn should be made to engage the plug inside the port by rotating and pushing upwards.

The assembly should be checked to be mechanically secure before support is removed. (The dropout of leads in non-persistent mode could result in a internal magnet voltage arc)

Once the assembly is connected and supported, the power supply current should be taken up to the persistent current by "FAST RAMP" to the current limit.

The persistent switch heater is then switched on to break the internal magnet circulation of current.

If this is done without power supply faults, the current can be slowly ramped down at the preset rate or increased to the desired new level.

The appearance of a fault (excessive voltage or drop of current) means the SCR shunt across the power supply has tripped. This will result in slow decrease of magnet current.

Once the current has ramped to zero the power supply can be switched off and the LHe allowed to evaporate.

If the magnet current was changed to a new level, the magnet should be placed persistent mode and the leads removed as soon as possible to minimize LHe loss.

THIS PAGE

INTENTIONALLY

LEFT BLANK

Appendix E. Computer Programming, Documentation and Material Report

R25-91

COMPUTER PROGRAMMING, DOCUMENTATION AND MATERIAL

A Superconducting Large-Angle Magnetic Suspension
June 3, 1991

Sponsor:
NASA Langley Research Center
Hampton, VA 23665

Contract No. NAS1-18853

SatCon Technology Corporation
12 Emily Street
Cambridge, MA 02176

TABLE OF CONTENTS

1. PROGRAM DOCUMENTATION

This section describes the computer code required to operate the superconducting large-angle magnetic suspension (LAMS) system. The source code is described and other required files are identified. The compiling and linking procedure is presented. Finally, the procedure for running the compiled and linked code is presented.

1.1 Source Code and Requirements

The source code of the main module of the LAMS suspension controller program is contained in the file SUSV2057.C. The source code can be modified using any text editor. A copy of the source code is supplied in Section 2.

For the compilation and link phases to run successfully the following header definition files and libraries and linker command files must be present.

1.1.1 Header Definition Files Required

stdio.h, spox.h, math.h, a30user.h, lamsmain.def, lamsmain.exp

1.1.2 Libraries Required

a30user.lib, c30user.lib, 1016c30.205, 1016c31.lib, waitst.obj
s30.o30, spox.a30, rtsx.lib

1.1.3 Linker Command file

susv2057.cmd

1.2 Compiling And Linking The Suspension Program

A batch file is provided for compiling, linking and generating executable code. To generate new executable code the batch file is invoked by issuing the following command.

```
C30SPOX SUSV2057
```

Note that the ".C" file extension is not used. On successful execution of this batch file the source code in file SUSV2057.C is converted to executable code and stored in a file SUSV2057.OUT

1.3 Running the Suspension Program on the Sonitech DSP board

After successfully generating executable code of the SUSV2057.C LAMS suspension program, it can be executed on the Sonitech DSP board by issuing the following command.

```
S30SPOX SUSV2057.OUT
```

The S30SPOX utility downloads the SUSV2057.OUT file to the DSP board and resets the DSP board to begin execution of the down loaded program. The program prints the following message in the screen.

```
Original version V 1.00 of LAMS suspension program.
x y z thx in FIXED coord. are output as observable signals
Commanded references are all in FIXED Coord Frame
Commanded can be manually increased
in steps to lift sphere
```

The measured values of the "x,y,z" translations and the "thx and thz" rotations are displayed after the prompt.

```
Initial x y z thx thz
```

The initial orientation of the sphere in Euler angles is displayed after the prompt.

```
Orientation of Sphere in Euler Angles
```

The reference inputs to the translations "x,y,z" and the "thx and thz" rotations are initially set to the measured values. This is confirmed by displaying the reference values after the prompt.

Reference x y z thx thz

The nominal ampere turns in each coil are next displayed after the prompt.

Scaled Bias Ampere Turns

The nominal controller loop gains are next displayed after the prompt.

Compensation Loop Gains

The SUSV2057 program prompts the user for various inputs. The user is required to respond to these prompts before the program proceeds to the next step. These are listed in the Table I together with nominal values responses of the user where applicable. Comments are in italic.

After Step 5, a delay of 10 seconds has been introduced before suspension is initiated. This to allow the transients of the digital filters to decay. After Step 7, the program loops back to Step 6. The program executes an orderly shut down when commanded to do so. It also executes an orderly shut down if the measured value of the orientation "thx" and "thz" are outside the nominal measurement range defined by

$$60 < thx < 80$$
$$98 < thz < 118.$$

Table I. User Responses to Prompts

	Program Prompt	**Response**
1	Enter reference for z in meters -->	1.0e-3
2	Enter 1-5 to change gain on loops x y z thx thz. Else enter 0 -->	0
3	Enter Loop Gain for Loop -->* *Only if response to 2 has been other than 0*	
4	Enter -1 to start Measurement loop -->	-1
5	Enter -1 to start Suspension loop -->	-1
6	Enter positive number to stop suspension loop -->* *The controller will terminate after a positive input*	-1
7	Current Reference for z in meters -->* *Displays the old z reference* Enter New Reference for z in meters -->	

2. SOURCE LISTING

```
/*
 *  ==== PROGRAM FOR SUSPENDING LAMS  1-April-1991 =======
 */
#include <stdio.h>
#include <spox.h>
#include <math.h>
#include <a30user.h>
#include <lamsmain.def>
#include <lamsmain.exp>

Int    DegOfFree, iflagg, tt0, tt1, TestChan, ErrorFlag1, ErrorFlag2;
Float Dummy, Theta, Psi, V10, V02, V03, SignalMul;

Void smain()

 {
  Int     iloop, ContNow, NNN;
  Ptr     Lptr0, Lptr1;

  asm("      AND 0FDFFH, IE  ");

  printf("\n Original version V 1.00 of LAMS suspension program. \n");
  printf("\n x y z thx in FIXED cood. are output as observable signals.");
  printf("\n Commanded references are all in FIXED Cood Frame");
  printf("\n z Commanded can be manually increased");
  printf(" in steps to lift sphere.");

  InitALL6();
  Ang_Init();
  *(Float *)ptrCapSenScal[0] = 0.0;
  *(Float *)ptrCapSenScal[1] = 0.0;
  *(Float *)ptrCapSenScal[2] = 0.0;

  ErrorFlag1 = 0;   ErrorFlag2 = -1;   iflagg  = 0;  tt0 = 0;
  TestChan = 1;     SignalMul = 0.0;

/* Set up Loop Gains  */
  *(Float *)ptrCompLGains       =  30000.0;
  *(Float *)(ptrCompLGains + 1) =  30000.0;
  *(Float *)(ptrCompLGains + 2) =  40000.0;
  *(Float *)(ptrCompLGains + 3) =  -700.0;
  *(Float *)(ptrCompLGains + 4) =   700.0;

  AD32in(ptrADinput, 16);
  SV_add2(ADinputOffSet, ADinput);

  CapSensor();
  Theta = 0.0;
  Psi = 70.0/57.3;
```

```
    V10 = *(Float *)(ptrADinput)   * 0.0061/16.0 * 0.82;
    V02 = *(Float *)(ptrADinput+2) * 0.0061/16.0 * 0.82;
    V03 = *(Float *)(ptrADinput+3) * 0.0061/16.0 * 0.82;
    printf("\n Coil voltages %e V10, %e V02 %e V03 ", V10, V02, V03);

    CoilAngles(V10, V02, V03, &Theta, &Psi, 3);
    *(Float *)(ptrMeas + 3)      =   Psi;
    *(Float *)(ptrMeas + 4)      =   1.884-Theta;

  /*  Set Commanded x y z thx thz to measured values          */

    SV_assign(MeasureMents, CommDR);
    *(Float *)(ptrCommDR)          = -1.0e-3;
    *(Float *)(ptrCommDR + 1)      =  1.0e-3;

    WRvector(" Initial x y z thx thz ", &MeasureMents);
    printf("\n Orientation of Sphere in Euler Angles \n");
    printf(" Theta-z : %6.2f deg. = %5.2f rad.\n",
                   *(Float *)(ptrMeas + 4)*57.3,*(Float *)(ptrMeas + 4));
    printf(" Theta-x': %6.2f deg. = %5.2f rad.\n",
                   *(Float *)(ptrMeas + 3)*57.3,*(Float *)(ptrMeas + 3));

    printf("\n Enter reference for z in metres  --> "); scanf("%e", &Dummy);
    *(Float *)(ptrCommDR + 2) = Dummy;
    WRvector(" Reference x y z thx thz ", &CommDR);

    ValidModelNum = -1;
    UpDateModel(-1);

    C16BiasCurr = 5.0;
                  /* Assign a value to Bias current in coil 1-6 */

    *(Float *)ptrAllBiasCur = C16BiasCurr * Coil16Turns;
    CalBiasCurrents();

    printf(" Entered Main Module \n");
    printf(" Valid Model  %d\n ", ValidModelNum);
    Dummy = 0.5;
    SV_muls(AllBiasCur, AllBiasCur, Dummy);
    WRvector (" Scaled Bias Ampere Turns " , &AllBiasCur);

    WRvector (" Compensation Loop Gains " , &CompLGains);
    NNN = 1;
    while ((NNN > 0 ) && (NNN < 6))
     {
      printf(" \n Enter 1-5 to change gain on loops x y z thx thz. \n ");
      printf(" Else enter 0  --> \n ");
      scanf("%d", &NNN);
      if ((NNN > 0 ) && (NNN < 6))
       {
       printf(" \n Enter Loop Gain for Loop %d ", NNN, " --> ");
       scanf("%f", &Dummy);
```

```
      *(Float *)(ptrCompLGains + NNN - 1) = Dummy;
      WRvector (" New Compensation Loop Gains " , &CompLGains);
      }
    }

  Lptr0 = ptrDAout;
  for (iloop = 0; iloop < 6; iloop++)
   {
    *(Float *)(Lptr0++) = 0.0;
   }
  DA16out(ptrDAout);
  printf(" \n Enter -1 to start Measurement loop    --> ");
  scanf("%d", &ContNow);

  if (ContNow < 0 )
   {
   Timer1Init(1.0/SampleFreq);
   asm("       OR  00200H, IE  ");
   asm("       OR  02000H, ST  ");
   ErrorFlag1 = 0;
   printf(" \n Enter -1 to start Suspension loop    --> ");
   scanf("%d", &ContNow);
   if ((ContNow < 0 ) && (ErrorFlag2 > -2 ))
    { while (iflagg < Pause5000) { tt0 = 0; }; ErrorFlag2 = 0; }
   }

  while ((ContNow < 0) && (ErrorFlag1 > -1) && (ErrorFlag2 > -1))
   {
    printf(" \n Enter positive number to stop suspension loop    --> ");
    scanf("%d", &ContNow);
    if ((ContNow < 0) && (ErrorFlag1 > -1) && (ErrorFlag2 > -1))
     {
      printf("\n Current Reference for z in metres  --> %e",
                                        *(Float *)(ptrCommDR + 2));
      printf("\n Enter New Reference for z in metres  --> ");
      scanf("%e", &Dummy);
      *(Float *)(ptrCommDR + 2) = Dummy;

      WRvector(" CommDR x y z thx thz ", &CommDR);
      WRvector(" Measured x y z thx thz ", &MeasureMents);
      WRvector(" DRError x y z thx thz ", &DRError);
      WRvector(" ContrSignals x y z thx thz ", &ContrSignals);
     }

   } /* while ((ContNow < 0) && (ErrorFlag1 > -1) && (ErrorFlag2 > -1 )
*/


   asm("       AND  0FDFFH, IE  ");

   ZeroOuts();
   SetUpAuxMeas();
```

```
/* Report Status */
   printf(" Error Flags 1= %d   2= %d \n", ErrorFlag1, ErrorFlag2);
   WRvector(" Reference x y z thx thz ", &CommDR);
   WRvector(" Measured x y z thx thz ", &MeasureMents);
   printf("\n Thx limits %f to %f ",  PsiZLow,    PsiZHi);
   printf(" Thz limits %f to %f  \n", 1.884-ThetaZHi, 1.884-ThetaZLow);

 } /* END  main  */

T1IntService()
 {
  Ptr   Lptr0, Lptr1;
  SM_Matrix    LPmat, LinvPmat, QStatTrs;
  Int   iloop;

  LPmat            = PltGains1;
  LinvPmat         = invPltGains1;
  QStatTrs         = QStatTrs1;

  if (ErrorFlag1 > -1)
   {

/* Read in the analogue inputs                                  */
  AD32in(ptrADinput, 19);
  SV_add2(ADinputOffSet, ADinput);

/* Calculate Rotations                                          */
  V10 = *(Float *)(ptrADinput)   * 3.12625e-4;
  V02 = *(Float *)(ptrADinput+2) * 3.12625e-4;
  V03 = *(Float *)(ptrADinput+3) * 3.12625e-4;

  Psi   = *(Float *)(ptrMeas + 3);   /* Starting estimate thx */
  Theta =   1.884 - (*(Float *)(ptrMeas + 4));
                                     /* Starting estimate thz */
  if (iflagg > Pause5000)
   {
  CoilAngles(V10, V02, V03, &Theta, &Psi, 3);
   }
  else
   {
    iflagg = iflagg + 1;
   }


/* Limit Theta to -+10 Tiene Angles, 118 - 98 degrees Euler */
  if (Theta < ThetaZLow)       { ErrorFlag2 = -2; }
  else if (Theta > ThetaZHi)   { ErrorFlag2 = -3; }

/* Limit Psi to 60  - 80 degrees Euler */
  if (Psi < PsiZLow)      { ErrorFlag2 = -4;}
  else if (Psi > PsiZHi) { ErrorFlag2 = -5;}
```

```
  *(Float *)(ptrMeas + 3)       =   Psi;
                                      /* New estimate of thx  */
  *(Float *)(ptrMeas + 4)       =   1.884-Theta;
                                      /* New estimate of thz  */

/* Calculate Translations                                     */

   CapSensor();

/* Compute the control signals                                */

   SV_sub3(CommDR, MeasureMents, DRError);

  *(Float *)(ptrDRError)      = *(Float *)(ptrDRError) +
                              (*(Float   *)(ptrADinput   +   17)   *   2.0
CapSenScalFac);
  *(Float *)(ptrDRError + 1) = *(Float *)(ptrDRError + 1) +
                              (*(Float   *)(ptrADinput   +   18)   *   2.0
CapSenScalFac);

  *(Float *)(ptrDRError + 4) = *(Float *)(ptrDRError + 4) +
                              (*(Float   *)(ptrADinput   +   16)   *   50.0
CapSenScalFac);

   SM_prodv(QStatTrs, DRError, QsDRError);

   CompFilter();
   SV_mul2(CompLGains, ContrSignals);  /* Control Signals after
                                          compensation are in
                                          ContrSignals vector */

  /* Apply the inverse tranform  to get drive signals */
  SM_prodv(invPltGains1, ContrSignals, DriveSignals);

 if (ErrorFlag2 > -1)
   {

/*  Add the bias ampere turns to the control ATs    */

  SV_setbase(AllBiasCur,1);
  SV_setlength(AllBiasCur,NoOfDOFs);
  SV_add2(AllBiasCur, DriveSignals);
  SV_setview(AllBiasCur, NULL);

/* Write Coil 1 bias ATs to output vector                  */
  *(Float *)ptrDAout = *(Float *)ptrAllBiasCur;

/* Write drive signals to DA convertors                       */
  SV_setbase(DAout,1);
  SV_setlength(DAout,NoOfDOFs);
  SV_assign(DriveSignals, DAout);
```

```
/*  Scale AT to Drive signal numbers    */
  SV_setview(DAout, NULL);
  SV_muls(DAout, DAout, ATtoAmps);
/* Select the output signals on DA channels 6-9
   and Drive Ampliers */

  SetUpAuxMeas();

  } /* if (ErrorFlag2 > -1)  */

 else  /* Commence shut down procedure  */
  {
   ZeroOuts();
   SetUpAuxMeas();
   if (ErrorFlag2 < -1 ) { ErrorFlag1 = -1; }
  }

 }   /* if (ErrorFlag1 > -1)  */

 }   /*  T1IntService()  */

void ZeroOuts()
  {
   *(Float *)(ptrDAout + 0) = 0.0;
   *(Float *)(ptrDAout + 1) = 0.0;
   *(Float *)(ptrDAout + 2) = 0.0;
   *(Float *)(ptrDAout + 3) = 0.0;
   *(Float *)(ptrDAout + 4) = 0.0;
   *(Float *)(ptrDAout + 5) = 0.0;
  } /*   ZeroOuts    */

 void SetUpAuxMeas()
  {
   SV_setview(DAout, NULL);
/* outputs errors in x y z                        */

  *(Float *)(ptrDAout + 6) = *(Float *)(ptrMeas )       * 1.0e7;
  *(Float *)(ptrDAout + 7) = *(Float *)(ptrMeas + 1)    * 1.0e7;

  *(Float *)(ptrDAout + 8) = (*(Float *)(ptrMeas + 3) - 1.22) * 1.0e5;
  *(Float *)(ptrDAout + 9) = (*(Float *)(ptrMeas + 4) - 1.90) * 1.0e5;

  SymClip(ptrDAout, ptrDAout, 10, 32000.0);
  DA16out(ptrDAout);

  } /*  SetUpAuxMeas()   */
```

3. BATCH FILE LISTING

File C30SPOX.BAT is a batch file which compiles and links the suspension program. A listing of the file appears below.

```
cl30 %1.c -z %1.cmd -o %1.out -m %1.map
```

REPORT DOCUMENTATION PAGE

Form Approved
OMB No. 0704-0188

1. AGENCY USE ONLY *(Leave blank)*	2. REPORT DATE	3. REPORT TYPE AND DATES COVERED
	December 1992	Contractor Report

4. TITLE AND SUBTITLE
A Superconducting Large-Angle Magnetic Suspension

5. FUNDING NUMBERS
C NAS1-18853
WU 324-02-01

6. AUTHOR(S)
James R. Downer, George V. Anastas, Jr., Dariusz A. Bushko, Frederick J. Flynn, James H. Goldie, Vijay Gondhalekar, Timothy J. Hawkey, Richard L. Hockney, and Richard P. Torti

7. PERFORMING ORGANIZATION NAME(S) AND ADDRESS(ES)
SatCon Technology Corporation
12 Emily Street
Cambridge, MA 02139

8. PERFORMING ORGANIZATION REPORT NUMBER

9. SPONSORING / MONITORING AGENCY NAME(S) AND ADDRESS(ES)
National Aeronautics and Space Administration
Langley Research Center
Hampton, VA 23681-0001

10. SPONSORING / MONITORING AGENCY REPORT NUMBER
NASA CR-189735

11. SUPPLEMENTARY NOTES
Langley Technical Monitor: Nelson J. Groom
Final Report - SBIR Phase II

12a. DISTRIBUTION / AVAILABILITY STATEMENT
FOR U.S. GOVERNMENT AGENCIES ONLY

Subject Category 18

12b. DISTRIBUTION CODE

13. ABSTRACT *(Maximum 200 words)*

SatCon Technology Corporation has completed a Small Business Innovation Research (SBIR) Phase II program to develop a Superconducting Large-Angle Magnetic Suspension (LAMS) for the NASA Langley Research Center. The Superconducting LAMS was a hardware demonstration of the control technology required to develop an advanced momentum exchange effector.

The Phase II research was directed toward the demonstration for the key technology required for the advanced concept CMG, the controller. The Phase II hardware consists of a superconductng solenoid ("source coil") suspended within an array of nonsuperconducting coils ("control coils"), a five-degree-of-freedom positioning sensing system, switching power amplifiers, and a digital control system. The results demonstrated the feasibility of suspending the source coil. Gimballing (pointing the axis of the source coil) was demonstrated over a limited range. With further development of the rotation sensing system, enhanced angular freedom should be possible.

14. SUBJECT TERMS	15. NUMBER OF PAGES
Control moment gyro, actuator, magnetic suspension system, gimbals, superconducting solenoid, source coil, control coil.	339
	16. PRICE CODE

17. SECURITY CLASSIFICATION OF REPORT	18. SECURITY CLASSIFICATION OF THIS PAGE	19. SECURITY CLASSIFICATION OF ABSTRACT	20. LIMITATION OF ABSTRACT
Unclassified	Unclassified		

1. STIMS 3X ACC# 9336274 IPS-FILE ADABAS # = 187806

FICHE AVAIL	= AD	HARD COPY AVL	= OK	COPYRIGHT	= N
ORIG AGENCY	= NASA	RECEIPT TYPE	= REG	ACQUIS TYPE	= REG
DOCUMENT CLASS	= TRP	ACCESS LEVEL	= O	ACCESS RESTR	= UNRES
LIMITATION CAT	= NONE	DOCUMENT SEC	= NC	TITLE SECURITY	= NC
SUBJECT CATGRY	= 31	SPECIAL HANDL	=	PAGE COUNT	= 00328
INC AUTHOR LST	= N	INC CNTRCT LST	= N	LANGUAGE	= EN
COUNTRY ORIGIN	= US	COUNTRY FINANC	= US	ABSTRACT PREP	= NON
PUB DATE	= 19921200	CORP SOURCE	= SC739580		

TITLE = A superconducting large-angle magnetic suspension
TITLE SUPP = Final Report
AUTHOR = DOWNER, JAMES R.
AUTHOR = ANASTAS, GEORGE V., JR.
AUTHOR = BUSHKO, DARIUSZ A.
AUTHOR = FLYNN, FREDERICK J.
AUTHOR = GOLDIE, JAMES H.
AUTHOR = GONDHALEKAR, VIJAY
AUTHOR = HAWKEY, TIMOTHY J.
AUTHOR = HOCKNEY, RICHARD L.
AUTHOR = TORTI, RICHARD P.
CONTRACT NUM = NAS1-18853
CONTRACT NUM = SBIR-09.01-0540A
CONTRACT NUM = RTOP 324-02-01
REPORT NUM = NASA-CR-189735
REPORT NUM = NAS 1.26:189735
SALES AGY PRIC = Contact the Langley SBIR Field Center Manager for
SALES AGY PRIC = further information
MAJOR TERMS = ATTITUDE CONTROL
MAJOR TERMS = CONTROL MOMENT GYROSCOPES
MAJOR TERMS = CONTROL SYSTEMS DESIGN
MAJOR TERMS = MAGNETIC SUSPENSION
MAJOR TERMS = SPACECRAFT CONTROL
MAJOR TERMS = SUPERCONDUCTIVITY
MINOR TERMS = BEARINGS
MINOR TERMS = DIGITAL SYSTEMS
MINOR TERMS = GIMBALS
MINOR TERMS = POWER AMPLIFIERS
FORM OF INPUT = HC

********** END OF ADABAS RECORD # 187806 **********